



National Library  
of Canada

Bibliothèque nationale  
du Canada

Canadian Theses Service

Service des thèses canadiennes

Ottawa, Canada  
K1A 0N4

## NOTICE

The quality of this microform is heavily dependent upon the quality of the original thesis submitted for microfilming. Every effort has been made to ensure the highest quality of reproduction possible.

If pages are missing, contact the university which granted the degree.

Some pages may have indistinct print especially if the original pages were typed with a poor typewriter ribbon or if the university sent us an inferior photocopy.

Previously copyrighted materials (journal articles, published tests, etc.) are not filmed.

Reproduction in full or in part of this microform is governed by the Canadian Copyright Act, R.S.C. 1970, c. C-30.

## AVIS

La qualité de cette microforme dépend grandement de la qualité de la thèse soumise au microfilmage. Nous avons tout fait pour assurer une qualité supérieure de reproduction.

S'il manque des pages, veuillez communiquer avec l'université qui a conféré le grade.

La qualité d'impression de certaines pages peut laisser à désirer, surtout si les pages originales ont été dactylographiées à l'aide d'un ruban usé ou si l'université nous a fait parvenir une photocopie de qualité inférieure.

Les documents qui font déjà l'objet d'un droit d'auteur (articles de revue, tests publiés, etc.) ne sont pas microfilmés.

La reproduction, même partielle, de cette microforme est soumise à la Loi canadienne sur le droit d'auteur, SRC 1970, c. C-30.

THE UNIVERSITY OF ALBERTA

Effect of Q Weighting on Self-Tuning Control of a Binary  
Distillation Column

by



James A. Langman

A THESIS

SUBMITTED TO THE FACULTY OF GRADUATE STUDIES AND RESEARCH  
IN PARTIAL FULFILMENT OF THE REQUIREMENTS FOR THE DEGREE

OF Master of Science

IN

Process Control

Department of Chemical Engineering

EDMONTON, ALBERTA

Fall 1987

Permission has been granted to the National Library of Canada to microfilm this thesis and to lend or sell copies of the film.

The author (copyright owner) has reserved other publication rights, and neither the thesis nor extensive extracts from it may be printed or otherwise reproduced without his/her written permission.

L'autorisation a été accordée à la Bibliothèque nationale du Canada de microfilmer cette thèse et de prêter ou de vendre des exemplaires du film.

L'auteur (titulaire du droit d'auteur) se réserve les autres droits de publication; ni la thèse ni de longs extraits de celle-ci ne doivent être imprimés ou autrement reproduits sans son autorisation écrite.

ISBN 0-315-40941-X

THE UNIVERSITY OF ALBERTA

RELEASE FORM

NAME OF AUTHOR

James A. Langman

TITLE OF THESIS

Effect of Q Weighting on Self-Tuning  
Control of a Binary Distillation  
Column

DEGREE FOR WHICH THESIS WAS PRESENTED Master of Science

YEAR THIS DEGREE GRANTED Fall 1987

Permission is hereby granted to THE UNIVERSITY OF  
ALBERTA LIBRARY to reproduce single copies of this  
thesis and to lend or sell such copies for private,  
scholarly or scientific research purposes only.

The author reserves other publication rights, and  
neither the thesis nor extensive extracts from it may  
be printed or otherwise reproduced without the author's  
written permission.

(SIGNED) *James Langman*

PERMANENT ADDRESS:

1617 - RALPH ST  
NORTH VANCOUVER B.C.  
V7K 1V6

DATED *JUNE 23* 1987



THE UNIVERSITY OF ALBERTA  
FACULTY OF GRADUATE STUDIES AND RESEARCH

The undersigned certify that they have read, and recommend to the Faculty of Graduate Studies and Research, for acceptance, a thesis entitled Effect of Q Weighting on Self-Tuning Control of a Binary Distillation Column submitted by James A. Langman in partial fulfilment of the requirements for the degree of Master of Science in Process Control.

.....  
Supervisor

.....  
V. Gourishanker

Date... 23 June, 1981 .....

Roses are red,  
Violets are blue;  
Since you put up with me, Annette,  
This is for you

## Abstract

This thesis represents another of a series of studies, both simulation and experimental, conducted in the Department of Chemical Engineering at the University of Alberta examining control of the terminal compositions of a binary distillation column. The focus of this work has been on the selection of the  $Q$  weighting polynomial used in a multivariable, multirate (MVMR) self-tuning controller. Both single and multirate forms of the controller have been employed. In addition, the performance that resulted using feedforward action based on the measured disturbance or an estimate of the disturbance was also investigated. Comparisons were made with multiloop control of the column using conventional proportional-integral-derivative (PID) controllers of the column.

Simulations were used to demonstrate different techniques aimed at using "tuned" PID controller constants for selection of the  $Q$  weighting coefficients. The various forms of the algorithm were then implemented on a pilot plant distillation column subjected to disturbances in the form of  $\pm 25$  step changes in the feed flow rate.

From the experimental tests most of the  $Q$  weighting schemes were at least as successful in controlling the column as the conventional PID controller. In general, multirate control improved the overall control of the column, as measured by the sum of absolute error (SAE) values, although the improvement in top composition control

was achieved at the expense of a deterioration in the control of the bottom composition. The use of an estimated or measured disturbance as the feedforward signal did not always result in improved control. This behavior would support the conjecture that the performance of the self-tuning controller may be further improved by following a procedure of "tuning" the weighting coefficients. The procedure of "tuning" the self-tuning controller parallels the procedure used in tuning a conventional PID controller.

## Acknowledgements

The author would like to express his thanks to the many individuals and groups, without whose support and encouragement completion of this work would not have been possible. Among those deserving of thanks are:

Dr. R.K. Wood and Dr. A.J. Morris for their guidance and supervision;

Mr. D. Sutherland, Mr. K. Faulder and the staff of both the electronics and machine shops for their prompt assistance in keeping the distillation column functional;

Mr. R.L. Barton and the DACS centre staff for their expertise and the use of the computing facilities;

The previous graduate students who have laid the groundwork for this thesis, notably F. Vagi, M. Tham and Y. Nazer;

The graduate students with whom over two years in graduate school became an enjoyable experience;

And, last but not least, the Natural Sciences and Engineering Council of Canada and the University of Alberta for financial assistance during the course of this work.

## Table of Contents

Chapter	Page
Abstract .....	v
Acknowledgements .....	vii
Nomenclature .....	xxv
1. Introduction .....	1
2. Literature Survey .....	3
2.1 Introduction .....	3
2.2 Why Adaptive Control? .....	3
2.3 Stochastic Adaptive Control .....	4
2.4 Control of Distillation Columns .....	12
2.5 Identification .....	14
2.6 Implementation of Stochastic Adaptive Controllers .....	14
2.7 Summary .....	15
3. Theoretical Development of the Self-tuning Controller .....	17
3.1 Introduction .....	17
3.2 Multi-input, Single-output Self-tuning Controller .....	18
3.2.1 Generalized Control Law Derivation .....	18
3.2.2 Minimum Variance Controller .....	26
3.3 Multivariable Self-tuning Controller .....	27
3.4 Distillation Column Control Law Implementation .....	34
3.5 Control with Multirate Sampling .....	37
3.6 Parameter Estimation .....	39
3.6.1 Multi-input, Single-output Parameter Estimation .....	40
3.6.2 Multivariable Parameter Estimation .....	42
3.7 Relative Disturbance Gain Theory .....	43

4.	Equipment .....	46
4.1	Introduction .....	46
4.2	Distillation Column Description .....	46
4.3	Computer Control .....	49
5.	Distillation Column Dynamics .....	54
5.1	Introduction .....	54
5.2	Linear Representation .....	55
5.3	Open Loop Test Results .....	56
5.3.1	Feed .....	57
5.3.2	Reflux .....	57
5.3.3	Steam .....	63
6.	Controller Parameters .....	67
6.1	Introduction .....	67
6.2	Sample Time .....	67
6.3	Conventional PID Controller Constants .....	68
6.4	Self-tuning Controller .....	71
6.4.1	Controller Polynomial Coefficients .....	71
6.4.2	Q Weighting Parameters .....	74
6.5	Controller Performance Criterion .....	82
7.	Simulation Results .....	83
7.1	Introduction .....	83
7.2	Single Transfer Function Plant Model Simulation .....	84
7.2.1	Introduction .....	84
7.2.2	PI Control .....	85
7.2.3	Parameter Identification .....	85
7.2.4	Minimum Variance Control .....	88
7.2.5	Generalized Minimum Variance Control .....	96

7.2.6	Single Transfer Function Simulation Summary .....	109
7.3	Two Transfer Function Plant Model Simulation ..	113
7.3.1	Introduction .....	113
7.3.2	PI Control .....	115
7.3.3	Parameter Identification .....	115
7.3.4	Minimum Variance Control .....	115
7.3.5	Generalized Minimum Variance Control ....	118
7.3.6	Two Transfer Function-Simulation Summary	140
7.4	Linear Distillation Column Model Simulation ...	142
7.4.1	Introduction .....	142
7.4.2	PI/PID Control .....	144
7.4.3	Minimum Variance Control .....	144
7.4.4	Generalized Minimum Variance Control ....	147
7.4.5	Linear Distillation Column Simulation Summary .....	157
8.	Experimental Results .....	165
8.1	Introduction .....	165
8.2	PI/PID Control .....	166
8.3	Commissioning the Self-tuning Controller .....	170
8.4	Minimum Variance Control .....	177
8.5	Generalized Minimum Variance Control .....	181
8.5.1	Introduction .....	181
8.5.2	Q Weighting Established from PI/PID Constants .....	182
8.5.3	Q Weighting Established from PI/PI Constants .....	196
8.5.4	Modified PI/PI Controller constants for Q Weighting .....	211



8.5.5 Q Weighting based on PI/PID constants with $g_0=0$ .....	234
8.5.6 Underestimating the Time Delay .....	247
8.5.7 Q Weighting Adapting with $g_0$ .....	261
8.6 Summary of Experimental Work .....	262
9. Conclusions .....	265
10. Recommendations .....	269
Bibliography .....	274
Appendices .....	284
Appendix A Example of Matrix Notation .....	285
Appendix B Differentiation of Cost Function .....	289
Appendix C Calibration Data for the Distillation Column .....	293
Appendix D Pseudocode for Distillation Column Routines .....	299

## List of Tables

Table	Page
4.1 Steady State Mass and Energy Balance Report.....	50
5.1 Transfer Functions Relating Feed Flow to Top and Bottom Compositions.....	60
5.2 Transfer Functions Relating Reflux Flow to Top and Bottom Compositions.....	62
5.3 Transfer Functions Relating Steam Flow to Top and Bottom Compositions.....	65
6.1 Cohen-Coon Constants.....	70
6.2 Initial PID Controller Constants.....	71
7.1 SAE Values for the Single Transfer Function Simulations.....	112
7.2 SAE Values for the Two Transfer Function Model Simulations.....	141
7.3 SAE Values for the Linear Distillation Column Simulations.....	162
8.1 SAE Values for PI/PID Control.....	170
8.2 SAE Values for Q Weighting based on PI/PID constants.....	196
8.3 SAE Values for Q Weighting based on PI/PI constants.....	210
8.4 Integral of Absolute Error Constants.....	218
8.5 SAE Values for Generalized Minimum Variance Control based on Modified PI/PI constants.....	233

8.6	SAE Values for Generalized Minimum Variance Control using $g_0=0$ .....	247
8.6	SAE Values for Generalized Minimum Variance Control using $g_0=0.0$ with the Time Delay Underestimated.....	261
8.8	Summary of Experimental Results.....	263
C.1	Top Product Analyzer Calibration.....	293
C.2	Top Product Flow Calibration.....	294
C.3	Reflux Flow Calibration.....	295
C.4	Feed Flow Calibration.....	296
C.5	Steam Flow Calibration.....	297
C.6	Bottom Product Flow Calibration.....	298

## List of Figures

Figure	Page
2.1 A Stochastic Adaptive Control System.....	5
4.1 University of Alberta Distillation Column.....	47
4.2 Simplified Flowchart for Control Timing.....	53
5.1 Open Loop Column Response to Feed Disturbances.....	58
5.2 Process Reaction Curve: Bottom Composition Response to Feed Disturbance.....	59
5.3 Open Loop Column Response to Reflux Disturbances....	61
5.4 Open Loop Column Response to Steam Disturbances....	64
7.1 Single Transfer Function Plant Model.....	84
7.2a PI Control of the Single Transfer Function.....	86
7.2b PI Control of the Single Transfer Function with No Time Delay.....	87
7.3a Parameters Identified during PI Control of the Single Transfer Function.....	89
7.3b Parameters Identified during PI Control of the Single Transfer Function with No Time Delay.....	90
7.4 Minimum Variance Control of the Single Transfer Function using Known Coefficient Values.....	91
7.5 Minimum Variance Control of the Single Transfer Function.....	93
7.6 Minimum Variance Control of the Single Transfer Function using 4 G Coefficients.....	95

7.7	Minimum Variance Control of the Single Transfer Function with the Time Delay Overestimated.....	97
7.8	Generalized Minimum Variance Control of the Single Transfer Function using Known Coefficient Values....	99
7.9	Generalized Minimum Variance Control of the Single Transfer Function with $g_0=0.5$ Initially.....	100
7.10	Generalized Minimum Variance Control of the Single Transfer Function with Zero Initial Parameter Values.....	101
7.11	Generalized Minimum Variance Control of the Single Transfer Function using 4 G Coefficients.....	103
7.12	Generalized Minimum Variance Control of the Single Transfer Function with $g_0=0.0$ .....	104
7.13	Generalized Minimum Variance Control of the Single Transfer Function using 4 G Coefficients and $g_0=0$ ..	105
7.14	Generalized Minimum Variance Control of the Single Transfer Function using 4 G Coefficients and the Time Delay Underestimated.....	107
7.15	Generalized Minimum Variance Control of the Single Transfer Function with $g_0=0.0$ and the Time Delay Underestimated.....	108
7.16	Generalized Minimum Variance Control of the Single Transfer Function with the Time Delay Underestimated.....	110
7.17	Generalized Minimum Variance Control of the Single Transfer Function with Q Weighting Adapted from $g_0$ ..	111
7.18	Two Transfer Function Plant Model.....	114
7.19a	PI Control of the Two Transfer Function Model.....	116

7.19b	Parameter Identification during PI Control of the Two Transfer Function Model.....	117
7.20	Minimum Variance Control of the Two Transfer Function Model (NFF).....	119
7.21	Minimum Variance Control of the Two Transfer Function Model (EFF).....	120
7.22	Minimum Variance Control of the Two Transfer Function Model (MFF).....	121
7.23	Generalized Minimum Variance Control of the Two Transfer Function Model using Known Coefficient Values (MFF).....	123
7.24	Generalized Minimum Variance Control of the Two Transfer Function Model using Known Coefficient Values (EFF).....	124
7.25	Generalized Minimum Variance Control of the Two Transfer Function Model using Known Parameter Values (NFF).....	125
7.26	Generalized Minimum Variance Control of the Two Transfer Function Model (NFF).....	127
7.27	Generalized Minimum Variance Control of the Two Transfer Function Model (EFF).....	128
7.28	Generalized Minimum Variance Control of the Two Transfer Function Model (MFF).....	129
7.29	Generalized Minimum Variance Control of the Two Transfer Function Model using 4 G parameters, $g_0=0.0$ and the Time Delay Underestimated (NFF).....	131
7.30	Generalized Minimum Variance Control of the Two Transfer Function Model using 4 G parameters, $g_0=0.0$ and the Time Delay Underestimated (EFF).....	132

7.31	Generalized Minimum Variance Control of the Two Transfer Function Model using 4 G parameters, $g_0=0.0$ and the Time Delay Underestimated (MFF).....	133
7.32	Generalized Minimum Variance Control of the Two Transfer Function Model with $g_0 = 0.0$ and the Time Delay Underestimated (NFF).....	134
7.33	Generalized Minimum Variance Control of the Two Transfer Function Model with $g_0 = 0.0$ and the Time Delay Underestimated (EFF).....	135
7.34	Generalized Minimum Variance Control of the Two Transfer Function Model with $g_0=0.0$ and the Time Delay Underestimated (MFF).....	136
7.35	Generalized Minimum Variance Control of the Two Transfer Function Model with Q Weighting adapting with $g_0$ (NFF).....	137
7.36	Generalized Minimum Variance Control of the Two Transfer Function Model with Q Weighting adapting with $g_0$ (EFF).....	138
7.37	Generalized Minimum Variance Control of the Two Transfer Function Model with Q Weighting adapting with $g_0$ (MFF).....	139
7.38	Linear Distillation Column Model.....	143
7.39	PI/PID Control of the Linear Column Model.....	145
7.40	PI/PI Control of the Linear Column Model.....	146
7.41	Minimum Variance Control of the Linear Column Model (NFF).....	148
7.42	Minimum Variance Control of the Linear Column Model (MFF).....	149
7.43	Generalized Minimum Variance Control of the Linear Column Model with Q Weighting based on PI/PID constants (NFF).....	151

7.44	Parameter Values for Generalized Minimum Variance Control of the Linear Column Model with Q Weighting based on PI/PID constants (NFF).....	152
7.45	Generalized Minimum Variance Control of the Linear Column Model with Q Weighting based on PI/PI constants (NFF).....	153
7.46	Generalized Minimum Variance Control of the Linear Column Model with $g_0=0.0$ and Q Weighting based on PI/PID constants (NFF).....	154
7.47	Generalized Minimum Variance Control of the Linear Column Model with $g_0=0.0$ and Q Weighting based on PI/PID constants (MFF).....	155
7.48	Generalized Minimum Variance Control of the Linear Column Model with $g_0=0.0$ and Q Weighting based on PI/PI constants (NFF).....	156
7.49	Generalized Minimum Variance Control of the Linear Column Model with $g_0=0.0$ , Q Weighting based on PI/PID constants and the Time Delay Underestimated (NFF).....	158
7.50	Generalized Minimum Variance Control of the Linear Column Model with $g_0=0.0$ , Q Weighting based on PI/PI constants and the Time Delay Underestimated (NFF).....	159
7.51	Generalized Minimum Variance Control of the Linear Column Model with $g_0=0.0$ , Q Weighting based on PI/PI constants and the Time Delay Underestimated (MFF).....	160
7.52	Generalized Minimum Variance Control of the Linear Column Model with Q Weighting adapting from $g_0$ and PI/PI constants (MFF).....	161
8.1	Single Rate PI/PID Control of the Column.....	167
8.2	Multirate PI/PID Control of the Column.....	169
8.3	Unsuccessful Column Start-up.....	172



8.4	Parameters for the Unsuccessful Column Start-up....	174
8.5	Successful Column Start-up.....	175
8.6	Parameters for the Successful Column Start-up.....	176
8.7	Minimum Variance Control of the Column.....	178
8.8	Parameters for Minimum Variance Control of the Column.....	180
8.9	Generalized Minimum Variance Control using Q Weighting based on PI/PID constants (SR,NFF).....	183
8.10	Parameters for Generalized Minimum Variance Control using Q Weighting based on PI/PID constants (SR,NFF).....	184
8.11	Generalized Minimum Variance Control using Q Weighting based on PI/PID constants (SR,EFF).....	185
8.12	Parameters for Generalized Minimum Variance Control using Q Weighting based on PI/PID constants (SR,EFF).....	186
8.13	Generalized Minimum Variance Control using Q Weighting based on PI/PID constants (SR,MFF).....	187
8.14	Parameters for Generalized Minimum Variance Control using Q Weighting based on PI/PID constants (SR,MFF).....	188
8.15	Generalized Minimum Variance Control using Q Weighting based on PI/PID constants (MR,NFF).....	190
8.16	Parameters for Generalized Minimum Variance Control using Q Weighting based on PI/PID constants (MR,NFF).....	191
8.17	Generalized Minimum Variance Control using Q Weighting based on PI/PID constants (MR,EFF).....	192

8.18	Parameters for Generalized Minimum Variance Control using Q Weighting based on PI/PID constants (MR,EFF).....	193
8.19	Generalized Minimum Variance Control using Q Weighting based on PI/PID constants (MR,MFF).....	194
8.20	Parameters for Generalized Minimum Variance Control using Q Weighting based on PI/PID constants (MR,MFF).....	195
8.21	Generalized Minimum Variance Control using Q Weighting based on PI/PI constants (SR,NFF).....	198
8.22	Parameters for Generalized Minimum Variance Control using Q Weighting based on PI/PI constants (SR,NFF).....	199
8.23	Generalized Minimum Variance Control using Q Weighting based on PI/PI constants (SR,EFF).....	200
8.24	Parameters for Generalized Minimum Variance Control using Q Weighting based on PI/PI constants (SR,EFF).....	201
8.25	Generalized Minimum Variance Control using Q Weighting based on PI/PI constants (SR,MFF).....	202
8.26	Parameters for Generalized Minimum Variance Control using Q Weighting based on PI/PI constants (SR,MFF).....	203
8.27	Generalized Minimum Variance Control using Q Weighting based on PI/PI constants (MR,NFF).....	204
8.28	Parameters for Generalized Minimum Variance Control using Q Weighting based on PI/PI constants (MR,NFF).....	205
8.29	Generalized Minimum Variance Control using Q Weighting based on PI/PI constants (MR,EFF).....	206

8.30	Parameters for Generalized Minimum Variance Control using Q Weighting based on PI/PI constants (MR, EFF) .....	207
8.31	Generalized Minimum Variance Control using Q Weighting based on PI/PI constants (MR, MFF) .....	208
8.32	Parameters for Generalized Minimum Variance Control using Q Weighting based on PI/PI constants (MR, MFF) .....	209
8.33	Generalized Minimum Variance Control using Q Weighting based on Modified PI/PI constants (SR, NFF) .....	212
8.34	Parameters for Generalized Minimum Variance Control using Q Weighting based on Modified PI/PI constants (SR, NFF) .....	213
8.35	Generalized Minimum Variance Control using Q Weighting based on Modified PI/PI constants (SR, EFF) .....	214
8.36	Parameters for Generalized Minimum Variance Control using Q Weighting based on Modified PI/PI constants (SR, EFF) .....	215
8.37	Generalized Minimum Variance Control using Q Weighting based on Modified PI/PI constants (SR, MFF) .....	216
8.38	Parameters for Generalized Minimum Variance Control using Q Weighting based on Modified PI/PI constants (SR, MFF) .....	217
8.39	Generalized Minimum Variance Control using Q Weighting based on Modified PI/PI constants (MR, NFF) .....	220
8.40	Parameters for Generalized Minimum Variance Control using Q Weighting based on Modified PI/PI constants (MR, NFF) .....	221

8.41	Generalized Minimum Variance Control using Q Weighting based on Modified PI/PI constants (MR,EFF).....	222
8.42	Parameters for Generalized Minimum Variance Control using Q Weighting based on Modified PI/PI constants (MR,EFF).....	223
8.43	Generalized Minimum Variance Control using Q Weighting based on Modified PI/PI constants (MR,MFF).....	224
8.44	Parameters for Generalized Minimum Variance Control using Q Weighting based on Modified PI/PI constants (MR,MFF).....	225
8.45	Generalized Minimum Variance Control using Q Weighting based on Tuned PI/PI constants (MR,NFF).....	227
8.46	Parameters for Generalized Minimum Variance Control using Q Weighting based on Tuned PI/PI constants (MR,NFF).....	228
8.47	Generalized Minimum Variance Control using Q Weighting based on Tuned PI/PI constants (MR,EFF).....	229
8.48	Parameters for Generalized Minimum Variance Control using Q Weighting based on Tuned PI/PI constants (MR,EFF).....	230
8.49	Generalized Minimum Variance Control using Q Weighting based on Tuned PI/PI constants (MR,MFF).....	231
8.50	Parameters for Generalized Minimum Variance Control using Q Weighting based on Tuned PI/PI constants (MR,MFF).....	232
8.51	Generalized Minimum Variance Control with $g_0=0.0$ (SR,NFF).....	235
8.52	Parameters for Generalized Minimum Variance Control with $g_0=0.0$ (SR,NFF).....	236

8.53	Generalized Minimum Variance Control with $g_0=0.0$ (SR,EFF).....	237
8.54	Parameters for Generalized Minimum Variance Control with $g_0=0.0$ (SR,EFF).....	238
8.55	Generalized Minimum Variance Control with $g_0=0.0$ (SR,MFF).....	239
8.56	Parameters for Generalized Minimum Variance Control with $g_0=0.0$ (SR,MFF).....	240
8.57	Generalized Minimum Variance Control with $g_0=0.0$ (MR,NFF).....	241
8.58	Parameters for Generalized Minimum Variance Control with $g_0=0.0$ (MR,NFF).....	242
8.59	Generalized Minimum Variance Control with $g_0=0.0$ (MR,EFF).....	243
8.60	Parameters for Generalized Minimum Variance Control with $g_0=0.0$ (MR,EFF).....	244
8.61	Generalized Minimum Variance Control with $g_0=0.0$ (MR,MFF).....	245
8.62	Parameters for Generalized Minimum Variance Control with $g_0=0.0$ (MR,MFF).....	246
8.63	Generalized Minimum Variance Control with $g_0=0.0$ and the Time Delay Underestimated (SR,NFF).....	249
8.64	Parameters for Generalized Minimum Variance Control with $g_0=0.0$ and the Time Delay Underestimated (SR,NFF).....	250
8.65	Generalized Minimum Variance Control with $g_0=0.0$ and the Time Delay Underestimated (SR,EFF).....	251

8.66	Parameters for Generalized Minimum Variance Control with $g_0=0.0$ and the Time Delay Underestimated (SR, EFF).....	252
8.67	Generalized Minimum Variance Control with $g_0=0.0$ and the Time Delay Underestimated (SR, MFF).....	253
8.68	Parameters for Generalized Minimum Variance Control with $g_0=0.0$ and the Time Delay Underestimated (SR, MFF).....	254
8.69	Generalized Minimum Variance Control with $g_0=0.0$ and the Time Delay Underestimated (MR, NFF).....	255
8.70	Parameters for Generalized Minimum Variance Control with $g_0=0.0$ and the Time Delay Underestimated (MR, NFF).....	256
8.71	Generalized Minimum Variance Control with $g_0=0.0$ and the Time Delay Underestimated (MR, EFF).....	257
8.72	Parameters for Generalized Minimum Variance Control with $g_0=0.0$ and the Time Delay Underestimated (MR, EFF).....	258
8.73	Generalized Minimum Variance Control with $g_0=0.0$ and the Time Delay Underestimated (MR, MFF).....	259
8.74	Parameters for Generalized Minimum Variance Control with $g_0=0.0$ and the Time Delay Underestimated (MR, MFF).....	260

## Nomenclature

### Abbreviations:

A/D	Analog / Digital
ASS	Above steady state
BSS	Below steady state
DACS	Data acquisition, control and simulation
DTF	Dual transfer function
DSS	Down to steady state
EFF	Estimated feedforward action
GC	Gas chromatograph
GMV	Generalized minimum variance
HP	Hewlett-Packard
LQG	Linear quadratic gaussian
LSI	Large scale integration
MFF	Measured feedforward action
MIMO	Multi-input multi-output
Min Var	Minimum variance
MISO	Multi-input single-output
MR	Model reference
MVMR	Multivariable multirate
NFF	No feedforward action
PI	Proportional integral
PID	Proportional integral derivative
RDG	Relative disturbance gain
RGA	Relative gain array
RLS	Recursive least squares

SAE Sum of absolute error  
 STF Single transfer function  
 UD Upper diagonal factorization  
 USS Up to steady state

Polynomials in  $z^{-1}$ :

A System output polynomial  
 B System input polynomial  
 C System polynomial associated with uncorrelated noise  
 D System disturbance polynomial  
 E Polynomial introduced with the separation of the noise into past and future terms  
 F Controller polynomial associated with the output  
 G Controller polynomial associated with the control input  
 H Controller polynomial associated with the stochastic noise term  
 L Controller polynomial associated with the feed-forward disturbance terms  
 P Polynomial weighting of the system output  
 $P_d$  Denominator of the output weighting polynomial  
 $P_n$  Numerator of the output weighting polynomial  
 Q Control weighting polynomial  
 R Set point weighting polynomial



## Polynomial Matrices in $z^{-1}$ :

- A System output polynomial matrix
- B System input polynomial matrix
- C System polynomial matrix associated with the uncorrelated random noise terms
- D System polynomial matrix associated with the disturbance terms
- E Polynomial matrix introduced with the separation of the noise terms into past and future elements
- F Controller polynomial matrix associated with the system outputs
- G Controller polynomial matrix associated with the control efforts
- H Controller polynomial matrix associated with the stochastic terms
- L Controller polynomial matrix associated with the feedforward disturbance terms
- P System output weighting polynomial matrix
- $P_d$  Denominator of the output weighting polynomial matrix
- $P_n$  Numerator of the output weighting polynomial matrix
- Q Control weighting polynomial matrix
- R Set point weighting polynomial matrix

### Variables:

$u, U$	Input
$y, Y$	Output
$v, V$	Disturbance
$\xi, \Xi$	Random, zero-mean noise
$k$	System delay
$d$	Disturbance delay
$J, J$	Cost function
$\sigma^2$	Variance of the noise
$X, X$	Observation vector (matrix)
$\theta, \theta$	Parameter estimate vector (matrix)
$\rho_1$	Variance of the noise in the Kalman filter approach
$\rho_2$	Forgetting factor, $\rho_1 = \rho_2$ for recursive least squares estimation (exponential forgetting factor)
$\beta$	Relative disturbance gain
$\lambda$	Relative gain
$s$	Laplace transform variable
$P_c$	Covariance matrix
$K$	Kalman gain
$K_p$	Process gain
$\tau_1$	First order time constant
$\theta_d$	Time delay
$PB$	Proportional band
$TI$	Integral time
$TD$	Derivative time
$K_c$	Proportional constant
$t_s$	Sample time

Superscripts:

Indicates an intermediate value

Indicates an estimated value

## 1. Introduction

Even a simple binary distillation column involves nonlinear, high order coupled dynamics with time delays. In industry, where almost every process employs some form of distillation, control of distillation columns, particularly the simultaneous control of product compositions, continues to present a challenge to the process industries. With distillation being a very energy intensive operation, improved distillation, column control can translate to significant economic benefits. The objective of this research is to increase the ease with which a self-tuning controller may be successfully implemented on an existing process. The particular multivariable, multirate self-tuning controller used in this study has been developed by Morris et al., [1982]. Several techniques are examined for establishing coefficients of the  $Q$  weighting polynomial of the self-tuning controller based on proportional-integral-derivative (PID) controller constants, assumed to be available from an existing, operative controller. The control performance obtained using both single and multirate forms of the control law is compared to conventional multiloop PID control of a pilot plant distillation column. In addition, the use of a measured or estimated value of the disturbance as a feedforward signal is also examined. This thesis is organized as follows.

Chapter 2 presents some background and current developments in the field of adaptive control through a

survey of some of the recent literature pertaining to the subject. In Chapter 3 the theoretical development of the multi-input, single-output (MISO) and multivariable, multi-rate (MVMR) self-tuning controllers are presented. Also included is some discussion relating to the recursive identification routine employed in this work. A description of the experimental equipment used in this study is given in Chapter 4. Chapter 5 presents the results of a series of open loop tests performed on the column to establish transfer functions to describe the dynamic behavior of the column. The approach used to obtain PI and PID controller constants is explained in Chapter 6, as are the different methods for selecting the  $Q$  weighting coefficients for self-tuning control.

The results of three linear simulations are presented in Chapter 7 in an attempt to illustrate some of the theoretical principles discussed in the earlier chapters. The experimental results for evaluating the different control algorithms are presented in Chapter 8. Chapter 9 contains the conclusions that may be drawn from this work, and the recommendations for future study are presented in Chapter 10.

## 2. Literature Survey

### 2.1 Introduction

To undertake a rigorous literature review encompassing all aspects of adaptive control would clearly be beyond the scope of this study. Instead, an attempt has been made to outline what adaptive control is, why it is necessary and what some of the latest developments in adaptive control are, including some examples of applications. To narrow the scope of the review further, an emphasis will be placed on stochastic adaptive control systems, although other forms of self-tuning controllers will be mentioned briefly. In keeping with this work, particular attention will be paid to applications of adaptive control on distillation columns.

### 2.2 Why Adaptive Control?

For a large proportion of industrial control applications, there is little advantage to be gained by using any control schemes more sophisticated than conventional proportional-integral-derivative (PID) control. However, on some processes that are difficult to model due to unknown or nonlinear dynamics, it may be necessary to retune the controllers if the operating conditions vary. Even for processes that are well understood, the dynamics may change with either changing production or wear or fouling of equipment. Occasionally, interactions may exist between control loops that add to the tuning difficulties,

or there may be a large number of loops such that even occasional retuning may represent a considerable amount of time and effort.

Controllers that are capable of retuning themselves have been available for several years and have been known by many names: adaptive, self-organizing, self-optimizing and learning controllers. The particular controllers of interest in this study fall into the category of stochastic adaptive controllers.

### 2.3 Stochastic Adaptive Control

A stochastic system is a system subjected to random or non-deterministic input disturbances so that the output of the system cannot be predicted exactly. Adaptive control techniques are frequently used to attempt to control stochastic processes. Two very important entities of any adaptive control scheme are the control law and the parameter estimation technique. It is assumed that the unknown process may be represented by a linear model and the coefficients of the model estimated. The underlying theory is based on the certainty equivalence principle which considers that the estimated coefficients may not be an accurate representation of the true coefficients, but that the estimated coefficients may be used in the control law to determine an input signal. In a stochastic adaptive controller the derivation of the control law takes into account the variation of the parameters by using a

stochastic model to describe the process. Figure 2.1 represents a block diagram of a stochastic adaptive controller.

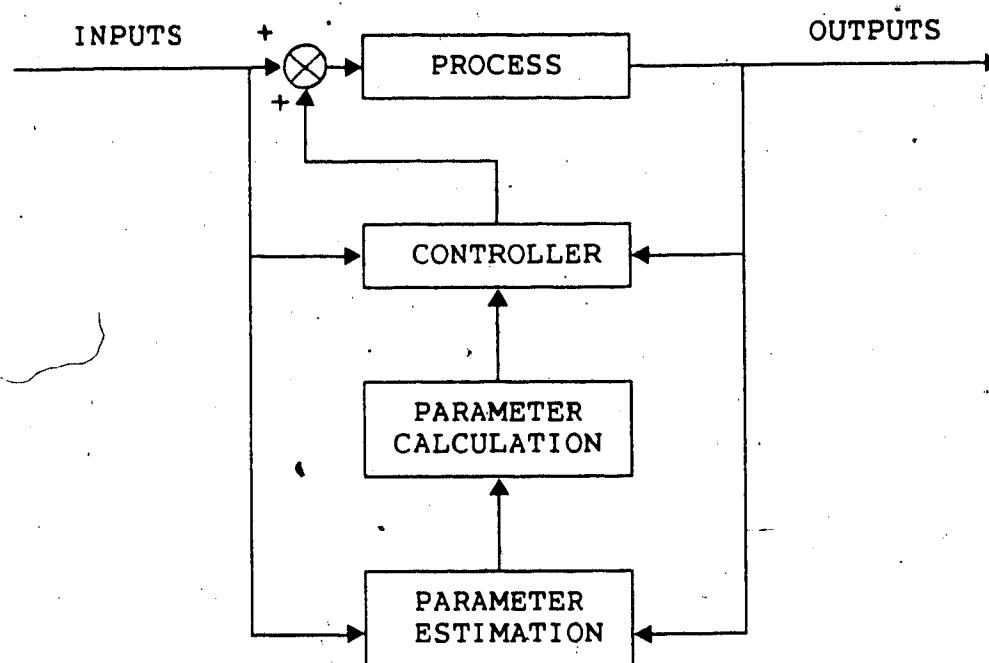


Figure 2.1 - A Stochastic Adaptive Control System

In Figure 2.1 an indirect, or explicit, scheme has been portrayed where the process model parameters are estimated and then the estimates are used to calculate the parameters found in the control law. The controller then determines the control action to be taken based on the process inputs and outputs, using the calculated controller parameters. Another possible scheme is to estimate the parameters used in the control law directly, bypassing the process model. This is the direct, or implicit, formulation and it has the



advantage of requiring fewer computations. The majority of the discussion in the remainder of this chapter focusses on the direct formulation.

The interest in stochastic adaptive controllers beginning in the early 1970's was fueled by the increase in availability of relatively inexpensive digital computing power. The basis for stochastic control theory was presented in the book of Åström [1970]. Some of the problems that had to be overcome to derive a controller based on a stochastic model were outlined by Åström and Wittenmark [1971]. Peterka, [1972], proposed an optimal regulator for a stationary stochastic plant with a single input and a single output. The objective was to minimize the variance of the plant output using a predicted stationary model, the coefficients of which were identified using an exponentially weighted, recursive least squares algorithm. However, it was the paper of Åström and Wittenmark, [1973], that initiated interest in the area of self-tuning regulators.

Åström et al., [1975], presented some of the first industrial applications, on a paper machine and an ore crusher, of the adaptive regulator based on recursive parameter estimation. At the same time Clarke and Gawthrop, [1975], extended the self-tuning regulator proposed by Åström and Wittenmark [1973] by adding a set point term and weighting on the control action in the control law. Clarke and Gawthrop, [1979], further refined their scheme by adding general weighting to the process input and output in

addition to the control action and thereby developed the controller known today as the "generalized minimum variance" controller.

These formulations were only concerned with single variable systems, so a natural extension of the single-input, single-output controller was to extend the theory to multi-input, multi-output situations as was done by Morris et al., [1977], and Koivo, [1980].

Many self-tuning controllers, or variations of self-tuning controllers, have been proposed. It is difficult to distinguish between many of the proposals since either the initial starting point for the controller derivation, or the end result, or both, appear quite similar to those of the generalized minimum variance controller. Several studies have outlined extensions or perturbations to the theory presented by Åström and Wittenmark, [1973], or Clarke and Gawthrop, [1975, 1979]. Among these are Bayoumi et al., [1981], in which a self-tuning regulator was applied to multivariable systems and Allidina and Hughes, [1982], where integral action was incorporated into the self-tuning controller. Latawiec and Chyra, [1983], studied the long term performance of the self-tuning controller subjected to low frequency disturbances using a time varying control weighting to avoid any closed loop identifiability problems. Clarke et al., [1983], extended the self-tuning controller to include a k-incremental prediction. Belanger, [1983], considered the stability of the self-tuning regulator.

As has been mentioned, there is no clear distinction between many of the control schemes and the generalized minimum-variance controller. An attempt has been made to group the following control schemes where a common link exists. For instance, one variation of self-tuning development not entirely separate from the stochastic adaptive controllers already discussed is the linear quadratic Gaussian (LQG) controller. This design technique employs a linear model, a quadratic cost function and assumes a Gaussian disturbance. The similarities between the previous self-tuning controller and the LQG design are outlined by Grimble, [1984], where the two techniques are shown to result in the same minimum variance criterion. The LQG approach to self-tuning control has also been considered by Åström, [1983b] and Clarke, [1983a,b]. An optimum, predictor based LQG controller design has been presented by Peterka, [1984], and Toivonen, [1983], has proposed the use of on-line adjustment to the weighting in the cost function.

Pole-placement controllers also appear to be very similar in some respects to the self-tuning controllers. Some of the more recent developments in the field of pole-placement controllers include: a multivariable adaptive controller based on pole-placement (Dion and Lozano, [1983]) and a self-tuning controller where the closed-loop poles and sampling period are determined on-line (McDermott and Mellichamp, [1984]). Additional studies on pole-placement controllers include those of Elliot and Wolovich, [1984],

which reviewed existing algorithms and proposed a new indirect pole-placement self-tuning controller. Ferreiro et al., [1985] and Jun et al., [1985], based multivariable self-tuning controllers on pole-assignment. Allidina and Yin, [1985], discussed an explicit pole-assignment self-tuning algorithm.

Another option for the design of a self-tuning controller which has undergone extensive investigation is that of model reference (MR) control. Although a parameter estimation scheme is required, MR control updates the control law parameters based on the agreement between the behavior of the controlled system and that predicted by a reference model. Some of the work in the area of self-tuning MR controllers is that of: Bar-Kana and Kaufman, [1983], who described a multivariable MR adaptive controller; Hahn, [1985], who developed a direct adaptive multivariable controller based on MR control; and Bittanti and Scattolini, [1985], who developed a self-tuning controller based on a model-following approach and demonstrated the performance by simulation employing a simple distillation column model.

Two examples of the state space approach to self-tuning control are provided by Warwick, [1981], and Bezanson and Harris, [1984].

There is a vast amount of self-tuning control literature that does not seem to clearly fall into any of the previously mentioned subdivisions of stochastic adaptive control, yet is probably still worthy of mention. These

include: Costin and Buchner, [1983a], who discussed minimum variance control of multivariable systems with different delays in the individual loops, and, in [1983b], discussed distributed control using self-tuning regulators; and Goodwin and Dugard, [1983], who developed a stochastic adaptive controller for linear multivariable systems which could be implemented with or without knowledge of the system interactor matrix. Grimbale, [1983], offered another form of the generalized minimum variance controller, with his weighted minimum variance controller. A multivariable controller which used an on-line solution of the Riccati equation was developed by Hallager and Jorgensen, [1983]. Silveria and Duraiswami, [1983], looked at a structure for an adaptive servomechanism controller which ensures asymptotic tracking with disturbance rejection. Mizuno and Fujii, [1983], designed a multivariable controller from a decomposed representation of an unknown plant. Yang and Lee, [1983], looked at the effects of model structure and the value of the measured disturbance on adaptive control. Huang et al., [1984], proposed a predictive, adaptive controller; and Martin-Sanchez et al., [1984], described a stable, adaptive predictive control system. Moir and Grimbale, [1984], discussed optimal self-tuning smoothing or filtering for linear multivariable processes. Kanniah and Malik, [1984], described a dual-rate self-tuning regulator that uses a smaller sampling interval than the control interval to update the controller parameters between periods of

constant control action. Habermayer and Keviczky, [1985], formulated an adaptive Smith predictor controller. Tsitsiklis and Athans, [1984], looked at robustness properties of nonlinear, stochastic multivariable optimal regulators.

Despite the extensive research into the broad area of adaptive control and the specific studies of self-tuning controllers, use of such control algorithms has not been readily accepted for industrial applications. One of the reasons is the widespread acceptance of the relatively simple PID controller. In an effort to incorporate the self-tuning capabilities into a controller which is accepted and proven in industry, many researchers have formulated a form of a self-tuning controller that has a PID structure. An early application was that of Yuwana and Seborg, [1982], who tuned the PID parameters on-line utilizing model parameters calculated from the set point response data generated from a single step change in the set point. Other approaches include: Bristol, [1983], who used a pattern-recognition design for adapting the PID controller; and Hetthessy et al., [1983], with an adaptive PID regulator which is based on the explicit identification of a second order model with time delay. Self-tuning feedback controllers that were structurally equivalent to a PID controller have been employed by Cameron and Seborg, [1983], and Song et al., [1984]. Kaya and Scheib, [1984], combined PID and Smith predictor algorithms with the ability to

automatically update process parameters; and Kraus, [1984], used heuristic reasoning in on-line tuning of a PID controller. Ortega and Kelly, [1984], reviewed some specific self-tuning PID algorithms.

Among the articles that have compared different adaptive algorithms are the following: Goodwin and Teoh, [1983], who examined several algorithms for the adaptive control of time varying systems with the emphasis on the concept of persistency of excitation; Kan et al., [1985a,b], used a simulation of a distillation column to compare the generalized minimum variance control strategy with pole/zero placement, state feedback, PID self-tuning, model reference and adaptive predictive controllers. Tham et al., [1985], compared a positional multivariable self-tuning controller to an incremental version of the controller under multirate control as well as single rate control; and Aloisi et al., [1985], studied single-input, single-output versions of minimum variance, model following and detuned minimum variance algorithms, focusing on their ability to control the top loop of a simulated distillation column.

## 2.4 Control of Distillation Columns

Recent applications of self-tuning or multivariable self-tuning control to distillation columns, aside from those already mentioned, include: Sastry et al., [1977], who studied the control of the top composition of a pilot scale column using a self-tuning regulator. Morris et al., [1981],

used the same column employed in this study to conduct single and multivariable studies of self-tuning control and extended the self-tuning controller to include multirate sampling [1982]. Martin-Sanchez and Shah, [1984], also studied the same distillation column, only they used an adaptive, predictive control system. Wiemer et al., [1983], who applied a multivariable model reference adaptive controller utilizing a filtered input signal to a pilot distillation column; and Tham et al., [1985], compared two multivariable self-tuning controllers for controlling the terminal compositions of a distillation column. Simulation studies employing nonlinear distillation column models have been performed by: Barcenas-Urbe and Alvarez-Gallegos, [1983], using a multivariable adaptive controller; and Goldschmidt et al., [1985], who used an explicit multivariable adaptive controller. Sanchez et al., [1985], used a multivariable adaptive controller which was based on LQ criterion and which followed a decoupled reference model; and Foss, [1985], applied multivariable control using a time-invariant, linear quadratic controller.

Alternatives to self-tuning, multivariable control of distillation columns have continued to appear in the literature. Some of the alternative control strategies can be found in: Wood, [1977], where feedforward techniques and computer aided designs that use multivariable frequency domain design, decoupling and characteristic loci techniques were discussed; Shah and Luyben, [1979], proposed nonlinear



composition estimators to eliminate the difficulties associated with direct on-line composition measurement. Dahlqvist, [1979], examined theoretically designed top and bottom composition controllers.

## 2.5 Identification

All the stochastic adaptive controllers discussed require a parameter estimation or identification routine. The identification literature is very extensive and will not be reviewed here. Some typical articles pertaining to identification for use with adaptive control schemes are: Sinha and Sen, [1975], who evaluated several on-line identification methods; and Dickmann and Unbehauen, [1979], where recursive identification of multi-input, multi-output systems was discussed. Both Fortescue et al., [1981], and Cordero et al., [1981], studied the use of a variable forgetting factor. Wong et al., [1983], compared several variations of the recursive least squares identification routine; and Hägglund, [1983], presented a new proposal for forgetting old data in recursive estimation schemes.

## 2.6 Implementation of Stochastic Adaptive Controllers

Some general implementation problems have been discussed by Clarke, [1980], Clarke and Gawthrop, [1980], and Wittenmark and Åström, [1984]. Apart from the applications mentioned previously in this chapter, many self-tuning regulators and controllers have been applied

successfully to pilot scale, and some industrial, equipment. Åström et al., [1977], were able to implement a self-tuning regulator on an industrial paper machine and an ore crusher, and Kurz et al., [1980], worked on an air heater. Fortescue et al., [1981], controlled a large scale CO<sub>2</sub> absorption-desorption pilot plant while Kegshenbaum and Fortescue, [1981], applied a self-tuning controller to a fractional crystallization bed. Latawiec and Chyra, [1983], developed a controller for a rotary cement kiln and Hallager and Jorgensen, [1983], performed their studies on a tubular fixed bed chemical reactor. Ferreira et al., [1984], examined level control of a middle tank cascaded with other tanks and Onderwater et al., [1985], controlled the temperature control of a catalytic tubular reactor.

## 2.7 Summary

A wide variety of stochastic adaptive control systems have been proposed and studied as indicated by the scope of the literature that has been reviewed. Details of the underlying theory and the applications of self-tuning controllers, can be obtained from review articles such as the following: Wittenmark, [1975], which reviewed early developments in stochastic adaptive control; and Åström et al., [1977], which discussed self-tuning regulators and their applications. Bartolini et al., [1981], examined adaptive controllers and problems with their implementation. Åström, [1983], and Seborg et al., [1983], reviewed leading

design techniques, experimental applications and their related problems. The work of Ray, [1983], represents an extensive survey of computer-aided control systems design, and that of Unbehauen, [1985], covers different structures of adaptive control systems.

### 3. Theoretical Development of the Self-tuning Controller

#### 3.1 Introduction

The self-tuning controller utilized in this study was originally developed by Clarke and Gawthrop [1975,1979]. Morris and Nazer [1977] extended the generalized minimum variance controller to include feedforward disturbance compensation, a discrete compensator to eliminate and stabilize the system closed loop response, and the ability to perform set point model following.

The theoretical development of the controller will be presented here in several stages. First, the derivation of the general multi-input, single-output (MISO) self-tuning controller will be presented in considerable detail followed by the specific case of the generalized MISO controller, the minimum variance controller. Next, the MISO controller is expanded to the multi-input, multi-output (MIMO) case, which, combined with the multirate theory, becomes the multivariable, multirate (MVMR) controller. This is followed by a discussion of the parameter estimation method used in conjunction with the self-tuning control law. The chapter concludes with an outline of the basic theory of the relative disturbance gain (RDG) analysis technique.

### 3.2 Multi-input, Single-output Self-tuning Controller

#### 3.2.1 Generalized Control Law Derivation

It is assumed that the process to be controlled may be represented by the following general discrete model:

$$\begin{aligned} y(t) + a_1 y(t-1) + \dots = z^{-k} [b_0 u(t) + b_1 u(t-1) + \dots] \\ + \xi(t) + c_1 \xi(t-1) + \dots \\ + z^{-d} [d_0 v(t) + d_1 v(t-1) + \dots] \end{aligned} \quad (3.1)$$

A more compact representation of the model is given by:

$$\begin{aligned} A(z^{-1})y(t) = z^{-k}B(z^{-1})u(t) + C(z^{-1})\xi(t) \\ + z^{-d}D(z^{-1})v(t) \end{aligned} \quad (3.2)$$

where  $A$ ,  $B$ ,  $C$  and  $D$  are polynomials in the backshift operator,  $z^{-1}$ , with  $a_0=1$ ,  $b_0 \neq 0$  and  $c_0=1$ . The vectors  $u(t)$  and  $y(t)$  are the process inputs and outputs at time  $t$ , respectively. The  $\xi(t)$  term is an uncorrelated, zero mean, random noise term and  $v(t)$  allows for input of measurable disturbances. The system delay, expressed as an integer multiple of the sampling period, is  $k$ , while  $d$  is the delay associated with the measured disturbance. It is assumed that the roots of  $C$  lie strictly inside the  $z$ -domain unit circle.

The objective of the controller design is to minimize the general cost function:

$$J = E\{[P(z^{-1})y(t+k) - R(z^{-1})w(t)]^2 + [Q'(z^{-1})u(t)]^2\} \quad (3.3)$$

where  $E\{*\}$  is the expectation operator.  $P(z^{-1})$ ,  $R(z^{-1})$  and  $Q'(z^{-1})$  are transfer functions in  $z^{-1}$  which allow general discrete weightings to be placed on the system output,  $y(t)$ , set point,  $w(t)$ , and control effort,  $u(t)$ , respectively. These transfer functions are expressed as polynomial ratios of the form:

$$P(z^{-1}) = \frac{P_n(z^{-1})}{P_d(z^{-1})}; \quad R(z^{-1}) = \frac{R_n(z^{-1})}{R_d(z^{-1})}; \quad Q'(z^{-1}) = \frac{Q'_n(z^{-1})}{Q'_d(z^{-1})}$$

The  $R(z^{-1})$  weighting provides set point tracking, and  $Q'(z^{-1})$  weighting is used to penalize excessive control effort.

In order to minimize the cost function in equation 3.3, knowledge of future terms of the weighted output,  $P(z^{-1})y(t+k)$ , are required. However, since at time  $t$  information is only known up to and including time  $t$ ,  $y(t+k)$  is unknown. It is therefore necessary to generate an estimate of the weighted output  $k$  steps ahead in the future. The system output,  $k$  steps ahead in time, is given from equation 3.2 as (omitting the  $z^{-1}$  arguments for simplicity):

$$y^*(t+k) = \frac{B}{A}u(t) + z^k \frac{C}{A}\xi(t) + z^{k-d} \frac{D}{A}v(t) \quad (3.4)$$

As long as the time delay associated with the disturbance is greater than or equal to that of the system, that is,  $d \geq k$ , then the output given in equation 3.4 will be realizable. If  $d < k$  it then becomes necessary to predict disturbance terms.

It is possible to express the noise terms of equation 3.4 as the sum of unknown future noise terms and known noise terms up to and including time  $t$ :

$$\begin{aligned} z^k \frac{C}{A} \zeta(t) &= [e_0 \zeta(t+k) + e_1 \zeta(t+k-1) + \dots + e_{k-1} \zeta(t+1)] \\ &+ \frac{1}{A} [f_0 \zeta(t) + f_1 \zeta(t-1) + \dots + f_j \zeta(t-j)] \quad (3.5) \\ j &= 0, 1, 2, \dots \end{aligned}$$

Or, if we let  $E' = e_0 + e_1 z^{-1} + e_2 z^{-2} + \dots + e_{k-1} z^{-(k-1)}$  and  $F' = f_0 + f_1 z^{-1} + \dots + f_j z^{-j}$ , then:

$$z^k \frac{C}{A} \zeta(t) = E' \zeta(t+k) + \frac{F'}{A} \zeta(t) \quad (3.6)$$

Substituting equation 3.6 into equation 3.4 yields:

$$y^*(t+k) = \frac{B}{A} u(t) + E' \zeta(t+k) + \frac{F'}{A} \zeta(t) + z^{k-d} \frac{D}{A} v(t) \quad (3.7)$$

Rearranging equation 3.2 it is possible to obtain an estimate of the noise at time  $t$  based on past and current measurable values as:

$$\zeta(t) = \frac{A}{C}y(t) - z^{-k}\frac{B}{C}u(t) - z^{-d}\frac{D}{C}v(t) \quad (3.8)$$

By replacing  $\zeta(t)$  in equation 3.7 with equation 3.8, the output  $k$  steps ahead in the future may be expressed as:

$$\begin{aligned} y^*(t+k) = & \frac{F'}{C}y(t) + E'\zeta(t+k) + \left[ \frac{C}{A} - z^{-k}\frac{F'}{A} \right] \frac{B}{C}u(t) \\ & + \left[ \frac{C}{A} - z^{-k}\frac{F'}{A} \right] z^{k-d}\frac{D}{C}v(t) \end{aligned} \quad (3.9)$$

With minor rearrangements, the identity used in equation 3.6 may be expressed as:

$$E' = \frac{C}{A} - z^{-k}\frac{F'}{A} \quad (3.10)$$

which can then be used to simplify equation 3.9 to:

$$y^*(t+k) = \frac{F'}{C}y(t) + E'\zeta(t+k) + \frac{E'B}{C}u(t) + z^{k-d}\frac{E'D}{C}v(t) \quad (3.11)$$

It is not possible to say exactly what the future noise terms will be except that, on average, they will be zero. Hence the best possible estimate of future noise terms is zero. The resulting prediction of the system output  $y$ ,  $k$  steps into the future, based on information up to and



including time  $t$ , is then:

$$y^*(t+k|t) = \frac{F'}{C}y(t) + \frac{E'B}{C}u(t) + z^{k-d}\frac{E'D}{C}v(t) \quad (3.12)$$

Multiplying equation 3.12 through by  $P$ , one obtains the weighted estimate of the system output which is what is required in the cost function (equation 3.3). Making the following substitutions:

$$E = P * E'; \quad F = P_n * F'$$

then the weighted  $k$ -step ahead prediction of the system output (based on known parameters and measured inputs, outputs and disturbances) is given by:

$$Py^*(t+k|t) = \frac{F}{CP_d}y(t) + \frac{EB}{C}u(t) + z^{k-d}\frac{ED}{C}v(t) \quad (3.13)$$

with the actual value being given by:

$$Py(t+k) = Py^*(t+k|t) + \epsilon(t+k) \quad (3.14)$$

The weighted output prediction error,  $\epsilon(t+k)$ , is assumed to be uncorrelated with past values of  $y(t)$ ,  $u(t)$  and  $v(t)$ . Similar to the noise, the error is assumed to have a mean value of zero, ie.  $E\{\epsilon(t+k)\} = 0$ . The variance of this error term is given by:

$$\begin{aligned}\sigma_{t+k}^2 &= E\{[e(t+k) - E\{e(t+k)\}]^2\} \\ &= E\{[e(t+k)]^2\}\end{aligned}\quad (3.15)$$

Now, substituting equation 3.14 into equation 3.3 yields:

$$\begin{aligned}J &= E\{[Py^*(t+k|t) + e(t+k) - Rw(t)]^2 + [Q'u(t)]^2\} \\ &= E\{[Py^*(t+k|t) - Rw(t)]^2 + [Q'u(t)]^2\} + \sigma_{t+k}^2\end{aligned}\quad (3.16)$$

In order to minimize the above function, the current control action,  $u(t)$ , is chosen so that the partial derivative of the cost function with respect to  $u(t)$  is zero (ie.  $\partial J / \partial u(t) = 0$ ). By removing the expectation operator, the minimization at each sampling instant becomes:

$$\begin{aligned}\frac{\partial J}{\partial u(t)} &= 2[Py^*(t+k|t) - Rw(t)] * \frac{\partial [Py^*(t+k|t)]}{\partial u(t)} \\ &\quad + 2Q'u(t) * \frac{\partial [Q'u(t)]}{\partial u(t)} = 0\end{aligned}\quad (3.17)$$

From equation 3.13 it is possible to see that  $Py^*(t+k|t)$  is a function of  $u(t)$ . Since only the first terms of the E, B and C polynomials are used in the differentiation,

$$\frac{\partial [Py^*(t+k|t)]}{\partial u(t)} = \frac{\partial}{\partial u(t)} \left[ \frac{EBu(t)}{C} \right] = \frac{e_0 b_0}{c_0}\quad (3.18)$$

Equation 3.17 then becomes:

$$\frac{e_0 b_0}{c_0} [Py^*(t+k|t) - Rw(t)] + Q'u(t)q_0' = 0 \quad (3.19)$$

By defining a new control weighting polynomial:

$$Q = \frac{Q'q_0'c_0}{e_0 b_0} \quad (3.20)$$

then it is possible to solve equation 3.19 for  $u(t)$  to get:

$$u(t) = \frac{1}{Q} [Rw(t) - Py^*(t+k|t)] \quad (3.21)$$

It is now desirable to obtain a more useful form of the control law by replacing  $Py^*(t+k|t)$  in equation 3.21. Using equation 3.13, let  $G = EB$ ,  $L = ED$  and  $C = 1 - z^{-1}H$  to get:

$$\begin{aligned} Py^*(t+k|t)[1 - z^{-1}H] &= Py^*(t+k|t) - HPy^*(t+k-1|t-1) \\ &= \frac{F}{P_d} y(t) + Gu(t) + z^{k-d}Lv(t) \end{aligned} \quad (3.22)$$

and now replace  $Py^*(t+k|t)$  in equation 3.21 to get:

$$\begin{aligned} u(t) = \frac{1}{Q} [Rw(t) - \frac{F}{P_d} y(t) - Gu(t) - z^{k-d}Lv(t) \\ - HPy^*(t+k-1|t-1)] \end{aligned} \quad (3.23)$$

Unfortunately,  $u(t)$  on the right hand side of equation 3.23 is unknown at the time of implementing  $u(t)$ . It is therefore necessary to factor out  $g_0$  from the  $G$  polynomial so that the control action at time  $t$  is:

$$u(t) = \frac{1}{[Q + g_0]} [Rw(t) - \frac{F}{P_d} y(t) - (G - g_0)u(t) - z^{k-d}Lv(t) - HPy^*(t+k-1|t-1)] \quad (3.24)$$

In the control law, equation 3.24, although  $R$ ,  $P$  and  $Q$  are to be selected by the control engineer, the numbers of coefficients in the  $F$ ,  $G$ ,  $H$  and  $L$  polynomials are fixed for a known system. However, although the structures of the polynomials are fixed, the coefficients themselves are usually unknown. Assuming a good estimation scheme is available, the best alternative in implementing the control law is to estimate the coefficients and use the estimates  $\hat{F}$ ,  $\hat{G}$ ,  $\hat{H}$  and  $\hat{L}$  in the control law. The resulting multi-input, single-output control law is then:

$$u(t) = \frac{1}{[Q + \hat{g}_0]} [Rw(t) - \frac{\hat{F}}{P_d} y(t) - (G - \hat{g}_0)u(t) - z^{k-d}\hat{L}v(t) - \hat{H}Py^*(t+k-1|t-1)] \quad (3.25)$$

The method used for estimating the unknown coefficients in equation 3.25 is discussed in Section 3.6.

### 3.2.2 Minimum Variance Controller

If the control effort is not of concern, it is possible to modify the cost function, equation 3.3, such that the controller would be designed to minimize the variance of the output from its set point, irrespective of the control effort. This is accomplished by setting  $Q' = 0$  and  $P = R = 1$  in equation 3.3 to get:

$$J = E\{[y(t+k) - w(t)]^2\} \quad (3.26)$$

Or, using the predicted output, the equivalent of equation 3.16 is:

$$J = E\{[y^*(t+k|t) - w(t)]^2\} + \sigma^2_{\epsilon,k} \quad (3.27)$$

The minimization of  $J$  with respect to  $u(t)$  then becomes:

$$\frac{\partial J}{\partial u(t)} = 2[y^*(t+k|t) - w(t)] \cdot \frac{\partial [y^*(t+k|t)]}{\partial u(t)} = 0 \quad (3.28)$$

Since the relation in equation 3.13 still holds, equation 3.28 is now:

$$\frac{e_0 b_0}{c_0} [(y^*(t+k|t) - w(t))] = 0 \quad (3.29)$$

Substituting for  $y^*(t+k|t)$  from equation 3.22, and solving for  $u(t)$  using a procedure similar to that used in the

previous Section, the control law can be found to be:

$$u(t) = \frac{1}{g_0} [w(t) - Fy(t) - (G - g_0)u(t) - z^{k-d}Lv(t) - Hy^*(t+k-1|t-1)] \quad (3.30)$$

or, using the estimated values of the controller parameters,

$$u(t) = \frac{1}{\hat{g}_0} [w(t) - \hat{F}y(t) - (\hat{G} - \hat{g}_0)u(t) - \hat{z}^{k-d}Lv(t) - \hat{H}y^*(t+k-1|t-1)] \quad (3.31)$$

which is the equivalent of equation 3.25 for  $Q = 0$ ,  $P_n = P_d = 1$  and  $P_n = P_d = 1$ .

### 3.3 Multivariable Self-tuning Controller

In this section the multi-input, multi-output (MIMO) self-tuning control law is developed. The derivation of the multivariable controller parallels the MISO self-tuning control law derivation with the extension from scalars and vectors to vectors and matrices, respectively.

An illustration of a multivariable system has been presented in Appendix A to clarify the notation. The extension of the MISO system may be represented by:

$$A(z^{-1})Y(t) = z^{-k}B(z^{-1})U(t) + C(z^{-1})E(t) + z^{-d}D(z^{-1})V(t) \quad (3.32)$$

where:

$\bar{A}(z^{-1})$ ,  $B(z^{-1})$ ,  $C(z^{-1})$  and  $D(z^{-1})$  are  $m \times m$  polynomial matrices in the backshift operator  $z^{-1}$ ,

$Y(t)$  is an  $m \times 1$  vector of measurable system outputs,

$U(t)$  is an  $m \times 1$  vector of control inputs,

$V(t)$  is an  $m \times 1$  vector of measurable disturbances,

$E(t)$  is a vector of random noise,

$k_{ij}$  is an integer multiple of the sampling time which corresponds to the delay between the  $i$ th control input and the  $j$ th process output and

$d_{ij}$  is an integer multiple of the sampling time which corresponds to the delay between the  $i$ th measurable disturbance and the  $j$ th process output.

A convenient assumption is that all system outputs are independent of each other. This results in  $\bar{A}(z^{-1})$  being a diagonal matrix, and is not a restrictive assumption. Similarly, if the noise terms are all independent of each other, the  $C(z^{-1})$  matrix is also a diagonal matrix. As in the MISO case, it is assumed that all the individual polynomial elements of the  $C(z^{-1})$  matrix have roots within the unit circle.

The objective of the generalized multivariable controller is to minimize the following cost function with respect to the controls,  $U(t)$ , on a loop by loop basis.

$$J = E\{[PY(t+k_{ii}) - RW(t)]'[PY(t+k_{ii}) - RW(t)] - [Q'U(t)]'[Q'U(t)]\} \quad (3.33)$$

Here,  $W(t)$  is an  $m \times 1$  vector consisting of the individual loop set points and  $P$ ,  $Q'$  and  $R$  are all  $m \times m$  diagonal transfer function matrices in the backshift operator (but with the  $z^{-1}$  arguments omitted for convenience), each element of which may be represented by numerator and denominator polynomials as described in Section 3.2.1.

Again, as in the MISO case,  $Y(t+k_{ii})$  is not known at time  $t$ , hence it is necessary to generate an estimate for the outputs  $k_{ii}$  steps ahead in the future. Note that  $k_{ii}$  relates  $u_i(t)$  to  $y_i$ . If equation 3.32 is multiplied through by  $z^{k_{ii}}$  and premultiplied by the inverse of  $A$ , the following estimate is obtained:

$$Y^*(t+k_{ii}) = z^{k_{ii}-k_{ij}} A^{-1} B U(t) + z^{k_{ii}} A^{-1} C E(t) + z^{k_{ii}-d_{ij}} A^{-1} D V(t) \quad (3.34)$$

$$k_{ii} \leq k_{ij} \text{ for all } j \neq i$$

Following the same procedure as in Section 3.2.1, define  $E'(z^{-1})$  and  $F'(z^{-1})$  as diagonal polynomial matrices which can be used to separate the noise terms into unknown future terms and known past terms by:



$$z^{k+1}A^{-1}C\Xi(t) = E'\Xi(t+k+1) + A^{-1}F'\Xi(t) \quad (3.35)$$

Now, substituting equation 3.35 into 3.34 to get:

$$\begin{aligned} Y^*(t+k+1) &= z^{k+1-k}A^{-1}BU(t) + E'\Xi(t+k+1) \\ &\quad + A^{-1}F'\Xi(t) + z^{k+1-d}A^{-1}DV(t) \end{aligned} \quad (3.36)$$

From equation 3.32 an estimate of the noise at time  $t$  based on past and current measurable values is given by:

$$\Xi(t) = C^{-1}AY(t) - z^{-k}C^{-1}BU(t) - z^{-d}C^{-1}DV(t) \quad (3.37)$$

Now, replace  $\Xi(t)$  in equation 3.36 using 3.37 and again take advantage of the matrices being diagonal to get:

$$\begin{aligned} Y^*(t+k+1) &= F'C^{-1}Y(t) + E'\Xi(t+k+1) \\ &\quad + [z^{k+1-k}A^{-1} - z^{-k}A^{-1}F'C^{-1}]BU(t) \\ &\quad + [z^{k+1-d}A^{-1} - z^{-d}A^{-1}F'C^{-1}]DV(t) \end{aligned} \quad (3.38)$$

Manipulating equation 3.35 yields:

$$[z^{k+1-k}A^{-1} - z^{-k}A^{-1}F'C^{-1}] = z^{k+1-k}E'C^{-1} \quad (3.39)$$

and

$$[z^{k+1-d}A^{-1} - z^{-d}A^{-1}F'C^{-1}] = z^{k+1-d}E'C^{-1} \quad (3.40)$$

By using equations 3.39 and 3.40 to replace the appropriate terms in equation 3.38, a simplified expression for the individual loop output,  $k+1$  steps ahead in time may be written as:

$$\begin{aligned} Y^*(t+k+1) &= F'C^{-1}Y(t) + E'E(t+k+1) \\ &\quad + z^{k+1-k}E'C^{-1}BU(t) \\ &\quad + z^{k+1-d}E'C^{-1}DV(t) \end{aligned} \quad (3.41)$$

If we maintain the assumption that the best possible estimate of all the noise terms is zero, then the best possible prediction of the output,  $Y(t)$ ,  $k+1$  steps in the future based on information up to and including time  $t$  is:

$$\begin{aligned} Y^*(t+k+1|t) &= F'C^{-1}Y(t) + z^{k+1-k}E'C^{-1}BU(t) \\ &\quad + z^{k+1-d}E'C^{-1}DV(t) \end{aligned} \quad (3.42)$$

Since equation 3.33 requires the weighted system output, it is necessary to multiply equation 3.46 through by the diagonal matrix  $P$ . In the multivariable case, it is desirable to decompose  $P$  into  $P_d * P_n$  where  $P_d$  and  $P_n$  are diagonal matrices containing the denominator and numerator portions of the  $P$  matrix, in their respective diagonal positions. At this point it is convenient to make the

following substitutions:

$$E = P * E'; \quad F = P_0 * F'$$

Equation 3.42 then becomes:

$$\begin{aligned} PY^*(t+k_{ii}|t) &= P_d F C^{-1} Y(t) + z^{k_{ii}-k_{ii}} E C^{-1} B U(t) \\ &\quad + z^{k_{ii}-d_{ii}} E C^{-1} D V(t) \end{aligned} \quad (3.43)$$

Again, realize that the predicted weighted outputs at time  $t$  are only estimates, and they are related to the actual values through the weighted output prediction error,  $\epsilon(t+k_{ii})$ :

$$PY(t+k_{ii}) = PY^*(t+k_{ii}|t) + \epsilon(t+k_{ii}) \quad (3.44)$$

Assume the noise to be uncorrelated with inputs and outputs, and that each loop has a mean noise value of zero, then the variance of the noise is given by:

$$\sigma_{t+k_{ii}}^2 = E\{[\epsilon(t+k_{ii})]^2\} \quad (3.45)$$

Substituting equation 3.48 into equation 3.37 to yield:

$$J = E\{[PY^*(t+k_{ii}|t) - RW(t)]'[PY^*(t+k_{ii}|t) - RW(t)] + [Q'U(t)][Q'U(t)]\} + \sigma_{ii}^2 \quad (3.46)$$

The details of the minimization of the cost function have been presented in Appendix B. The results of the differentiation of the cost function with respect to  $U(t)$  have been shown to be:

$$\frac{\partial J}{\partial U(t)} = 2E(0)C(0)B(0)'[PY^*(t+k_{ii}|t) - RW(t)] + 2Q'(0)Q'U(t) \quad (3.47)$$

or, setting the derivative equal to zero:

$$0 = E(0)C(0)B(0)'[PY^*(t+k_{ii}|t) - RW(t)] + Q'(0)Q'U(t) \quad (3.48)$$

By defining a new control weighting polynomial matrix as:

$$Q = [B(0)']^{-1}C(0)E(0)Q'(0)Q' \quad (3.49)$$

then it is possible to rearrange equation 3.48 to yield:

$$QU(t) = [RW(t) - PY^*(t+k_{ii}|t)] \quad (3.50)$$

By replacing  $PY^*(t+k_{ii}|t)$  in equation 3.50 using equation 3.43 and letting  $G = EB$ ,  $L = ED$  and  $C = I - z^{-1}H$  it follows that:

$$\begin{aligned} [z^{k_{ii}-k_{ij}}G + Q]U(t) &= RW(t) - P_d FY(t) \\ &- z^{k_{ii}-d_{ij}}LV(t) \\ &- HPY^*(t+k_{ii}-1|t-1) \end{aligned} \quad (3.51)$$

Analogous to the MISO case, the actual values of  $F$ ,  $G$ ,  $H$  and  $L$  are usually unknown, and the best available alternative is to replace the parameters with their estimated values to get:

$$\begin{aligned} [z^{k_{ii}-k_{ij}}\hat{G} + Q]U(t) &= RW(t) - P_d \hat{F}Y(t) \\ &- z^{k_{ii}-d_{ij}}\hat{L}V(t) \\ &- \hat{H}PY^*(t+k_{ii}-1|t-1) \end{aligned} \quad (3.52)$$

### 3.4 Distillation Column Control Law Implementation

The generalized multivariable self-tuning control law presented in equation 3.52 may be simplified when applying it to a particular process. This work is concerned with control of the top and bottom compositions of a distillation column subject to disturbances in the feed flow rate. The distillation column is represented by a 2\*2 system, with the top composition control loop as loop #1 and the bottom

composition control loop as loop #2. Equation 3.52 may be expressed for loop #1 as:

$$\begin{aligned}
 [Q_{11} + G_{11}(0)]u_1(t) = & R_{11}w_1(t) - \frac{1}{P_{d11}} F_{11}y_1(t) \\
 & - \sum_{i=1}^{nG_{11}-1} G_{11}(i)u_1(t-i) \\
 & - G_{12}u_2(t+k_{11}-k_{12}) \\
 & - L_{11}v_1(t+k_{11}-d_{11}) \\
 & - H_{11}P_{11}y_1^*(t+k_{11}-1|t-1) \quad (3.53)
 \end{aligned}$$

This is based on the assumption that  $k_{12} > k_{11}$ . If  $k_{12} = k_{11}$ ,  $u_2(t+k_{11}-k_{12})$  on the left hand side of equation 3.53 becomes  $u_2(t)$  and, since  $u_2(t)$  is unknown at time  $t$ , some rearrangement must take place. In this case where two loops are being controlled, it is necessary to solve for  $u_1(t)$  and  $u_2(t)$  simultaneously. This is accomplished by using the following equations. For loop #1:

$$\begin{aligned}
 [Q_{11} + G_{11}(0)]u_1(t) + G_{12}(0)u_2(t) = & R_{11}w_1(t) \\
 & - \frac{1}{P_{d11}} F_{11}y_1(t) \\
 & - \sum_{i=1}^{nG_{11}-1} G_{11}(i)u_1(t-i) \\
 & - \sum_{i=1}^{nG_{12}-1} G_{12}(i)u_2(t-i) \\
 & - L_{11}v_1(t+k_{11}-d_{11}) \\
 & - H_{11}P_{11}y_1^*(t+k_{11}-1|t-1) \quad (3.54)
 \end{aligned}$$

and for loop #2:

$$\begin{aligned}
 [Q_{22} + G_{22}(0)]u_2(t) + G_{21}(0)u_1(t) &= R_{22}w_2(t) \\
 &- \frac{1}{P_{22}} F_{22}y_2(t) \\
 &- \sum_{i=1}^{nG_{22}-1} G_{22}(i)u_2(t-i) \\
 &- \sum_{i=1}^{nG_{21}-1} G_{21}(i)u_1(t-i) \\
 &- L_{22}v_2(t+k_{22}-d_{22}) \\
 &- H_{22}P_{22}y_2^T(t+k_{22}-1|t-1) \quad (3.55)
 \end{aligned}$$

Using matrix notation equations 3.54 and 3.55 may be represented as:

$$SU(t) = \Phi(t) \quad (3.56)$$

where:

$$S = \begin{bmatrix} Q_{11} + G_{11}(0) & G_{12}(0) \\ G_{21}(0) & Q_{22} + G_{22}(0) \end{bmatrix} \quad (3.57)$$

and  $T(t)$  consists of the right hand sides of equations 3.54 and 3.55. Providing  $S$  is non-singular, the control law becomes:

$$U(t) = S^{-1}T(t) \quad (3.58)$$

The solution to equation 3.58 is accomplished using Cramer's rule.

In the event that  $k_{ij} > k_{ji}$ , for  $j \neq i$ , it may be necessary to either change the manipulated and controlled variable pairings, control more than one variable with one manipulated variable, or consider using a different self-tuning controller. One possible control scheme that would handle this situation is discussed by Martin-Sanchez and Shah [1984].

### 3.5 Control with Multirate Sampling

In multiloop control, individual loops frequently have their own individual optimum sampling times. Under multivariable control, it is common practice to arrive at a single sampling interval for all loops which represents a compromise between all the ideal sampling intervals. Frequently, in a realistic situation, a process analyzer is required to determine one or more of the outputs. Analyzers require a particular cycle time to accomplish the analysis which is, unfortunately, often much longer than the desired sampling period.

In an effort to improve the control of loops not constrained by analyzers and having optimum sampling times less than the smallest cycle time, a natural extension of



the multivariable controller would be to allow for different sampling rates for the individual loops. This is accomplished in the MVMR self-tuning controller with the only restriction being that all the individual sampling intervals of the various loops should be integer multiples of the smallest sampling interval,  $t_s$ .

Loop #2 of the distillation column, the bottoms composition control loop, is constrained to a large cycle time due to the gas chromatograph analysis of the bottom composition. Control of loop #1, the top composition control loop, may be improved by using a smaller sampling interval than that of loop #2.

$$(t_s)_2 = m(t_s)_1, \quad m = 1, 2, \dots \quad (3.59)$$

Loop #1 will have  $m$  control actions calculated for every single control action on loop #2. The control law derivation parallels the development of the multivariable controller. However, since it is expected that parameter identification will be required, a problem arises in the calculations for loop #2. In loop #1, the interaction between the two loops is taken into consideration by using the most recent value of  $u_2(t)$ . However, in loop #2 with multirate sampling there will be the need to contend with inter-sample control actions from the top loop. To attempt to include the inter-sample interactions, the inter-sample control actions from the faster loop may be averaged, and

the average value of the manipulated variable used in place of  $u_i(t)$  in equation 3.55. The averaging may be accomplished using:

$$u(av) = (1/m) \sum_{i=1}^m u_i(t-i+1) \quad (3.60)$$

However, Tham, [1985], concluded that better control may be achieved by ignoring the inter-sample interactions. For this study the interactions will therefore be ignored. Hence no modifications to the algorithm derived in Section 3.3 are required when implementing multirate control.

### 3.6 Parameter Estimation

There are two critical components of adaptive control schemes; the control law; and, since there is rarely sufficient a priori knowledge of the system to be controlled, a parameter estimation scheme. A method of estimating the F, G, L and H parameters for the control schemes must be employed to implement the control schemes.

Several recursive on-line estimation algorithms are available [Reinholt, 1984]. These include recursive least squares, extended least squares, recursive learning method and recursive square root, to mention a few. All the parameter estimation schemes must start with the same information.

### 3.6.1 Multi-input, Single-output Parameter Estimation

Beginning with a slightly rearranged form of equation 3.22, and replacing the  $F$ ,  $G$ ,  $H$  and  $L$  parameters with their estimated values gives:

$$\begin{aligned} Py^*(t+k|t) = & \frac{\hat{F}}{\hat{P}_d} y(t) + \hat{G}u(t) + z^{k-d}\hat{L}v(t) \\ & + \hat{H}Py^*(t+k-1|t-1) \end{aligned} \quad (3.61)$$

If an observation, or input-output vector,  $X(t)$ , is defined as;

$$\begin{aligned} X(t) = [ & y(t)/\hat{P}_d, y(t-1)/\hat{P}_d, \dots, y(t-nf+1)/\hat{P}_d, \\ & u(t), u(t-1), \dots, u(t-ng+1), \\ & v(t+k-d), v(t+k-d-1), \dots, v(t+k-d-nl+1), \\ & Py^*(t+k-1|t-1), Py^*(t+k-2|t-2), \dots, \\ & Py^*(t+k-nh|t-nh) ]^t \end{aligned} \quad (3.62)$$

where

$nf$  is the order of the  $\hat{F}$  polynomial,  
 $ng$  is the order of the  $\hat{G}$  polynomial,  
 $nl$  is the order of the  $\hat{L}$  polynomial and  
 $nh$  is the order of the  $\hat{H}$  polynomial.

For a vector containing the parameter estimates defined as:

$$\Theta(t) = \begin{bmatrix} f_0, f_1, \dots, f(nf-1), \\ \hat{g}_0, \hat{g}_1, \dots, \hat{g}(ng-1), \\ l_0, l_1, \dots, l(nl-1), \\ \hat{h}_0, \hat{h}_1, \dots, \hat{h}(nh-1) \end{bmatrix} \quad (3.63)$$

equation 3.61 can be written more compactly as:

$$Py^*(t+k|t) = X(t)' \Theta \quad (3.64)$$

Since good success has been achieved using the recursive least squares (RLS) method with upper diagonal factorization (UD) of the covariance matrix [Tham, 1985], this work will employ this estimation technique. The following algorithm outlines the steps used by the RLS estimation scheme:

Output prediction:-

$$Py^*(t+k|t) = X(t)' \Theta \quad (3.65)$$

Gain calculation:

$$K(t+k) = \frac{P_c(t)X(t)}{[\rho_1 + X(t)'P_c(t)X(t)]} \quad (3.66)$$

Parameter estimation:

$$\Theta(t+1) = \Theta(t) + K(t+1) \left[ \frac{y(t)}{P_d} - Py^*(t+k|t) \right] \quad (3.67)$$

Covariance update;

$$P_c(t+1) = [I - K(t+1)X(t)'] \frac{P_c(t)}{\rho_2} \quad (3.68)$$

where

$\rho_1$  is the variance of the noise

$\rho_2$  is the forgetting factor

$P_c$  is the covariance matrix

and  $K$  is the Kalman gain.

The conventional UD method was developed by Bierman [1976], but this scheme was subsequently modified by Morris et al., [1979], to yield a more numerically stable algorithm while using a constant forgetting factor. Due to the symmetry of the covariance matrix, in the actual implementation of the algorithm, a vector is used to store the upper triangular portion of the  $P_c$  matrix. This provides a significant reduction in the storage requirements. Details of the recursive UD estimation scheme employed in this work are given by Reinholt, [1984].

### 3.6.2 Multivariable Parameter Estimation

The same parameter estimation technique is employed in the MIMO case as was used for the MISO situation. Notation is simplified by letting:

$$X(t) = \begin{bmatrix} X_{11}(t) & & 0 \\ & X_{22}(t) & \\ & & \dots \\ 0 & & & X_{mm}(t) \end{bmatrix} \quad (3.69)$$

with each  $X_{ii}$  defined as described in equation 3.62, but applied to a single loop. If:

$$\theta(t) = [\theta_1(t), \theta_2, \dots, \theta_m(t)]' \quad (3.70)$$

then, on a loop by loop basis it follows that:

$$P_{i,j}y^*(t+k_{i,j}|t) = X_{i,j}(t)' \theta_i(t) \quad (3.71)$$

### 3.7 Relative Disturbance Gain Theory

The relative disturbance gain (RDG) is a technique which may be used to analyze closed loop performance of multivariable control systems from open loop, steady state process gains. As described by Marino-Galarrraga et al., [1985], the RDG may be used to evaluate relative gain array (RGA) results. RDG analysis has an advantage over RGA methods in that RDG considers the nature of the disturbance affecting the system.

Setting up the RDG starts with the steady state gain matrix. This matrix, illustrated with a 2\*2 system including the gains for an arbitrary disturbance, is:

$$\begin{bmatrix} y_1 \\ y_2 \end{bmatrix} = \begin{bmatrix} G_{11} & G_{12} & G_{13} \\ G_{21} & G_{22} & G_{23} \end{bmatrix} \begin{bmatrix} u_1 \\ u_2 \\ v \end{bmatrix} \quad (3.72)$$

The RDG,  $\beta_1$ , is defined as the change in the controller output for loop 1 that is required to counteract a disturbance,  $v$ , and bring  $y_1$  back to its set point, and is given for loop #1 by:

$$\beta_1 = \lambda \left[ 1 - \frac{G_{23}G_{12}}{G_{13}G_{22}} \right] \quad (3.73)$$

where  $\lambda$  is the relative gain for the 2x2 system:

$$\lambda = \frac{1}{1 - (G_{12}G_{21}/G_{11}G_{22})} \quad (3.74)$$

By symmetry:

$$\beta_2 = \lambda \left[ 1 - \frac{G_{13}G_{21}}{G_{23}G_{11}} \right] \quad (3.75)$$

or, by multiplying equations 3.73 and 3.75 together:

$$\beta_2 = \frac{(1 - \beta_1)\lambda}{(\lambda - \beta_1)} \quad (3.76)$$

Although the discussion by Marino-Galarraga et al., [1985], focusses on decoupling loops controlled using PID controllers, the main result of interest is that when  $|\beta_1| > 1$ , interaction between the loops is unfavourable and

decoupling should be considered.



## 4. Equipment

### 4.1 Introduction

The experimental work conducted in this project represents another study of distillation column control conducted using the pilot plant distillation column located in the Department of Chemical Engineering at the University of Alberta. Some of the most recent work has been done in conjunction with the Department of Chemical Engineering at the University of Newcastle-Upon-Tyne, particularly the self-tuning controller evaluations.

### 4.2 Distillation Column Description

The pilot scale distillation column in the Department of Chemical Engineering used for control studies is a 22.9 cm diameter, glass column that contains eight trays. The trays are spaced 30.5 cm apart and each contains four 4.8 cm diameter bubble caps arranged on a square pitch. The column is equipped with a total condenser and a thermosyphon reboiler. Figure 4.1 is a schematic representation of the column.

The feed to the column is a binary mixture of 50 mass percent methanol and water. The feed enters the column on the fourth tray, numbered from the bottom, after being preheated to 61°C.

Vapour from the top of the column is condensed using one of two available cooling water sources for the U-tube

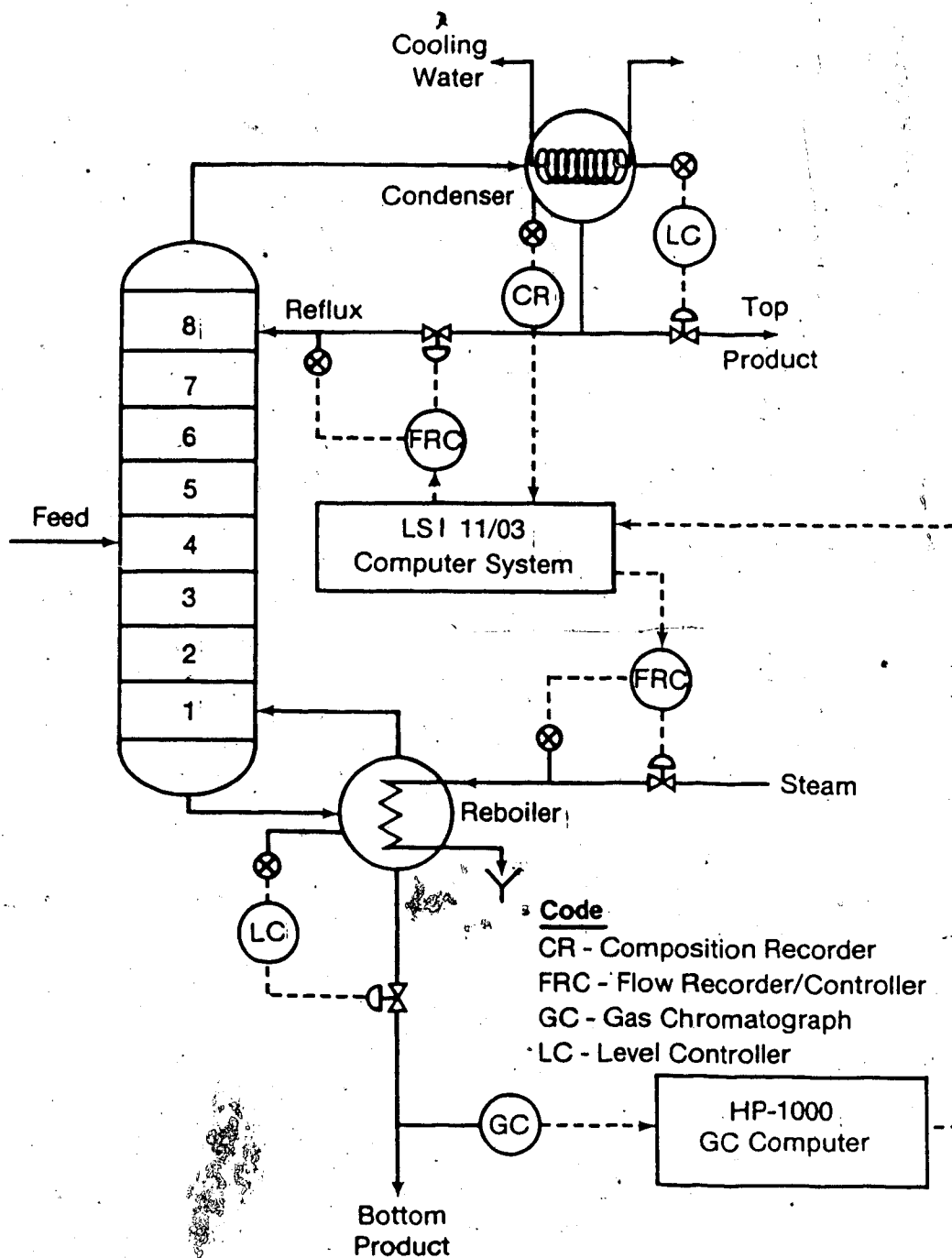


Figure 4.1 - University of Alberta Distillation Column

condenser. It was found that the domestic cooling water could provide a lower and more consistent inlet temperature, hence it was used instead of the constant head water supply system. A valve on the cooling water outlet was found to be critical in providing sufficient back pressure to fill the exchanger and provide adequate cooling. The cooling water flow was used to maintain the column pressure at approximately atmospheric pressure.

Distillate composition is analyzed continuously by an in-line capacitance cell. The reflux flow rate is used to maintain the top composition at 95.0 mass percent methanol. Reflux, returned to tray one of the column, is heated to 55°C. The level in the condenser is controlled by the top product flow.

Bottom product flow is used to regulate the level in the reboiler and steam flow rate is used to maintain the bottom composition at 5.0 mass percent methanol. An on-line gas chromatograph (HP5720A) is used to analyze the bottoms composition. An A/D converter (HP18652A) facilitates transmission of the signal from the detector of the gas chromatograph (GC) to the HP1000 computer for analysis of the chromatogram. A standard HP GC package on the HP1000 is used to generate the GC analysis suitable for transmission to the LSI 11/03. Bottom and top product streams return to a feed tank where a recirculation system is employed to ensure uniform temperature and composition in the feed.

Feed, steam, reflux, top and bottom flows are all recorded and controlled using pneumatic controllers. Thermocouples are used to continuously monitor all stream temperatures as well the individual tray temperatures. An example of the material and energy balance calculations generated from the temperature and flow data is presented in Table 4.1. Calibration data for the individual flow recorders are included in Appendix C.

#### 4.3 Computer Control

The distillation column may be operated under local automatic control with set points for the controllers entered manually on the control panel, or under the control of an LSI 11/03 16 bit microcomputer. The LSI is interfaced to the column with all the necessary pneumatic/current, current/pneumatic transmitters and analog/digital and digital/analog converters. The computer runs under the real time RT 11 operating system with all the control routines written in FORTRAN. Several control options, including manual, proportional-integral-derivative (PID) and self-tuning control are currently available. Eight-inch floppy diskettes are used for program and data storage.

Timing of the GC sampling and the required control actions takes place using a real-time clock. Incoming data from the GC report initiates the control program. The program allows for on-line changes to the controller parameters, setting of disturbances as well as selective

Table 4.1  
Steady State Mass and Energy Balance Report.

11 January 1986 1230 hrs

STEADY STATE CONDITIONS  
(119. SAMPLES 1 SECOND INTERVAL)

FLOW DATA

	FLOW(g/s)	STANDARD DEVIATION
STEAM	10.143	0.045
REFLUX	9.397	0.031
FEED	17.976	0.080
TOP PRODUCT	8.900	0.183
BOTTOM PRODUCT	8.481	1.148
COOLING WATER	464.237	29.294

TEMPERATURE DATA

	TEMP(DEG C)	STANDARD DEVIATION
FEED INLET	61.682	0.428
REFLUX	48.364	0.069
REFLUX INLET	54.822	0.164
TOP VAPOUR	64.227	0.219
CWATER IN	5.651	0.085
CWATER OUT	14.760	0.208
STEAM IN	116.409	0.371
STEAM CONDS	100.892	0.000
REB VAPOUR	90.242	0.201
BOTTOM PRODUCT	37.977	0.292
REBOILER LIQ	91.762	0.158
FEED	32.119	0.057
CONDENSER LIQ	50.265	0.207

COMPOSITION DATA (MASS% METHANOL)

TOP = 94.920 FEED = 49.800 BOTTOM = 5.101

Table 4.1 (cont)  
Steady State Mass and Energy Balance Report.

MATERIAL BALANCE

	FLOW (g/s)	COMPOSITION (MASS%MEOH)	METHANOL (g/s)	WATER (g/s)
FEED	17.976	49.800	8.952	9.024
BOTTOM PRODUCT	8.481	5.101	0.433	8.049
TOP PRODUCT	8.900	94.920	8.448	0.452
% ERROR	3.31		0.80	5.80

ENERGY BALANCE

	ENTHALPY IN (J/s)	ENTHALPY OUT (J/s)
FEED	3961.811	
REFLUX INLET	1513.925	
STEAM	27437.400	4315.726
COOLING WATER	11689.585	30502.873
CONDENSER OUT		2655.873
BOTTOM PRODUCT		3240.834
TOTAL	44602.723	40715.305
HEAT LOSS =	3887.418 (J/s)	
=	8.716 (% OF TOTAL HEAT INPUT)	

monitoring of inputs via a keyboard input. In addition, a foreground/background configuration is used which allows for the simultaneous execution of control algorithms in the foreground and less important tasks in the background. A simplified flowchart of the real-time control routine is given in Figure 4.2. More details of the programming are given in Appendix D in the form of pseudocode.

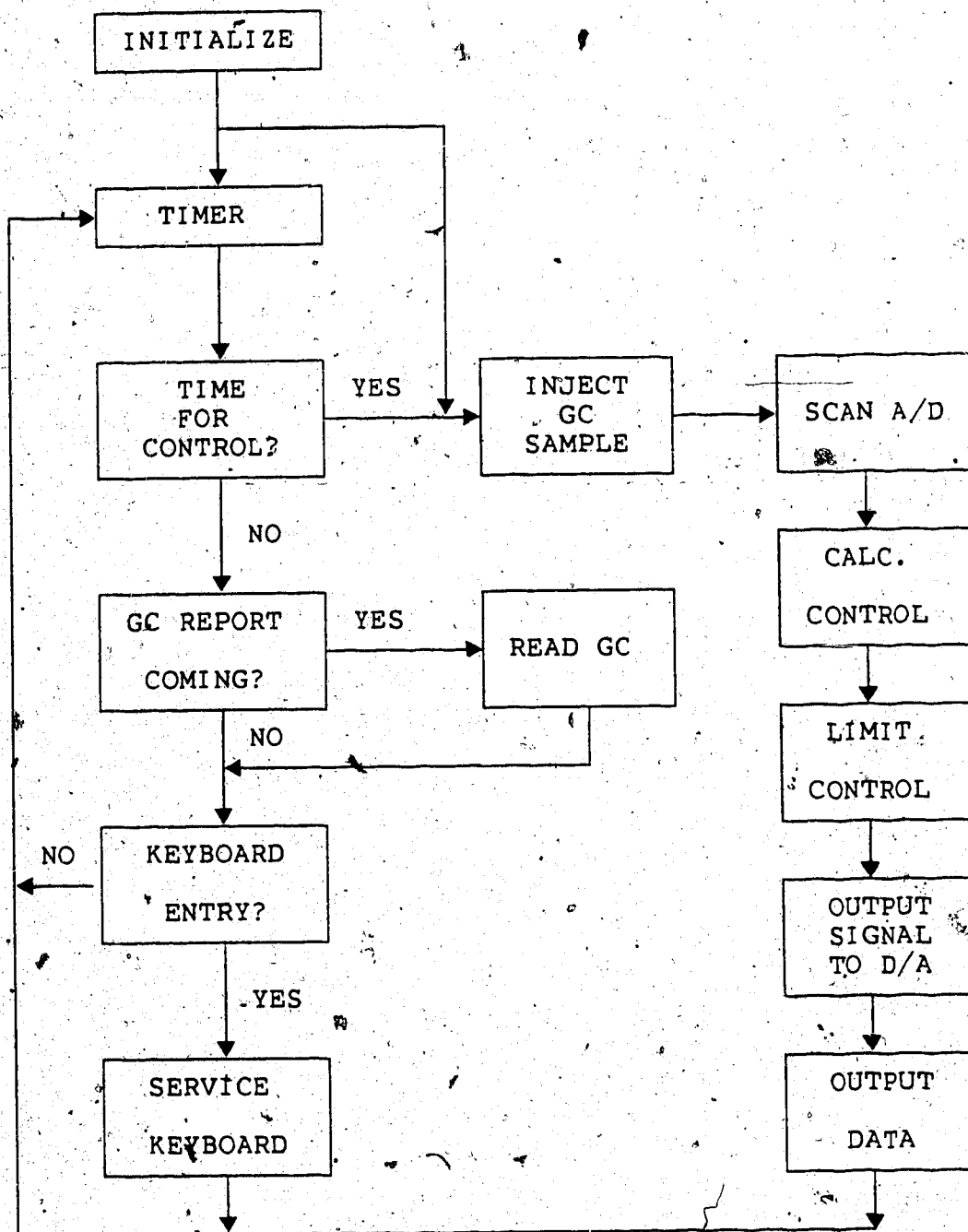


Figure 4.2 - Simplified Flowchart for Control Timing.



## 5. Distillation Column Dynamics

### 5.1 Introduction

Even for the simple binary distillation column used in this study, inherent interactions and nonlinear dynamic behavior exist. In order to properly design either a conventional PID controller or a self-tuning controller, some knowledge of the dynamic behavior of the column, including any time delays, is essential.

Despite the nonlinear behavior of the column, it is desirable to approximate the column with a linear model. In previous control studies, [Vagi, 1987], it was found that it was possible to approximate the high-order, nonlinear dynamics of the same column used in this study with first order plus time delay representations.

Due to several changes in the operating conditions of the column; fluctuations in the supply steam pressure between 90 and 60 psig; recalibrations of the flow and composition recorders that resulted in different steady state steam and reflux values; and using a different cooling water supply for the condenser, reinvestigation of the column dynamics was justified.

There are a variety of techniques that can be used to obtain the process gain, time constant and the time delay needed to characterize the system. Open loop step tests, pulse testing or PRBS testing may be used to generate data, with the data analyzed either graphically or by numerical

search techniques. Due to its simplicity, the method chosen for this work involved performing open loop step tests on the column. Three different methods were used to fit the open loop data to first order plus time delay models; a program, MODFIT.FOR, which was a modified version of the program MODEL [Desphande and Ash, 1981] in which a sum of errors squared is minimized to match up with the experimental results; a graphical technique which utilizes a tangent line drawn on the process response curve through its point of maximum slope, which is the method preferred by Lopez et al. [1967]; and a second, relatively quick graphical method which utilizes two points on the reaction curve [Smith and Corripio, 1985]. This last method has the advantage of not relying on the position or slope of the tangent line used in the first graphical method. The three methods will be referred to as MOD, LOP and SMI respectively.

## 5.2 Linear Representation

The dynamic behavior of many processes, although inherently nonlinear, may be approximated by a first order plus time delay model:

$$G_{11}(s) = \frac{K_p e^{-\theta_d s}}{\tau_1 s + 1} \quad (5.1)$$

where

$K_p$  is the process gain (mass%/g/s),

$\tau_1$  is the first order time constant (min) and

$\theta_1$  is the time delay (min).

In the case of the distillation column, there are two process outputs, the top and bottom compositions, and three inputs of interest, the reflux, steam and feed flows. The following transfer function matrix can be used to represent the 2\*3 system:

$$\begin{bmatrix} y_1(s) \\ y_2(s) \end{bmatrix} = \begin{bmatrix} G_{11}(s) & G_{12}(s) & G_{13}(s) \\ G_{21}(s) & G_{22}(s) & G_{23}(s) \end{bmatrix} \begin{bmatrix} u_1(s) \\ u_2(s) \\ u_3(s) \end{bmatrix} \quad (5.2)$$

where

$y_1$  is the top composition,  $y_2$  the bottom composition,  $u_1$  is the reflux,  $u_2$  the steam, and  $u_3$  the feed, and  $G_{ij}$  is a transfer function relating output  $i$  to input  $j$ .

### 5.3 Open Loop Test Results

The response of the distillation column to unit step changes in the feed, steam or reflux flows provides a method of generating data to be analyzed by one of the earlier mentioned techniques to establish a transfer function.

### 5.3.1 Feed

The response of the top and bottom compositions to a square wave pattern of  $\pm 12.4\%$  changes in the steady state feed flow rate is shown in Figure 5.1. Note that, although a steady state has not been reached in either the first or second steps of the disturbance (possibly due to flooding in the column), the resulting final value of the top composition dropped below the original steady state value for both an increase and a decrease in the feed flow. This is an illustration of the nonlinear behavior of the column. The response of the top and bottom compositions may be split into four process reaction curves, one corresponding to each of the four steps of the disturbance. A typical example of one such process reaction curve, showing the bottom composition reacting to an increase in feed flow, is given in Figure 5.2. The transfer functions obtained through analysis of the process reaction curves are presented in Table 5.1.

### 5.3.2 Reflux

The open loop test to determine the effect of reflux on the top and bottom compositions involved manipulating the reflux flow in a similar square wave pattern, with the reflux changed by  $\pm 6.9\%$  from the steady state value. The response of the top and bottom compositions is shown in Figure 5.3. Through analysis of the process reaction curves, the transfer functions presented in Table 5.2 are obtained.

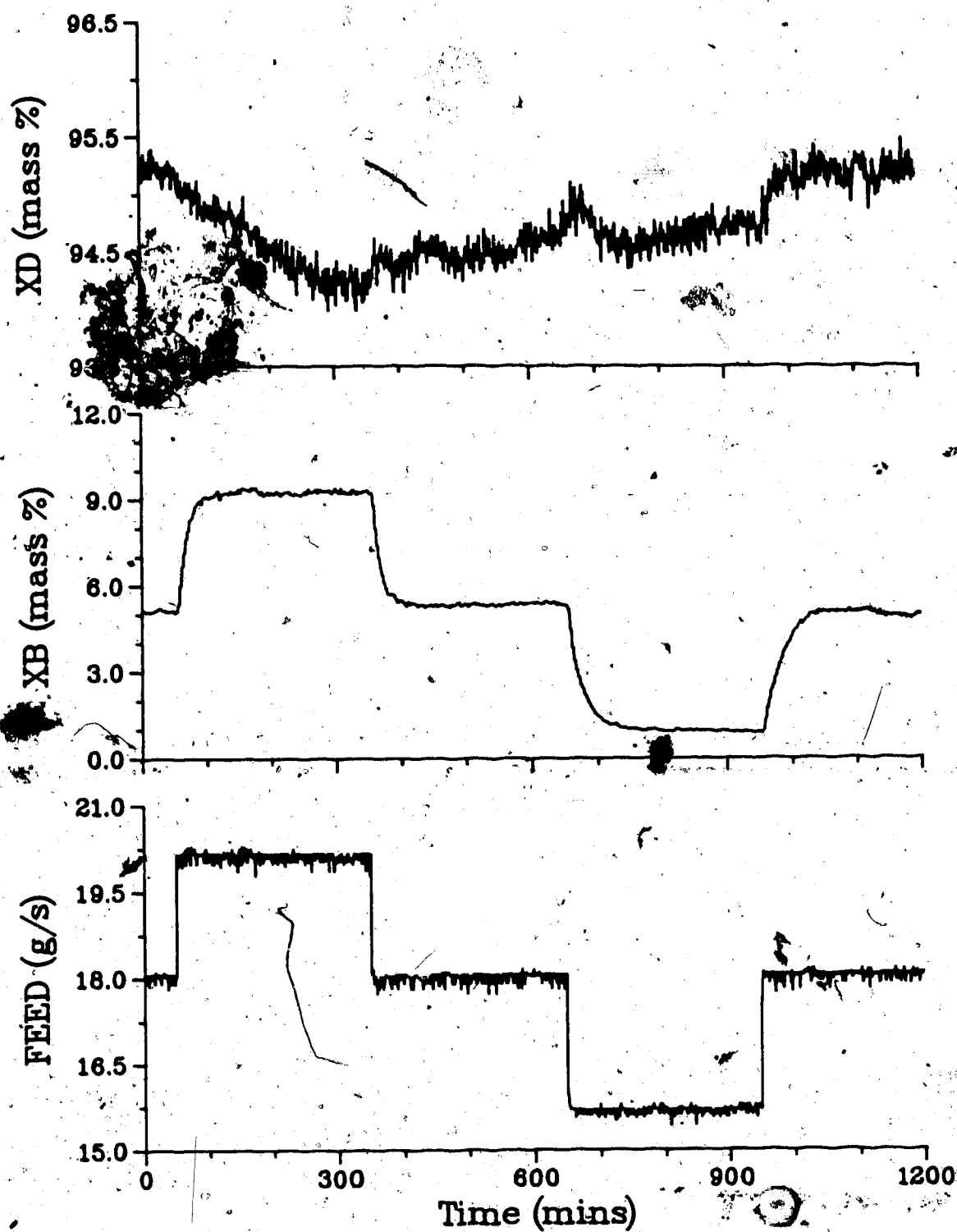


Figure 5.1 - Open Loop Column Response to Feed Disturbances ( $\pm 12.4\%$ )

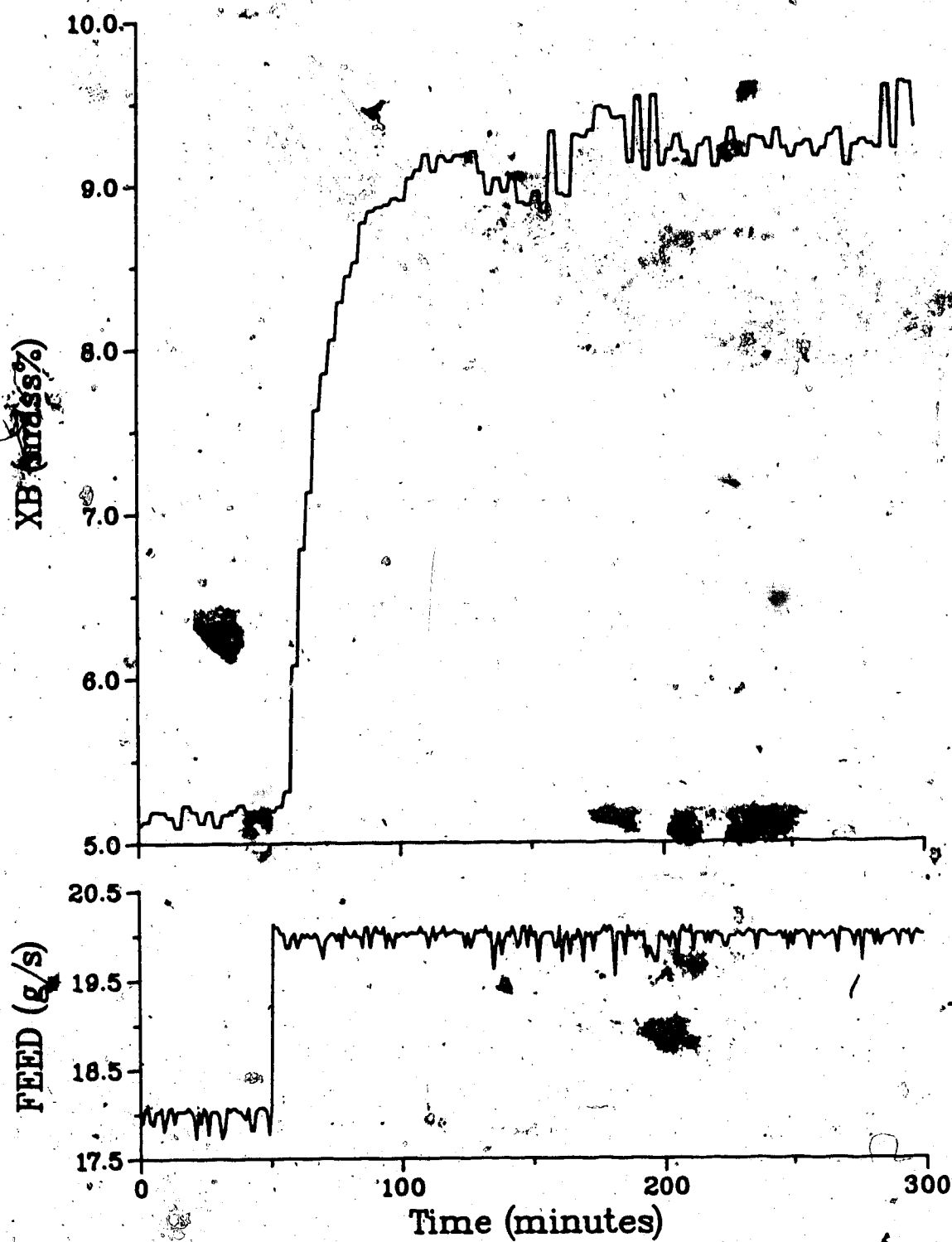


Figure 5.2 - Process Reaction Curve: Bottom Composition Response to Feed Disturbance (+12.4%)

Table 5.1

Transfer Functions Relating Feed Flow  
to Top and Bottom Compositions

Operating Region	Above Steady State(SS)		Below Steady State(SS)	
	Increase from SS	Decrease to SS	Decrease from SS	Increase to SS
$G_{13}(s)$ MOD	$\frac{-.799e^{-0s}}{276s+1}$	$\frac{-.124e^{-0s}}{20.9s+1}$	$\frac{-.017e^{-2s}}{0.088s+1}$	$\frac{.204e^{-7s}}{25.3s+1}$
$G_{13}(s)$ LOP	$\frac{-.456e^{-3.5s}}{138.s+1}$	$\frac{-.146e^{-4.7s}}{7.80s+1}$	$\frac{-.057e^{-1.2s}}{6.38s+1}$	$\frac{.234e^{-10.6s}}{20.1s+1}$
$G_{13}(s)$ SMI	$\frac{-.456e^{-26.8s}}{114.s+1}$	$\frac{-.146e^{-6.9s}}{5.67s+1}$	$\frac{-.057e^{-2.6s}}{4.96s+1}$	$\frac{.234e^{-12.5s}}{22.0s+1}$
$G_{23}(s)$ MOD	$\frac{1.98 e^{-5s}}{14.5s+1}$	$\frac{1.90 e^{-4s}}{14.3s+1}$	$\frac{1.87 e^{-4s}}{20.1s+1}$	$\frac{1.79 e^{-5s}}{29.0s+1}$
$G_{23}(s)$ LOP	$\frac{1.86e^{-6.3s}}{13.2s+1}$	$\frac{1.74e^{-4.7s}}{12.0s+1}$	$\frac{1.98e^{-6.6s}}{12.3s+1}$	$\frac{1.83e^{-7.6s}}{20.9s+1}$
$G_{23}(s)$ SMI	$\frac{1.86e^{-7.5s}}{14.1s+1}$	$\frac{1.74e^{-6.7s}}{11.7s+1}$	$\frac{1.98e^{-5.7s}}{19.1s+1}$	$\frac{1.83e^{-10.6s}}{23.4s+1}$

MOD - Transfer functions via MODFIT.FOR program

LOP - Transfer functions via Lopez et al. [1967] method

SMI - Transfer functions via Smith and Corripio [1985]  
method

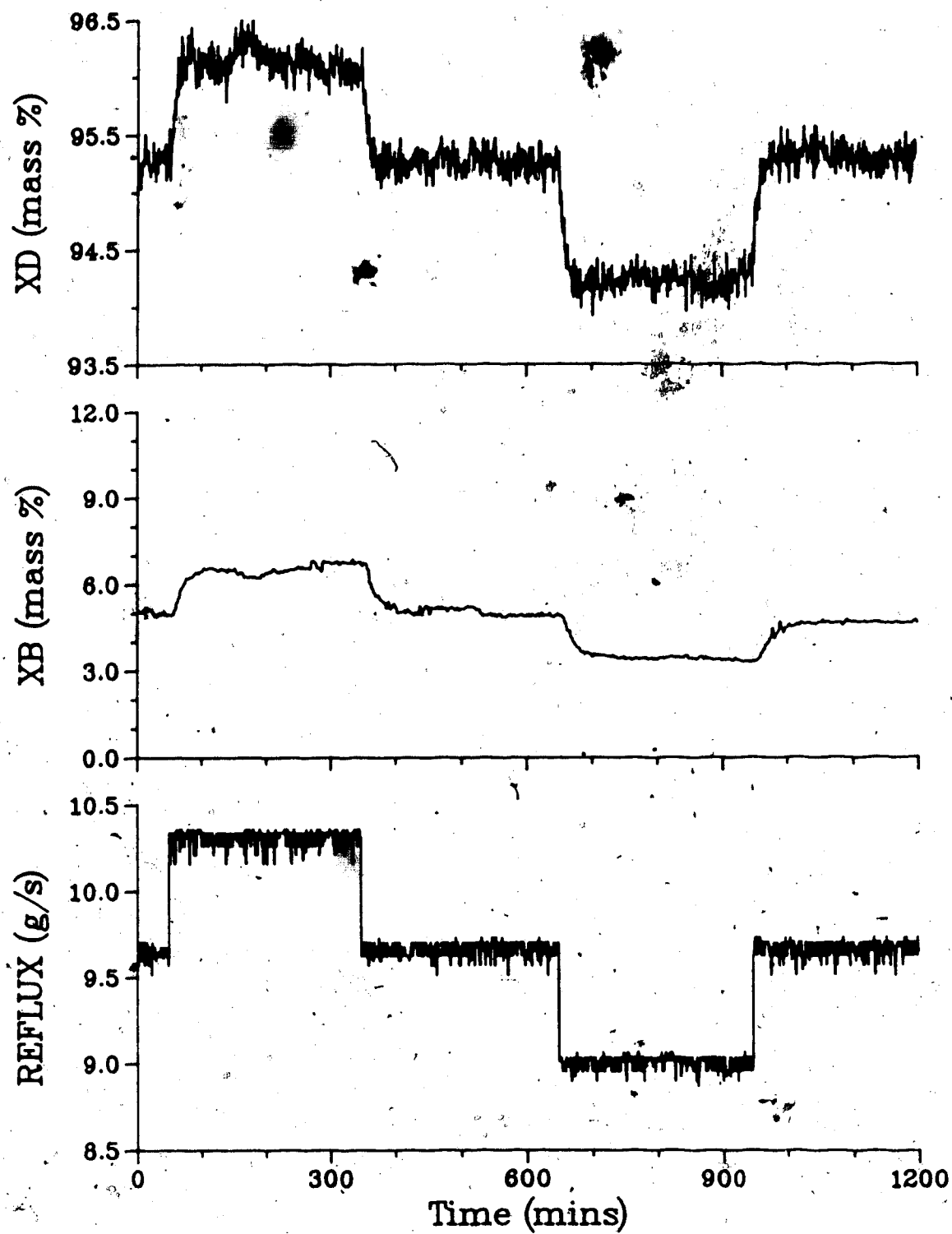


Figure 5.3 - Open Loop Column Response to Reflux Disturbances ( $\pm 6.9\%$ )



Table 5.2

Transfer Functions Relating Reflux Flow  
to Top and Bottom Compositions

Operating Region	Above Steady State(SS)		Below Steady State(SS)	
	Increase from SS	Decrease to SS	Decrease from SS	Increase to SS
$G_{11}(s)$ MOD	$\frac{1.33 e^{-0.5}}{7.73s+1}$	$\frac{1.26 e^{-0.5}}{7.53s+1}$	$\frac{1.55 e^{-0.5}}{7.81s+1}$	$\frac{1.55 e^{-0.5}}{8.36s+1}$
$G_{11}(s)$ LOP	$\frac{1.30 e^{-1.2s}}{8.74s+1}$	$\frac{1.23 e^{-0.7s}}{9.92s+1}$	$\frac{1.58 e^{-1.4s}}{8.50s+1}$	$\frac{1.63 e^{-0.9s}}{10.2s+1}$
$G_{11}(s)$ SMI	$\frac{1.30 e^{-2.8s}}{7.09s+1}$	$\frac{1.23 e^{-2.1s}}{8.50s+1}$	$\frac{1.58 e^{-2.1s}}{7.80s+1}$	$\frac{1.63 e^{-2.6s}}{8.50s+1}$
$G_{21}(s)$ MOD	$\frac{2.21 e^{-5s}}{15.8s+1}$	$\frac{2.67 e^{-5s}}{18.0s+1}$	$\frac{2.31 e^{-5s}}{20.3s+1}$	$\frac{1.98 e^{-6s}}{25.4s+1}$
$G_{21}(s)$ LOP	$\frac{2.40 e^{-7.6s}}{16.1s+1}$	$\frac{2.70 e^{-8.3s}}{11.6s+1}$	$\frac{2.30 e^{-5.2s}}{8.50s+1}$	$\frac{2.03 e^{-9.4s}}{18.9s+1}$
$G_{21}(s)$ SMI	$\frac{2.40 e^{-8.1s}}{13.1s+1}$	$\frac{2.70 e^{-7.8s}}{15.9s+1}$	$\frac{2.30 e^{-8.4s}}{15.9s+1}$	$\frac{2.03 e^{-11.1s}}{29.8s+1}$

### 5.3.3 Steam

The response of the compositions to a  $\pm 10.8\%$  change in the steam flow is presented in Figure 5.4. Although the bottom composition changes markedly with each step in the steam flow, only an increase in steam flow from the steady state value has a significant effect on the top composition. This is a further illustration of the nonlinear dynamic characteristics of the distillation column. The transfer functions obtained are presented in Table 5.3.

From the twenty-four transfer functions presented for each analysis technique in Tables 5.1, 5.2 and 5.3, it is desirable simulation studies to employ a matrix of only six transfer functions. In this study, the parameters for the transfer functions of the transfer function matrix are taken as the average values. For each of the analysis techniques, the transfer function matrix was calculated to be:

MOD

$$Y(s) = \begin{bmatrix} \frac{1.42e^{-1.0s}}{7.86s+1} & \frac{-0.669e^{-3.8s}}{15.0s+1} & \frac{-0.183e^{-3.8s}}{80.6s+1} \\ \frac{2.29e^{-6.5s}}{19.9s+1} & \frac{-4.54e^{-5.3s}}{18.5s+1} & \frac{1.89e^{-5.5s}}{19.5s+1} \end{bmatrix} U(s) \quad (5.3)$$

LOP

$$Y(s) = \begin{bmatrix} \frac{1.44e^{-1.1s}}{9.34s+1} & \frac{-0.700e^{-3.4s}}{11.6s+1} & \frac{-0.106e^{-5.0s}}{43.1s+1} \\ \frac{2.36e^{-7.6s}}{13.8s+1} & \frac{-4.49e^{-5.3s}}{16.0s+1} & \frac{1.85e^{-6.3s}}{14.6s+1} \end{bmatrix} U(s) \quad (5.4)$$

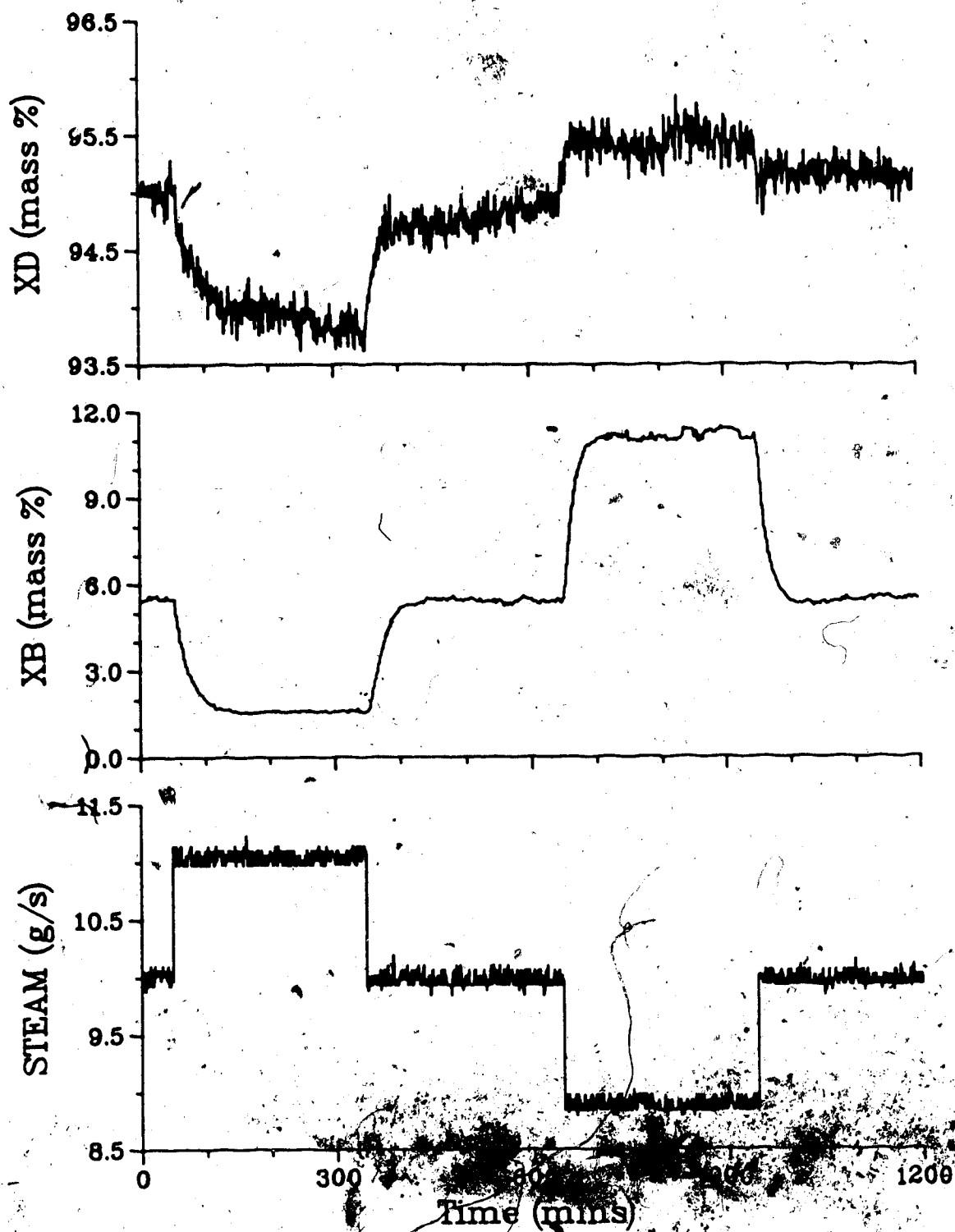


Figure 5.4 - Open Loop Column Response to Steam Disturbances ( $\pm 10.8\%$ )

Figure 5.3

Transfer Functions Relating Steam Flow  
to Top and Bottom Compositions

Operating Region	Above Steady State(SS)		Below Steady State(SS)	
	Increase from SS	Decrease to SS	Decrease from SS	Increase to SS
$G_{12}(s)$	$\frac{-1.04e^{-3s}}{34.0s+1}$	$\frac{-.874e^{-3s}}{16.4s+1}$	$\frac{-.516e^{-1s}}{7.93s+1}$	$\frac{-.244e^{-4s}}{1.82s+1}$
MOD				
$G_{12}(s)$	$\frac{-1.04e^{-5.4s}}{19.1s+1}$	$\frac{-.995e^{-2.8s}}{12.3s+1}$	$\frac{-.538e^{-2.1s}}{10.9s+1}$	$\frac{-.226e^{-3.1s}}{4.25s+1}$
LOP				
$G_{12}(s)$	$\frac{-1.04e^{-1.9s}}{36.9s+1}$	$\frac{-.995e^{-1.5s}}{20.2s+1}$	$\frac{-.538e^{-4.1s}}{8.86s+1}$	$\frac{-.226e^{-3.4s}}{3.90s+1}$
SMI				
$G_{22}(s)$	$\frac{-3.81e^{-3s}}{20.3s+1}$	$\frac{-3.59e^{-5s}}{24.5s+1}$	$\frac{-5.29e^{-5s}}{15.5s+1}$	$\frac{-5.45e^{-4s}}{13.6s+1}$
MOD				
$G_{22}(s)$	$\frac{-3.66e^{-5.4s}}{13.5s+1}$	$\frac{-3.59e^{-6.9s}}{20.3s+1}$	$\frac{-5.39e^{-4.7s}}{16.1s+1}$	$\frac{-5.32e^{-4.3s}}{14.2s+1}$
LOP				
$G_{22}(s)$	$\frac{-3.66e^{-5.3s}}{18.8s+1}$	$\frac{-3.59e^{-8.1s}}{23.0s+1}$	$\frac{-5.39e^{-7.2s}}{13.8s+1}$	$\frac{-5.32e^{-6.4s}}{12.0s+1}$
SMI				

SMI

$$Y(s) = \begin{bmatrix} \frac{1.44e^{-2.4s}}{7.97s+1} & \frac{-0.700e^{-2.7s}}{17.5s+1} & \frac{-0.106e^{-12.2s}}{36.7s+1} \\ \frac{2.36e^{-8.9s}}{16.2s+1} & \frac{-4.49e^{-6.8s}}{16.9s+1} & \frac{1.85e^{-7.8s}}{17.1s+1} \end{bmatrix} U(s); \quad (5.5)$$

By comparing the transfer function matrices determined by the three methods for analyzing the process reaction curves, it may be seen that all methods yield similar results. All the gain values show close agreement. Of the time constants only the time constant associated with the effect of the change in feed rate on the top composition differed significantly between the methods. Use of the LOP method resulted in four of the six time delays being slightly higher than values established by the MOD method. Use of the SMI method resulted in significantly higher time delays for five of the six transfer functions compared with MOD.

Despite the large time constant for the  $G_{13}$  transfer function that results from using the MODFIT program, since this technique does not require a graphical procedure, the transfer function matrix given by equation 5.3 will be used for the controller design calculations and simulations that follow.

## 6. Controller Parameters

### 6.1 Introduction

Caution must be used by the control engineer when implementing any control algorithm. For the multivariable, multirate, self-tuning controller developed in Chapter Three it is possible to vary the number of parameters for each of the controller polynomials, the values of the coefficients used in the weighting transfer functions, and the sampling time. Some guidelines have been established to provide initial estimates for specifying the various elements in the control law based on the dynamics of the system [Morris & Nazer, 1977]. Since column control using proportional-integral-derivative (PID) controllers are used in this study as a base case for comparison of control performance using the other algorithms, the selection of the PID controller settings will be included along with those for the self-tuning controller.

### 6.2 Sample Time

As discussed in Chapter Four, the bottom composition control loop is restricted by the GC cycle time to a minimum sample interval of three minutes. To avoid any additional delays, a sample time of three minutes was then chosen for the single rate control interval.

Since there is continuous measurement of the composition of the top product it is possible to control the

top composition of the column with a smaller sampling interval than the bottom composition control loop. Stephanopoulos, [1984], suggests that the sample time should be less than one time constant. If  $\tau_1$  is the dominant first order time constant then, from practical experience, the sampling time should be selected from:

$$0.1\tau_1 < t_s < 0.2\tau_1 \quad (6.1)$$

From the transfer function matrix determined from the column dynamics, equation 5.3, the dominant time constant is 7.86 minutes so the sample time suggested by equation 6.1 is between 47.2 seconds and 94.3 seconds. For convenience, the multirate controller was chosen to operate with a control interval of one minute for the top composition control loop, so that the bottom product sampling time is an integer multiple of that of the top composition control loop.

### 6.3 Conventional PID Controller Constants

The discrete form of the PID algorithm used in this study is:

$$u_n = u_{n-1} + K_c \left\{ \left[ 1 + \frac{t_s}{2T_I} + \frac{TD}{t_s} \right] e_n + \left[ \frac{t_s}{2T_I} - 1 - \frac{2TD}{t_s} \right] e_{n-1} + \frac{TD}{t_s} e_{n-2} \right\} \quad (6.2)$$

where

$K_c$  is the proportional constant ( $=100./PB$ ),

$T_I$  is the integral time,

$T_D$  is the derivative time,

$t_s$  is the sample time,

$u_n$  is the control action at time  $n$ , and

$e_n$  is the error at time  $n$ .

There are many methods available to select controller constants for PID controllers [Lopez et al., 1969; Yuwana & Seborg, 1982; Stephanopoulos, 1984]. Previous work done at the University of Alberta by Vagi, [1987], indicated that the Cohen-Coon method would provide the best initial parameter values, hence the Cohen-Coon design technique will be used here. It should be pointed out that any method for selecting initial controller constants rarely yields the optimum parameters. The estimated controller constants should only be thought of as suitable initial values.

Miller et al., [1967], compared several different techniques for estimating controller constants including the Cohen-Coon method, with the results presented in equations of the form:

$$K * K_c = A(\theta_d / \tau_1)^{-B} \quad (6.3)$$

$$T_I / \tau_1 = C(\theta_d / \tau_1)^D \quad (6.4)$$

$$T_D / \tau_1 = E(\theta_d / \tau_1)^F \quad (6.5)$$



where  $K$  is the process gain with the constants  $A, B, C, D, E$  and  $F$  for the Cohen and Coon method given in Table 6.1.

Table 6.1  
Cohen-Coon Constants  
[Miller et al., 1967]

Mode	A	B	C	D	E	F
PI	.928	.946	.928	.583		
PID	1.370	.950	.740	.738	.365	.950

Moore et al., [1969], suggest the use of an equivalent time delay in equations 6.3 to 6.5,  $\theta_d = (\theta_d + t_s/2)$ , to provide better estimates for digital control implementation due to sampling.

Previous work, [Vagi, 1987], has indicated that improved control performance is achieved by operating the bottom control loop of the column under PID control as opposed to PI control. A PI controller is satisfactory for the top control loop while under multiloop control, but it may be advantageous to use PID control for the top control loop when multirate control is implemented. The controller constants used as initial estimates in this study are given in Table 6.2.

Table 6.2  
Initial PID Controller Constants

TOP LOOP		GAIN = 1.42 mass%/g/s		
		TIME CONSTANT = 471.6 s		
		TIME DELAY = 60.0 s		
$t_s$ (s)	Kc	PB	TI	TD
60.0	3.131	31.93	166.6	0.0
60.0	4.654	21.49	102.8	35.69
180.0	1.931	51.78	224.4	0.0
BOTTOM LOOP		GAIN = -4.54 mass%/g/s		
		TIME CONSTANT = 1110.0 s		
		TIME DELAY = 318.0 s		
$t_s$ (s)	Kc	PB	TI	TD
180.0	0.781	128.1	392.4	156.6

## 6.4 Self-tuning Controller

### 6.4.1 Controller Polynomial Coefficients

Morris and Nazer, [1977], provide a set of guidelines for specifying the number of controller parameters to use when implementing the self-tuning controller. If  $N$  is the sum of the model orders assumed for the individual transfer functions that are used in each loop, then there will be  $N + k$  coefficients in the  $G$  polynomial, where  $k$  is the delay associated with the manipulated variable for the particular loop. The  $F$ ,  $H$  and  $E$  controller polynomials will contain  $N$ ,

$N + 1$  and  $N + k$  coefficients respectively.

Since the  $H$  polynomial coefficients are directly linked to the system noise, assumed to have a mean of zero, the  $H$  parameters are not easily identified. It is found that the coefficient values vary from positive to negative values, around zero, without convergence. Consequently it is realistic to ignore the  $H$  polynomial, as was done for this study.

In Chapter Five the dynamics of the column were determined by a series of open loop tests. For each product composition the response to the direct manipulated variable, interacting manipulated variable and to the disturbance were all assumed to be represented by first order plus time delay transfer functions. Hence, for both the top and bottom loops, the accumulative model order, based on the assumed transfer functions is 3, so  $N = 3$ . From equation 5.3 the delay relating the top composition and the reflux is 1.0 minute. Under single rate control where both the top and bottom compositions are sampled at three minute intervals, this one minute delay is taken as three minutes, one sampling interval, rather than not allow for any time delay. Under multirate control where the top composition is sampled every minute,  $k$  will be set to 1, corresponding to a time delay of one minute. This is a much better approximation to the actual time delay than was possible for single rate sampling. From the assumed transfer functions, for both single rate and multirate control the number of coefficients

for the  $G_{11}$ ,  $F$ ,  $L$  and  $G_{12}$  polynomials in the top composition controller are 4, 3, 4, and 4, respectively.

As the bottom composition was sampled at a three minute interval for both single rate and multirate control, the 5.3 minute delay between the steam and the bottom composition was approximated as two sample intervals,  $k = 2$ , so the number of  $G_{22}$ ,  $F$ ,  $L$  and  $G_{21}$  coefficients for the bottom composition controller are therefore 5, 3, 5 and 5 respectively.

Although the number of coefficients in the  $G$ ,  $F$  and  $L$  polynomials given above are based on the assumed model structure and column dynamics, it may be possible, in practice, to use fewer coefficients. Reducing the number of coefficients should reduce the computing time required for parameter estimation and enhance the rate of convergence of the remaining parameters.

An indication as to whether or not the interacting  $G$  coefficients are required is given by the relative disturbance gain technique discussed in Section 3.7. For the system represented by equation 5.3:

$$\lambda = 1.312 \quad ; \quad \beta_1 = 3.308 \quad ; \quad \beta_2 = 1.516$$

Since  $|\beta_i| > 1.0$  for both  $i = 1$  and  $i = 2$ , some undesirable interaction exists and it is useful to include decoupling between the two ends of the column, so no  $G_{12}$  or  $G_{21}$  parameters were eliminated for the initial tests.

If the last coefficient in any polynomial is identified to a value close to zero compared to the other coefficients in the same polynomial, the last coefficient may be eliminated since its contribution to the control action is insignificant. Overspecifying the number of coefficients in the controller polynomials, and successively reducing the number through a series of runs by eliminating the insignificant coefficients is an acceptable method of obtaining the optimum number of coefficients for a particular process. However, for this work the number of coefficients in the controller polynomials will not be reduced.

#### 6.4.2 Q Weighting Parameters

Although the number of coefficients for the  $G$ ,  $F$ ,  $L$  and  $H$  polynomials have been specified, with their values to be determined through a parameter estimation scheme, the weighting employed by the  $P$ ,  $R$  and  $Q$  transfer function matrices must also be chosen by the control engineer. The majority of the work done using this type of controller has involved setting  $P = R = I$ . Seborg et al., [1983] include simulations where the  $P$  and  $R$  diagonal polynomial matrices were not taken as identity matrices, but their work only involved MISO systems. Although  $P$  and  $R$  weighting is an area that should be explored further, for this study,  $P$  and  $R$  were both set equal to identity matrices.

As discussed in Section 3.2.2, setting  $Q$  equal to 0 will yield the minimum variance controller. To date, no definitive method exists for determining the structure of the  $Q$  weighting polynomial. Lieuson, [1980], recognized that the control law presented in equation 3.21 is similar to a standard feedback control law. This can be seen by rewriting equation 6.2 as:

$$u_n - u_{n-1} = K_1 e_n + K_2 e_{n-1} + K_3 e_{n-2} \quad (6.6)$$

where

$$K_1 = K_c \left[ 1 + \frac{t_s}{2TI} + \frac{TD}{t_s} \right] \quad (6.7)$$

$$K_2 = K_c \left[ \frac{t_s}{2TI} - 1 - \frac{2TD}{t_s} \right] \quad (6.8)$$

$$K_3 = K_c \frac{TD}{t_s} \quad (6.9)$$

Now, if the backward shift operator,  $z^{-1}$ , is substituted into equation 6.6, rearrangement yields:

$$u_n = \left[ \frac{K_1 + K_2 z^{-1} + K_3 z^{-2}}{1 - z^{-1}} \right] e_n \quad (6.10)$$

This equation is similar to equation 3.21, given below,

$$u(t) = \frac{1}{Q} [Rw(t) - Py^*(t+k|t)] \quad (3.21)$$

with the control action a function of the error  $[Rw(t) - Py^*(t+k|t)]$ . Lieuson also argued that under self-tuning control the output is being predicted and, as a result, any existing delays between inputs and outputs are removed. Without any delay, it was felt that the derivative term of a PID compensator may be omitted ( $K3 = 0$ ). In the studies of Lieuson, and also by Vagi, [1987],  $Q$  weighting was derived from an inverse PI structure:

$$Q = \frac{1 - z^{-1}}{Q_0 + Q_1 z^{-1}} = \frac{1 - z^{-1}}{K1 + K2 z^{-1}} \quad (6.11)$$

Aloisi et al., [1985], also used the  $Q$  weighting given by equation 6.11.

However, as shown in Section 3.2.1, when  $Py^*(t+k|t)$  is replaced in equation 3.21 using equation 3.13, an additional term,  $g_0$ , must be factored out to make the equation realizable and written as:

$$u(t) = \frac{1}{[Q + g_0]} \left[ Rw(t) - \frac{F}{P_d} y(t) - (G - g_0)u(t) - z^{-1} [Lv(t) - HPy^*(t+k-1|t-1)] \right] \quad (6.12)$$

In equation 6.12, the term in brackets still represents a "deviation" from the set point,  $Rw(t)$ , although the sum of

the terms subtracted from the set point do not equal the predicted output. However, it would be very convenient if equation 6.12 could still be looked upon as being similar to equation 6.10. This is particularly useful in the case of implementing a self-tuning controller on an existing plant where reasonable PID controller parameters are likely to be known. In order to obtain the desired correspondence between the  $Q$  polynomial and the standard feedback compensator, it is necessary to equate:

$$\frac{1 - z^{-1}}{K_1 + K_2 z^{-1} + K_3 z^{-2}} = \frac{1 - z^{-1}}{q_0 + q_1 z^{-1} + q_2 z^{-2}} + g_0 \quad (6.13)$$

If one is able to force  $g_0 = 0$ , there is a direct relationship between  $q_0$ ,  $q_1$  and  $q_2$  and  $K_1$ ,  $K_2$  and  $K_3$  as seen in equation 6.13. The  $Q$  weighting then results from the inverse form of the PID compensator found in equation 6.10. As mentioned earlier, this represents a very convenient form for the  $Q$  weighting polynomial. Setting  $g_0 = 0.0$ , does not, however, bring the term in brackets in equation 6.12 any closer to representing the set point minus the predicted output as in equation 3.21.

The various  $Q$  weighting polynomial representations used in this study can be illustrated by considering a single-input, single-output process, with no noise or disturbances, represented as:



$$Ay(t) = z^{-k}Bu(t) \quad (6.14)$$

If the process may be represented by a first order plus time delay transfer function such as:

$$y(s) = \frac{2.0 e^{-2s}}{10.0s + 1} u(s) \quad (6.15)$$

then the discrete representation is:

$$\frac{y(t)}{u(t)} = \frac{z^{-k}B}{A} = \frac{0.19033 z^{-2}}{1 + .90484z^{-1}} \quad (6.16)$$

Comparison with equation 6.14 shows that:

$$A = 1 + .90484z^{-1} = 1 + a_1z^{-1} \quad (6.17)$$

$$B = 0.19033 = b_0 \quad (6.18)$$

Since the model delay is 2 and the order of the model is 1, it follows that 1 F and 3 G coefficients are required so the E polynomial (cf. Section 3.2.1) would have 3 coefficients with the G polynomial expressed as:

$$G = b_0e_0 + b_0e_1z^{-1} + b_0e_2z^{-2} \quad (6.19)$$

resulting in the output prediction given by:

$$\begin{aligned} \hat{y}^*(t+2|t) = & f_0 y(t) + b_0 e_0 u(t) + b_0 e_1 u(t-1) \\ & + b_0 e_2 u(t-2) \end{aligned} \quad (6.20)$$

By choosing  $P = R = 1$ , the control law is then:

$$\begin{aligned} u(t) = & \frac{1}{[Q + b_0 e_0]} [w(t) - f_0 y(t) - b_0 e_1 u(t-1) \\ & - b_0 e_2 u(t-2)] \end{aligned} \quad (6.21)$$

or

$$u(t) = \frac{1}{[Q + g_0]} [w(t) - (\hat{y}^*(t+2|t) - g_0 u(t))] \quad (6.22)$$

From equation 6.22 it is obvious that the term subtracted from the set point is not exactly equal to the predicted output since  $g_0 = b_0 e_0 \neq 0.0$ . Forcing  $g_0 = 0.0$  would allow the  $Q$  polynomial to take the inverse PID structure, but would leave only two  $G$  parameters in the controller polynomial so the prediction term would be:

$$\hat{y}^*(t+2|t) = f_0 y(t) + b_0 e_1 u(t-1) + b_0 e_2 u(t-2) \quad (6.23)$$

The prediction given by equation 6.23 does not correspond to the prediction given by equation 6.20, causing a detrimental effect on the ability of the controller to predict the output. If an extra  $G$  coefficient were added, the prediction would become:

$$y^*(t+2|t) = f_0 y(t) + b_0 e_1 u(t-1) + b_0 e_2 u(t-2) + b_0 e_3 u(t-3) \quad (6.24)$$

This results in the correct number of terms in the prediction, but by comparing equations 6.20 and 6.24, it can be seen that the incorrect  $u(t)$  terms are used, so the prediction will still not be correct. However, if the model time delay was underestimated by one interval and an extra coefficient was added to the B polynomial, the model of the process would be:

$$\frac{z^{-k}B}{A} = \frac{z^{-1}(b_0 + b_1 z^{-1})}{1 + a_1 z^{-1}} \quad (6.25)$$

Comparing equation 6.16 with equation 6.25, it should be noted that if equation 6.25 is to correctly represent the process (cf. equation 6.10) then  $b_0 = 0.0$  and  $b_1 = 0.19033$ . The E polynomial would now have only 2 coefficients since the time delay is assumed to be 1. The G polynomial is then:

$$G = b_0 e_0 + (b_0 e_1 + b_1 e_0) z^{-1} + b_1 e_1 z^{-2} \quad (6.26)$$

so the output prediction becomes:

$$y(t+1|t) = f_0 y(t) + b_0 e_0 u(t) + (b_0 e_1 + b_1 e_0) u(t-1) + b_1 e_1 u(t-2) \quad (6.27)$$

Since  $b_0 = 0.0$ , the prediction of the output will not change by rearranging  $b_0 e_0 u(t)$  to solve for  $u(t)$  as is necessary in deriving the control law (equation 6.21). This procedure achieves the desired objectives of setting  $g_0 = 0.0$  and allowing the  $Q$  weighting polynomial to directly take on the inverse PID structure.

A further option considered in this work is to not set  $g_0 = 0.0$  and use the assumption made by Lieuson that the derivative term is not required in calculating  $Q$  weighting coefficients since the self-tuning controller has the ability to predict the output. Then equation 6.13 becomes:

$$\frac{1 - z^{-1}}{K1 + K2z^{-1}} = \frac{1 - z^{-1}}{q_0 + q_1 z^{-1}} + g_0 \quad (6.28)$$

Solving for  $q_0$  and  $q_1$ :

$$q_0 = \frac{K1}{1 - g_0 K1} ; \quad q_1 = \frac{K2}{1 + g_0 K2} \quad (6.29)$$

If  $q_0$  and  $q_1$  are left as functions of  $g_0$ , the  $Q$  weighting coefficients will adapt as  $g_0$  adapts. The effect on control performance of this option as well as the other options considered in this section, are examined in Chapter

7 by simulations using a simple linear model.

#### 6.5 Controller Performance Criterion

To provide a quantitative measure for the purpose of comparing one control scheme with another, the sum of absolute error, SAE, will be used. SAE weights errors on the response curve equally, hence offset and overshoot will be treated equally. This is convenient since in controlling the distillation column the elimination of offset and the minimization of overshoot are both considered important. It will also allow for comparisons with previous results. Other performance criterion (Stephanopoulos, [1984]), might well be employed to provide a quantitative measure of control performance to supplement visual comparisons.

## 7. Simulation Results

### 7.1 Introduction

In this work a variety of simulation studies were performed to evaluate the control strategies. Initially a single transfer function was used as the plant to be controlled. The conventional PID algorithm as well as the minimum variance and generalized minimum variance forms of the self-tuning controller were employed with the results presented in Section 7.2. The results provide some insight into the aspect of parameter tuning.

In Section 7.3, simulation results involving a model consisting of two transfer functions are used to demonstrate the effect of using the disturbance or an estimate of the disturbance as a feedforward signal. Results obtained using the distillation column transfer function model given by equation 5.3 are presented in Section 7.4.

To perform the simulations a program LINSIM.FOR was used. LINSIM.FOR is a slightly modified version of MIST.FOR, a program developed at the University of Newcastle-Upon-Tyne [Nazer, 1981]. Up to four transfer functions of different orders may be used in either of two loops. Integration is carried out using a fourth order Runge Kutta routine. The original program which required the time delays associated with the plant model to be integer multiples of the controller sampling time was altered to allow for mismatch between the time delay in the model and the controller

sampling time.

## 7.2 Single Transfer Function Plant Model Simulation

### 7.2.1 Introduction

To illustrate some of the control concepts developed in Chapters 3 and 6, a first order single transfer function has been used as the plant model to be controlled:

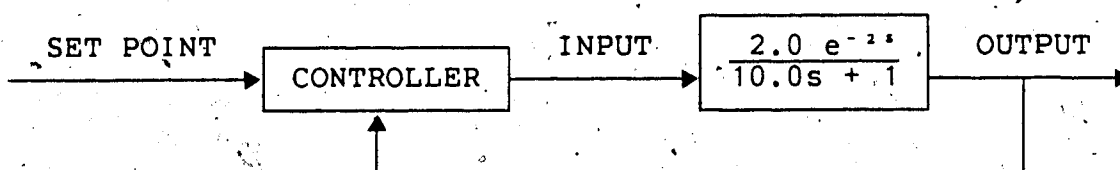


Figure 7.1 - Single Transfer Function (STF) Plant Model

In the simulation, a sample interval of one minute was employed. For a first order transfer function with a time delay of 2 sampling intervals, 3 G coefficients and 1 F coefficient will be required in the self-tuning controller to exactly model the "process".

In each of the following tests, the set point has been varied in a square wave pattern: at 60 minutes the set point was increased from 0.0 to 6.0; at 110 minutes it was decreased to 0.0; at 160 minutes it was decreased further to -6.0 and at 210 minutes the set point was returned to 0.0. Parameter identification began at 10 minutes and control at 30 minutes. Since neither the input nor output signal

contained any noise, no parameter adaptation or control action took place prior to the first set point change.

### 7.2.2 PI Control

To provide a base case, conventional PI control was applied to the model in Figure 7.1. A series of runs were made with various controller constants to obtain a tuned controller. The tuned constants were found to be a proportional band (PB) of 38.0 and an integral time (TI) of 12.0. The responses obtained by using this controller are presented in Figure 7.2a: The control achieved was not particularly good, but this is due to the presence of the time delay. A derivative term in the control law was used, but found to provide negligible improvement in the control performance.

To demonstrate that it is the presence of the time delay that causes the poor control performance under PI control, the time delay was removed from the model. The results in Figure 7.2b were obtained using the same PI controller constants. The control has been greatly improved.

### 7.2.3 Parameter Identification

While employing the tuned PI controller to control the model given in Figure 7.1 the identification routine was run independently to track the identification of the self-tuning parameters. As is typical for most of the tests,  $g_0$ , the first coefficient of the G polynomial, was initially set to



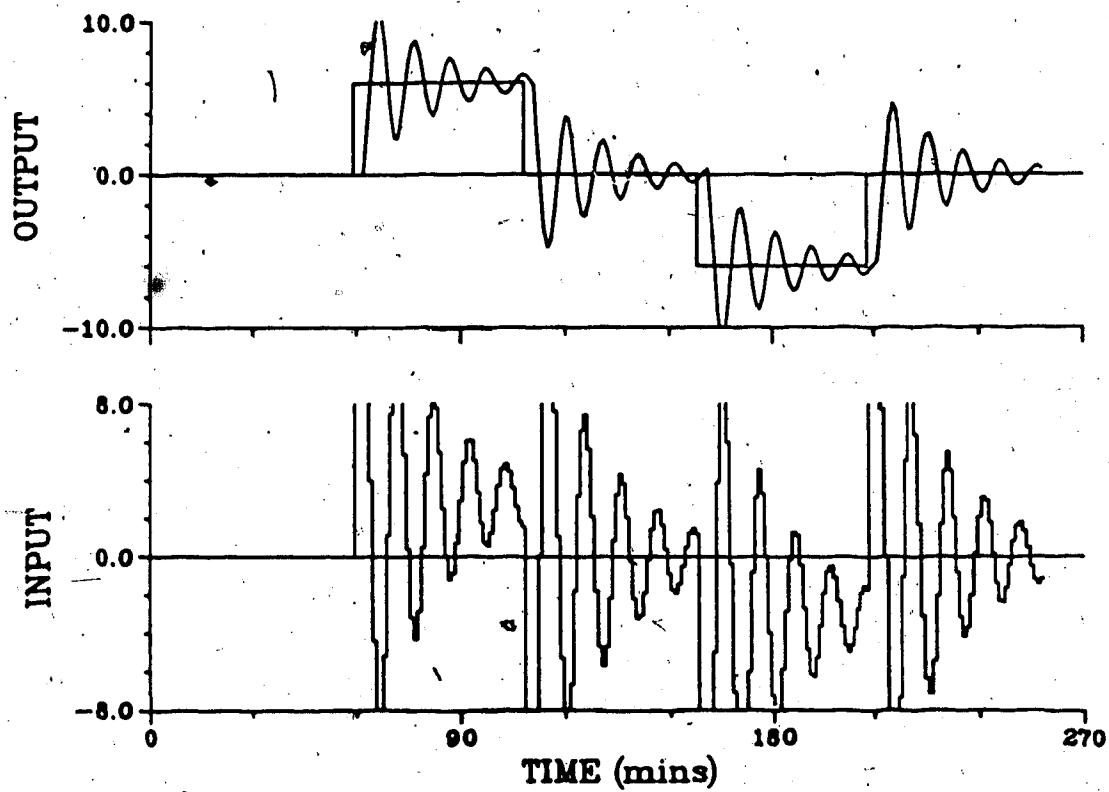


Figure 7.2a - PI Control of the Single Transfer Function  
with  $PB=38.0$ ,  $TI=12.0$

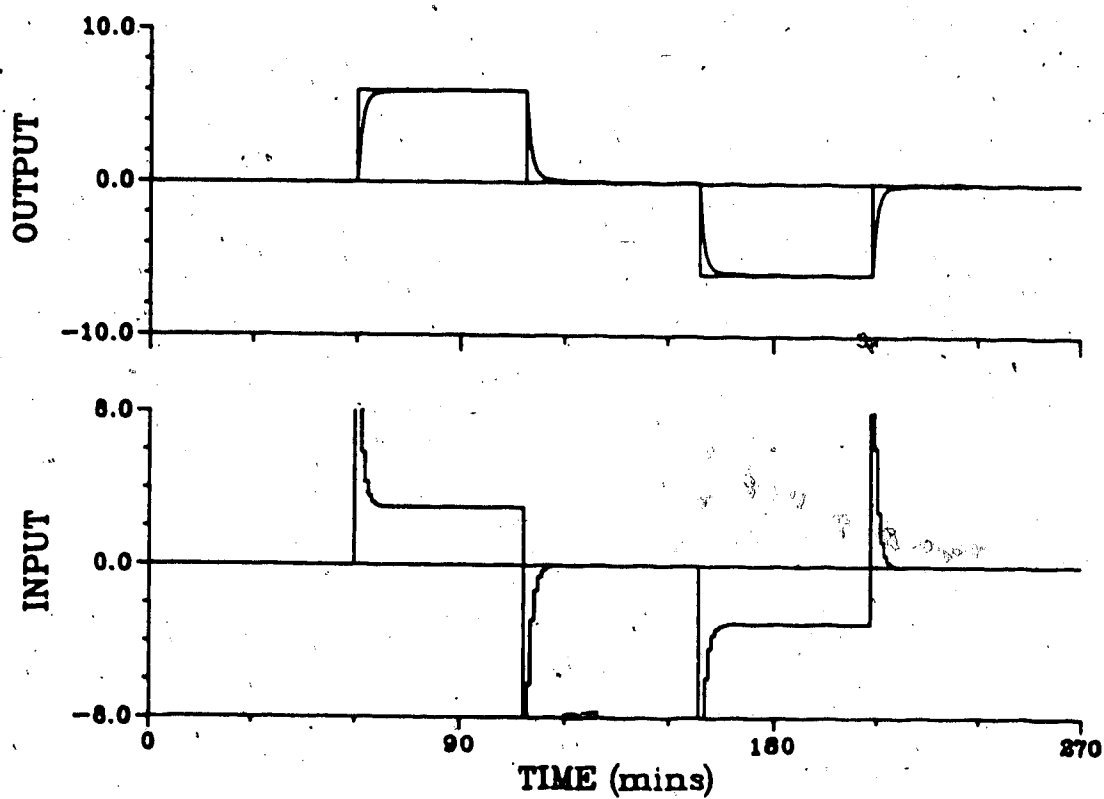


Figure 7.2b - PI Control of the STF with the Time Delay Removed and  $PB=38.0$ ,  $TI=12.0$

0.5. This is explained further in Section 7.2.4. Despite the fact that PI control is providing rather poor control, the self-tuning parameters converge to their true values very quickly as shown in Figure 7.3a. The true values of  $g_0 = 0.19033$ ,  $g_1 = 0.17221$ ,  $g_2 = 0.15583$  and  $f_0 = 0.74082$  were found by converting the transfer function in Figure 7.1 to its equivalent Z-transform.

In the case where the time delay has been removed, only one G parameter is required. This is illustrated in Figure 7.3b by the identification of only one nonzero G coefficient, despite specifying three coefficients for the identification routine. The final value of the F coefficient in Figure 7.3b is 0.9048.

#### 7.2.4 Minimum Variance Control

Minimum variance (MIN VAR) control, where the Q weighting polynomial is set equal to zero, has the characteristic of utilizing very large changes in control action to quickly return a deviating output to its set point. For simulations this is not a problem, but in practice this will cause excessive wear on final control elements.

If the exact values of the controller polynomial coefficients are known, it is possible to achieve very good control. In Figure 7.4 the true coefficient values given above have been used. The output returns to the set point in one sample interval after the delay of two sample intervals,

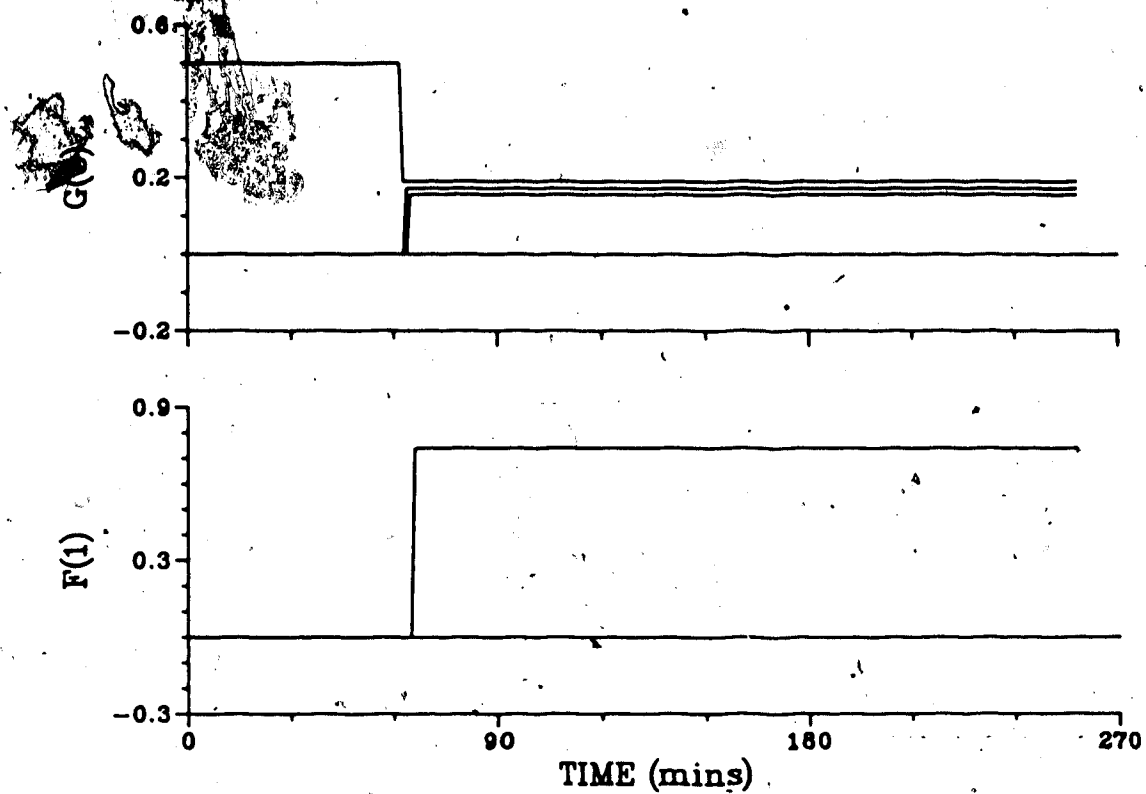


Figure 7.3a - Parameters Identified during PI Control of the Single Transfer Function

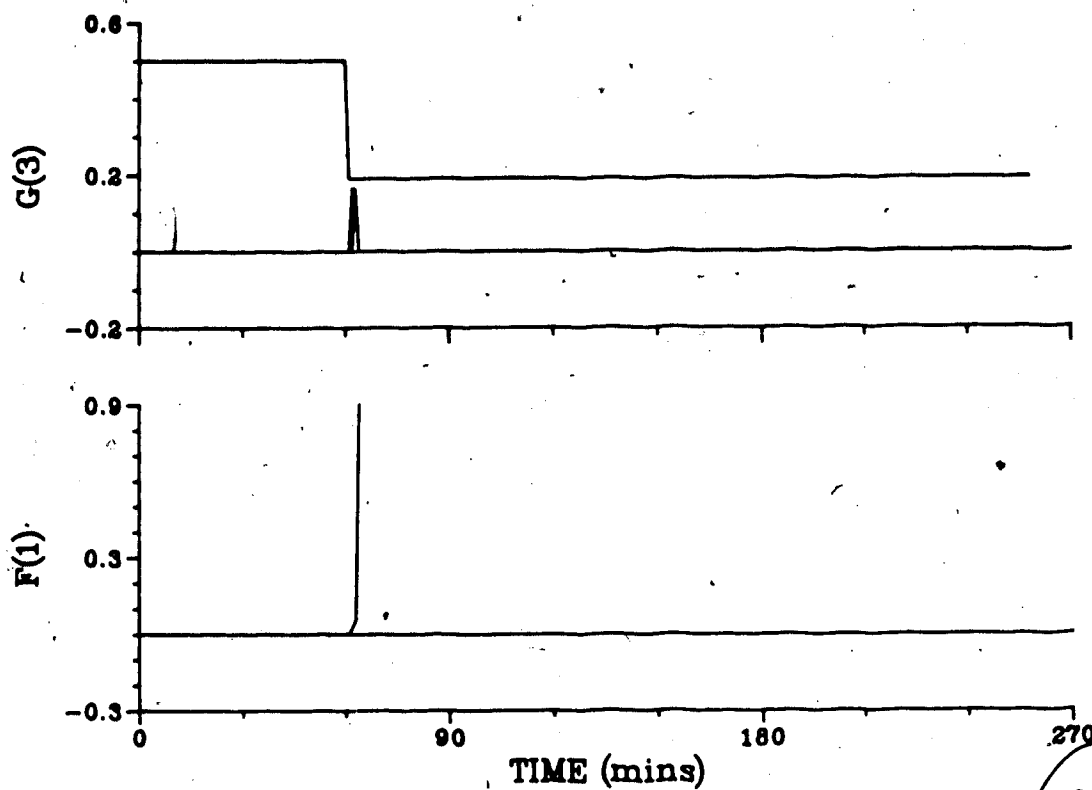


Figure 7.3b - Parameters Identified during PI Control of the Single Transfer Function with No Time Delay

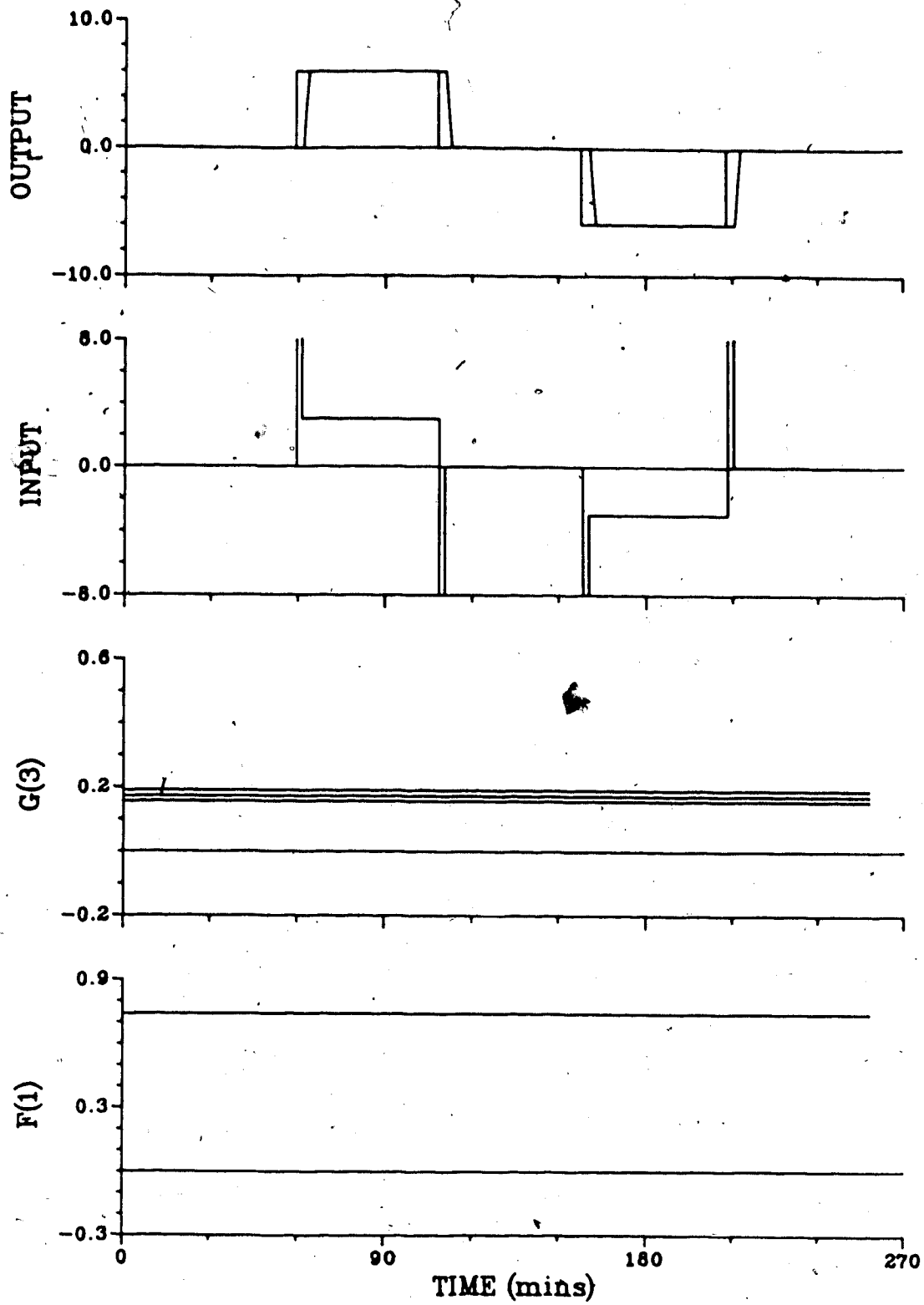


Figure 7.4 - Minimum Variance Control of STF using Known Coefficient Values ( $g_0=0.19033$ ,  $g_1=0.17221$ ,  $g_2=0.15583$  and  $f_0=0.74082$ )

and no adjustments to the values of the coefficients are necessary. Note that since no limits have been placed on the control (input) action, a very severe action is taken to return the output to the set point as quickly as possible. As a result of scaling the figures the maximum and minimum values of the control action have been cut off.

In a practical situation, the actual coefficient values are unknown, which is why an identification scheme is required. A logical starting point would be to set all the coefficients to zero, except for  $g_0$ . Since the control action in the minimum variance case is an "error" multiplied by  $1 / g_0$ , care must be taken to ensure that  $g_0 \neq 0.0$ . This is initially accomplished by setting  $g_0 = 0.5$ . Although the choice of 0.5 is somewhat arbitrary, it has been used in previous studies, [Tham, 1985, Vagi, 1987], since it is of the same order of magnitude as the expected final value of  $g_0$ . Figure 7.5 presents the results of a simulation in which minimum variance control has been used and the values of the parameters are assumed to be unknown. Although once identification takes place the parameters converge rapidly to their exact values, during the first set point change the output overshoots the set point. Once the parameters have converged, the response is identical to the case for known parameters.

If four G coefficients are used instead of the three that would be specified based on the known model form, the extra coefficient,  $g_3$ , converges to a value of zero. This

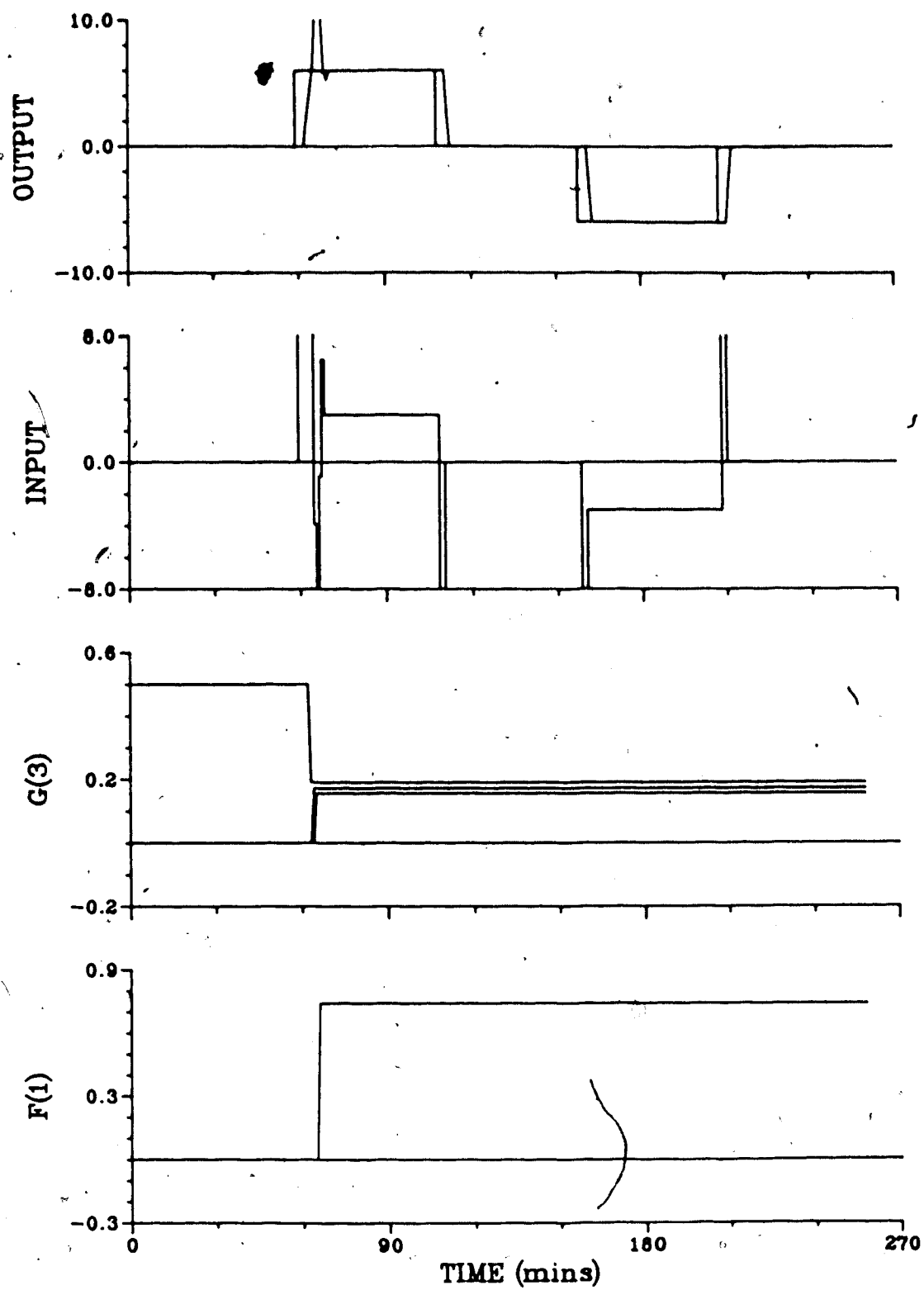


Figure 7.5 - Minimum Variance Control of STF for initial parameter values of  $g_0=0.5$ ,  $g_1=g_2=f_0=0.0$



behavior, illustrated in Figure 7.6, confirms the conjecture that over-specifying the number of coefficients is not necessarily detrimental to control performance. This suggests that if the actual number of coefficients required to model a particular process was not known, over-specifying and then successively reducing the number of coefficients until none of the coefficients are identified as zero, is an acceptable method of determining the actual number of coefficients.

In all of the minimum variance results that have been presented, there has been no mismatch in terms of model structure or time delays between the process model and the assumed model used to establish the controller parameters. To examine the effect of a poor estimate of the time delay of the process model, simulations were performed for underestimation and overestimation of the time delay in the assumed model. It was found that when the process time delay was underestimated by one sample interval, the control performance was so poor that the results have not been presented. This extremely poor performance results because the controller expects the process output to change faster than it actually does. When the output does not appear to respond to a control action, a larger than necessary controller output is produced. It is this action coupled with the fact that  $g_0$  is approaching 0.0 as it is identified, that causes the very poor control behavior. In contrast, overestimation of the assumed time delay in the

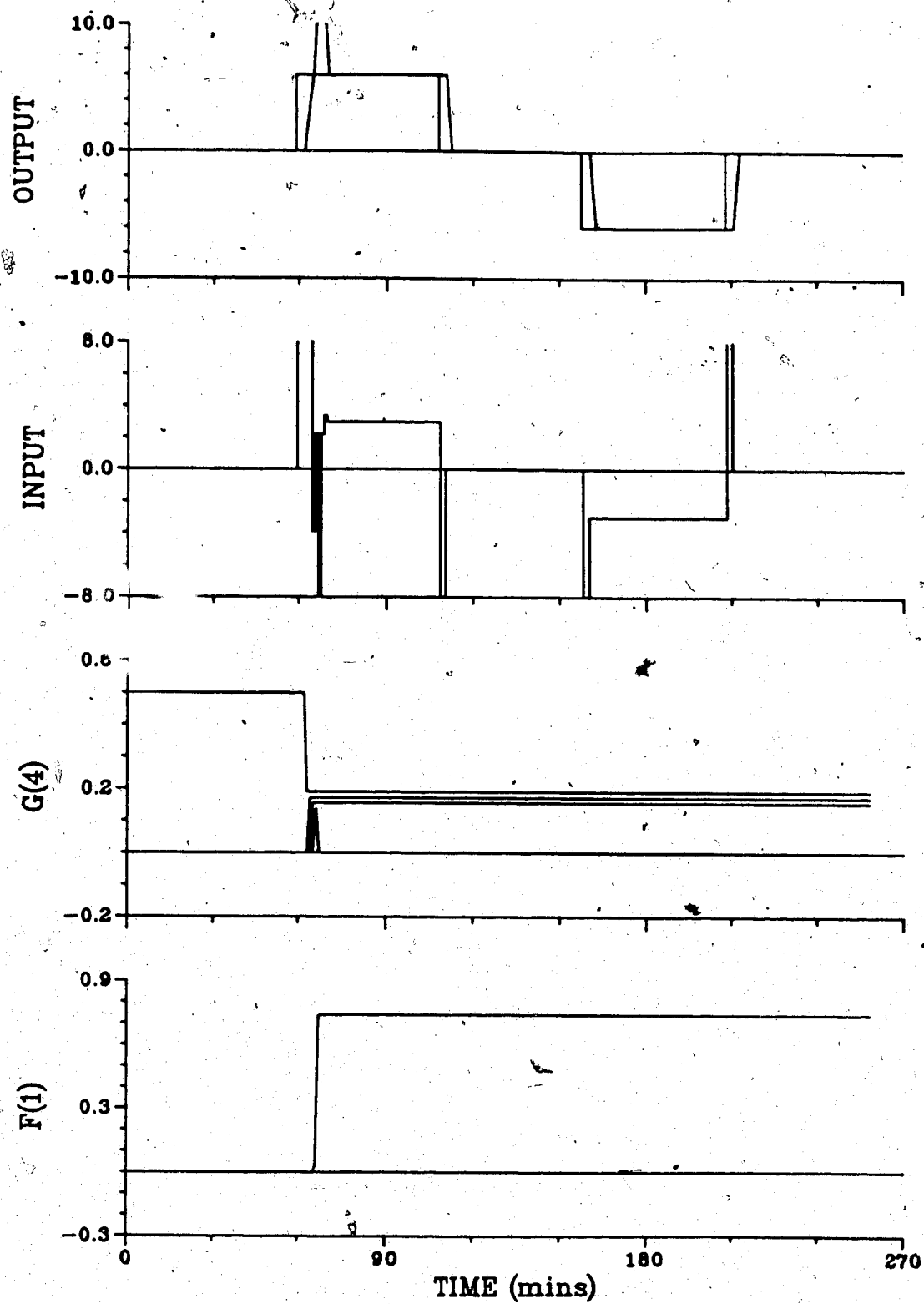


Figure 7.6 - Minimum Variance Control of STF using 4 G Coefficients

model, which effectively overestimates the number of controller polynomial coefficients, still results in reasonable control. The results for the case where the model structure for the controller is based on an assumed delay of 3 sampling intervals are shown in Figure 7.7. This demonstrates that if there is any doubt as to the correct value of the process time delay, it is preferable that the time delay be overestimated than underestimated when the minimum variance control strategy is used.

#### 7.2.5 Generalized Minimum Variance Control

The generalized minimum variance (GMV) controller utilizes the  $Q$  weighting polynomial to place some weighting on the control action. This has the effect of decreasing the severity with which the control action changes and, in practice, should extend the life of the final control element. As discussed in Section 6.4.2, it is convenient to think of the  $1 / [Q + g_0]$  term in equation 6.12 as being similar to a PID-type compensator. Unless otherwise stated, the  $Q$  weighting polynomial coefficients are established from the PID compensator as outlined earlier, except that no derivative term has been used so subsequent references will be to a PI compensator. From  $PB = 38.0$  and  $TI = 12.0$ , the  $Q$  weighting coefficients may be calculated from equation 6.11 to be:  $q_0 = 2.74$  and  $q_1 = -2.52$ . Since  $PB$  and  $TI$  are more familiar terms than  $q_0$  and  $q_1$ , they will be used when specifying how the  $Q$  coefficients were calculated.

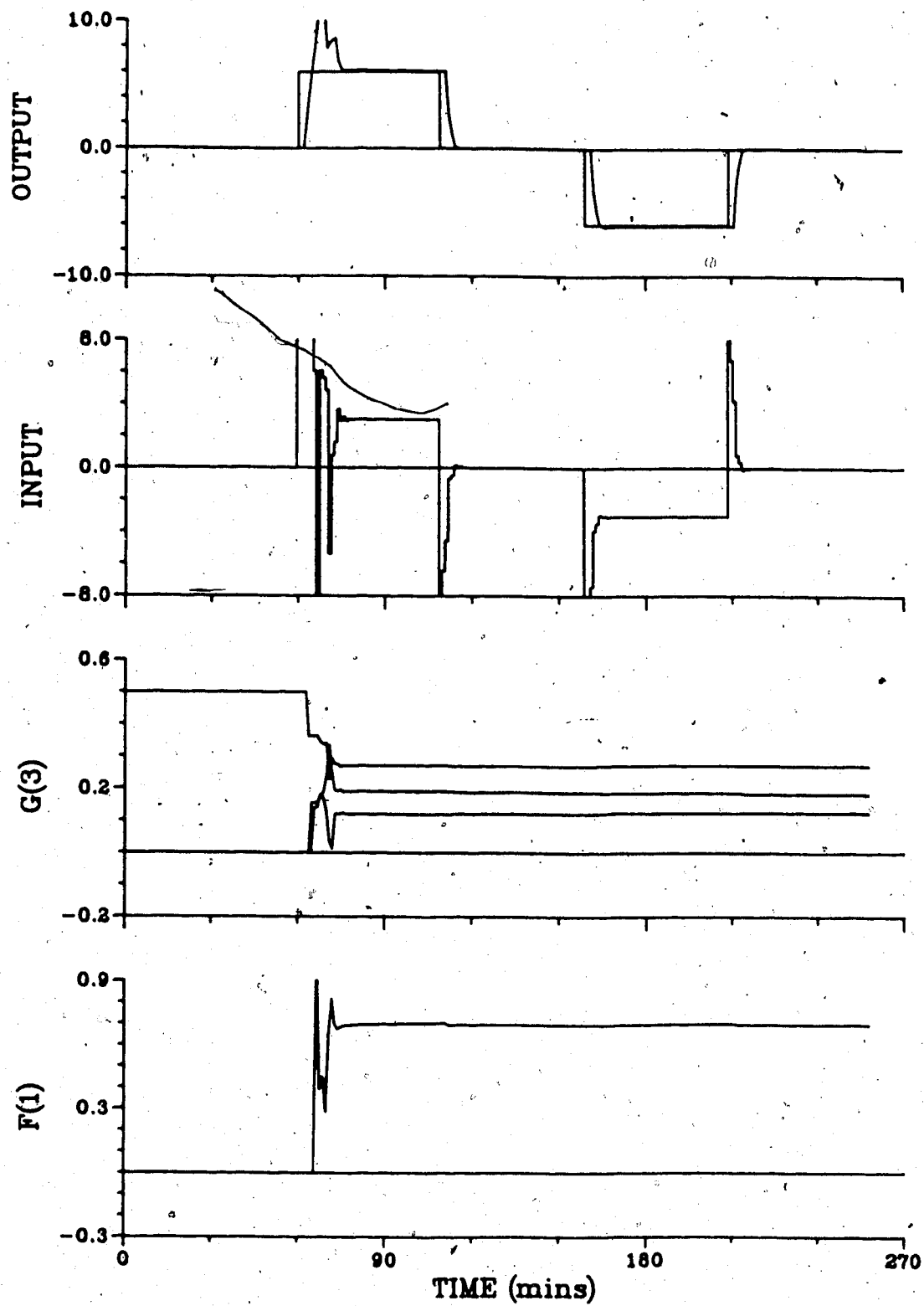


Figure 7.7 - Minimum Variance Control of STF with the Process Time Delay Overestimated

As can be seen from the results shown in Figure 7.8, if the actual values of the controller polynomial coefficients are known, very good control behavior results. Comparison of the process outputs plotted in Figures 7.4 and 7.8 show that the GMV controller did not perform as well as the MIN VAR controller, but the changes in the manipulated variable in Figure 7.8 are more acceptable. Although the initial control action in each step is quite large, a step change in the setpoint represents a very sudden, large error for the controller to correct.

Obviously, if the actual coefficients had not been known, the initial tuning-in period, commencing with the first step change, would display poorer control performance than that shown in Figure 7.8. Once the parameters have converged, the responses of the known parameter and the unknown parameter cases should be identical as is observed by comparing the output plots of Figures 7.8, 7.9 and 7.10. Figure 7.9 shows the control performance for the case where all the coefficients are initially set to 0.0, except for  $g_0$ , which is set to 0.5 to start. Since  $g_0$  is not the only term in the denominator (cf. equation 6.12) it is also possible to set  $g_0 = 0.0$ . This was done to obtain the output response shown in Figure 7.10. It can be seen from Figure 7.10 that during the tuning-in period the control behavior is not satisfactory. Hence, where applicable,  $g_0$  will initially be taken as 0.5.

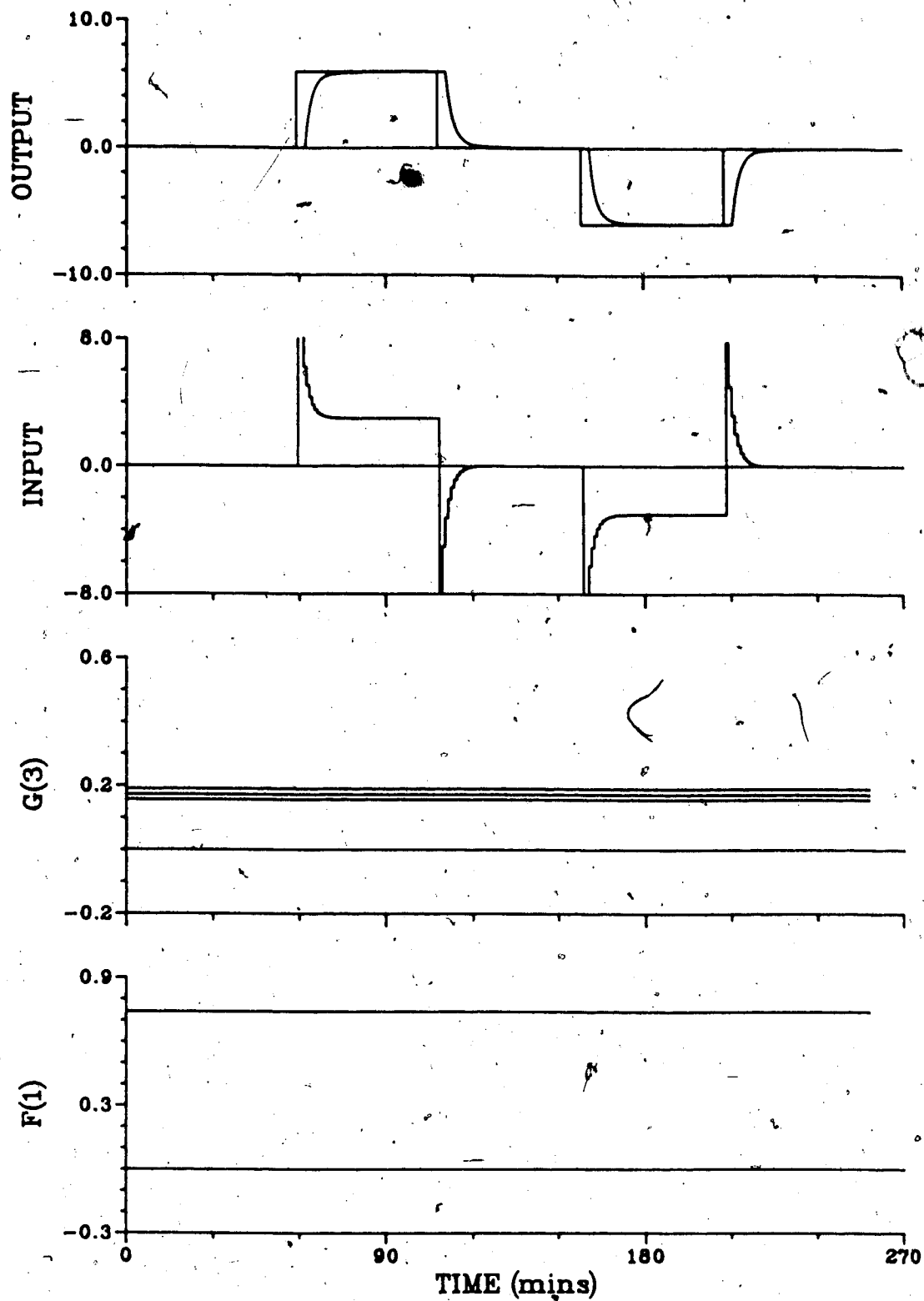


Figure 7.8 - Generalized Minimum Variance Control of STF using Known Coefficient Values ( $g_0=0.19033$ ,  $q_1=0.17221$ ,  $q_2=0.15583$  and  $f_0=0.74082$ )

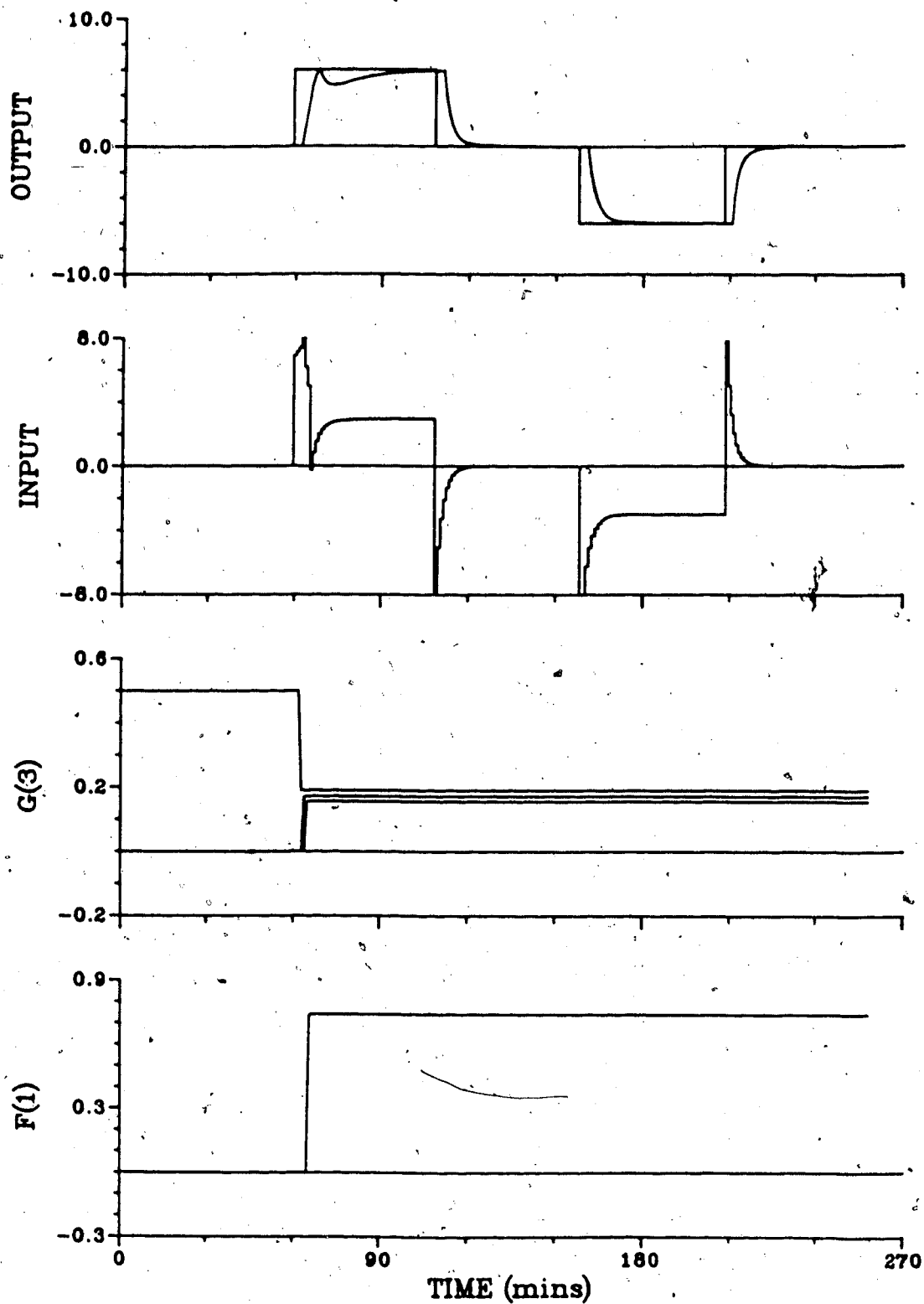


Figure 7.9 - Generalized Minimum Variance Control of STF with initial parameter values of  $g_0=0.5$ ,  $a_1=a_2=f_0=0.0$

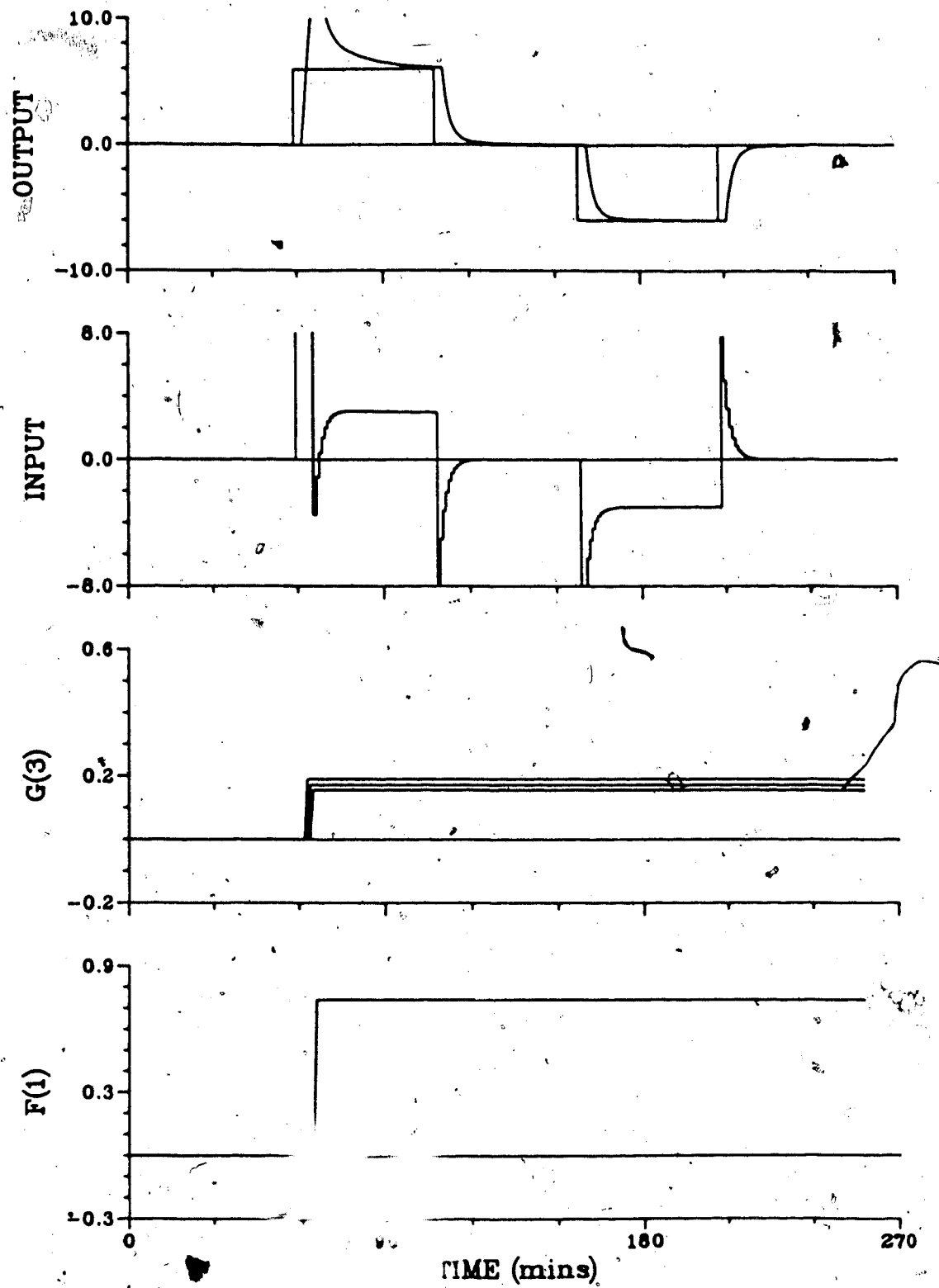


Figure 7.10 - Generalized Minimum Variance Control of STF for zero initial parameter values



As was illustrated for the minimum variance control strategy, addition of an extra  $G$  coefficient will result in the extra coefficient being identified as 0.0 leading to the parameter adaption pattern shown in Figure 7.11.

In Section 6.4.2 it was suggested that one method of obtaining a direct correspondence between the PID-type compensator and the  $Q$  weighting polynomial is to set  $g_0 = 0.0$  and not adapt the value. The results of treating  $g_0$  in this manner are presented in Figure 7.12. Setting  $g_0 = 0.0$  in effect reduces the number of  $G$  coefficients to two. Despite this fact, after the tuning-in period, control is still quite acceptable. However, the large deviations of the output from the set point experienced during the parameter tuning phase may not be acceptable.

In an effort to avoid reducing the order of the model used by the controller, but to force  $g_0$  to 0.0, it is possible to add a fourth  $G$  coefficient. Even when  $g_0 = 0.0$ , 3  $G$  coefficients will remain to model the system. From the  $G$  parameters plotted in Figure 7.13 it is seen that one of the coefficients is identified to practically zero, which may have been expected. Adding the fourth  $G$  coefficient does not result in any improvement in the output response to the set point changes.

As discussed in Section 6.4.2, if the time delay assumed for the model structure of the controller was reduced to 1 sampling interval, thereby underestimating the model time delay, instead of  $g_0$ ,  $g_1$  and  $g_2$  being identified,

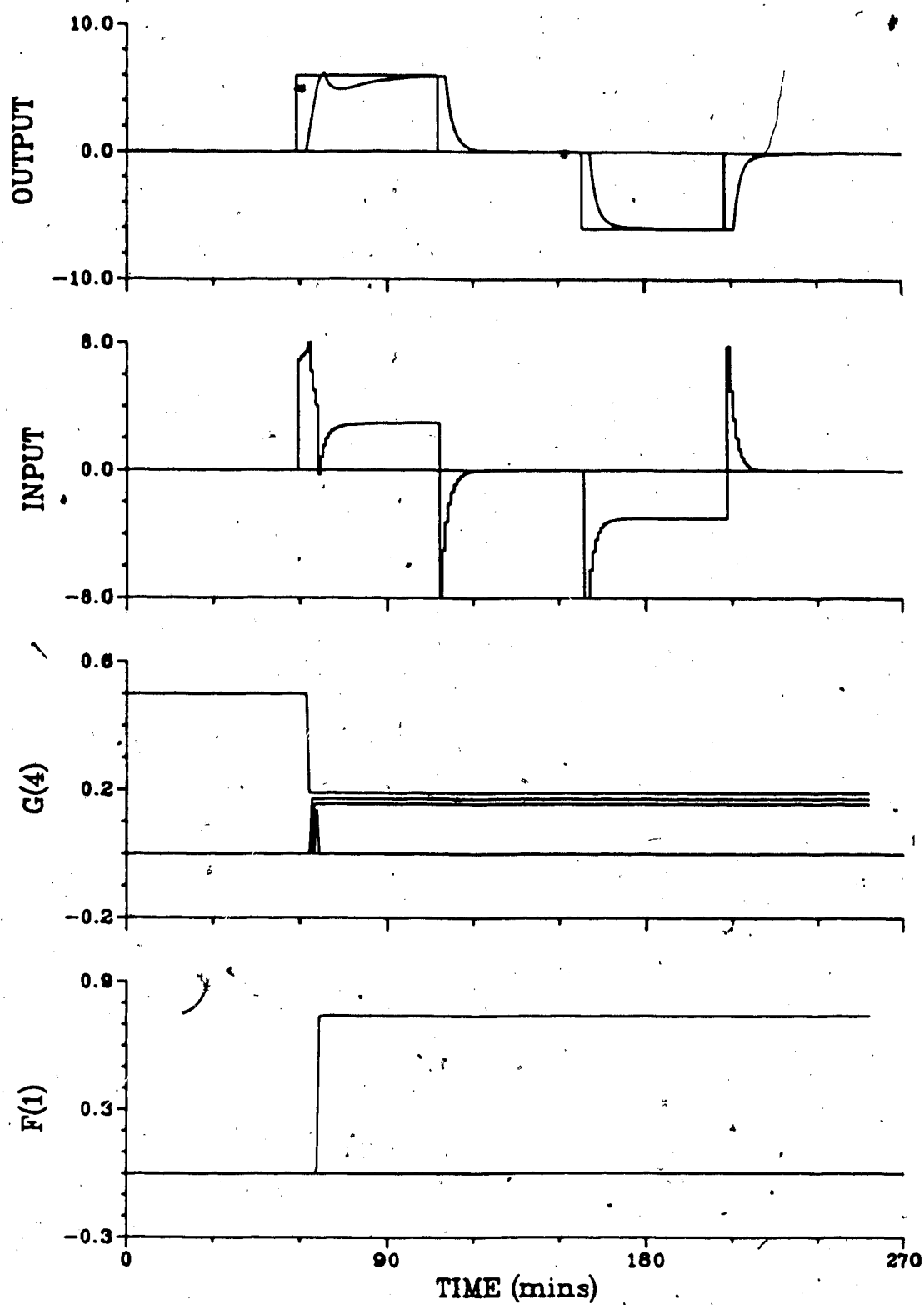


Figure 7.11 - Generalized Minimum Variance Control of STF using 4 G Coefficients

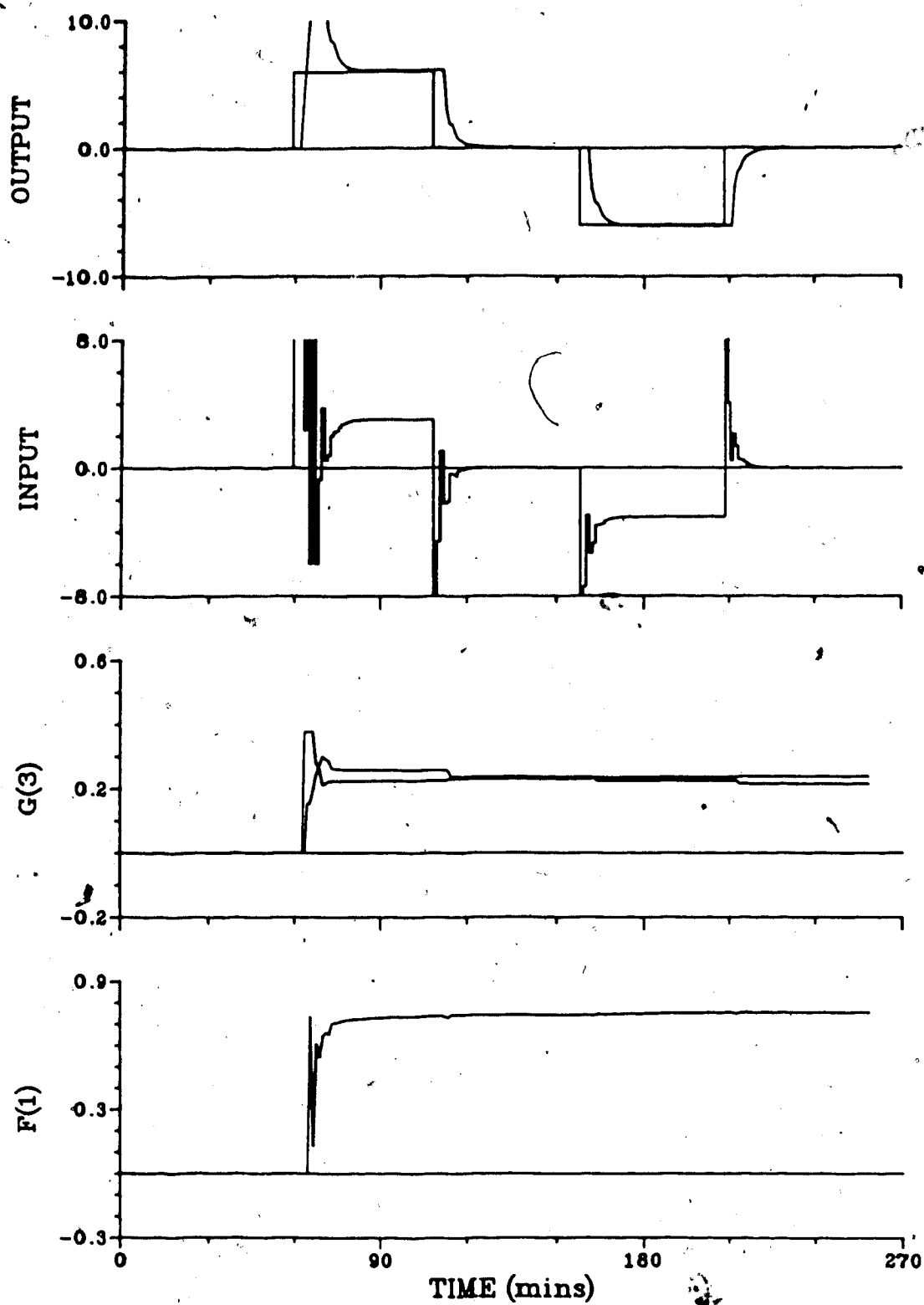


Figure 7.12 - Generalized Minimum Variance Control of STF for a set value of  $g_0=0.0$

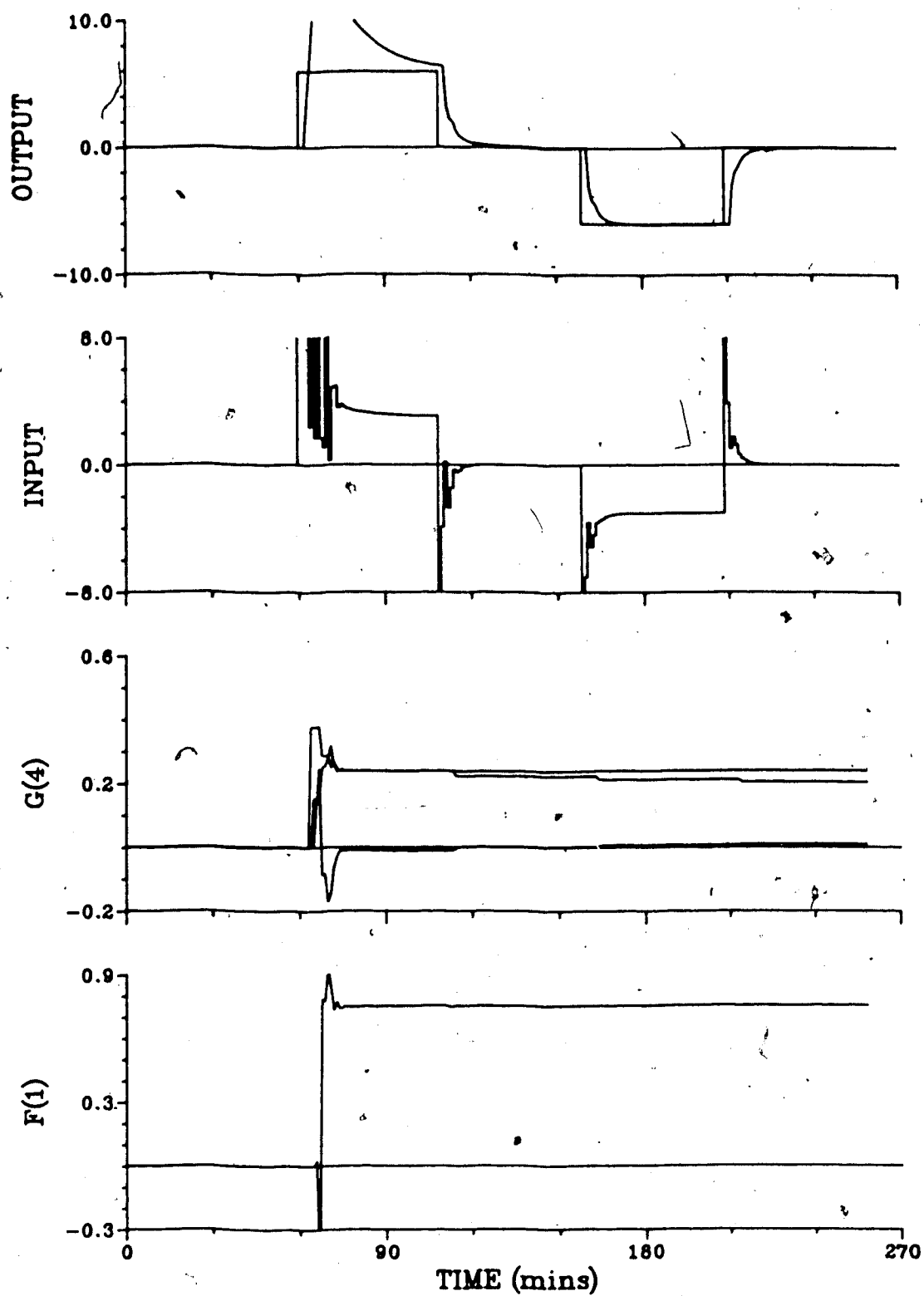


Figure 7.13 - Generalized Minimum Variance Control of STF using 4 G Coefficients and a set value of  $g_0=0.0$

$g_1$ ,  $g_2$  and  $g_3$  should now be identified to the previous values of  $g_0$ ,  $g_1$  and  $g_2$ . From the  $G$  parameter plots given in Figure 7.14, it is apparent that underestimation of the time delay does, in fact, reduce the order of the model used by the controller. Since the control performance presented in Figure 7.14 is an improvement over the minimum variance strategy, this suggests that the difficulties experienced when underestimating the delay in the minimum variance case arose strictly due to the fact the  $g_0$  was approaching a very small number, and the control action calculation involved dividing by  $g_0$ .

A simulation was also performed where the process time delay was again underestimated in the model structure of the controller (taken as 1 sampling interval). For a first order process with a time delay of 1, two  $G$  coefficients would be required so, in order that  $g_0$  may be set to a fixed value of 0.0 and two  $G$  coefficients identified, three  $G$  parameters were specified. As can be seen from the responses in Figure 7.15, this approach results in better control performance than that achieved in the other simulations. It can be seen that the initial tuning phase was not too severe, and the control performance obtained once the parameters had converged was quite good. This suggests that underestimating the time delay is not necessarily the detriment to control performance observed when using the minimum variance control strategy.

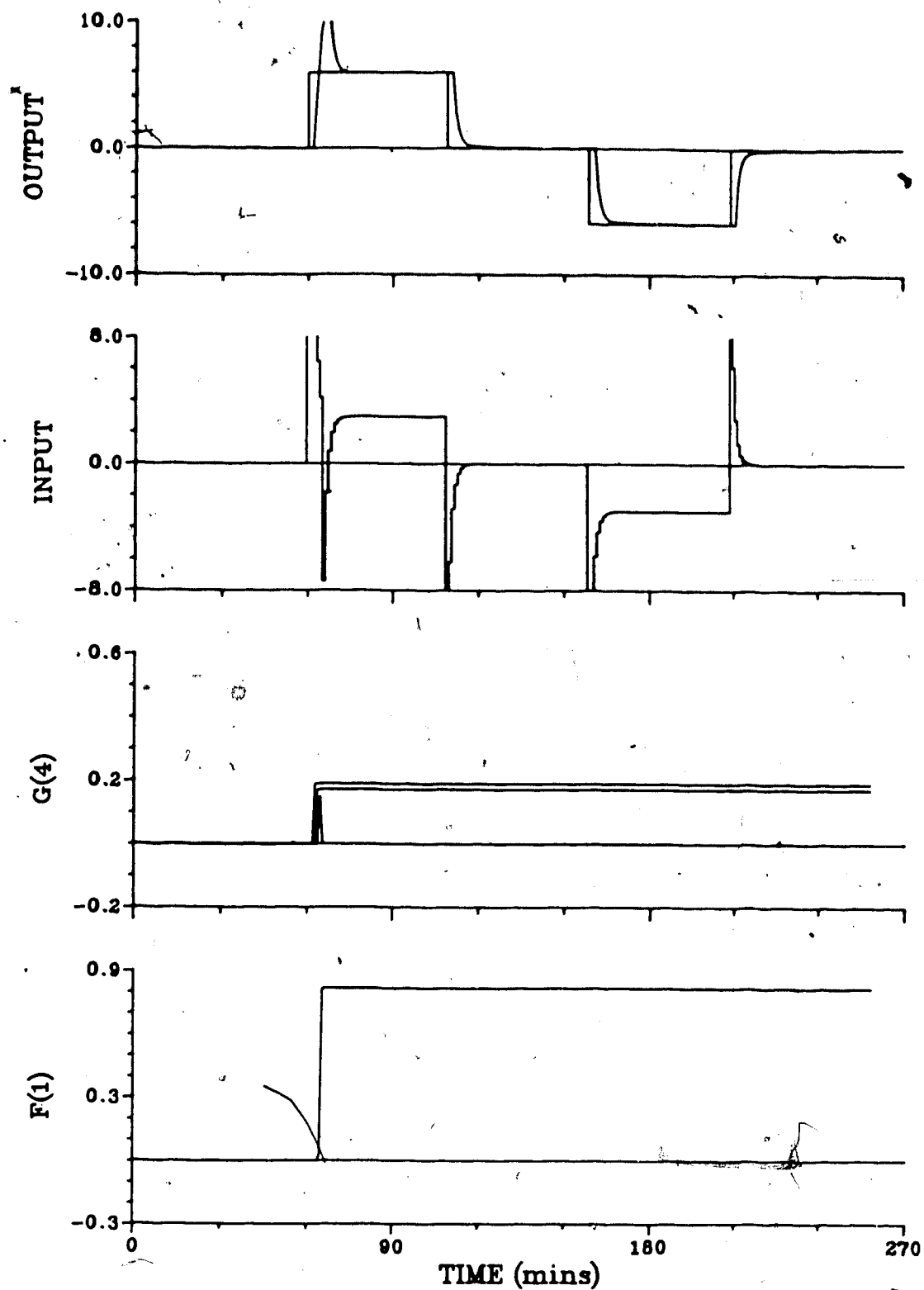


Figure 7.14 - Generalized Minimum Variance Control of STF using 4 G Coefficients and the Time Delay Underestimated

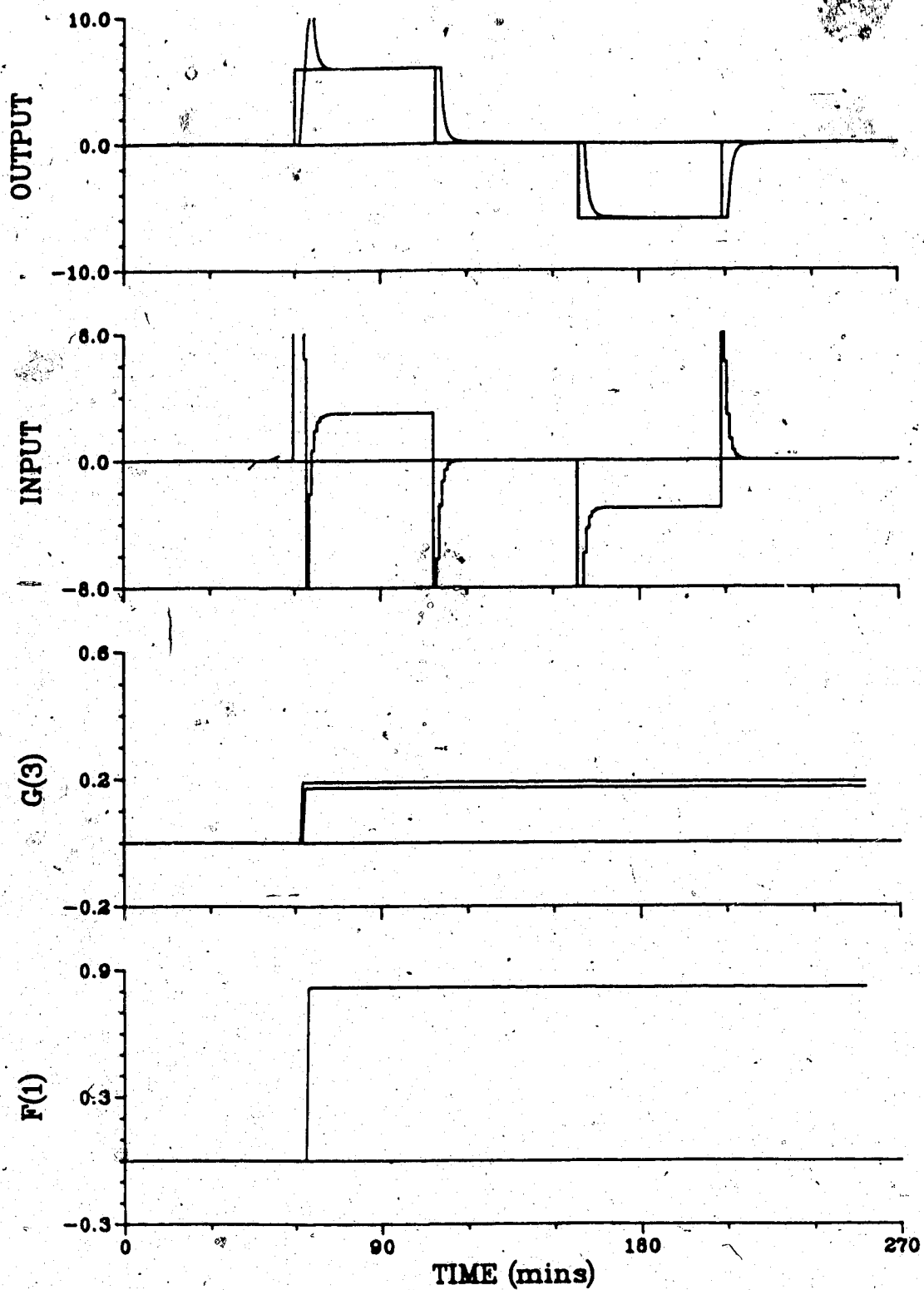


Figure 7.15 - Generalized Minimum Variance Control of STF with  $g_0=0.0$  and the Time Delay Underestimated.

The control performance was also simulated for the case in which the process time delay was underestimated by one sample interval and three G parameters were used, with  $g_0$  not fixed at 0.0. These conditions are the GMV equivalent of the minimum variance test for which the control performance was so poor that no plot has been included. It can be observed from the control performance shown in Figure 7.16 that the large deviations of the output from the set point that occurred in the minimum variance test did not occur in the GMV case since  $Q$  is nonzero. In this case letting  $g_0$  approach 0.0, does not have any detrimental effect on the control.

The final method of accounting for the  $g_0$  term that was suggested in Section 6.4.2, involved letting  $q_0$  and  $q_1$  be functions of  $g_0$ . This was evaluated by simulation leading to the response presented in Figure 7.17. Although the control performance is very good once the parameters have tuned in, the tuning-in stage is noticeably worse when compared with Figure 7.15.

#### 7.2.6 Single Transfer Function Simulation Summary

The sum of absolute error (SAE) values for all of the single transfer function simulations that were performed are compiled in Table 7.1. The total SAE value is the value for all four set point changes, while the tuned SAE value is only the SAE from the second set point change (110 minutes) which covers the portion of the test for converged parameter



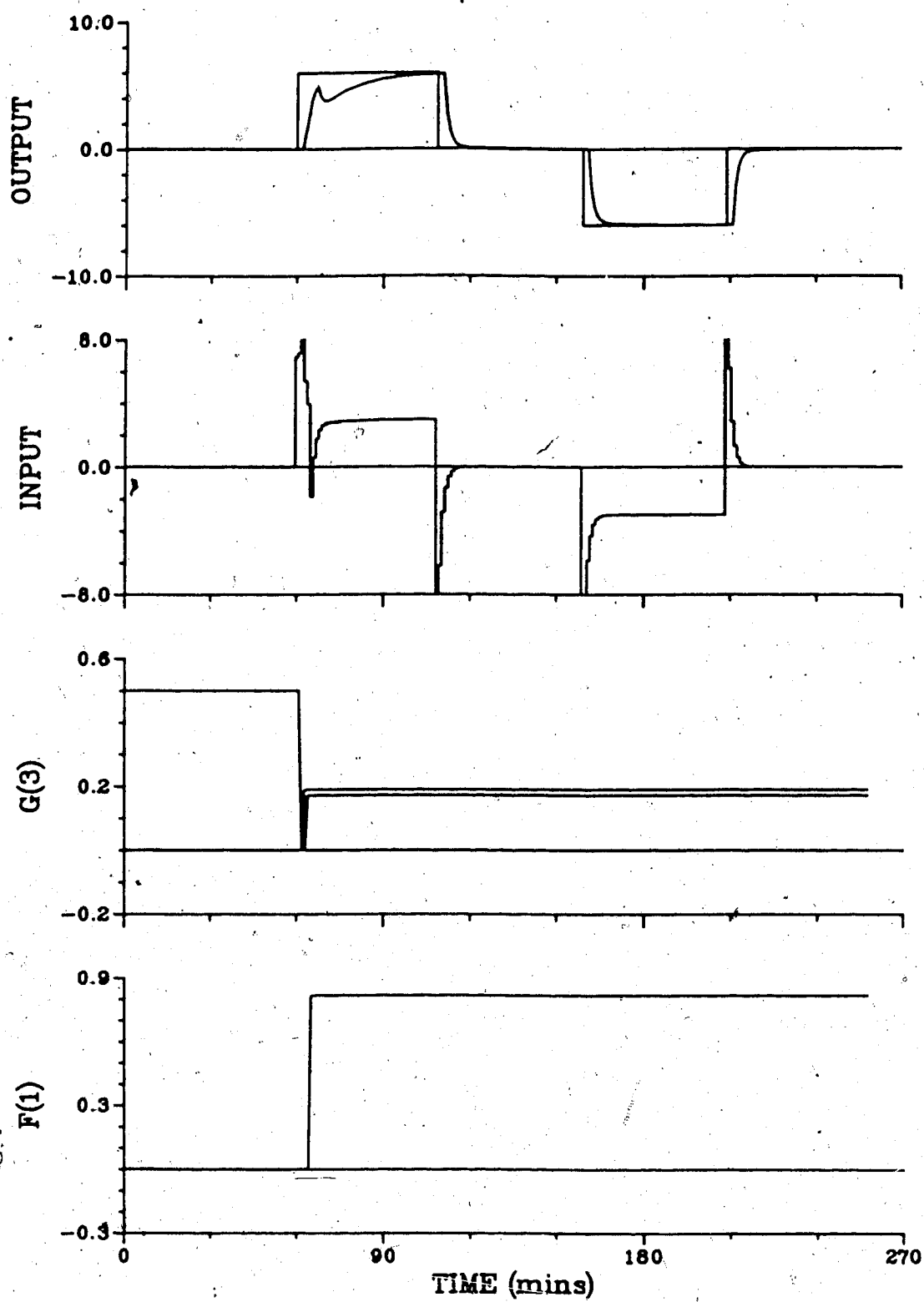


Figure 7.16 - Generalized Minimum Variance Control of STF with the Time Delay Underestimated

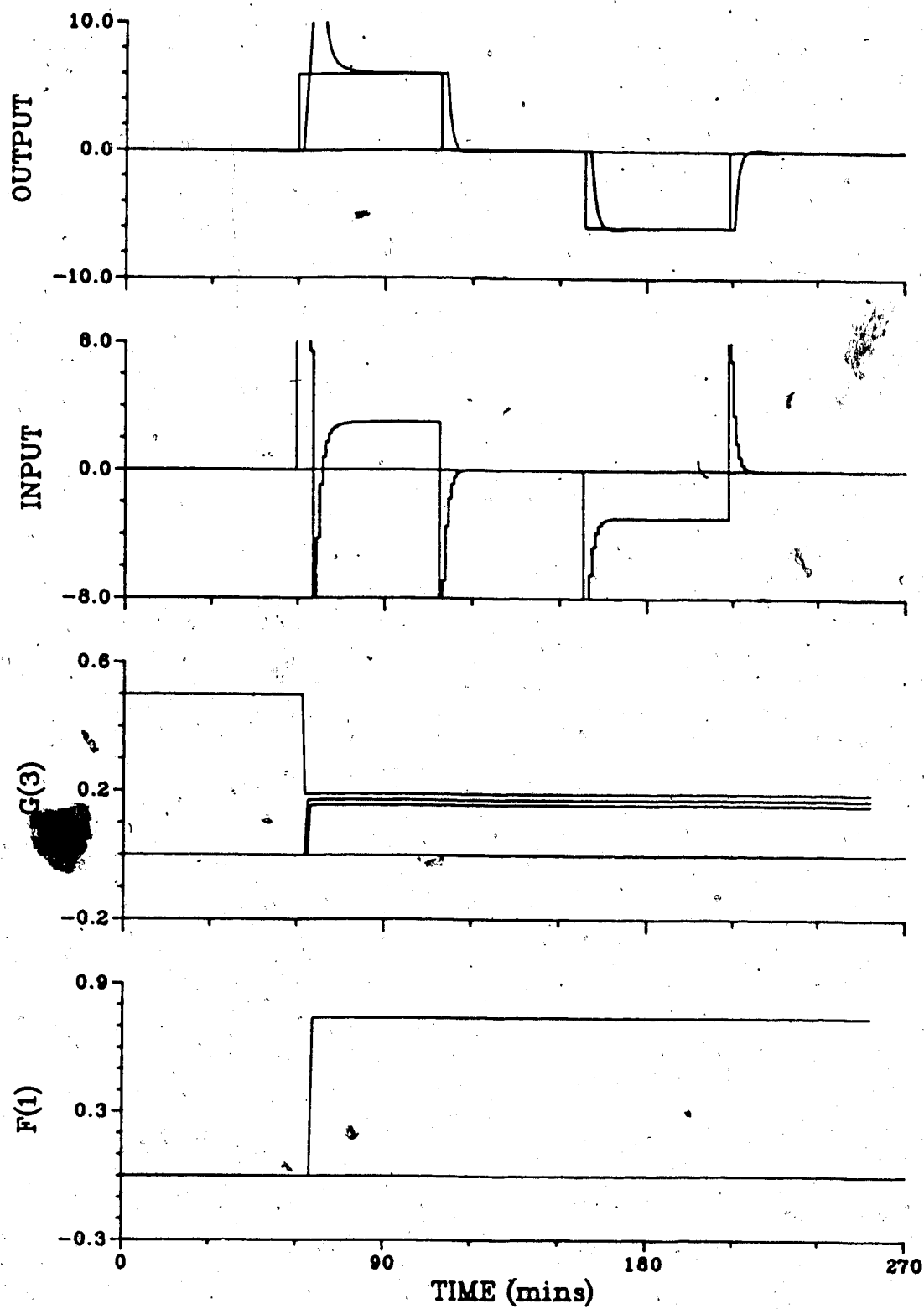


Figure 7.17 - Generalized Minimum Variance Control of STF with Q Weighting Adapted from  $g_0$

Table 7.1  
SAE Values for the Single Transfer Function Simulations

Control/Strategy	Total SAE	Tuned SAE	Figure
PI	328.81	241.34	7.2
PI / No Delay in Model	54.44	34.83	7.3
MIN VAR / Known Coefficients	82.30	55.72	7.4
MIN VAR / Unknown Coefficients	123.54	55.72	7.5
MIN VAR / 4 G's	105.98	55.72	7.6
MIN VAR / Underestimated Delay	Large	Large	—
MIN VAR / Overestimated Delay	122.91	63.51	7.7
GMV / Known Coefficients	126.33	88.73	7.8
GMV / $g_0=0.5$ Initially	144.75	87.83	7.9
GMV / $g_0=0.0$ Initially	188.03	90.23	7.10
GMV / 4 G's	142.83	87.84	7.11
GMV / $g_0=0.0$	157.90	83.31	7.12
GMV / 4 G's, $g_0=0.0$	118.44	70.72	7.13
GMV / 4 G's, Underestimated Delay	118.44	70.72	7.14
GMV / $g_0=0$ , Underestimated Delay	114.32	63.51	7.15
GMV / Underestimated Delay	139.83	69.51	7.16
GMV / Q's = function of $g_0$	135.97	66.38	7.17

values.

In all cases, except underestimating the time delay while under minimum variance control, self-tuning control provided a considerable improvement over PI control. Once the parameters have converged, minimum variance control proved to be superior to generalized minimum variance control. However, as observed from the response of the manipulated variables, minimum variance control is characterized by excessive control actions, which is of no consequence for a simulation, but would not be acceptable in practice.

Generalized minimum variance control using well tuned PI controller parameters directly in the  $Q$  weighting polynomial represents a considerable improvement over PI control. For  $g_0$  nonzero, control may be improved by attempting to remove the effect of  $g_0$  and allow  $1 / [Q + g_0]$  to take on the inverse PID structure. A combination of underestimating the time delay and setting  $g_0 = 0.0$  provided good control performance. The best results minimized deviations from the set point during the tuning-in phase and, once the parameters had converged, provided good set point following. These results were obtained when the correct number of  $G$  coefficients was used for the process time delay, but the time delay in the controller model was decreased by one sampling interval and  $g_0$  was fixed at 0.0. From Table 7.1 it may be seen that forcing  $g_0$  to 0.0 provides a considerably better tuning-in period, and a slightly better control than the case where  $g_0$  was not fixed at 0.0.

### 7.3 Two Transfer Function Plant Model Simulation

#### 7.3.1 Introduction

In Section 7.2 where a single transfer function is used as the model, it is only possible to examine servo control, the response to set point changes. With the addition of a second transfer function it is possible to examine regulatory control performance, that is, the response to a

disturbance other than a set point change. This is desirable since in the experimental work that follows, the column has been subjected to disturbances in the form of feed flow changes and not set point changes. With an additional transfer function to simulate a disturbance to the process output, it is also possible to evaluate various feedforward strategies. For these simulations the two transfer function model shown in Figure 7.18 is used.

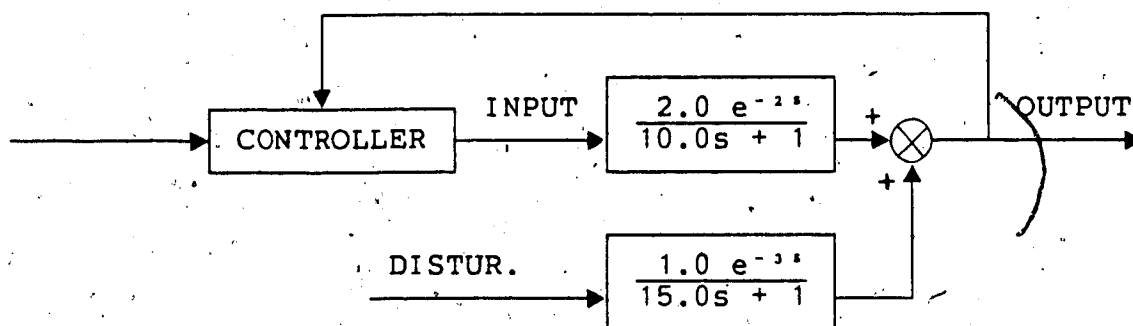


Figure 7.18 - Two Transfer Function Plant Model

The disturbance consists of a square wave pattern of 50 minute steps beginning at 60 minutes, with a magnitude of 2.0. As for the single transfer function simulations, identification began at 10 min and control at 30 minutes for each run. No noise was added to any of the signals and a sample interval of one minute was used.

### 7.3.2 PI Control

A series of simulations were made employing conventional PI control with the controller constants varied to obtain a "best" response. As in Section 7.2.2, derivative action was not found to be beneficial in controlling the process. The tuned controller constants were determined to be  $PB = 45.0$  and  $TI = 4.0$ . The output of the process when subjected to the disturbance and controlled with the PI strategy utilizing tuned constants is shown in Figure 7.19a along with the input and disturbance signals.

### 7.3.3 Parameter Identification

While the process was under PI control, the parameter identification routine was performed with the G, F and L parameters identified as shown in the parameter plots in Figure 7.19b. From the L parameter plot it is evident that no L parameters are identified. This may have been anticipated since the L parameters are associated with the feedforward signal of the assumed model, and no feedforward action was used in the simulation.

### 7.3.4 Minimum Variance Control

Three different strategies were evaluated using a minimum variance control strategy. In each simulation different amounts of information about the disturbance were used in determining the signal to provide feedforward action. The results presented in Figure 7.20 were obtained

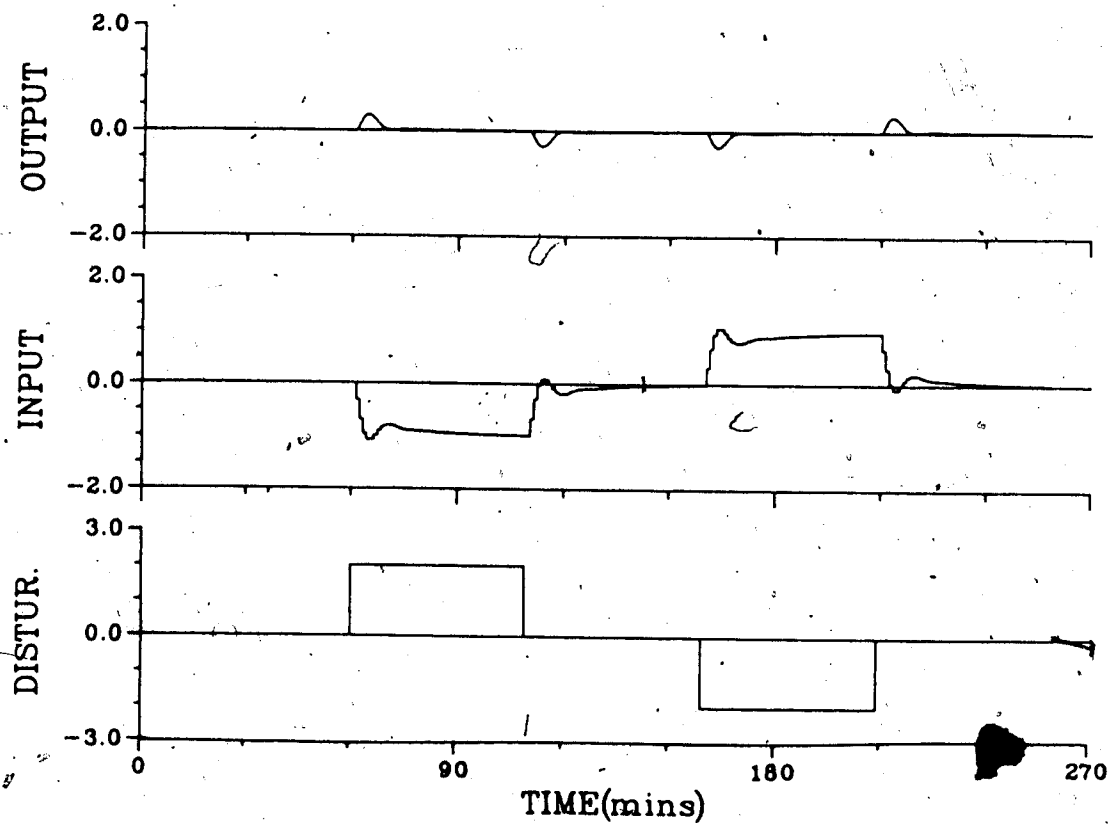


Figure 7.19a - PI Control of the Dual Transfer Function  
Model with  $PB=45.0$ ,  $TI=4.0$

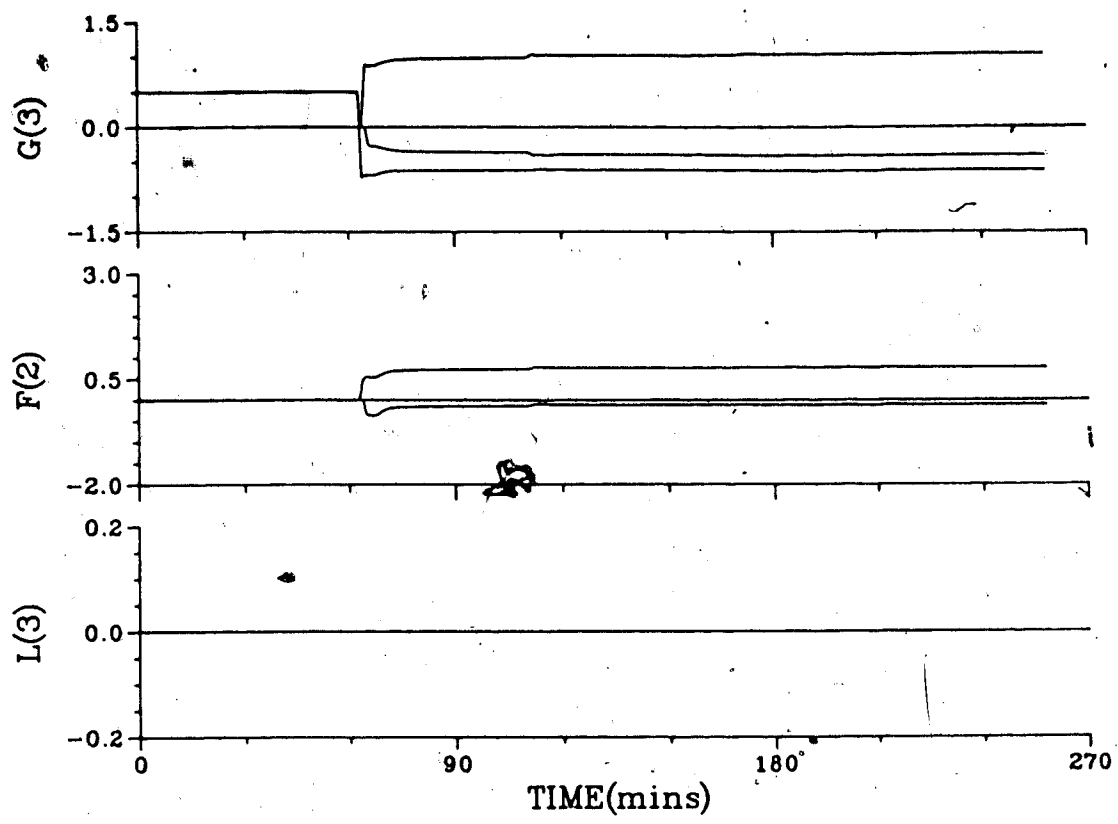


Figure 7.19b - Parameter Identification while Under PI Control of the Dual Transfer Function Model



using no feedforward action, and those in Figure 7.21 resulted from using an estimate of the disturbance,  $y(t) - y^*(t-k)$ . When the disturbance was measured the performance that resulted is shown in Figure 7.22.

As was observed for the simulations with the single transfer function system, the control performance is characterized by relatively severe changes in the manipulated variable. It does, however, provide very good control performance, particularly once the controller parameters have converged. Aside from the parameter values, there appears to be very little difference in the output response for the case of using no feedforward signal and when an estimated feedforward signal is used. The ability to measure the disturbance and use the measurement as a feedforward signal provides far superior control, as can be seen from the response of the controlled variable shown in Figure 7.22.

### 7.3.5 Generalized Minimum Variance Control

Evaluation of the performance of the generalized minimum variance controller was conducted using  $Q$  coefficients based on proportional band and integral time values used for PI control. The calculated values of the  $Q$  coefficients are:  $q_0 = 2.50$  and  $q_1 = -1.94$ . From a knowledge of the system transfer functions as given in Figure 7.18, the theoretical values for the polynomial coefficients of the controller were calculated to be:  $g_0 = 0.19033$ ,  $g_1 =$

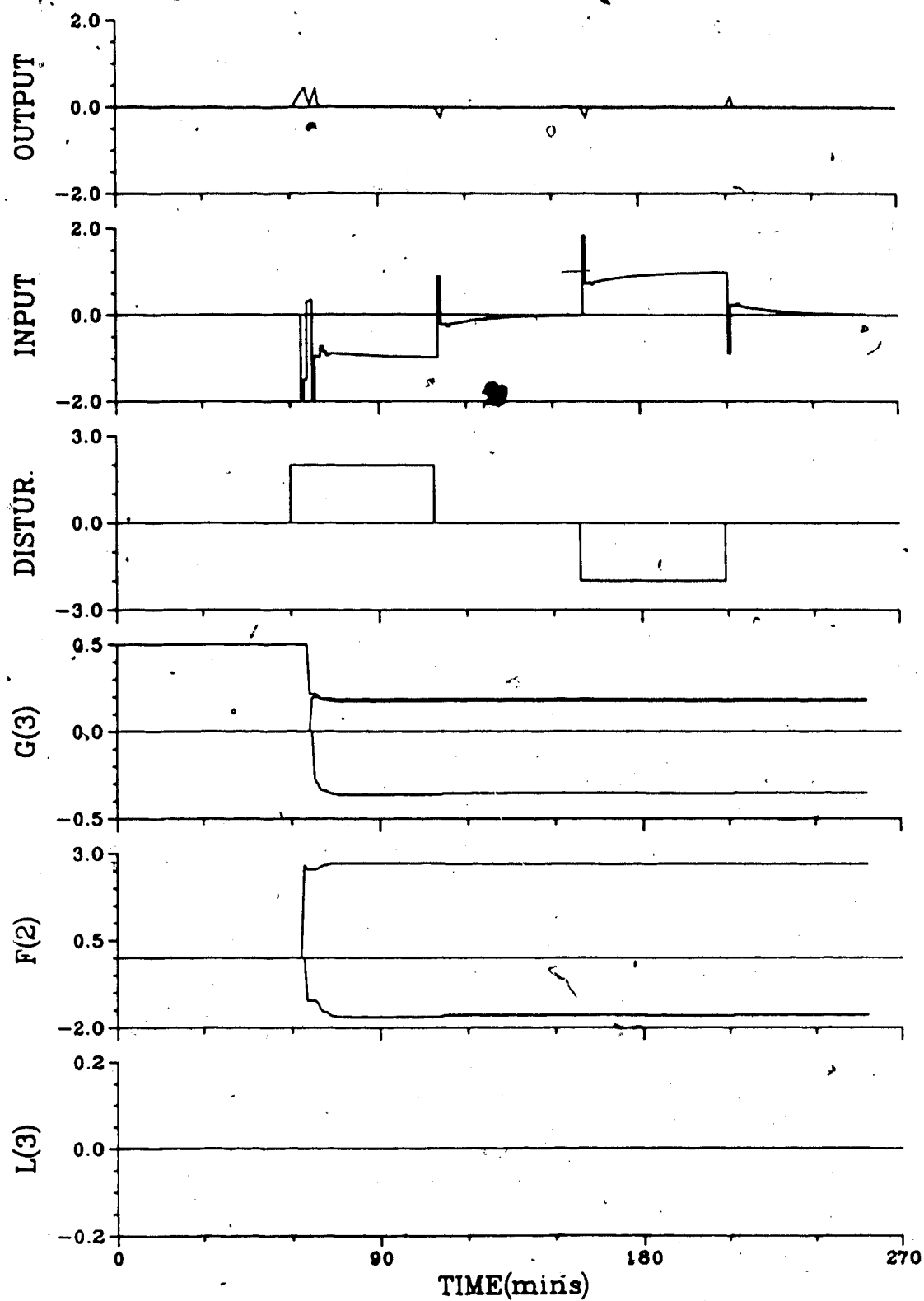


Figure 7.20 - Minimum Variance Control of the Two Transfer Function Model with No Feedforward Action (NFF)

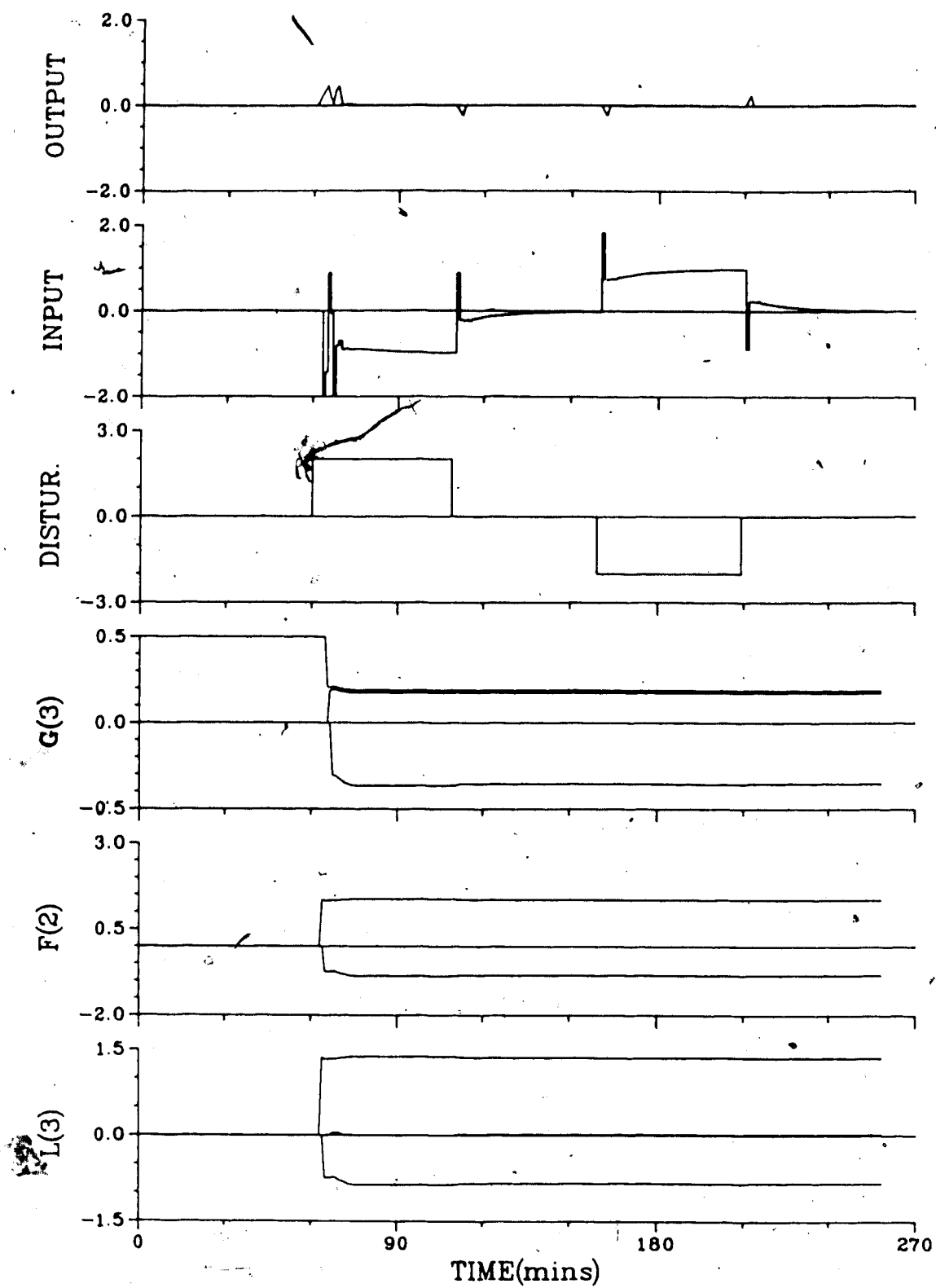


Figure 7.21 - Minimum Variance Control of the Two Transfer Function using Estimated Feedforward Action (EFF)

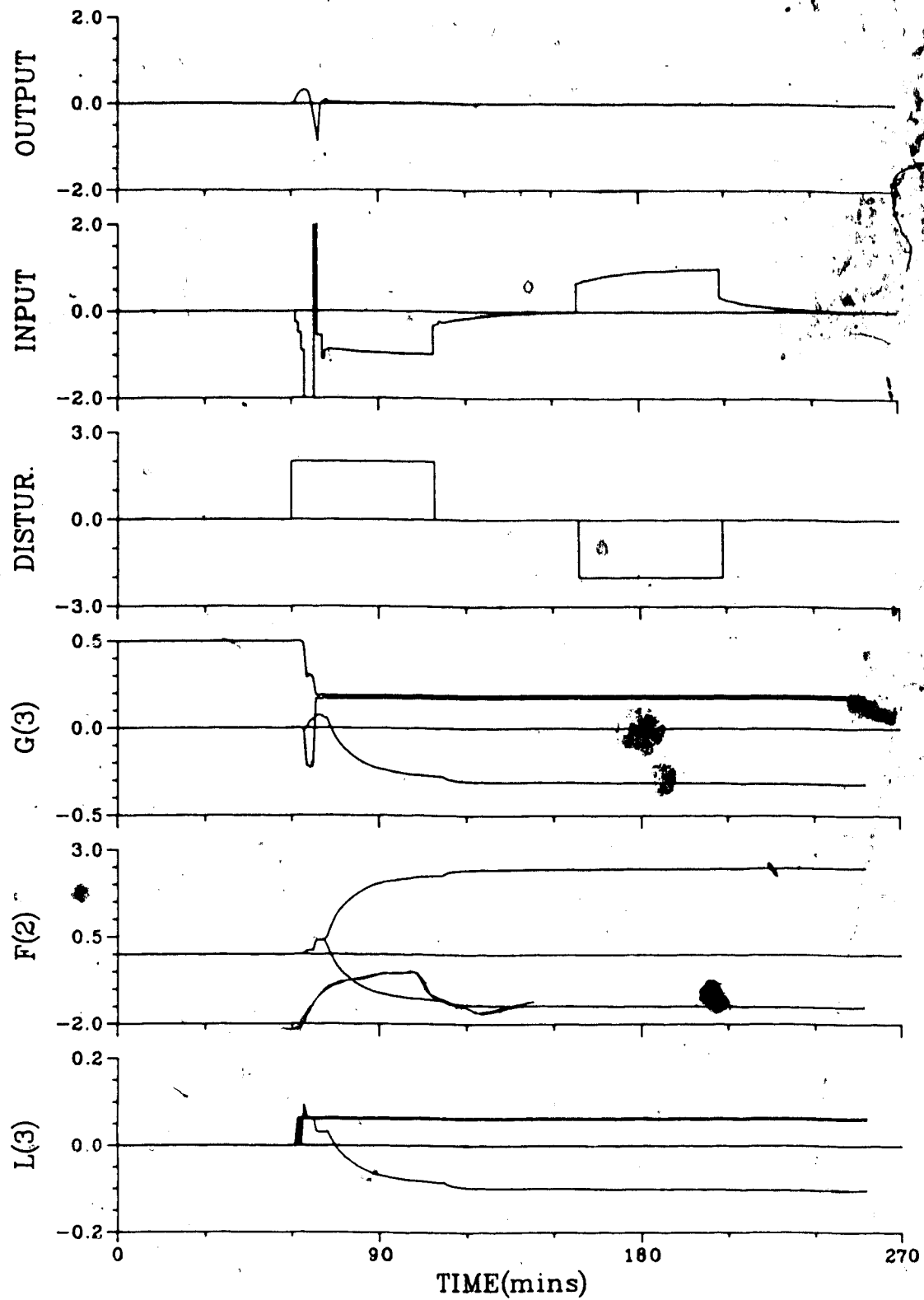


Figure 7.22 - Minimum Variance Control of the Two Transfer Function Model using the Measured Disturbance for Feedforward Action (MFF)

0.17221,  $g_2 = -0.32767$ ,  $f_0 = 2.5404$ ,  $f_1 = -1.5578$ ,  $l_0 = 0.064493$ ,  $l_1 = 0.060334$ , and  $l_2 = -0.10739$ .

If these values of the controller polynomial coefficients are used as initial coefficient values, very good control results. This can be seen from the results in Figure 7.23, obtained using the known values of the coefficients in conjunction with the measurement of the disturbance to establish the feedforward action. As expected, the changes in the manipulated variable are much less abrupt than in the minimum variance case, due to the weighting applied to the control effort. It should be noted that the known coefficient values have been calculated assuming that the measurement of the disturbance is used for feedforward action, so if estimated feedforward action or no feedforward action is used, the initial parameter values will no longer be the correct values and the identification routine adapts the parameters to different values. This is illustrated by the adaption of the parameter values shown in Figures 7.24 and 7.25 for estimated feedforward action and no feedforward action, respectively. Since some parameter adaptation is taking place, the control suffers slightly as the F, G and L parameters approach their steady state values in the latter two cases, as compared to the measured feedforward case.

For the case of assuming that the initial parameter values are unknown, all the initial values are set to zero except for  $g_0 = 0.5$ . The performance that results for no

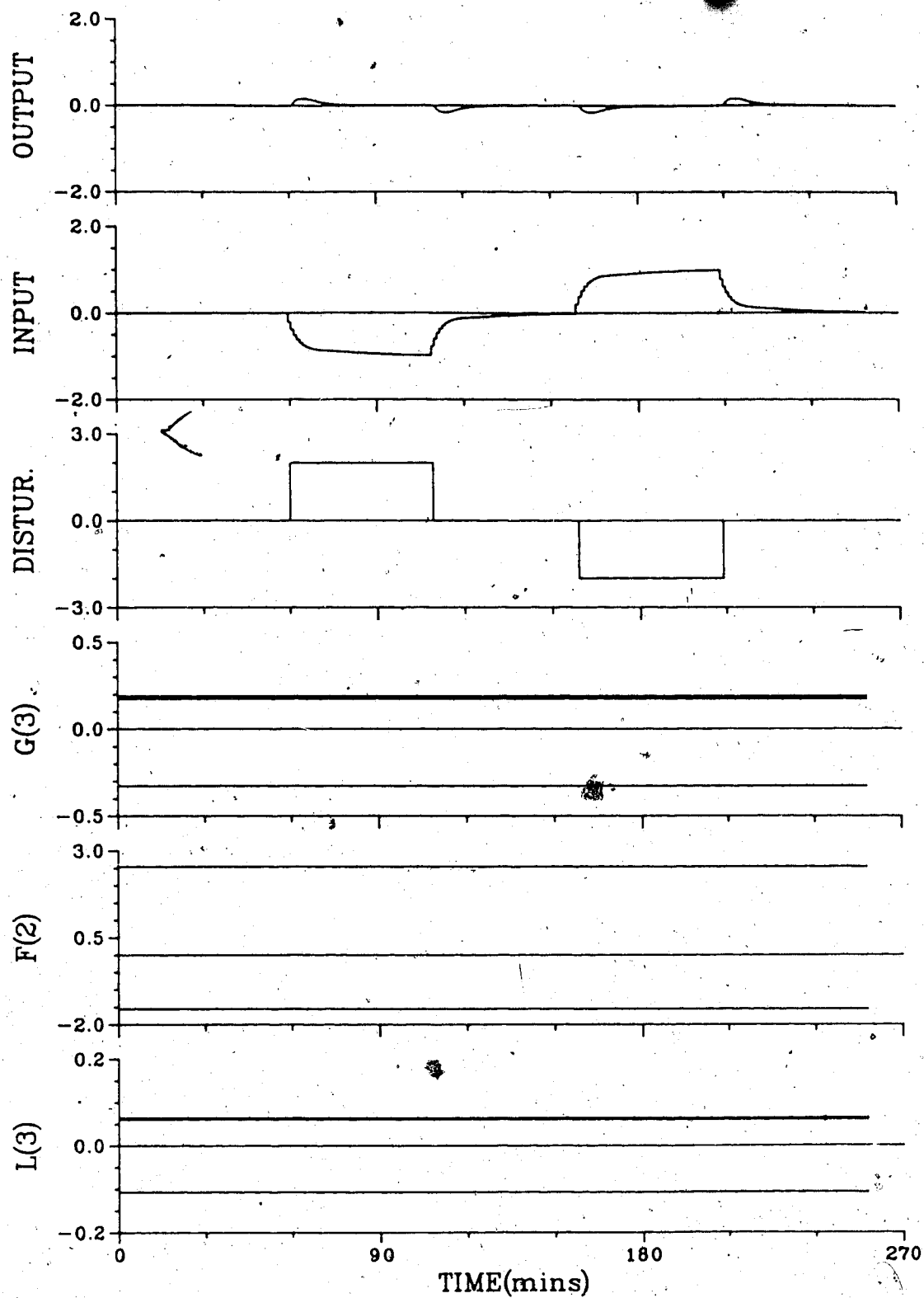


Figure 7.23 - Generalized Minimum Variance Control of the Two Transfer Function Model using Known Coefficient Values and MFE

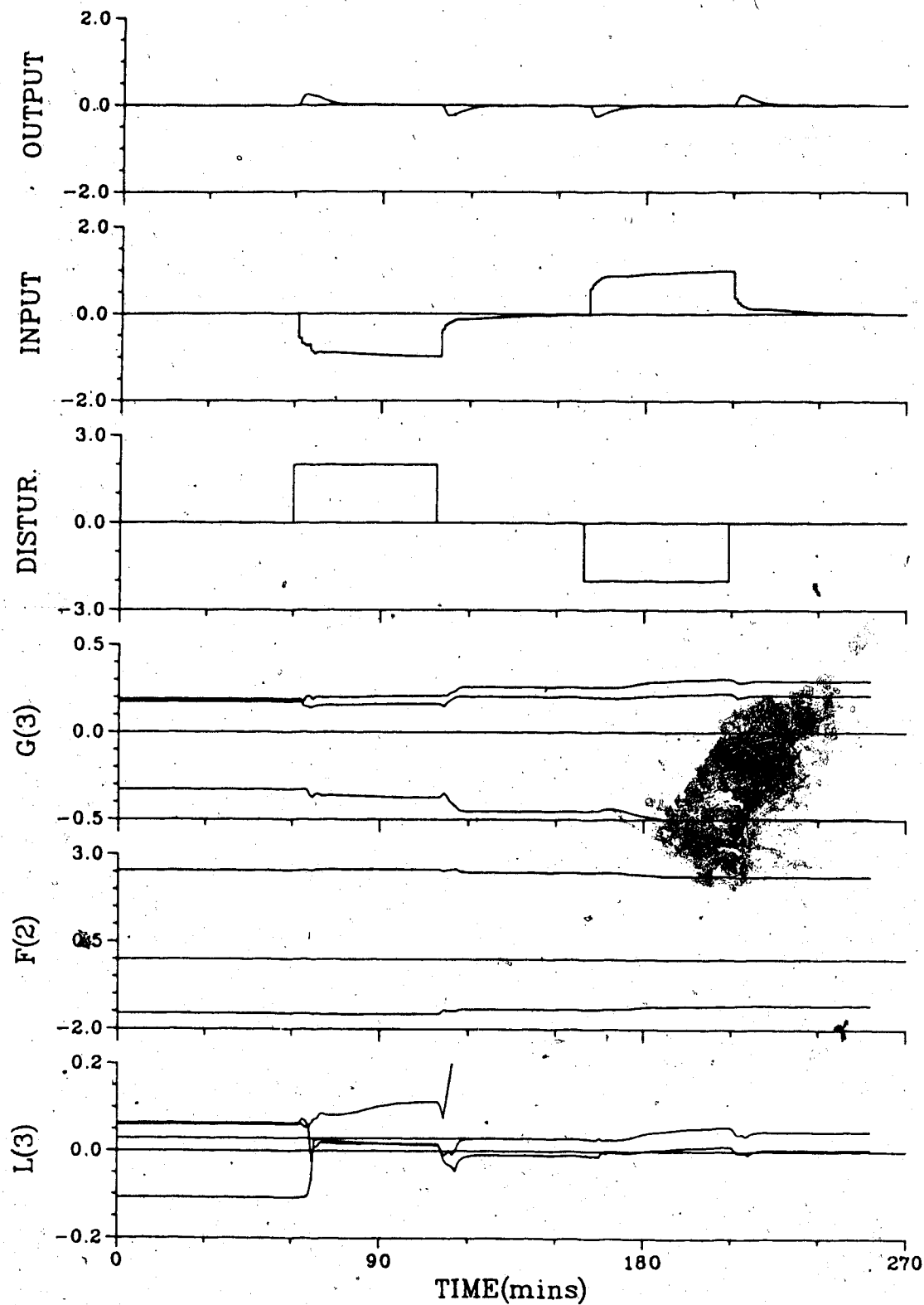


Figure 7.24 - Generalized Minimum Variance Control of the Two Transfer Function Model using Known Coefficient Values and EFF

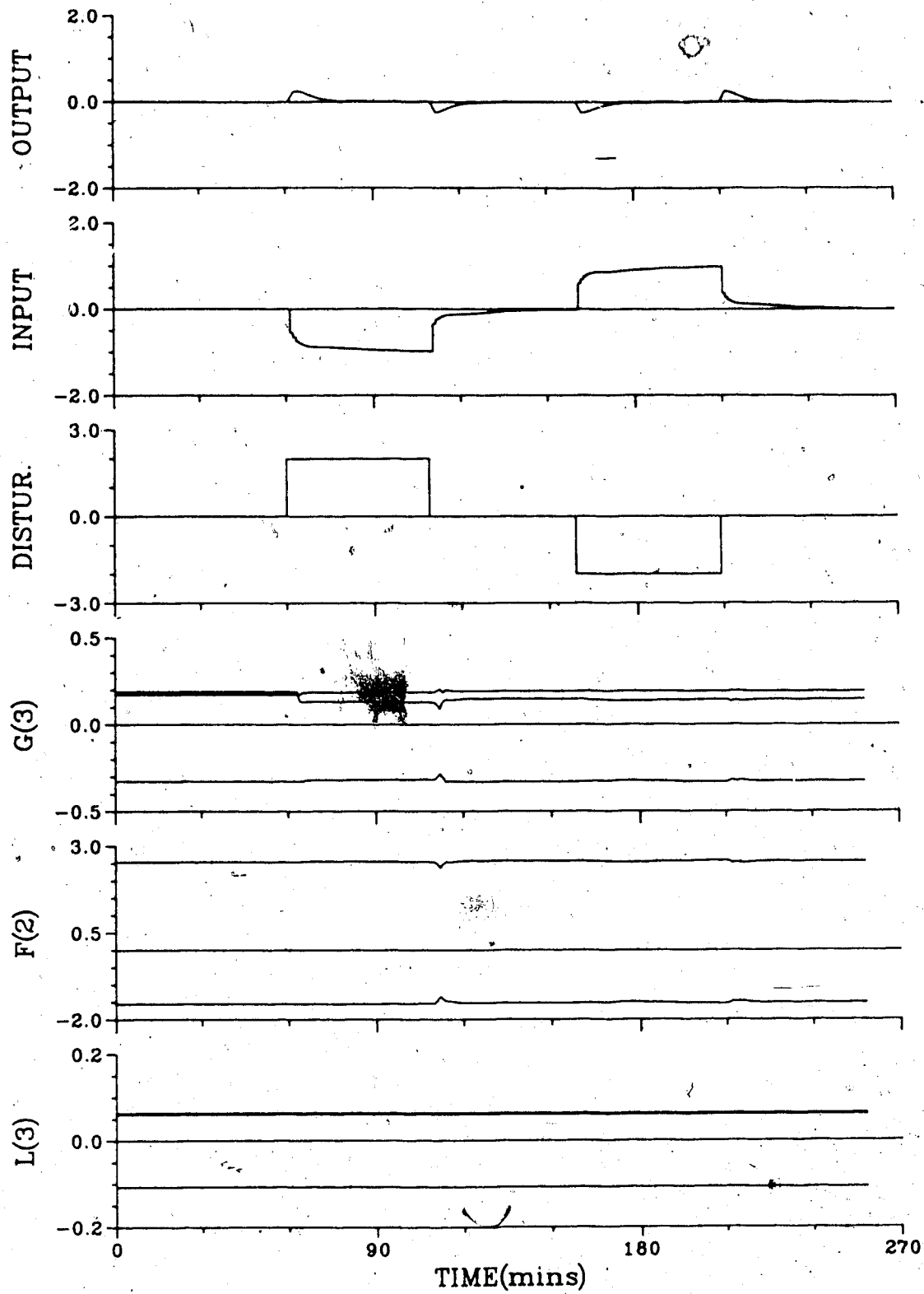


Figure 7.25 - Generalized Minimum Variance Control of the Two Transfer Function Model using Known Coefficient Values with NFF



feedforward action, an estimate of the disturbance for the feedforward action, and the measured disturbance as the feedforward action is displayed in Figures 7.26, 7.27 and 7.28. It should be noted (Dickmann and Unbehauen, [1979]) that now that the process consists of more than a single transfer function, there is no reason to expect the controller parameters to converge to their theoretical values. Of these three tests, as would be expected, the case in which the measured value of the disturbance is used as the feedforward action provided superior results and, upon close examination, it can be seen that for this case the manipulated variable responds 2 sample intervals sooner to a disturbance than either of the other two schemes. The performance exhibited by the results of the tests using an estimate of the disturbance or no feedforward action are practically indistinguishable once the parameters have converged, although with an estimate of the disturbance the parameters require a longer tuning period. It can be seen that a considerable amount of time is required for the parameters to converge and the response of the manipulated variable indicates an overdamped system when compared to the response of the manipulated variable using the PI control strategy. Only with measurement of the disturbance is better control achieved than resulted under PI control.

In an effort to improve the control behavior by removing the effect of  $g_0$ , simulations were performed using an extra G parameter with  $g_0$  fixed at 0.0 and the time delay

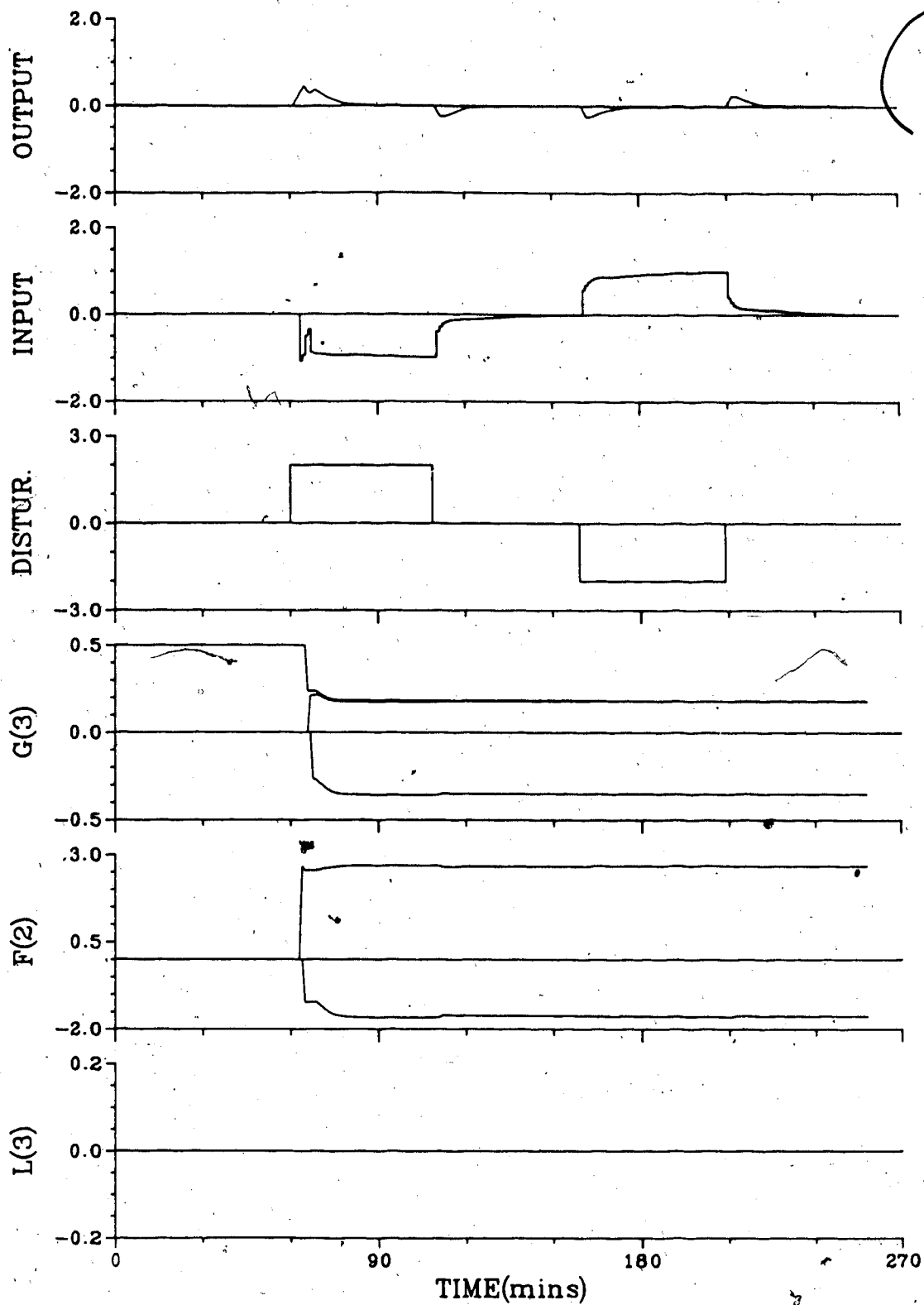


Figure 7.26 - Generalized Minimum Variance Control of the Two Transfer Function Model with NFF

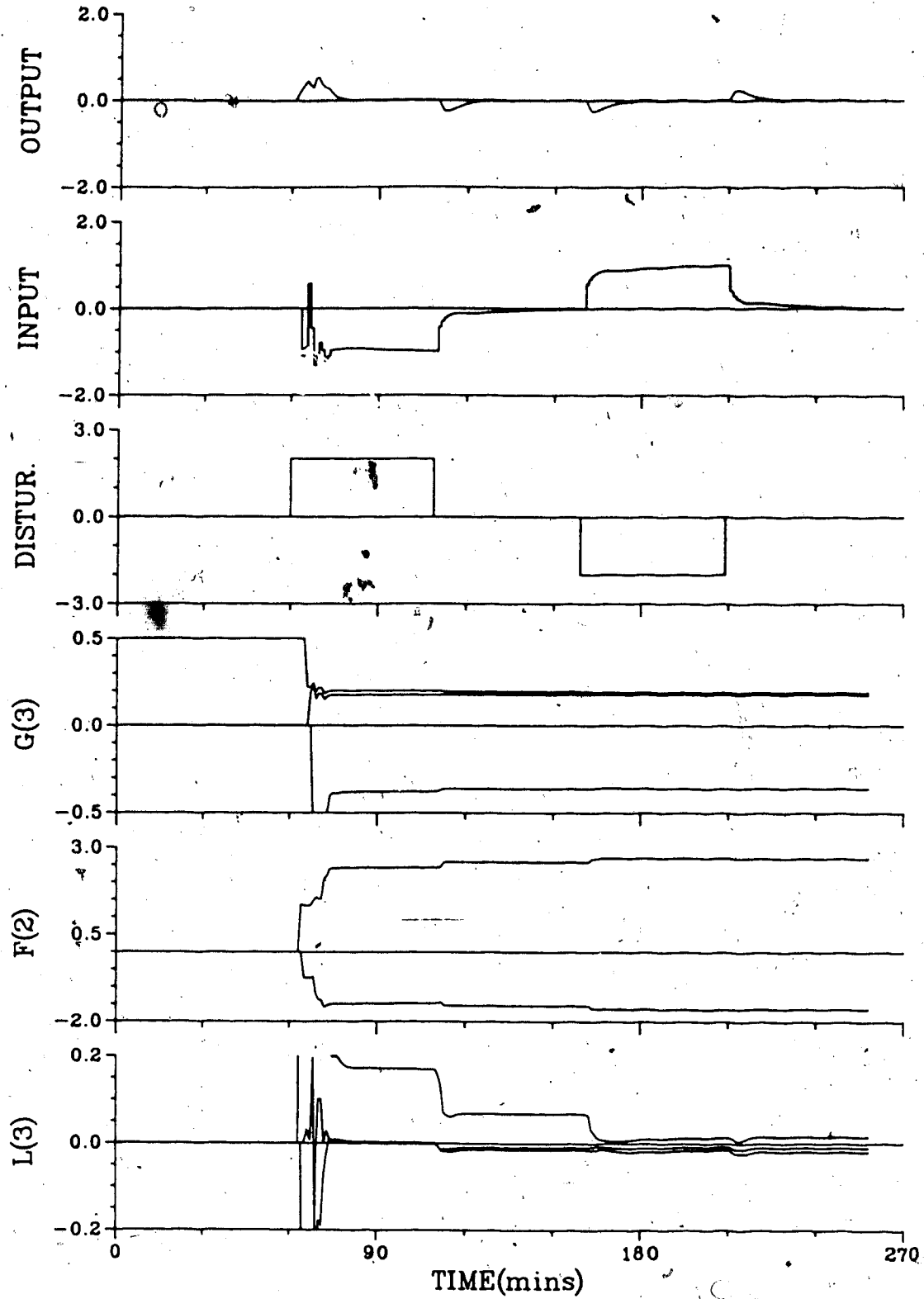


Figure 7.27 - Generalized Minimum Variance Control of the Two Transfer Function Model using EFF

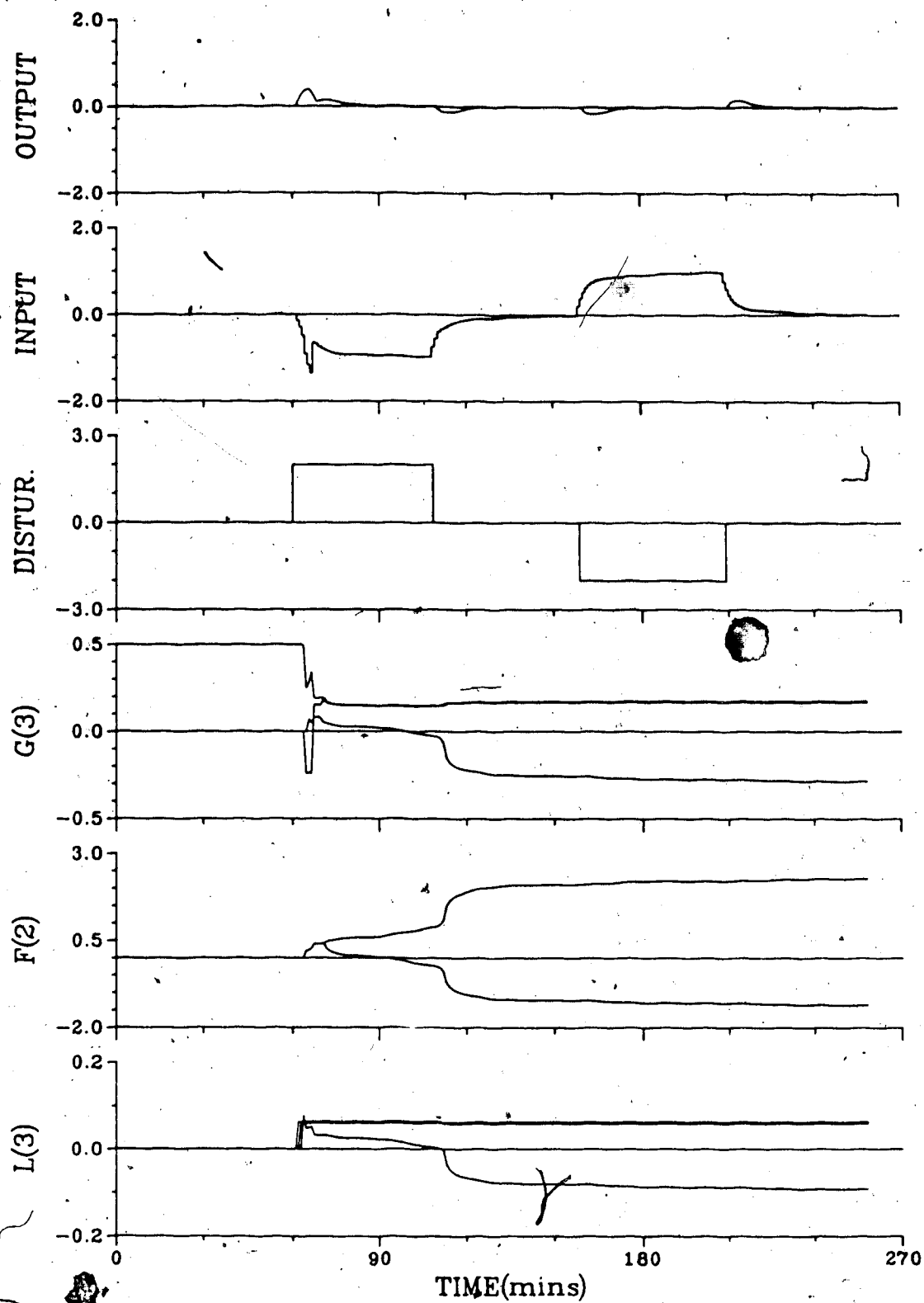


Figure 7.28 - Generalized Minimum Variance Control of the Two Transfer Function Model using MFF

underestimated by one sampling interval. The behavior that resulted with this form of control law for the separate cases of no feedforward action, estimated or measured feedforward action is shown in Figures 7.29, 7.30 and 7.31 respectively. It can be seen that control of the output variable has improved over the previous GMV results for the initial step disturbance, although the control performance for the other three disturbance changes has not appreciably improved.

Since the parameter estimation behavior in Figures 7.29 to 7.31 shows that only two G parameters were identified as being significantly nonzero, simulations were performed using only three G parameters. The results of these simulations are presented in Figures 7.32, 7.33 and 7.34 for the no feedforward action, estimated and measured feedforward action cases. Comparison of this control performance, using only three G parameters, with that shown in Figures 7.29 to 7.31 shows that the performance is essentially identical for each case.

The control performance of this system was also studied using a weighting that involved letting  $q_0$  and  $q_1$  be functions of  $g_0$ , as shown in equation 6.29. The results for the no feedforward action, estimated and measured feedforward action tests are presented in Figures 7.35, 7.36 and 7.37. Very good control performance resulted when using a measurement of the disturbance for feedforward action, especially once the parameters had adapted. The other two

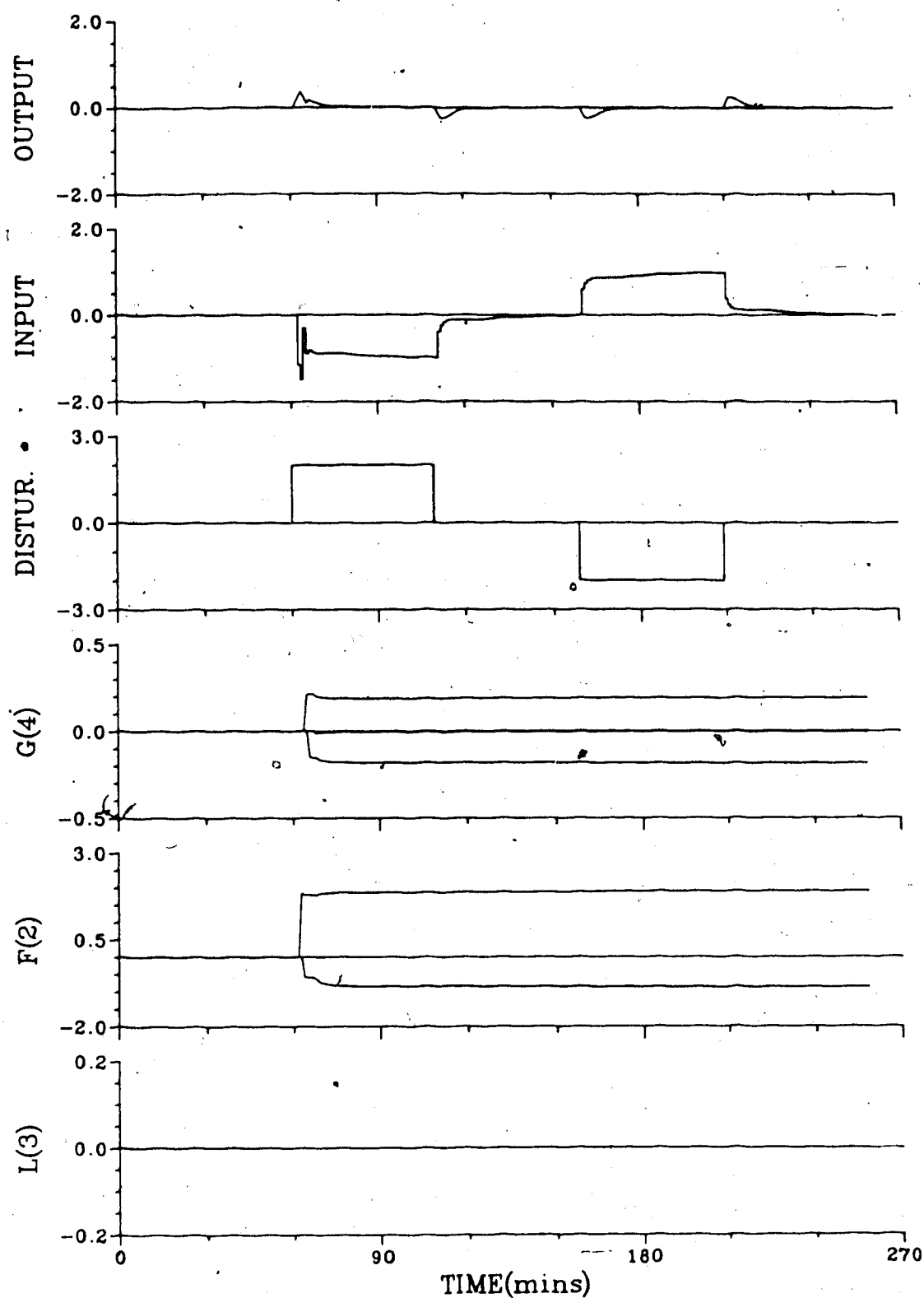


Figure 7.29 - Generalized Minimum Variance Control of the Two Transfer Function Model with 4 G param.,  $g_0=0.0$ , Delay Underestimated and with NFF

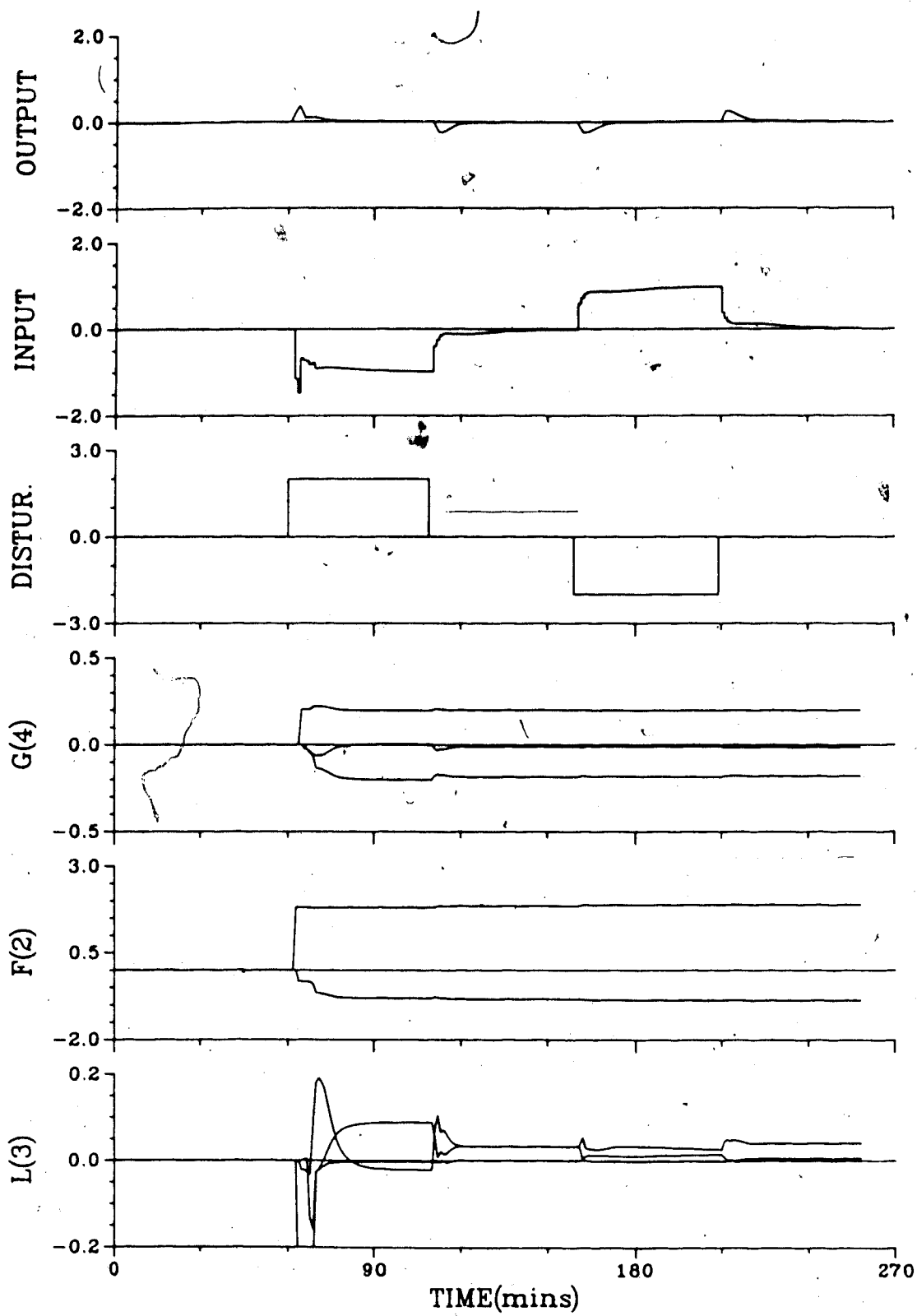


Figure 7.30 - Generalized Minimum Variance Control of the Two Transfer Function Model with 4 G param.,  $g_0=0.0$ , Delay Underestimated and using EFF

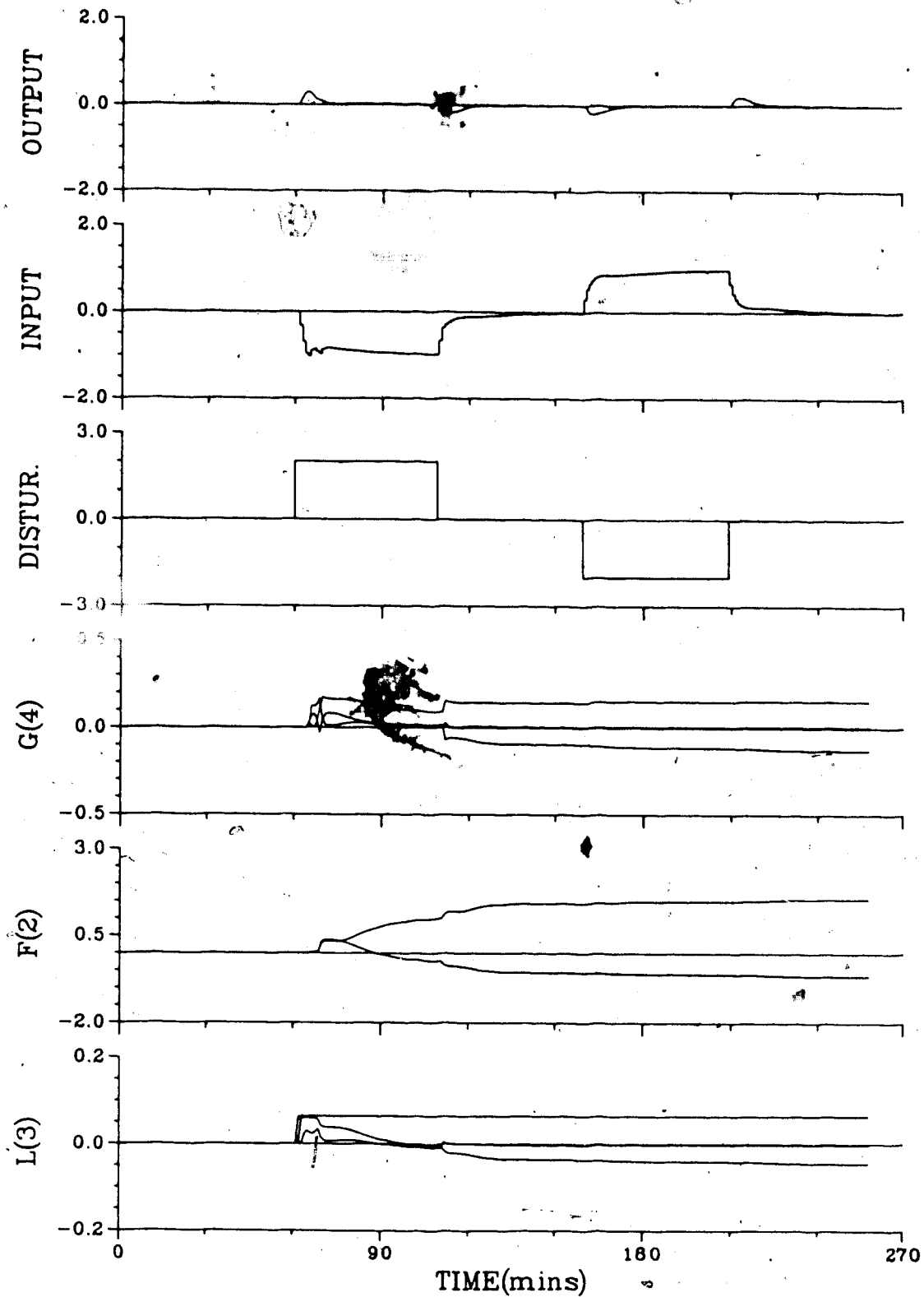


Figure 7.31 - Generalized Minimum Variance Control of the Two Transfer Function Model with 4 G param.,  $g_0=0.0$ , Delay Underestimated and using MFF



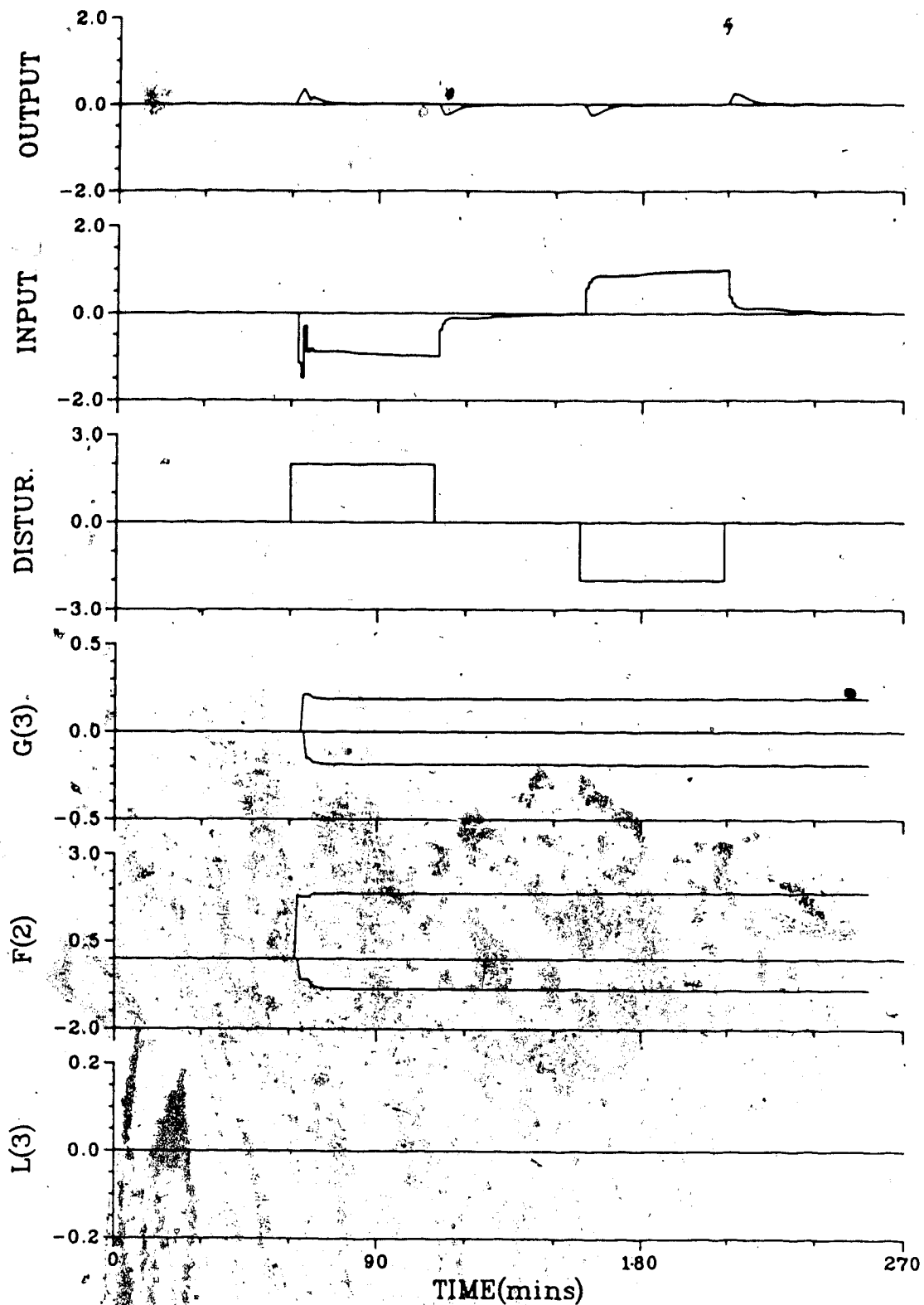


Figure 7-32 - Generalized Minimum Variance Control of the Two Transfer Function Model with  $g_0=0$ , the Time Delay Underestimated and with NFF

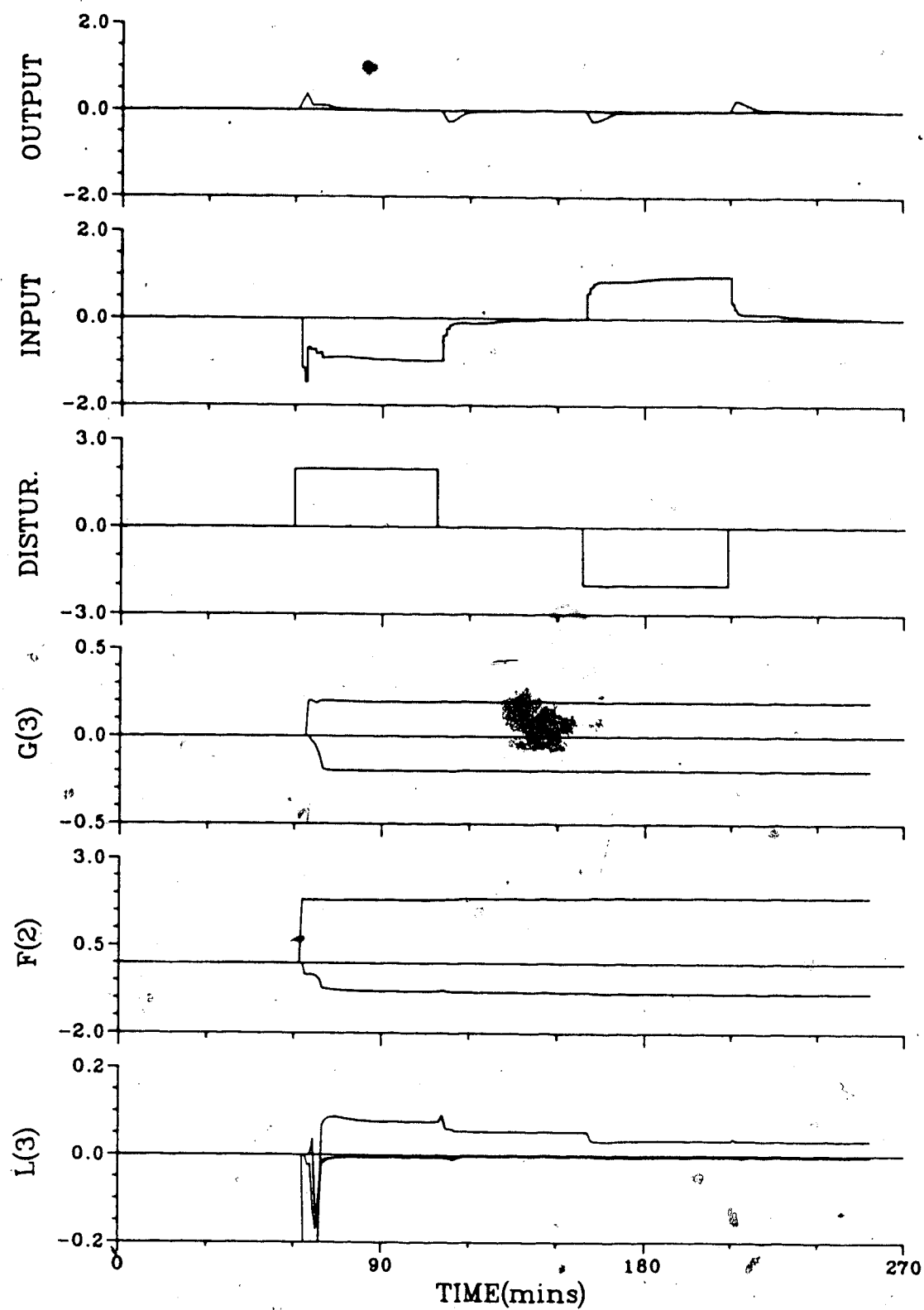


Figure 7.33 - Generalized Minimum Variance Control of the Two Transfer Function Model with  $g_0=0$ , the Time Delay Underestimated and using EFF

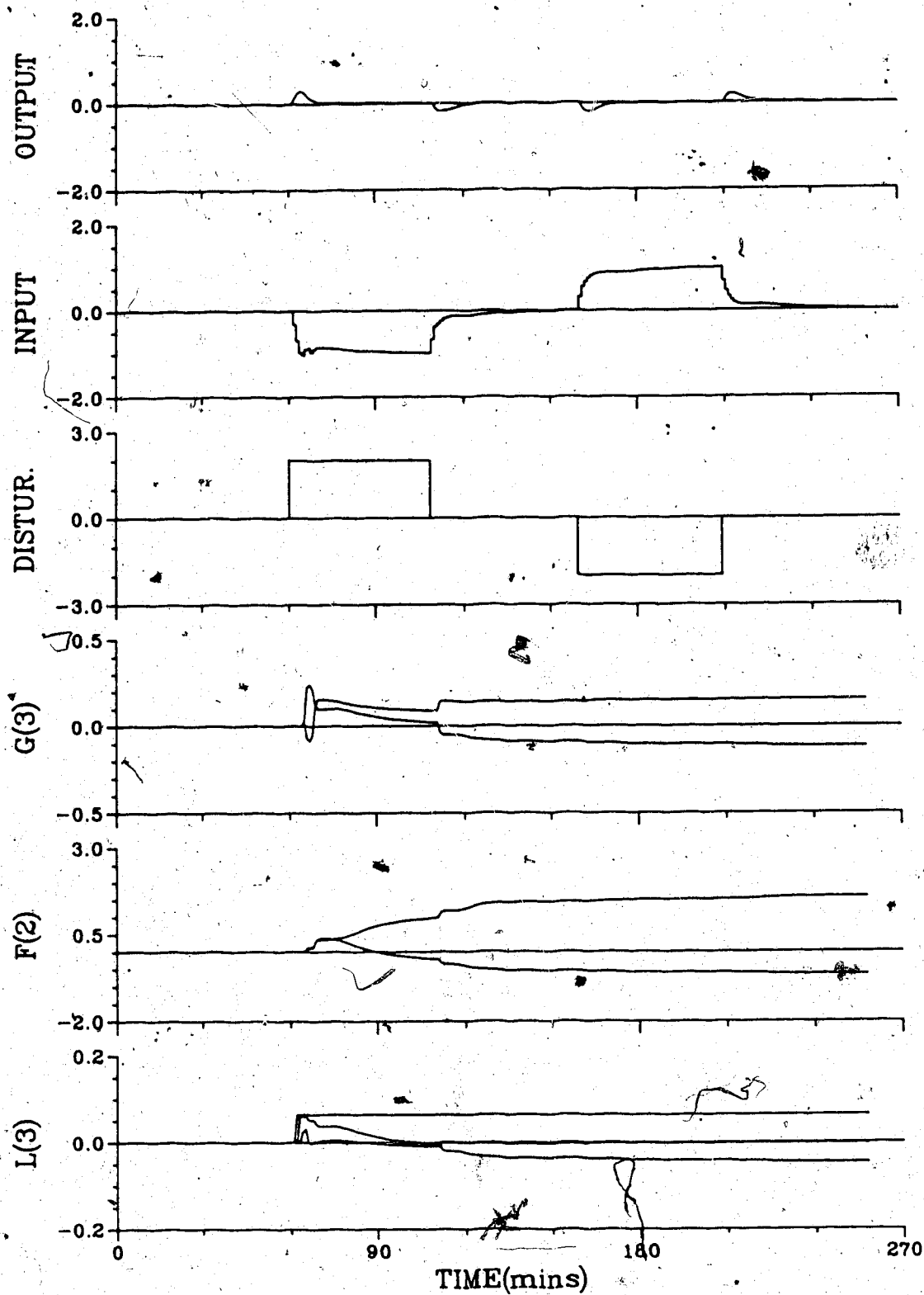


Figure 7.34 - Generalized Minimum Variance Control of the Two Transfer Function Model with  $g_0=0$ , the Time Delay Underestimated and using MFF

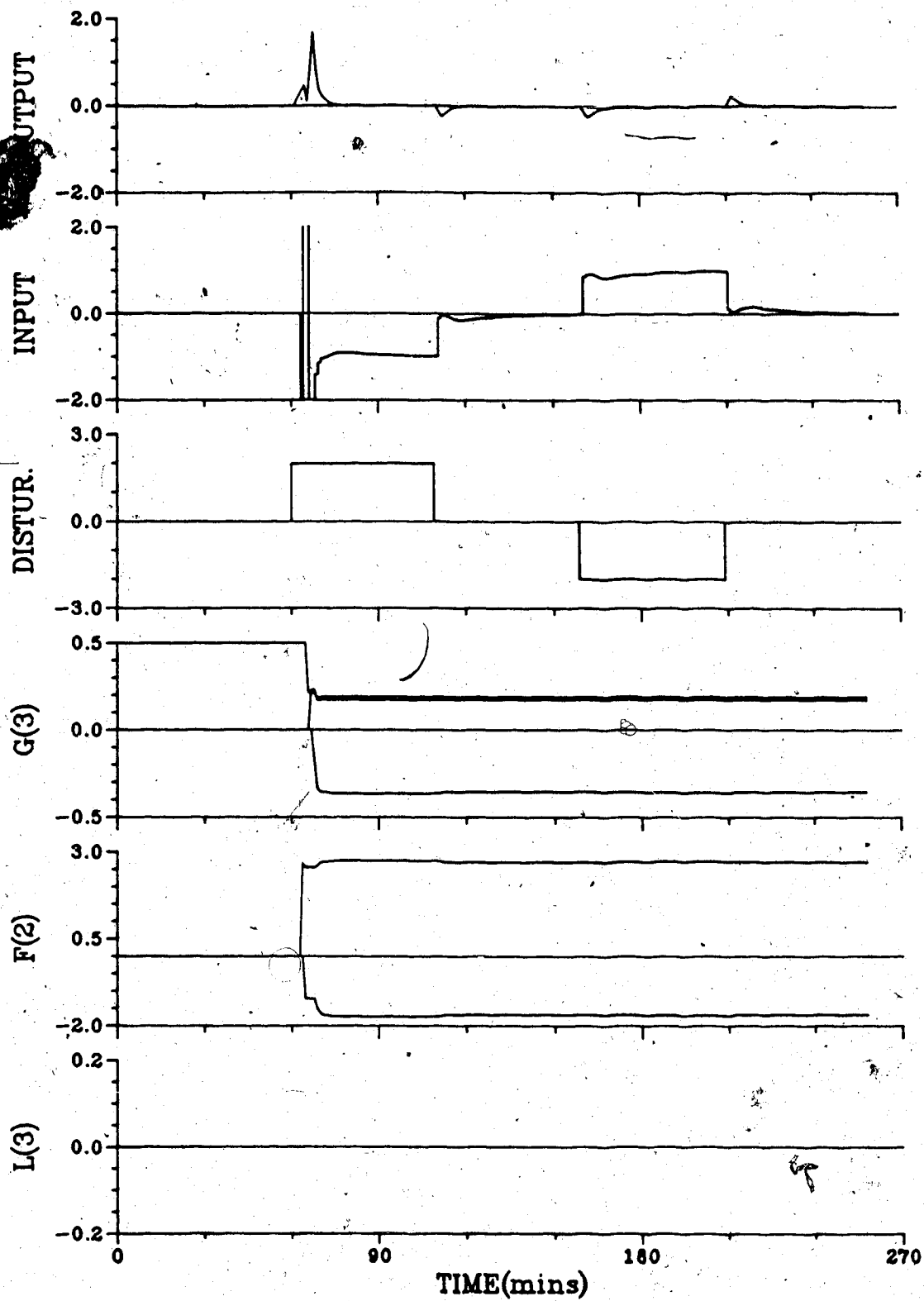


Figure 7.35 - Generalized Minimum Variance Control of the Two Transfer Function Model with the Q Weighting adapting with  $g_0$  and NFF

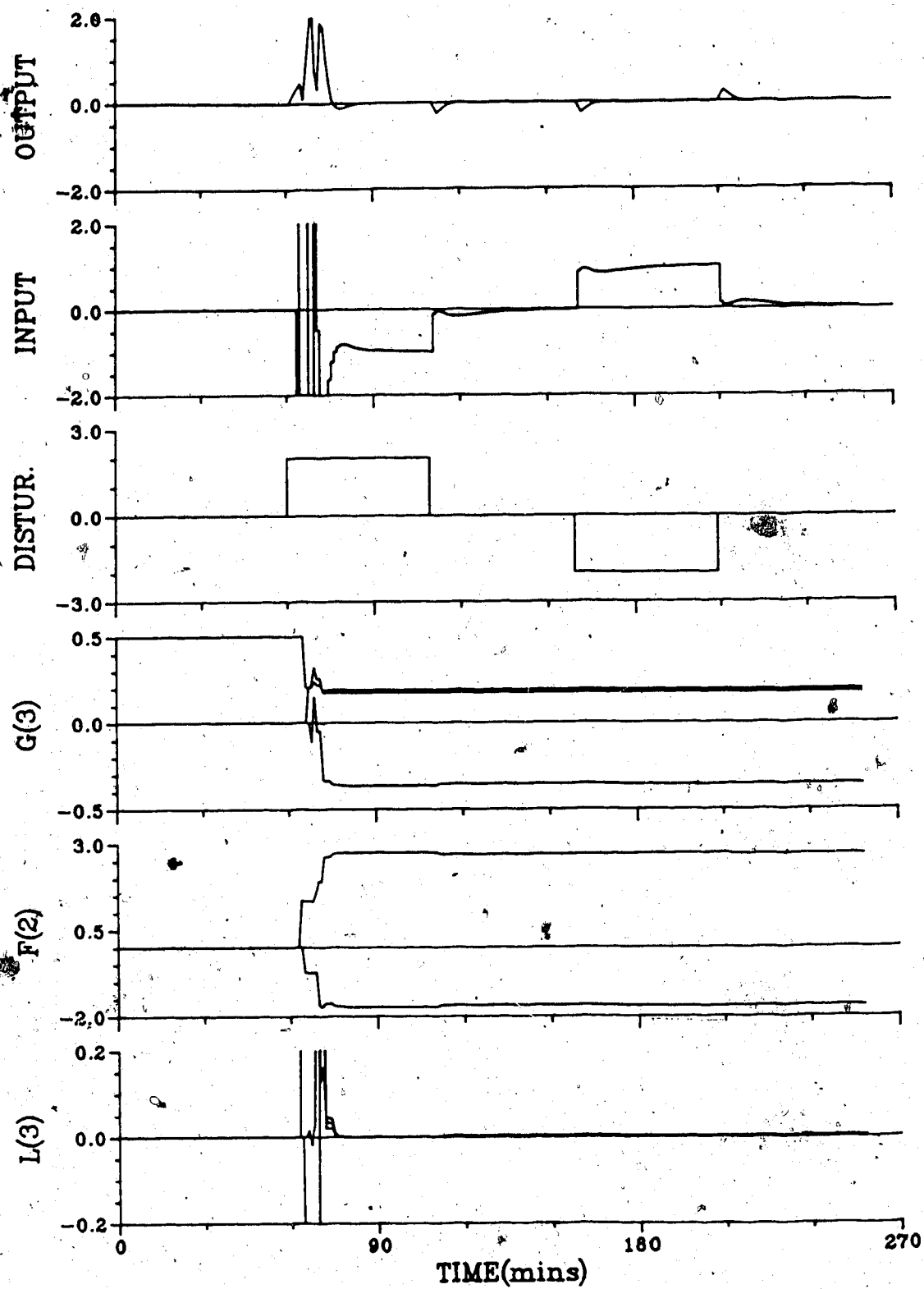


Figure 7.36 - Generalized Minimum Variance Control of the Two Transfer Function Model with the  $Q$  Weighting adapting with  $g_0$  using EFF

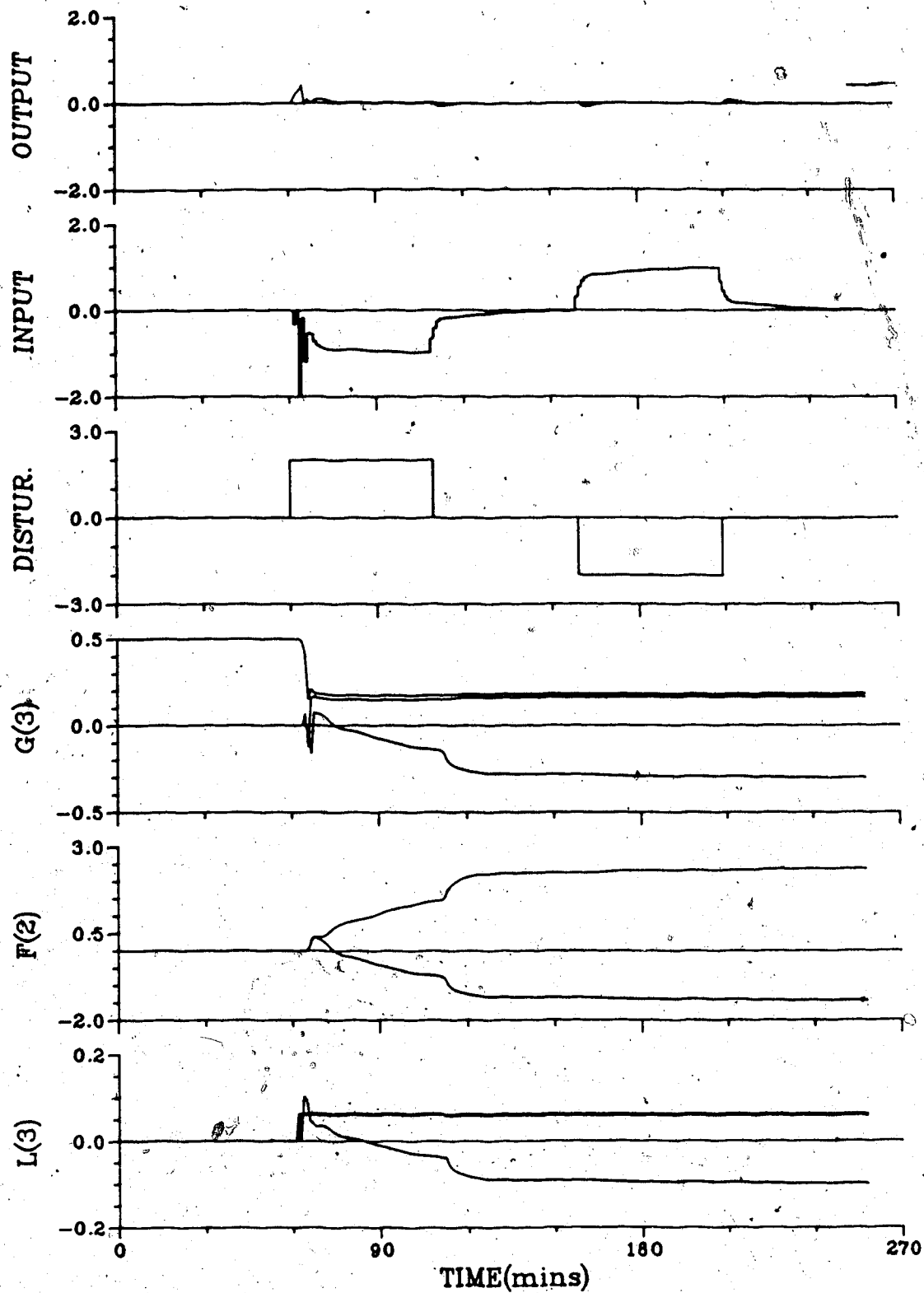


Figure 7.37 - Generalized Minimum Variance Control of the Two Transfer Function Model with the  $Q$  Weighting adapting with  $g_0$  using MFF

schemes required a longer tuning-in period before the control improved.

### 7.3.6 Two Transfer Function Simulation Summary

Since many of the controlled responses that have been presented in this section are very similar, it is convenient to compare the responses using a performance index. The total SAE value and the tuned SAE value, computed from the time of the second disturbance (110 minutes), for the different simulations are presented in Table 7.2.

Examination of these values shows that minimum variance control provides the best control both during and after the initial parameter tuning period for each of the three different schemes. It can also be seen that for minimum variance control, use of estimated feedforward action produces only slightly better control performance than with no feedforward control action, and produces a slightly poorer control during the tuning period. The use of measured feedforward control action provides much better control especially once the parameters have converged.

Control of the system using the generalized minimum variance algorithm resulted in improved behavior compared with the use of the PI algorithm when measured feedforward action was employed, or when the Q weighting was taken as a function of  $g_0$ . In general, the performance obtained using estimated feedforward action resulted in only slightly better performance during the tuning than was the case for

Table 7.2  
SAE Values for the Two Transfer Function Model  
Simulations for Various Control Strategies

Control/Strategy	Total SAE	Tuned SAE	Figure
PI	7.06	5.29	7.19
MIN VAR / NFF	4.04	1.69	7.20
MIN VAR / EFF	4.13	1.68	7.21
MIN VAR / MFF	3.54	0.21	7.22
GMV / Known Coefficients, NFF	8.85	6.53	7.25
GMV / Known Coefficients, EFF	8.68	8.85	7.24
GMV / Known Coefficients, MFF	7.04	5.28	7.23
GMV / NFF	11.29	6.76	7.26
GMV / EFF	11.49	6.84	7.27
GMV / MFF	8.59	4.78	7.28
GMV / 4 G's, Underestimated Delay, $g_0=0.0$ , NFF	7.83	5.76	7.29
GMV / 4 G's, Underestimated Delay, $g_0=0.0$ , EFF	7.90	5.77	7.30
GMV / 4 G's, Underestimated Delay, $g_0=0.0$ , MFF	7.19	5.04	7.31
GMV / $g_0=0.0$ , Underestimated Delay, NFF	7.81	5.77	7.32
GMV / $g_0=0.0$ , Underestimated Delay, EFF	7.82	5.77	7.33
GMV / $g_0=0.0$ , Underestimated Delay, MFF	7.23	5.03	7.34
GMV / Q's adapting from $g_0$	9.13	3.44	7.35
GMV / Q's adapting from $g_0$	16.70	3.47	7.36
GMV / Q's adapting from $g_0$	3.71	1.51	7.37

the use of no feedforward action. The SAE values show that underestimating the time delay and setting  $g_0 = 0.0$  provided consistently good control. However, the best control performance achieved using GMV resulted when the Q weighting was taken as a function of  $g_0$  and the measured value of the disturbance was used for the feedforward action.



It should be noted that, under PI control, the addition of a feedforward signal would normally require retuning of the controller parameters to achieve control that was at least as good as that obtained prior to the use of a feedforward signal. It is conceivable, then, that the control behavior obtained when employing an inverse PI structure for the Q weighting polynomial may be improved with some further tuning if an estimated or measured feedforward signal is used.

## 7.4 Linear Distillation Column Model Simulation

### 7.4.1 Introduction

A linear model of the distillation column expressed in terms of the 6 transfer functions obtained from the open loop tests, given by equation 5.3, has also been used to evaluate various control strategies. The transfer functions used in this model are given in Figure 7.38.

To compare the various control strategies, a disturbance of  $\pm 4.5$  in a square wave pattern was used with steps of 100 minutes, starting at 50 minutes. For all of the simulation results presented in this section, a sample time of 3 minutes has been used for the bottom composition control loop. To illustrate multirate sampling, a sampling time of 1 minute has been used on the top composition control loop. For each simulation, the identification began at 30 minutes, with operation starting at 40 minutes.

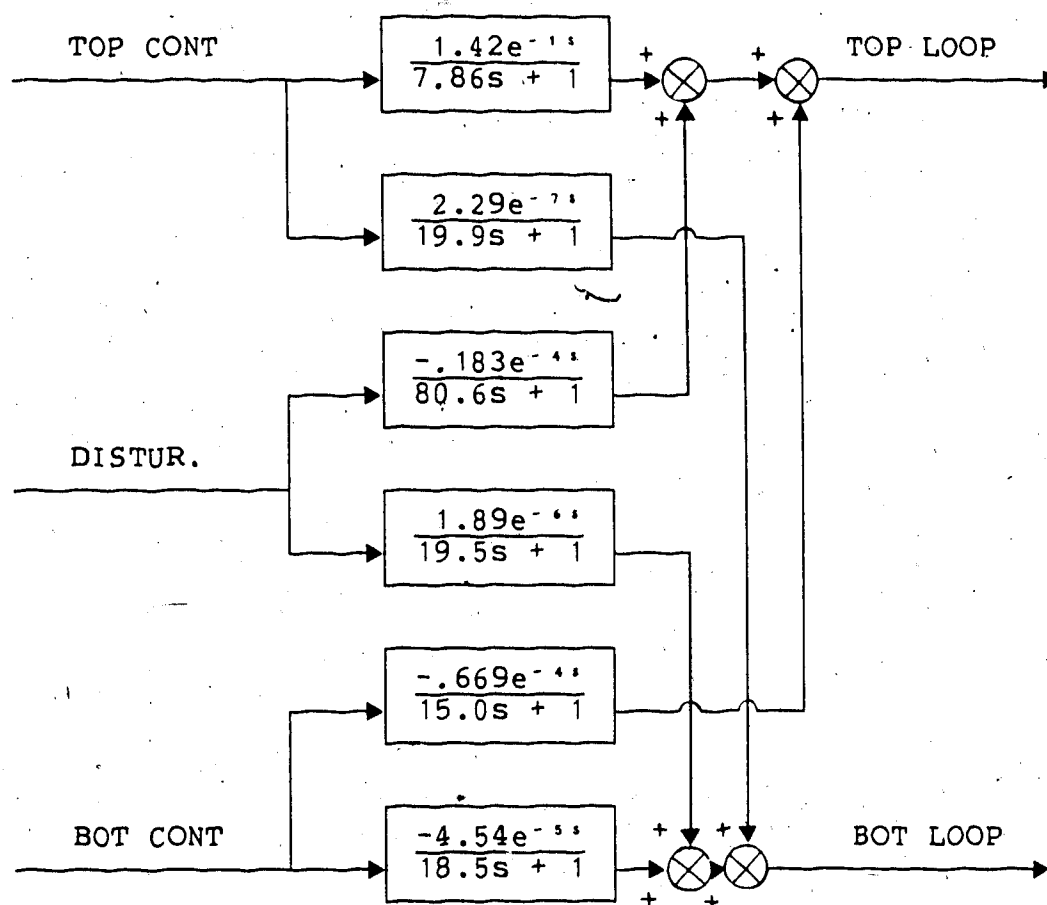


Figure 7.38 - Linear Distillation Column Model

#### 7.4.2 PI/PID Control

To provide a base case for comparison of performance with the self-tuning controller, conventional multiloop PID control was employed. A PI controller was used in the top composition loop, and a PID controller in the bottom composition loop. The controllers were tuned using various combinations of controller constants, until the control performance shown in Figure 7.39 was obtained. This performance was achieved with controller constants of  $PB = 25.0$  and  $TI = 4.8$  for the top loop and, for the bottom loop,  $PB = 70.0$ ,  $TI = 4.5$  and  $TD = 3.5$ . To illustrate the importance of derivative action in the bottom loop, the derivative action was removed. The results, plotted in Figure 7.40, show that without derivative action to counteract the large time delays, the response becomes oscillatory.

#### 7.4.3 Minimum Variance Control

When using the self-tuning controller to control the linear model of the column, the number of coefficients in each of the controller polynomials must be specified. As outlined in Section 6.4.1, the number of  $G_{11}$ ,  $F$ ,  $L$  and  $G_{12}$  polynomials will be 4, 3, 4 and 4 for the top loop, and 5, 3, 5 and 5 for the bottom loop.

Once the self-tuning controller is used on this interacting model, the problems associated with tuning the controller parameters are immediately evident, as can be

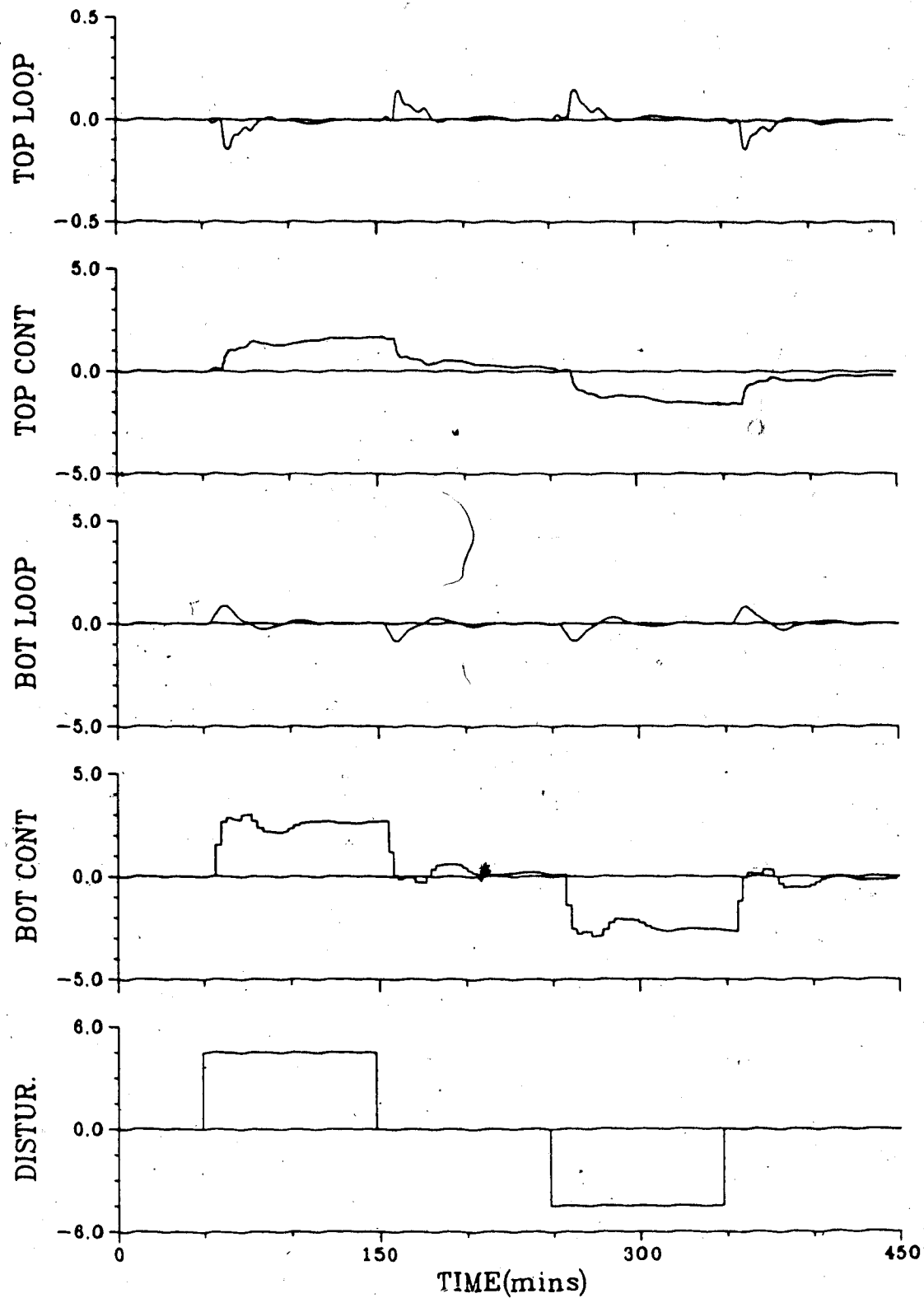


Figure 7.39 - PI/PID Control of the Linear Column Model  
Top: PB=25.0, TI=4.8  
Bottom: PB=70.0, TI=4.5, TD=3.5

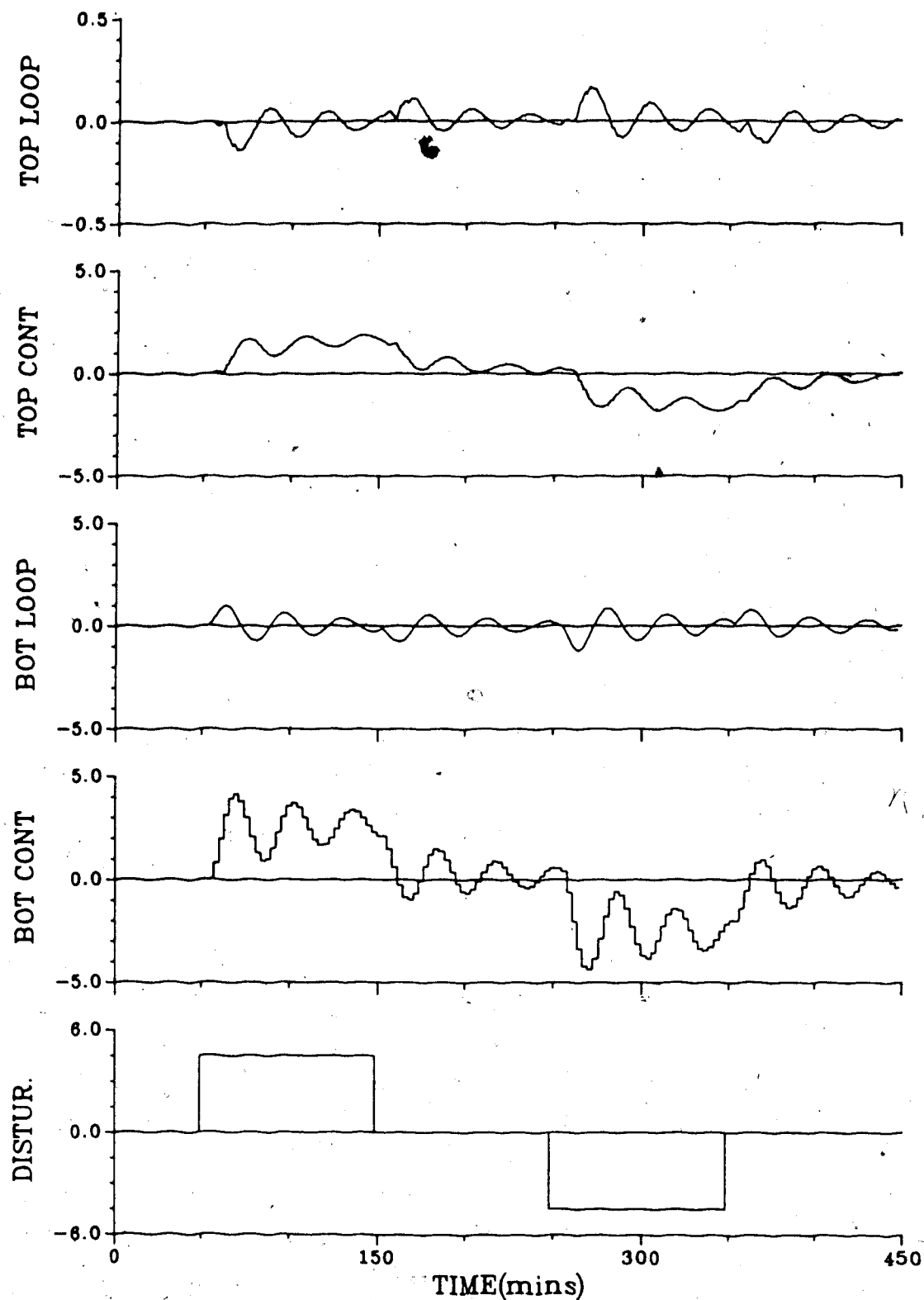


Figure 7.40 - PI/PI Control of the Linear Column Model  
Top: PB=25.0, TI=4.8  
Bottom: PB=70.0, TI=4.5

seen from the responses shown in Figure 7.41. This performance, which utilized the minimum variance control strategy, shows that it takes approximately 125 minutes after the disturbance occurs (roughly 42 control intervals on the bottom loop) before the bottom composition is near the set point. Even at this point the control actions are still very large, resulting in oscillatory behavior, as may have been expected under minimum variance control. Although the composition in the bottom loop fluctuates, control of the bottom composition has been achieved. Once the parameters have adapted, the top loop composition appears to be controlled very well. When the measured value of the disturbance is used to provide the feedforward action, much of the "on-off" effect is eliminated, as can be seen by the more stable response in Figure 7.42. However, a tuning-in period of over 100 minutes is still required.

A test using an estimate of the disturbance as the feedforward action has been performed and the results of this run are tabulated in the summary section.

#### 7.4.4 Generalized Minimum Variance Control

Unless a specific point is to be illustrated, for the rest of the simulations, only the situation where no feedforward action was used has been plotted. Simulations employing an estimated and a measured feedforward action are reported in tabular form in Table 7.3.

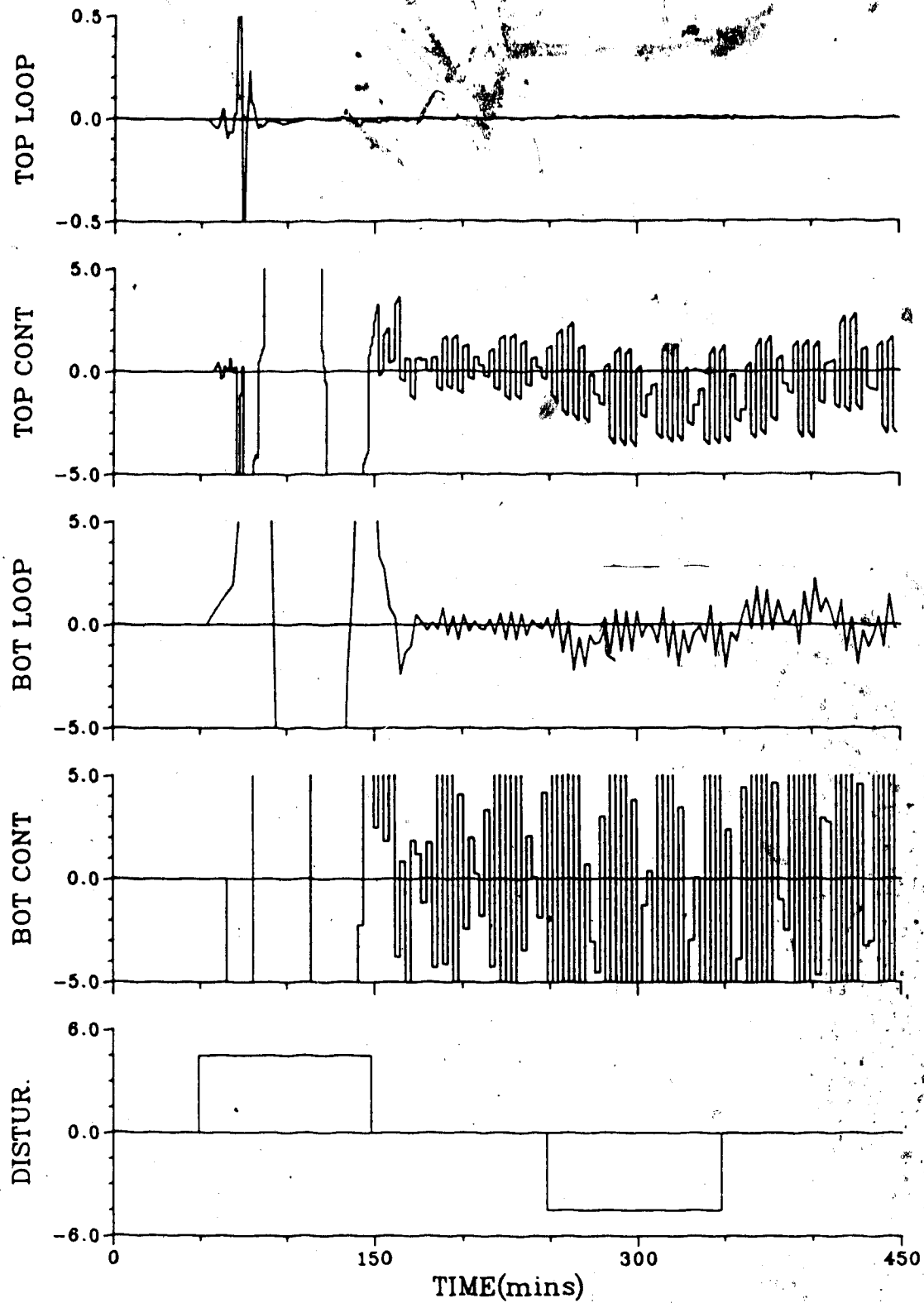


Figure 7.41 - Minimum Variance Control of the Linear Column  
Column Model with NFF

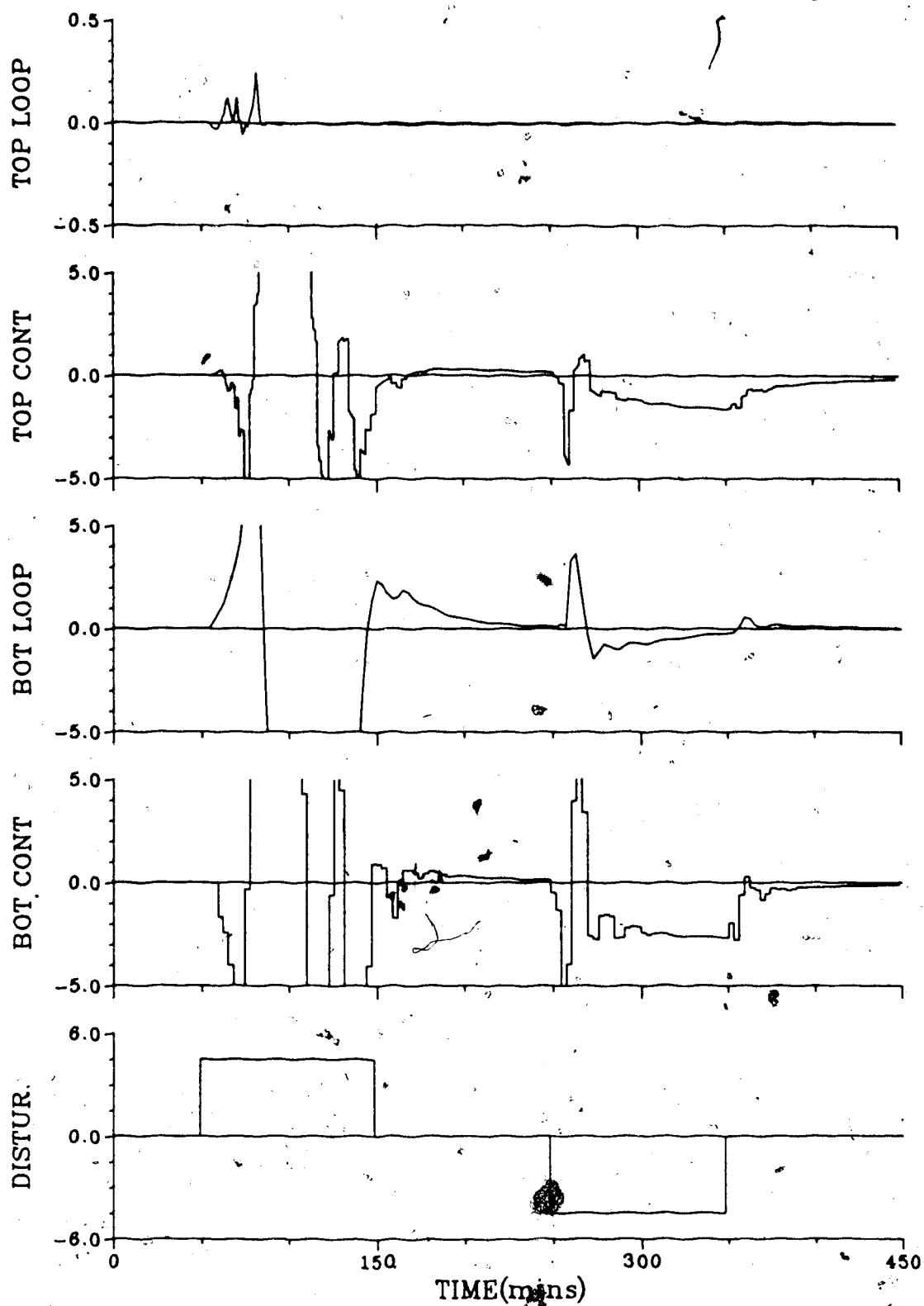


Figure 7.42 - Minimum Variance Control of the Linear Column  
Column Model using MFF



When  $Q$  weighting was established from the inverse PID structure, the self-tuning controller responded to disturbances acting on the modelled process to produce the results shown in Figure 7.43. Figure 7.44 contains the parameters corresponding to the data plotted in Figure 7.43. Removing derivative action when calculating the  $Q$  coefficients in the bottom loop resulted in poorer control of that loop, although little change in top composition control has occurred. These can be seen by comparing the composition responses in Figures 7.43 with those in 7.45. In addition, the tuning-in period for the top composition loop has been degraded.

Employing the scheme of setting  $g_0 = 0.0$  without any underestimating of the time delay and using no feedforward action was not very effective. The corresponding responses are shown in Figure 7.46. The addition of the measured value of the disturbance to provide the feedforward action improved not only the control performance, but also the tuning-in portion of the test, as can be observed from the responses shown in Figure 7.47. Removing the derivative action when calculating the  $Q$  coefficients for the bottom composition controller results in an improvement over the case in which no feedforward action was used, as observed by comparing the responses in Figures 7.46 and 7.48.

If the time delay is underestimated in conjunction with setting  $g_0 = 0.0$ , it is again advantageous to drop the derivative action when calculating the  $Q$  coefficients for

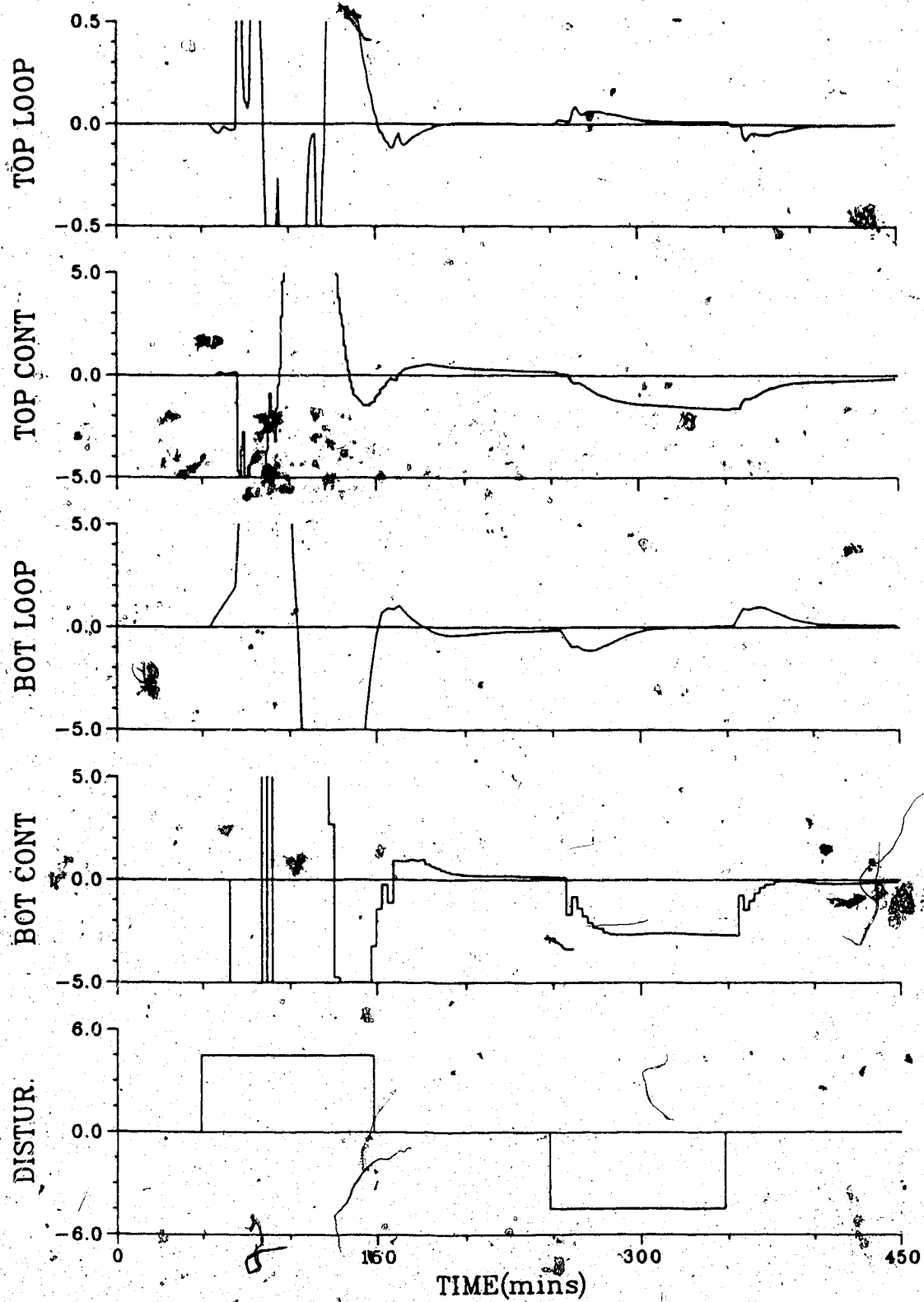


Figure 7.43 - G<sub>MV</sub> Control of the Linear Column Model with  
 NFF From: Top: PB=25.0, TI=4.8  
 Bottom: PB=70.0, TI=4.5, TD=3.5

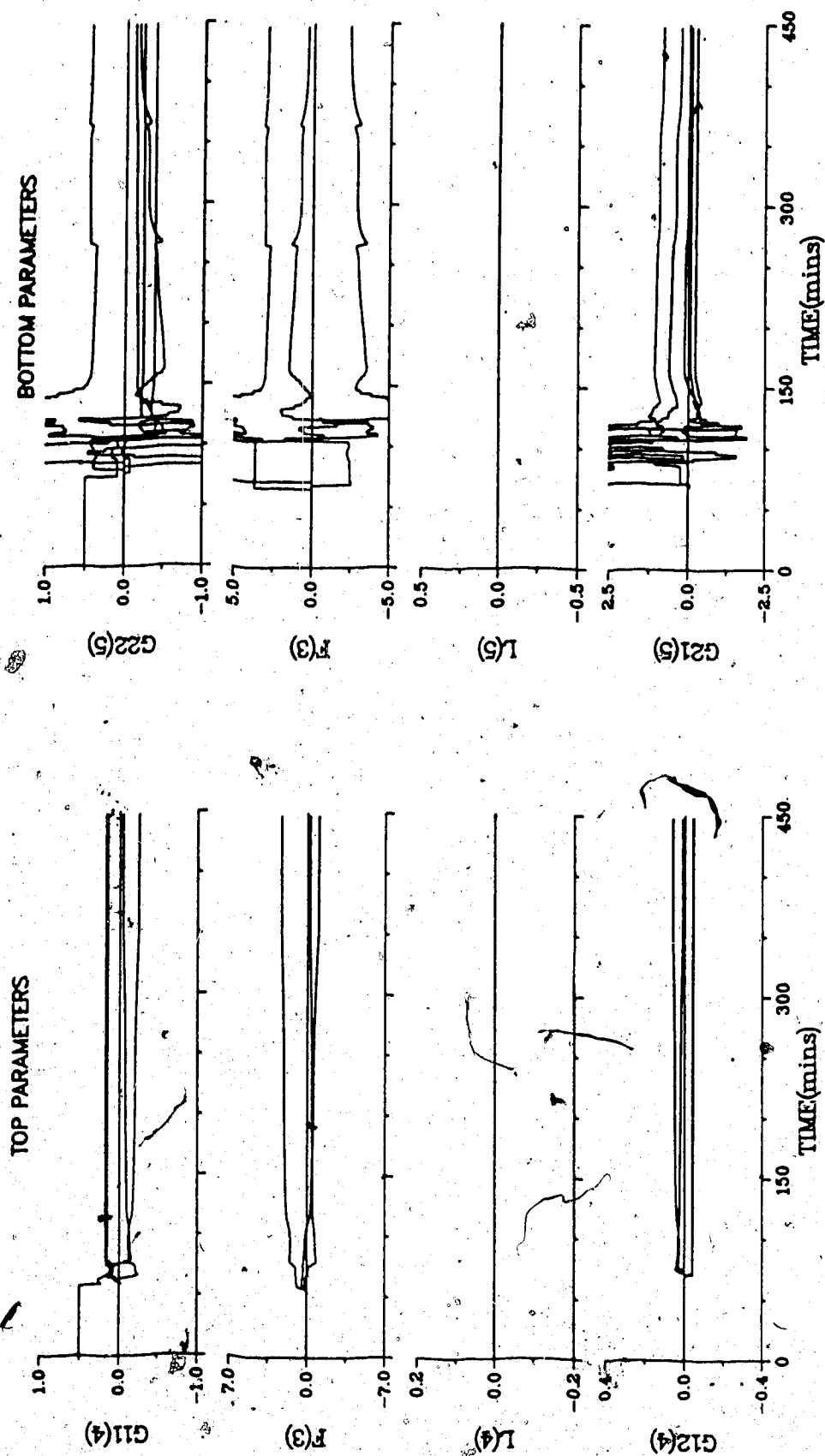


Figure 7.44 - Parameters for GMV Control of the Linear Column Model with NFF

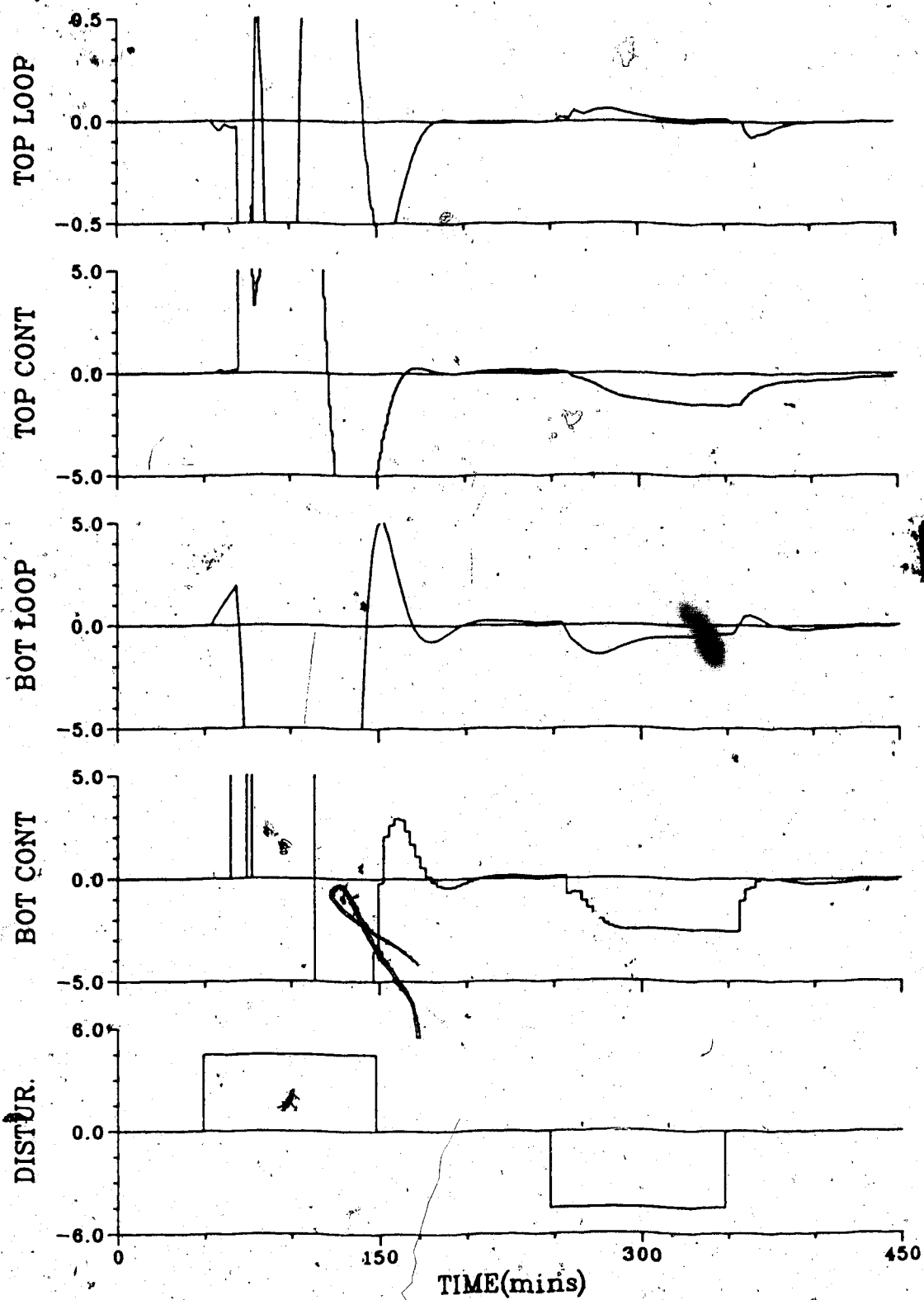


Figure 7.45 - GMV Control of the Linear Column Model with  
 NEF From: Top: PB=25.0, TI=4.8  
 Bottom: PB=70.0, TI=4.5

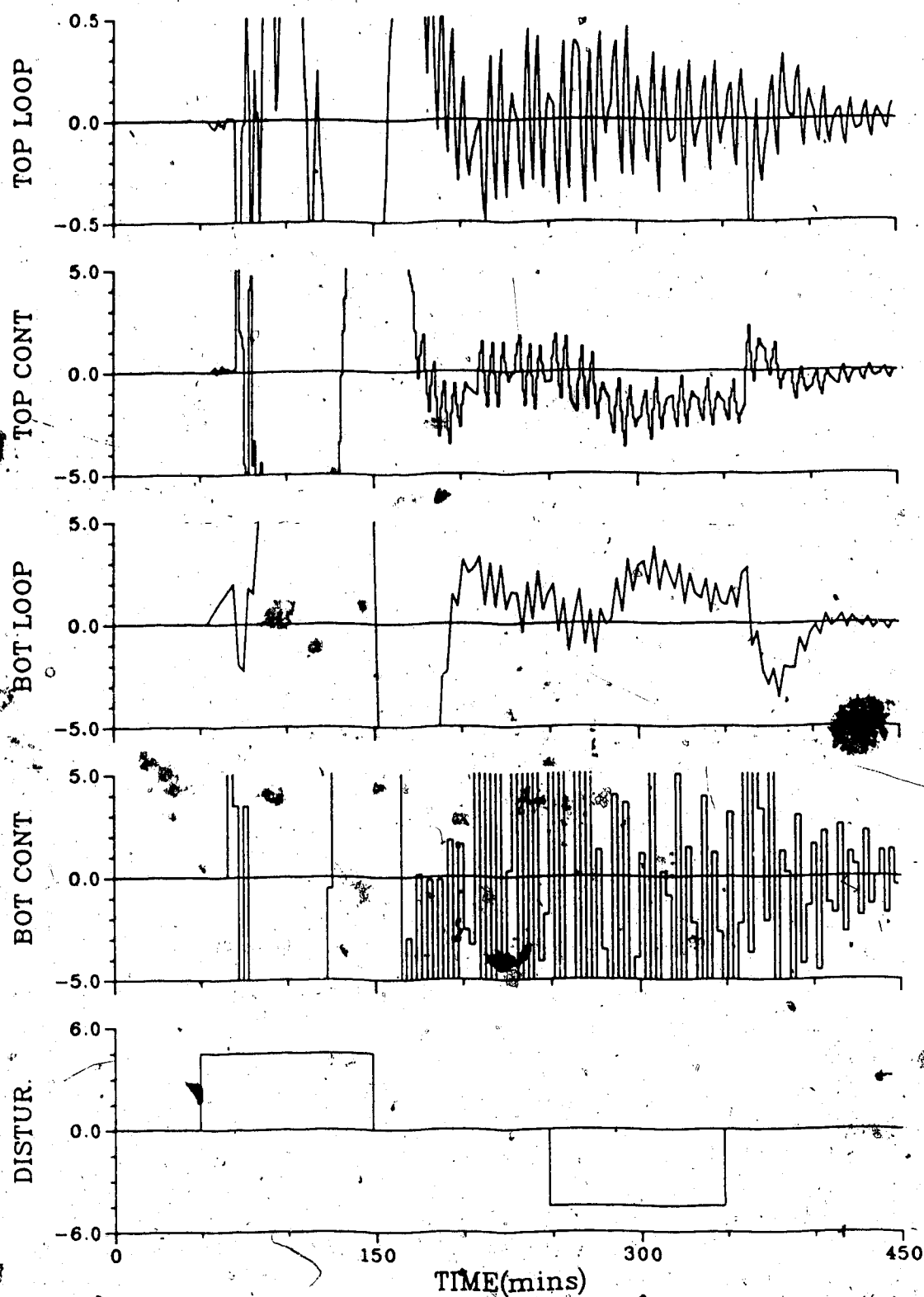


Figure 7.46 - GMV Control of the Linear Column Model with  $g_0=0.0$ , Q Weighting from PI/PID and NFF.

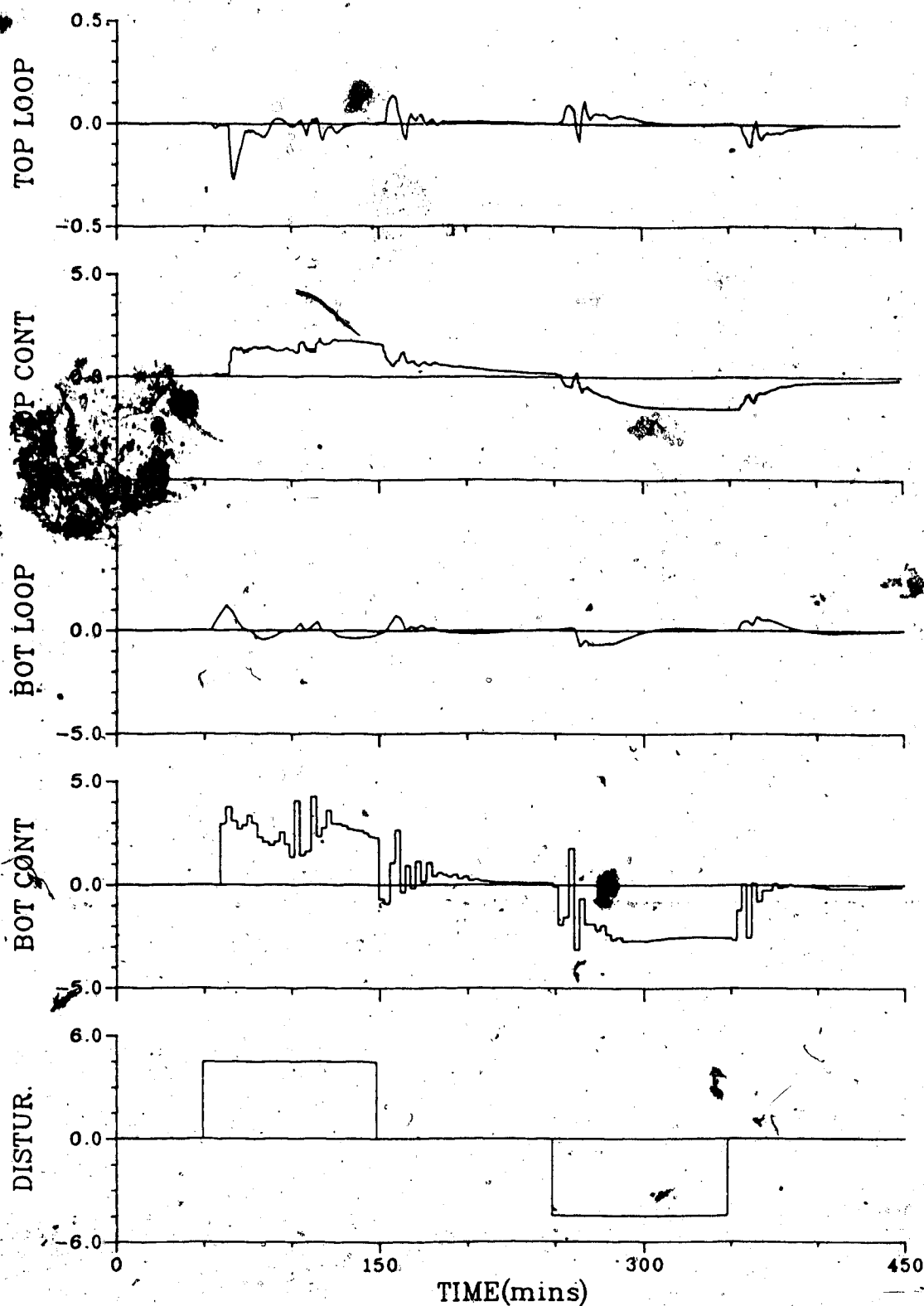


Figure 7.47 - GMV Control of the Linear Column Model with  $g_0=0.0$ , Q Weighting from PI/PID using MFF

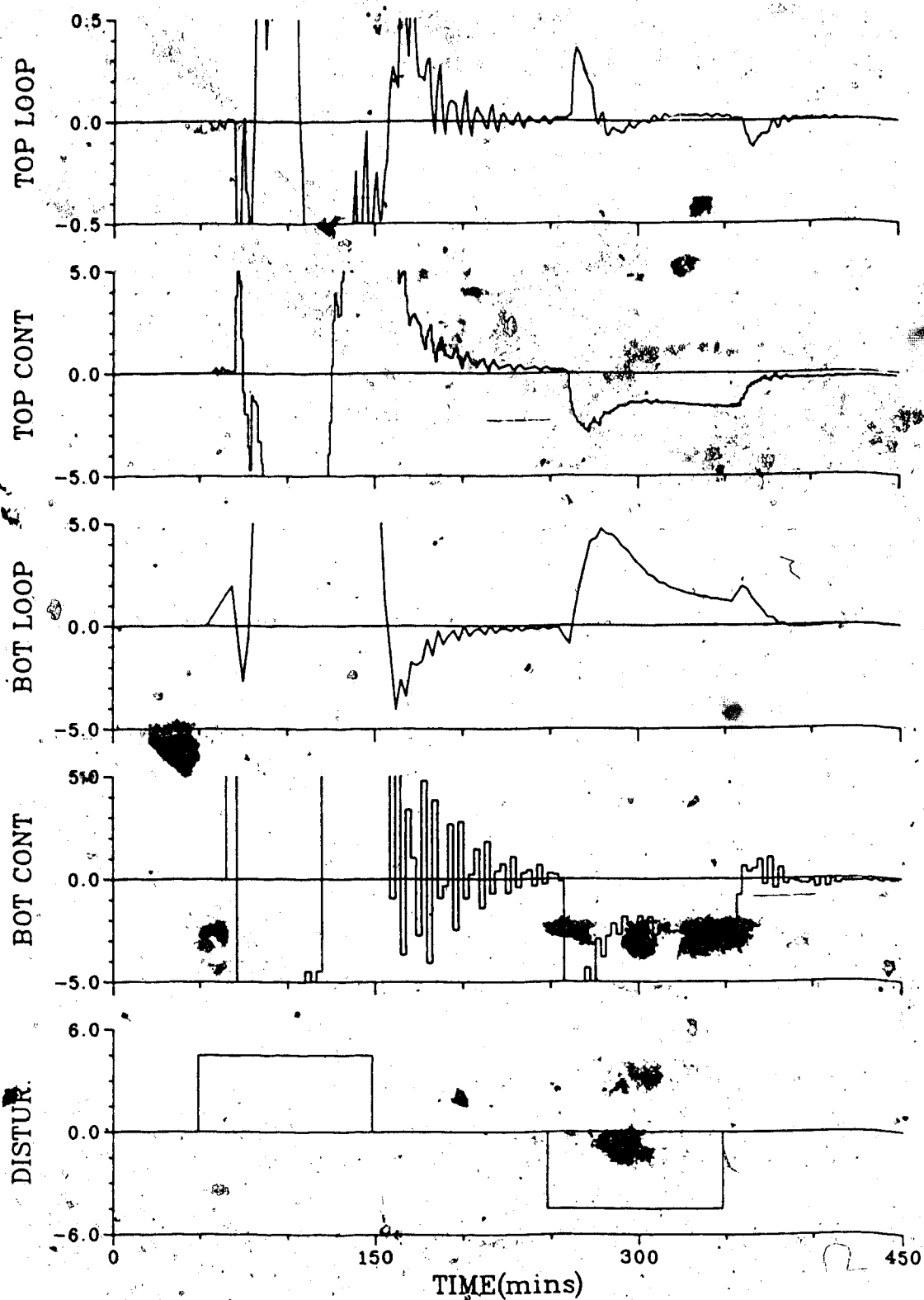


Figure 7.48 - GMV Control of the Linear Column Model with  $q_0=0.0$ , Q Weighting from PI/PI and NFF

the bottom composition controller. This can be seen by comparing the top and bottom composition responses shown in Figures 7.49 and 7.50, where derivative action was and was not used in the calculations, respectively. By including the measured disturbance to provide the feedforward action, the tuning and control may be further improved. Figure 7.51 represents the results of a simulation in which the time delay was underestimated,  $g_0 = 0.0$ , PI constants were used to determine the Q weighting coefficients, and the measured disturbance was used as the feedforward signal.

The final option considered was to allow the Q weighting parameters to adapt along with  $g_0$  as outlined in equation 6.29. Using this technique, the results plotted in Figure 7.52 were obtained. Very good control performance was achieved with this test.

#### 7.4.5 Linear Distillation Column Simulation Summary

The SAE values of all the tests that were plotted, for the tests where both estimated and measured feedforward action have been employed, and for some selected single rate tests are given in Table 7.3. The SAE values listed in Table 7.3 represent the SAE from 250 minutes until the end of the test. The single rate tests used the same PID constants to determine the Q weighting coefficients of the GMV controller as had been used in the multirate tests. Retuning the controller while employing single rate control was attempted but negligible improvement resulted.



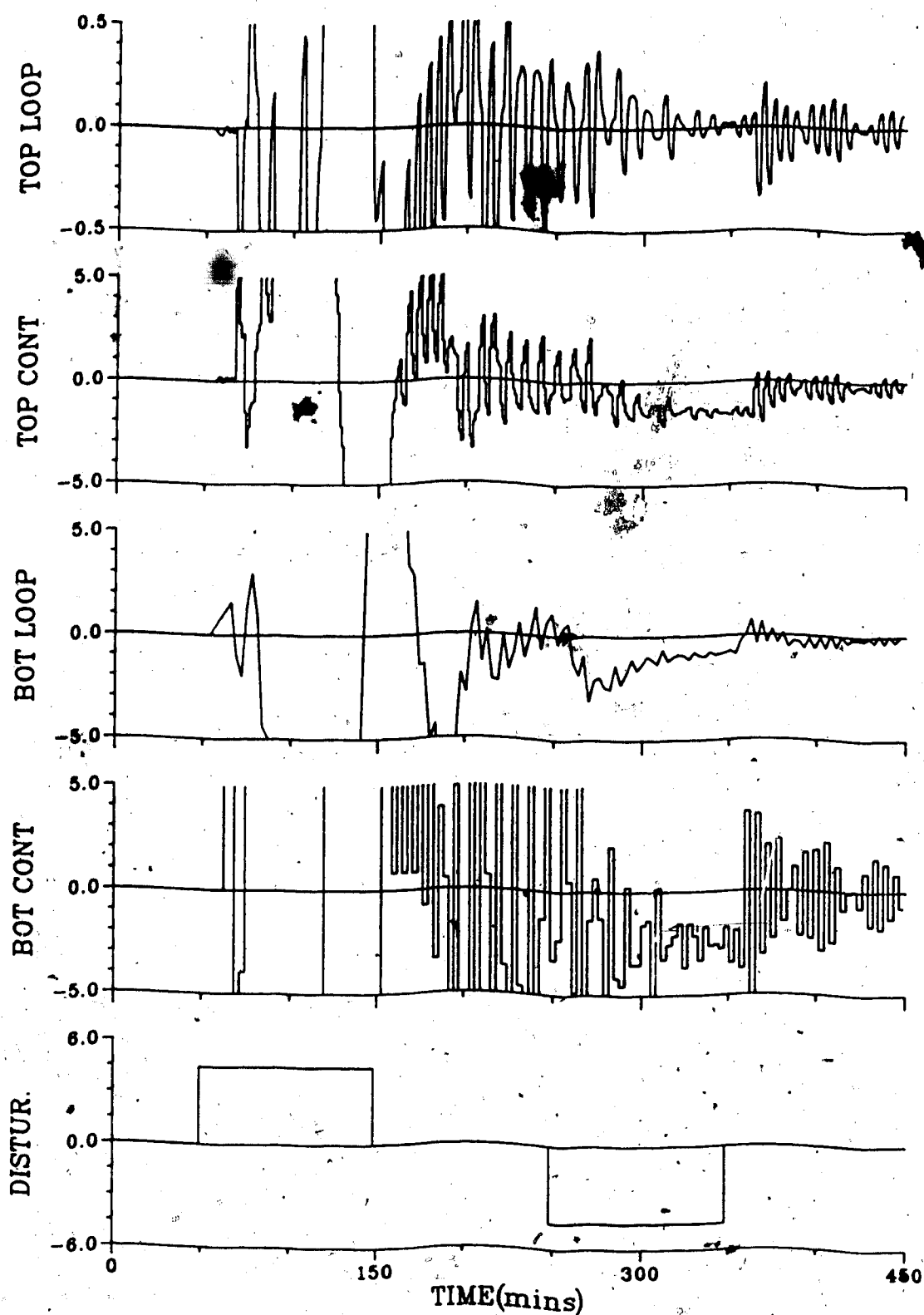


Figure 7.49 - GMV Control of the Linear Column Model with  $g_0=0.0$ , Q Weighting from PI/PID and the Time Delay Underestimated with NFF

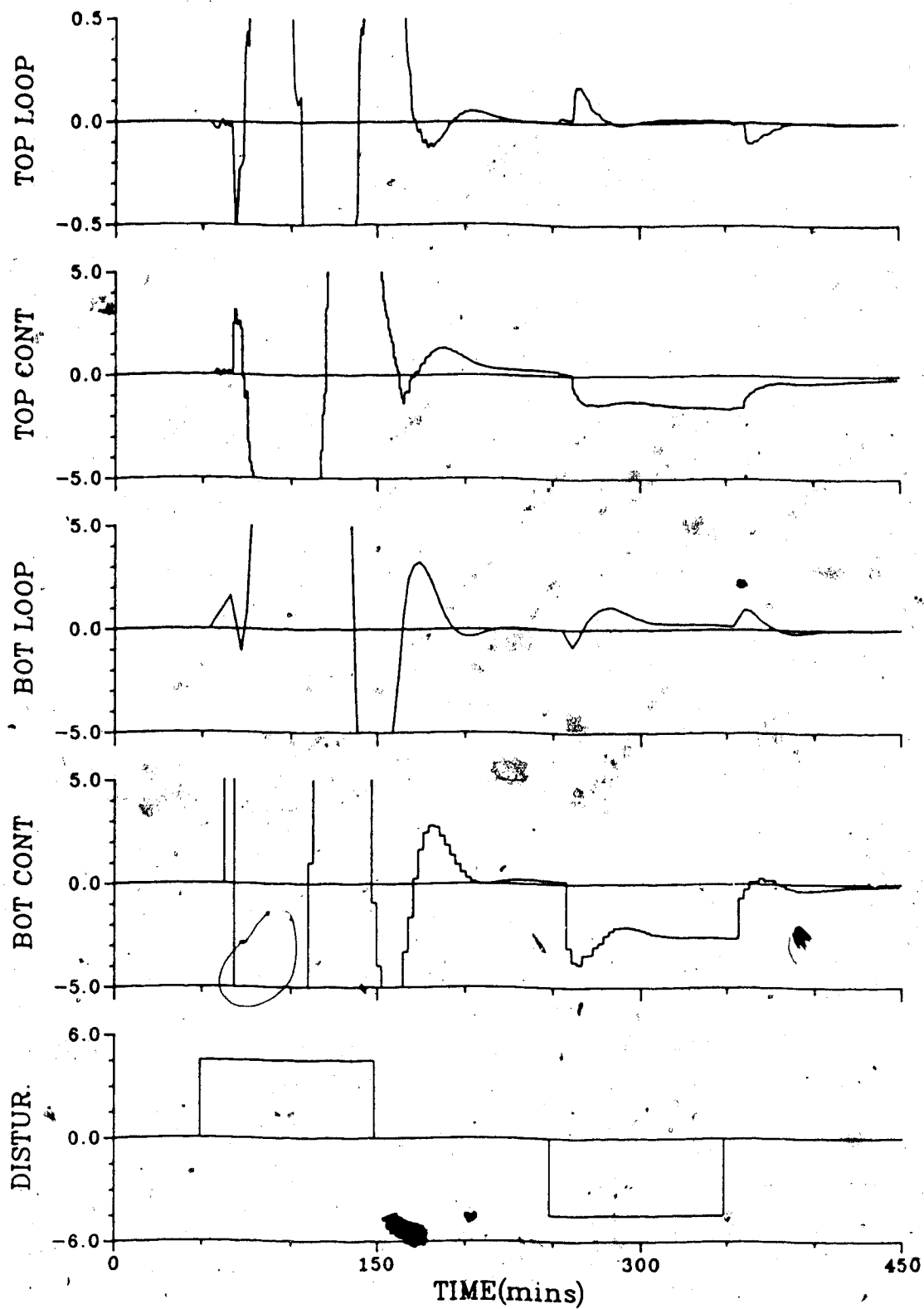


Figure 7.50 - GMV Control of the Linear Column Model with  $g_0=0.0$ , Q Weighting from PI/PI and the Time Delay Underestimated with NFF

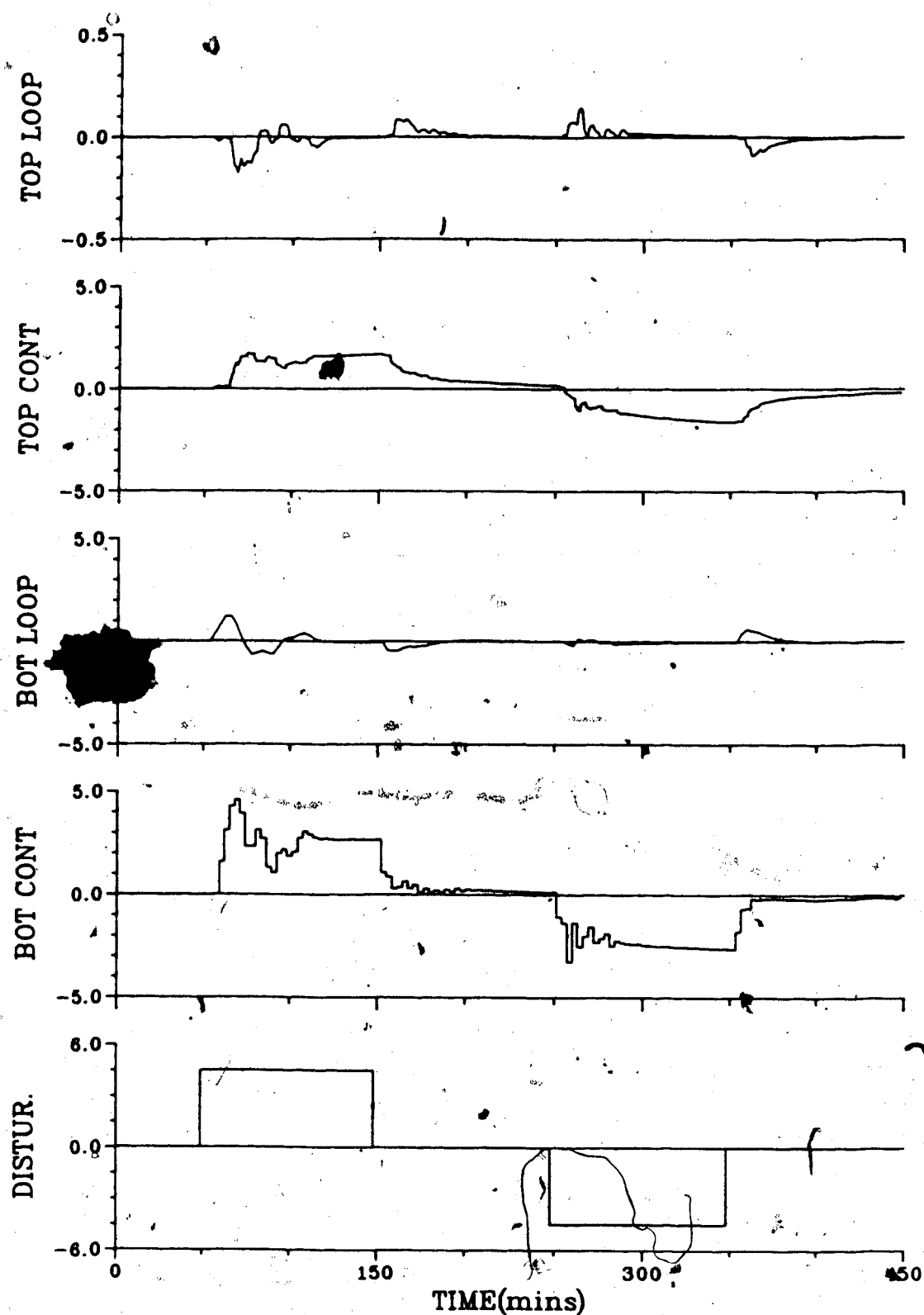


Figure 7.51 - GMV Control of the Linear Column Model with  $g_0=0.0$ ,  $Q$  Weighting from PI/PI and the Time Delay Underestimated using MFF

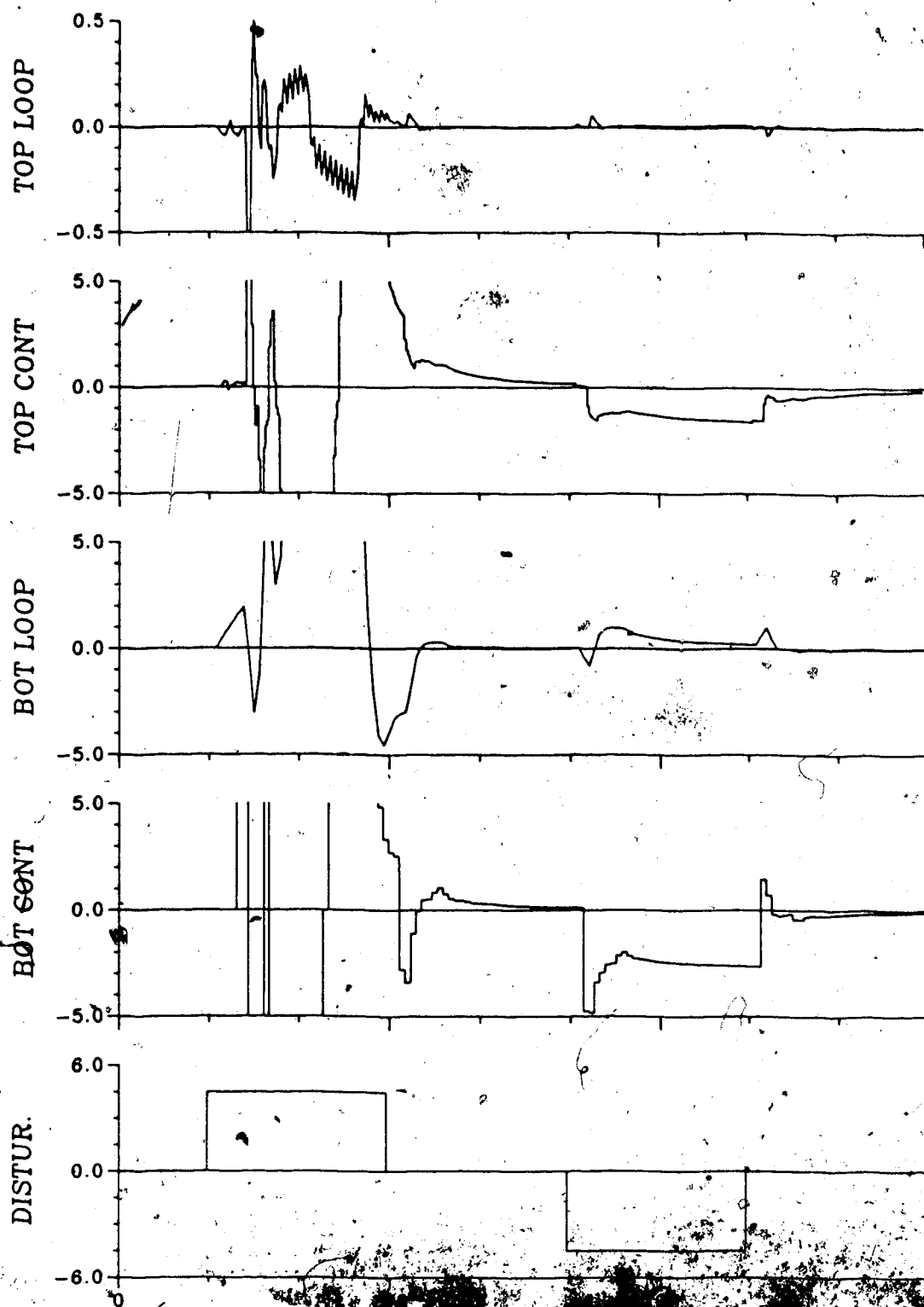


Figure 7.52 - GMV Control of the Linear Column Model with  $Q$  weighting adapting from  $g_0$  and  $PI/PI$  constants with NFF

Table 7.3  
SAE Values for the Linear Distillation Column  
Simulations for Various Control Strategies

Control/ Strategy	SAE value		
	NFF	EFF	MFF
TOP LOOP			
PID	4.15		
PID / Single rate	4.51		
PI	8.59		
MIN VAR	0.13	1.11	0.75
GMV / PID	4.33	4.72	4.67
GMV / PID, Single rate			109.9
GMV / PI	4.19	4.86	3.96
GMV / PID, $g_0 = 0.0$	27.99	24.62	3.93
GMV / PID, $g_0 = 0.0$ , Single rate			691.4
GMV / PI, $g_0 = 0.0$	7.09	6.37	4.60
GMV / PID, $g_0 = 0.0$ , Underestimated Delay	20.67	14.78	9.04
GMV / PID, $g_0 = 0.0$ , Underestimated Delay, Single rate			158.8
GMV / PI, $g_0 = 0.0$ , Underestimated Delay	4.29	5.70	3.85
GMV / Q's adapting from $g_0$	1.36	1.23	1.59
BOTTOM LOOP			
PID	32.50		
PID / Single rate	32.77		
PI	72.53		
MIN VAR	170.3	235.4	89.84
GMV / PID	72.37	108.6	92.48
GMV / PID, Single rate			184.6
GMV / PI	91.57	109.6	49.03
GMV / PID, $g_0 = 0.0$	259.6		40.47
GMV / PID, $g_0 = 0.0$ , Single rate			991.5
GMV / PI, $g_0 = 0.0$	263.8	164.6	40.81
GMV / PID, $g_0 = 0.0$ , Underestimated Delay	158.7	63.43	41.74
GMV / PID, $g_0 = 0.0$ , Underestimated Delay, Single rate			141.8
GMV / PID, $g_0 = 0.0$ , Underestimated Delay	62.70	100.4	16.68
GMV / Q's adapting from $g_0$	54.48	39.36	76.56

One simulation not reported in Table 7.3 was that for the GMV test in which the feedforward action consisted of an estimate of the disturbance,  $g_0 = 0.0$ , and PID constants were used to establish the  $Q$  weighting coefficients. The SAE value for the initial portion of the test was too high to actually be reported, making it impossible to obtain a value for the tuned portion of the test.

In general, being able to measure the disturbance and use the measured value as the feedforward action in the controller improves the performance of the controller. The use of no feedforward action was in general, but not always, the least successful of the various schemes. As mentioned earlier, when using an estimated or measured value of the disturbance in the feedforward action, retuning the PID controller will be required to maintain reasonable control. Hence it may be expected that retuning the parameters used in calculating the  $Q$  weighting coefficients will improve the control once a feedforward signal is added.

Using the self-tuning controller with  $Q$  weighting coefficients calculated without derivative action, with a few exceptions, improved the control performance. The test where  $g_0 = 0.0$ , the process time delay was underestimated and the derivative action was not included in the calculations, and the test where the  $Q$  coefficients were adapted from  $g_0$  both produced quite low SAE values for all feedforward options. The minimum variance control strategy resulted in the smallest SAE values in the top loop, but in

the bottom loop most of the other control strategies outperformed minimum variance, probably owing to the mismatch between the process time delays and the time delays used in the controller model. In very few cases did the self-tuning controller actually outperform the tuned PID controller.

## 8. Experimental Results

### 8.1 Introduction

This chapter summarizes the experimental work performed on the distillation column during the course of this study. Following the pattern used for the simulation studies, a base case was determined by applying conventional PI/PID control to the column under both single and multirate configurations. Discussion of the approach used to commission the self-tuner, that is, the transfer of control of the column to self-tuning control, will be conducted in Section 8.3. Minimum variance control was attempted on the column, followed by a series of generalized minimum variance control tests designed to evaluate the various schemes for selecting the  $Q$  weighting, and the various feedforward options under both single and multirate control.

All the experimental tests involved subjecting the column to  $\pm 25$  mass percent changes in the feed flow in a square wave pattern, with the duration of each step being 150 minutes. Under single rate control, a sampling time of three minutes was used for both the top and bottom composition control loops. Multirate control involved sampling the top loop at one minute intervals. The SAE values for all of the tests are tabulated to assess the performance achieved using the different forms of the control algorithms.



## 8.2 PI/PID Control

To provide a base case, the column was operated under PI control of the top composition and PID control of the bottom composition with the loops treated independently, that is, under multiloop control. Initially, the controller constants calculated in Chapter 6 were used. In an effort to improve the control a series of tests with various controller constants was performed in which the proportional band, the integral time and the derivative time (in the case of the bottom composition controller) were varied with the objective of reducing the total absolute error. For both loops the third disturbance, the step decrease in flow rate from steady state, proved to be the most difficult disturbance to control. It is possible to tune the controllers to minimize the error resulting from this disturbance, but when the controller is well tuned for this disturbance, control behavior during the other three disturbances results in a total SAE value that is no longer a minimum overall. Consequently the well tuned controller constants were chosen to provide the most satisfactory behavior for composition control for all four feed flow rate disturbances. Figure 8.1 shows the performance for the single sampling rate case using a sampling time of three minutes for both the top and bottom composition control loops. The addition of derivative action was not found to improve the control on the top loop. The controller constants used to achieve the control performance shown in

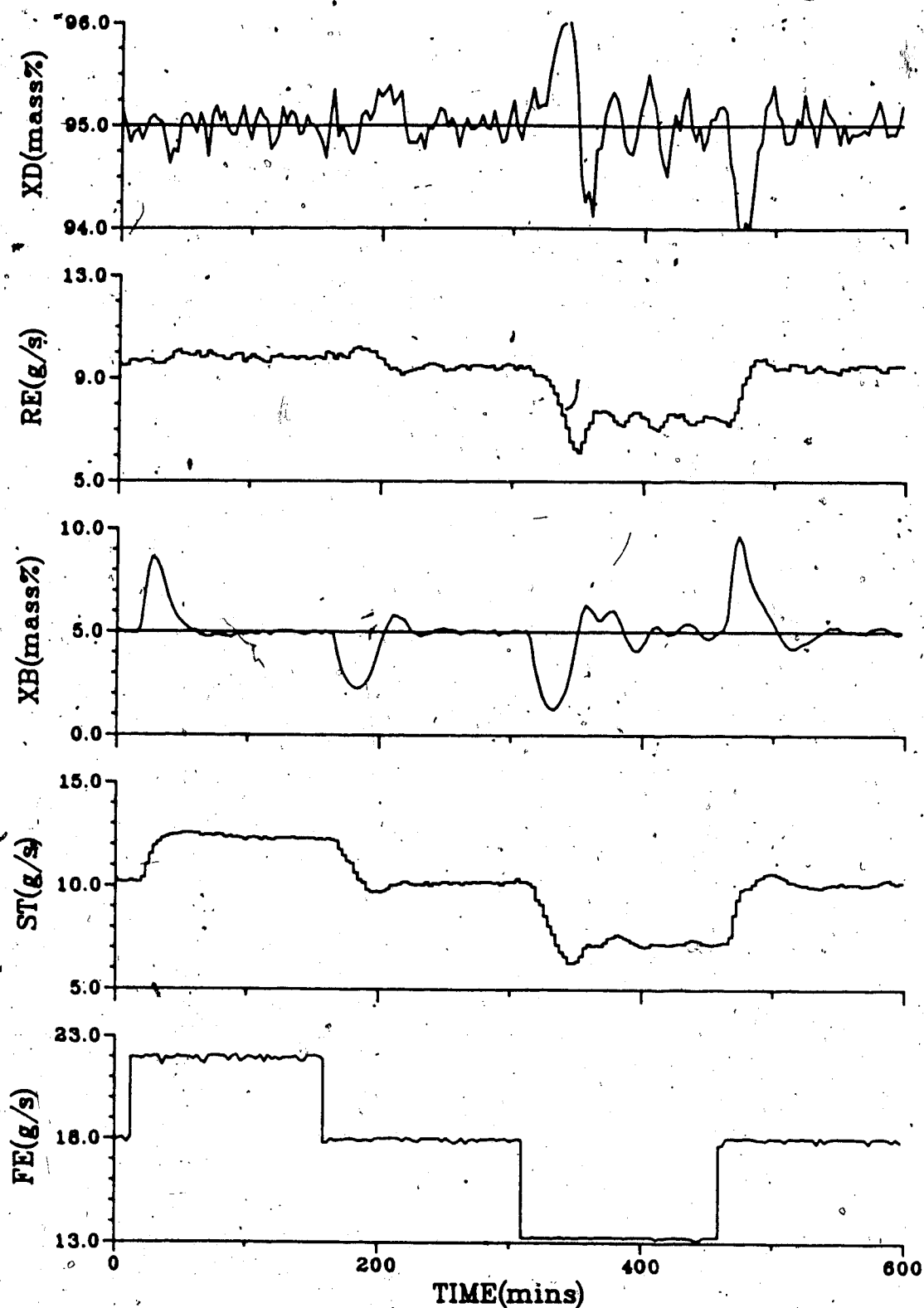


Figure 8.1 - Single Rate PI/PID Control of the Column

Top: PB=30.0 TI=170.0

Bottom: PB=65.0 TI=425.0 TD=125.0

Figure 8.1, were  $PB = 30.0$  and  $TI = 170.0$  for the top composition loop and  $PB = 65.0$ ,  $TI = 425.0$  and  $TD = 125.0$  for the bottom loop.

Under multirate control, with the top composition sampled at one minute intervals, the control performance that resulted is shown by the response in Figure 8.2. As for the single rate sampling test, there was no improvement by use of derivative action for the top composition controller with well tuned controller constants established as  $PB = 20.0$  and  $TI = 170.0$  for the top loop and  $PB = 65.0$ ,  $TI = 425.0$  and  $TD = 125.0$  for the bottom loop.

There is no noticeable difference between the control behavior in Figures 8.1 and 8.2, but it is interesting to compare the SAE values for these two tests, and the tests performed using the initial controller constants, shown in Table 8.1. In this summary, the four consecutive steps in feed flow rate have been referred to as: ASS, the step above steady state; DSS, the step down to steady state; BSS, the step below steady state; and USS, the step up to steady state. From Table 8.1 it can be observed that a considerable reduction in the total SAE value for the top loop has been achieved by both using multirate sampling and by using the tuned controller constants. Even though tuning PI/PID controllers is a time consuming process, the SAE values show that the control performance can be improved considerably over the results obtained using the initial estimated controller constants.

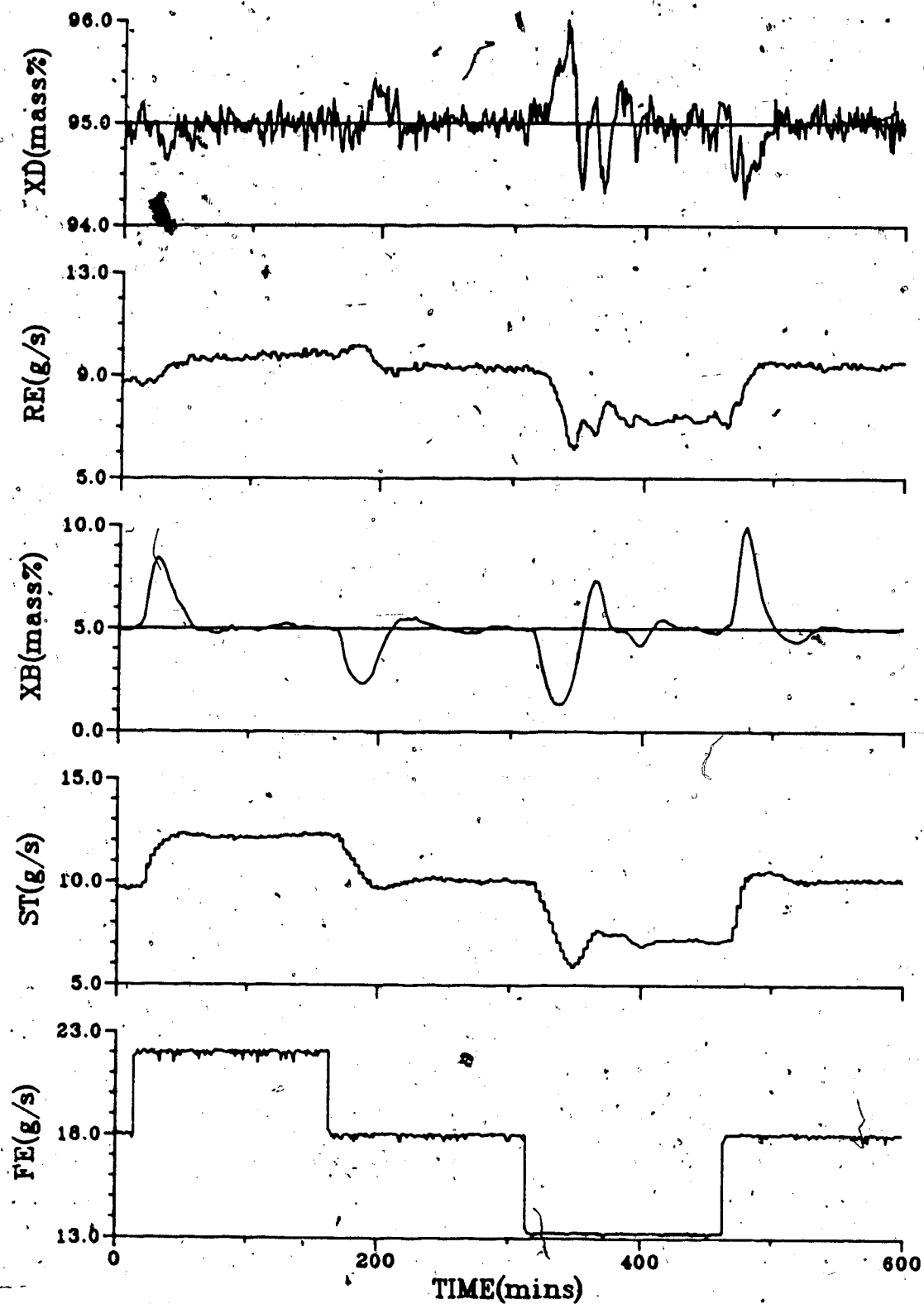


Figure 8.2 - Multirate PI/PID Control of the Column

Top: PB=20.0 TI=170.0

Bottom: PB=65.0 TI=425.0 TD=125.0

Table 8.1  
SAE Values for PI/PID Control

PI/PID Total Constants	SAE for the step:					
	Loop	ASS	DSS	BSS	USS	SAE
Single Rate Control						
Initial Values	Top	20.0	34.8	62.4	42.2	159.4
	Bottom	122.2	149.2	182.0	158.0	611.4
	Both	142.2	184.0	244.4	200.2	770.8
Well Tuned Values Figure 8.1	Top	15.5	20.5	49.5	32.2	117.7
	Bottom	78.0	89.1	142.8	111.8	421.7
	Both	93.5	109.6	192.3	144.0	539.4
Multirate Control						
Initial Values	Top	14.9	23.9	30.6	26.1	95.5
	Bottom	123.5	135.8	226.9	171.8	658.0
	Both	148.4	159.7	257.5	197.9	753.5
Well Tuned Values Figure 8.2	Top	14.0	15.1	32.4	21.6	83.1
	Bottom	81.3	87.0	142.0	99.0	409.3
	Both	95.3	102.1	174.4	120.6	492.4

### 8.3 Commissioning the Self-tuning Controller

The difficulties associated with starting up the self-tuning controller arise because the identification routine requires some time to properly identify the parameters used in the self-tuning control law. It is necessary, before any identification is performed, to initialize the data vectors that are used by the

identification routine to contain the actual column steady state flow rates and set points for at least a number of sample intervals equal to or greater than the system order plus the largest time delay. After that, experience dictates that identification should take place for a period of time before the self-tuning controller is turned on.

Identification of the process parameters is required to establish the relationships between the process inputs and outputs in the control law. Under some circumstances the system may be sufficiently excited, through noise or drifting outputs, to allow the control law coefficients to be properly identified. However, for the actual distillation column operating at steady state there is insufficient excitation for the parameter identification to properly take place, as illustrated by the responses in Figure 8.3. For this test the column operated under PI/PID control until steady state conditions were deemed to exist. Identification began at 30 minutes on the plot and continued for 3 hours. As is typical of all the start-ups, no feedforward action was used. Six minutes after the self-tuning controller was turned on, at approximately 215 minutes in the figure, the steam flow unexpectedly dropped, resulting in the bottom composition rapidly increasing. After the bottom composition rose above 15%, the column was switched on to manual control as a safety precaution and the identification was turned off. By examining the adaptation pattern of the parameters shown in Figure 8.4, it can be seen that there is a

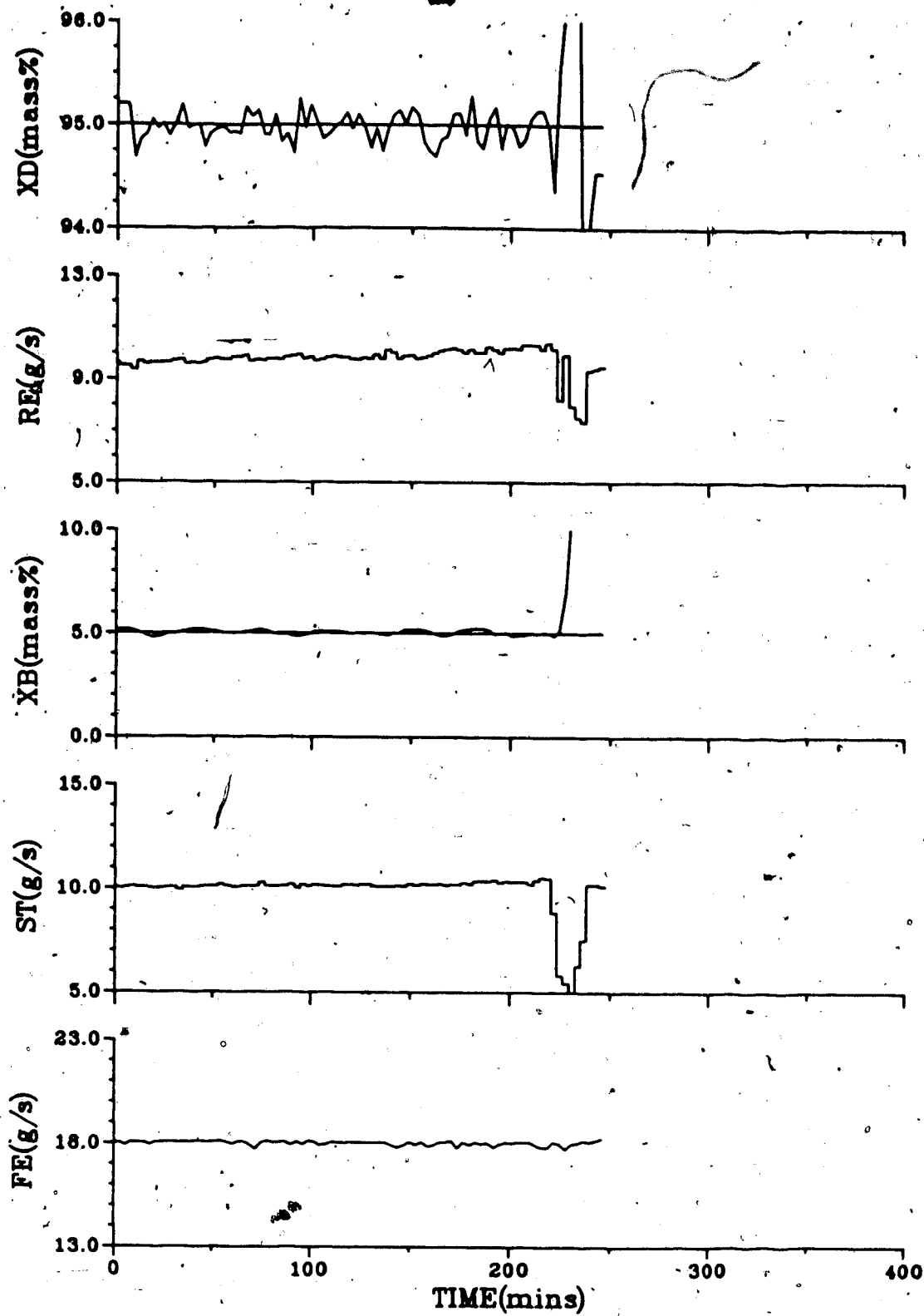


Figure 8.3 - Unsuccessful Column Start-up

significant change in the parameter values after the self-tuning controller was turned on. The identification routine was unable to identify acceptable controller parameter values in time to prevent the switch to manual control.

After attempting several different techniques for improving the initialization of the self-tuning controller, a start-up pattern which proved to be satisfactory for most of the tests performed during this study was adopted and is shown in Figure 8.5. Identification was started 30 minutes following the start of data collection (data collection is considered to coincide with the origin of the figures). After a minimum of 2 hours of identification a  $\pm 5\%$  feed disturbance was introduced, with the column still under PID control, to force some change in both the reflux and steam flow rates. Each step of the disturbance was 45 minutes in duration. After the end of the fourth step, the column was left to attain steady state, still under PID control, for at least an additional hour, at which time the column was switched to self-tuning control. Upon making the change from PID to self-tuning control, some deviation in the reflux and steam flows resulted since, as can be seen in Figure 8.6, the parameters still had not converged to their final values. Note that the final adapting period was short and that once the parameters converged, they remained steady. After self-tuning control began, the column was left for at least 2.5 hours to reach a steady state before any tests



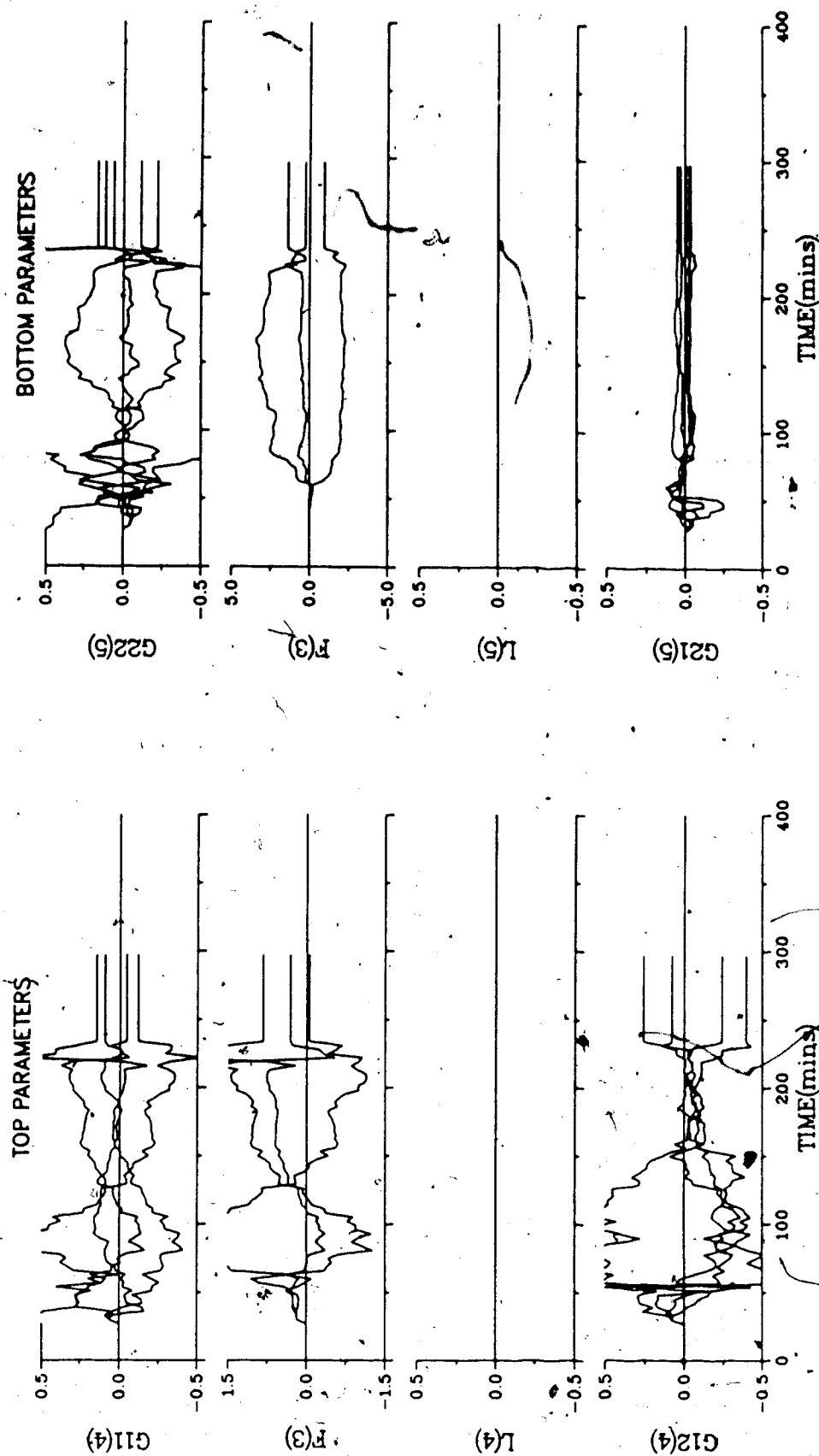


Figure 8.4 - Parameters for the Unsuccessful Column Start-up

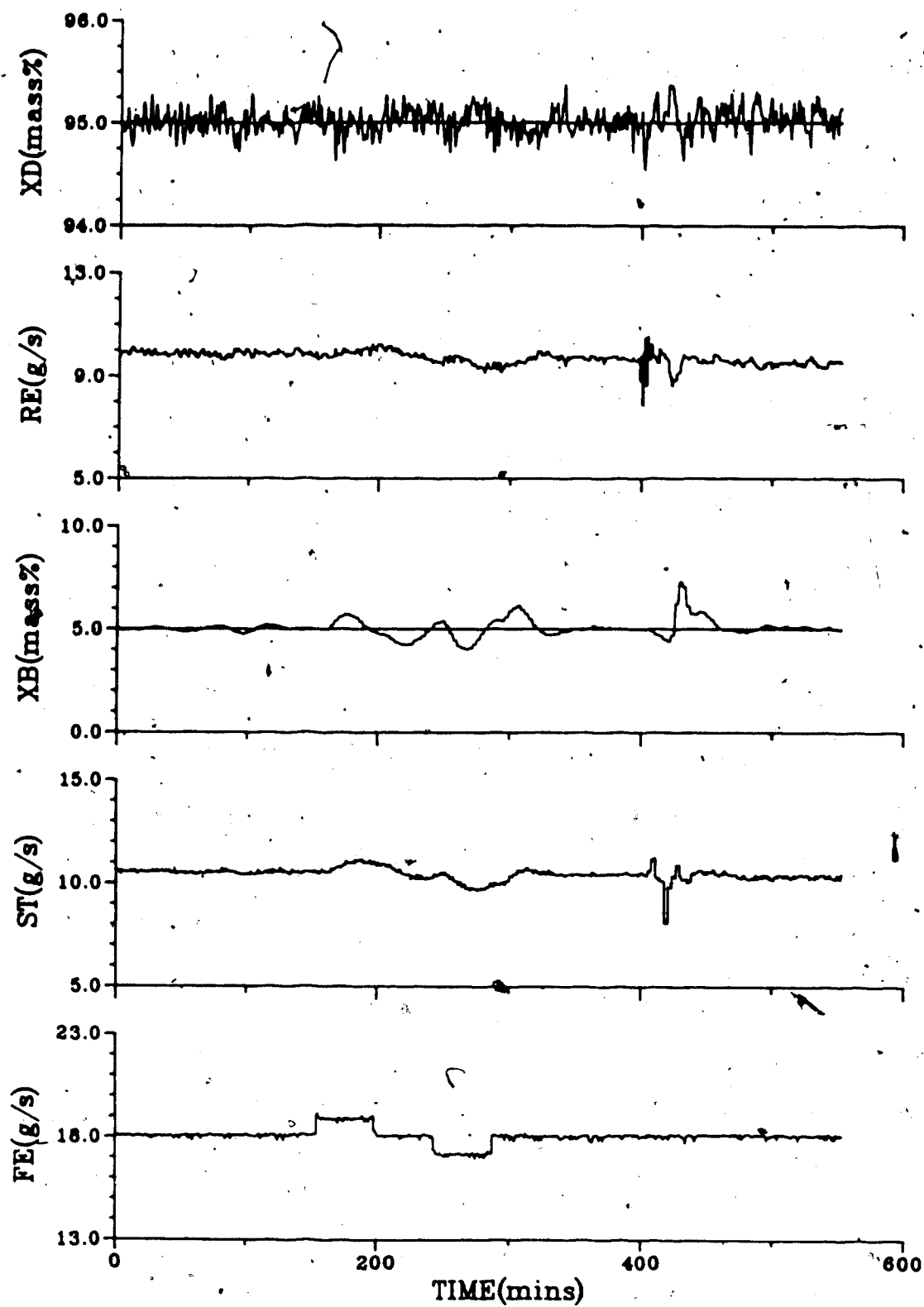


Figure 8.5 - Successful Column Start-up

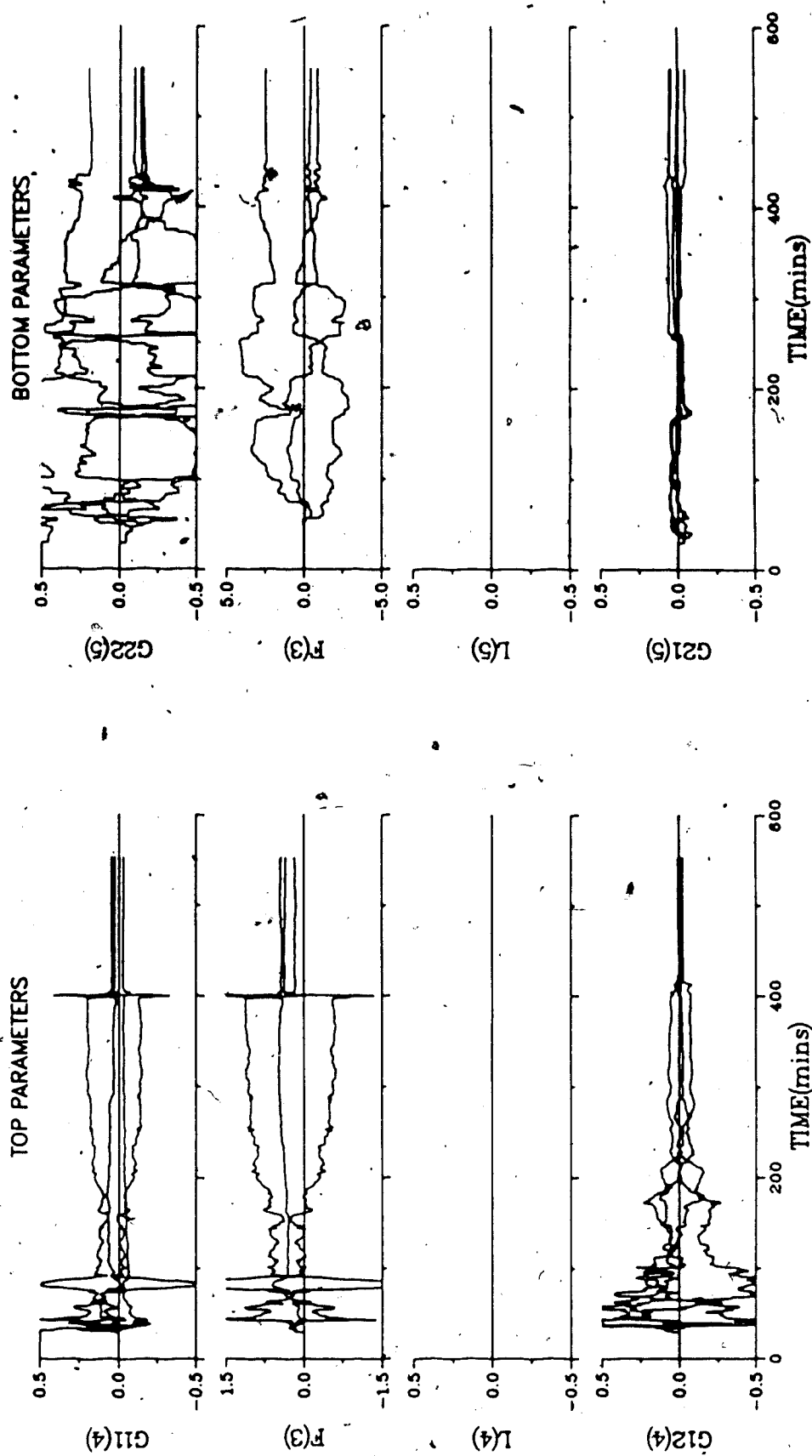


Figure 8.6 - Parameters for the Successful Column Start-up

were performed. The size of the deviation of the top and bottom compositions from their set points that was caused by switching the self-tuning controller on was a function of the duration of the  $\pm 5\%$  disturbance steps and the time left after the last step before the self-tuning controller was started.

Commissioning the self-tuning controller was not a straightforward process and for someone inexperienced with this aspect of adaptive control, unwarranted disappointment with the controller may result. For the majority of the results that follow, the start-up procedure was similar to that just described and the tests were initiated after the self-tuning controller had run at steady state for a minimum of one hour.

#### 8.4 Minimum Variance Control

The simulations in Chapter 7 indicated that although minimum variance control employs large steps in the control action, very good control performance results. Hence a minimum variance control test was performed with single rate sampling and no feedforward control action, leading to the responses shown in Figure 8.7. As can be seen from Figure 8.7, control of the top composition was very poor. One factor that may cause this behavior is the difference between the actual one minute process time delay in the top loop and the assumed delay of three minutes (one sample interval) used to establish the structure of the controller.

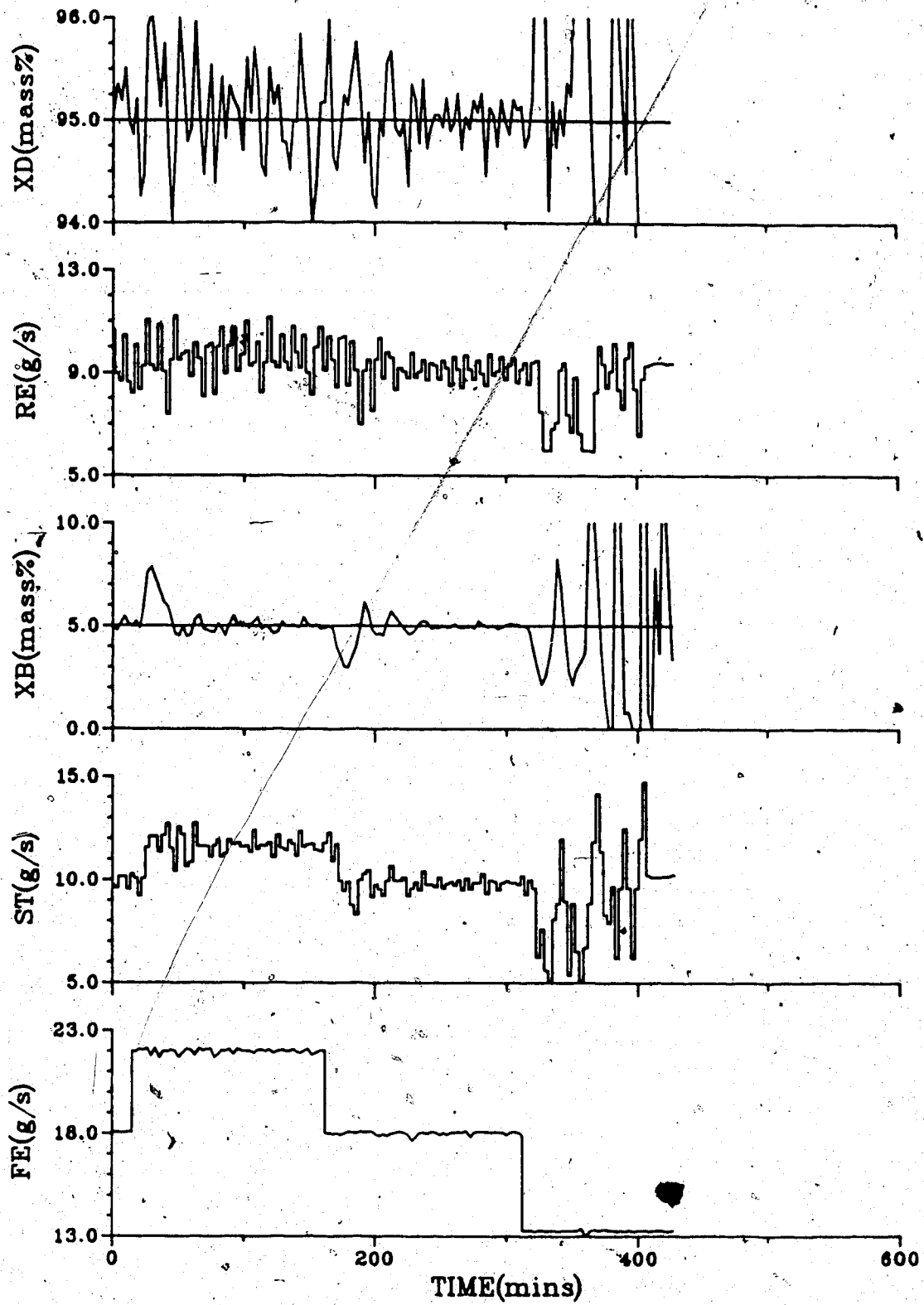


Figure 8.7 - Minimum Variance Control of the Column

Another factor is no doubt the lack of weighting on the control action which resulted in a bang-bang type of control action. In the bottom loop the initial deviations of the bottom composition from its set point for each of the first two changes in feed flow were substantially reduced compared with the deviations that resulted using a PID controller. However, once the bottom composition was brought to its set point the controller continued to make abrupt changes in the steam flow which prevented the bottom composition from remaining at the set point. The third step change in the feed flow resulted in such poor control that the column was switched from self-tuning to manual control at approximately 410 minutes.

The response of the controller parameters corresponding to the control behavior shown in Figure 8.7 is presented in Figure 8.8. The amount of adaptation taking place after the third step indicates that either the new operating conditions represented a considerable change from the previous operating conditions, or that the identification routine experienced difficulty relating the control actions taking place with the resulting changes in the outputs. The poor control achieved was probably a combination of these two possibilities.

A test was attempted using the multirate minimum variance controller, but the control performance was so poor that it was not possible to maintain control of the column even at steady state. Setting  $Q = 0.0$  to obtain minimum

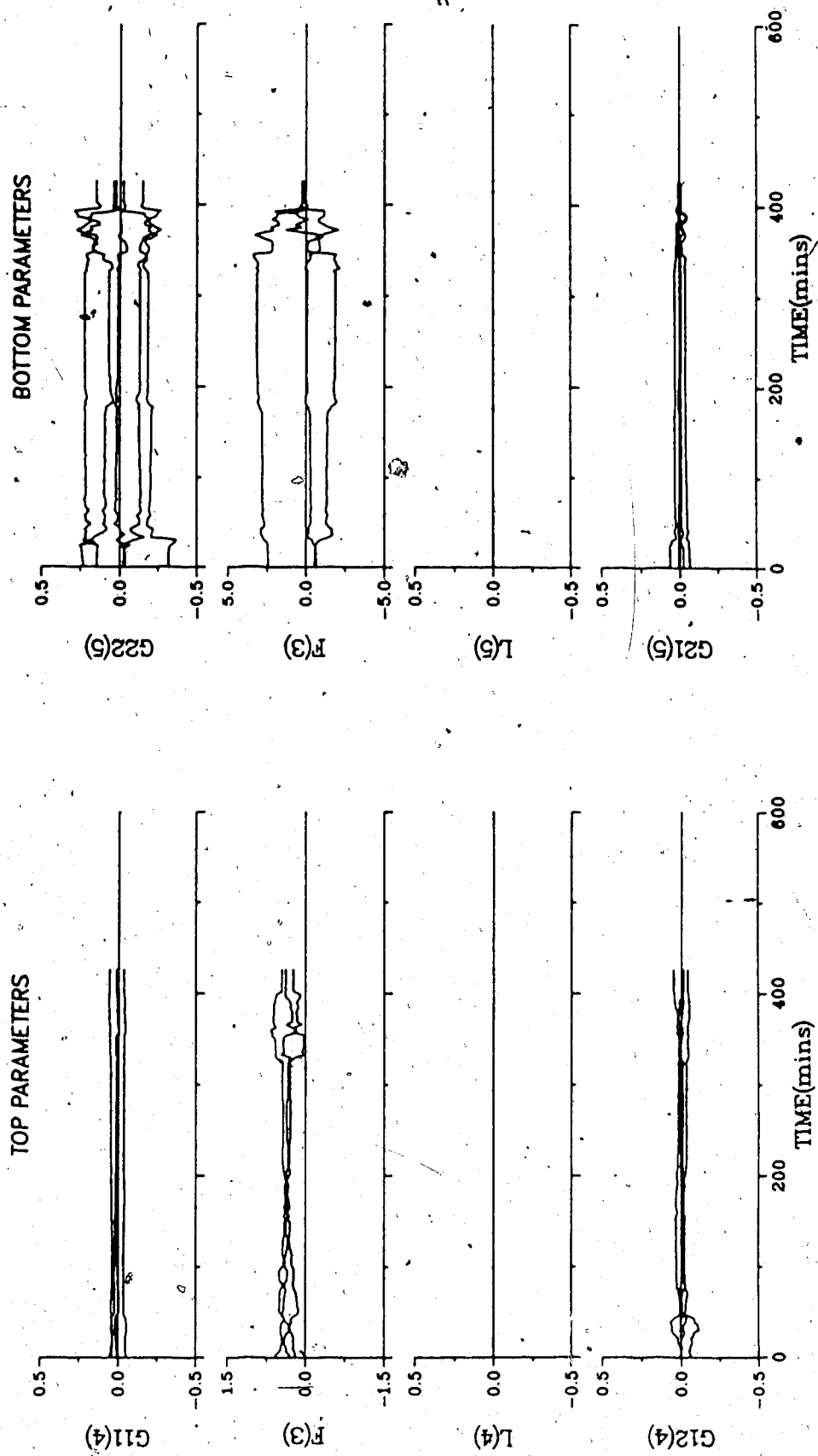


Figure 8.8 - Parameters for Minimum Variance Control of the Column

variance control, either single or multirate, was not successful in controlling the column and will therefore not be considered further.

## 8.5 Generalized Minimum Variance Control

### 8.5.1 Introduction

This section presents results from experimental tests performed on the column using the various techniques which allow the  $Q$  weighting polynomial to resemble the PID structure as discussed in Section 6.4.2. For each of the techniques, the experimental tests were repeated with the use of no feedforward control action (NFF), an estimate of the effect of the feed flow rate change on the output for use with feedforward control action (EFF), and direct measurement of the feed flow rate change for use with feedforward control action (MFF). The difference between the output and the predicted output,  $y(t) - y^*(t-k)$ , was used to implement the feedforward control action when it was assumed that measured values of the feed flow rate were not available. Most of the tests were performed using both single rate (SR) and multirate (MR) forms of the control algorithm. Each set of results includes two plots: one showing the manipulated and controlled variables, and another showing the parameters for the two loops.



### 8.5.2 Q Weighting Established from PI/PID Constants

The simplest method of assigning values to the Q weighting polynomial parameters is to ignore the  $q_0$  term and assume that the Q weighting has the form of an inverse PID compensator. For this choice the tuned PID controller constants may be used to calculate the Q coefficients. Since there was virtually no time delay associated with the top composition control loop, no derivative action was warranted, so an inverse PI compensator is used in the calculations. The controller constants employed to calculate the Q coefficients for the results shown in Figures 8.9-8.14 were  $PB = 30.0$  and  $TI = 170.0$  for the top loop. These correspond to  $q_0 = 3.36$  and  $q_1 = -3.30$ . For the bottom loop  $PB = 65.0$ ,  $TI = 425.0$  and  $TD = 125.0$ , so  $q_0 = 65.6$ ,  $q_1 = -130$  and  $q_2 = 64.1$ . Figures 8.9 and 8.10 use no feedforward action, while the value used for the feedforward action has been estimated in Figures 8.11 and 8.12, and measured in Figures 8.13 and 8.14.

From Figures 8.9, 8.11 and 8.13, it can be seen that use of the measured disturbance as the feedforward signal reduces the oscillations in the reflux flow that occurred during the third step of the tests where the measured disturbance is not available. Of the three tests, measuring the disturbance for the feedforward action resulted in the best control of top composition, particularly during the third and fourth steps.

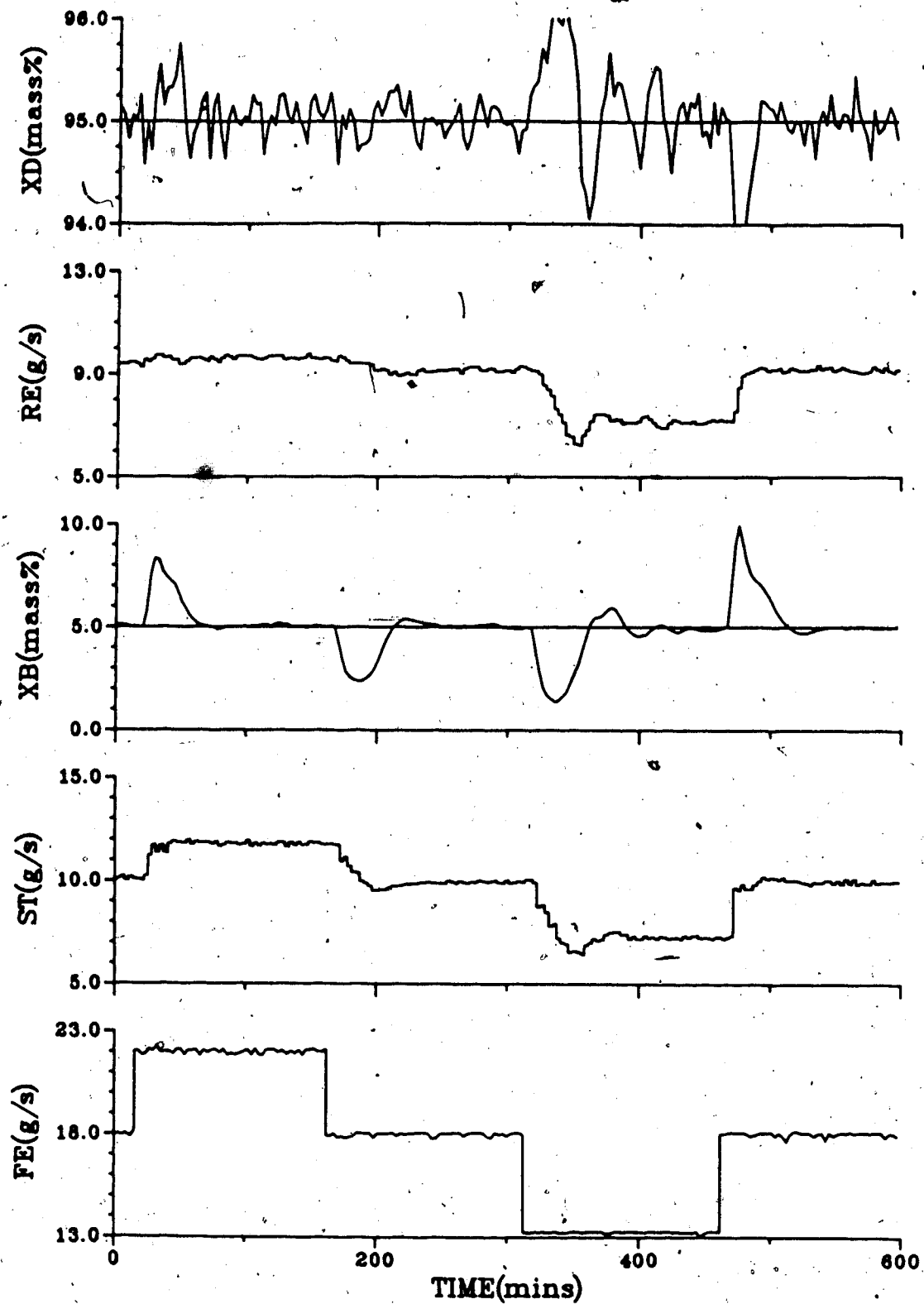


Figure 8.9 - Generalized Minimum Variance Control  
with Q Weighting based on PI/PID  
constants (SR,NFF)

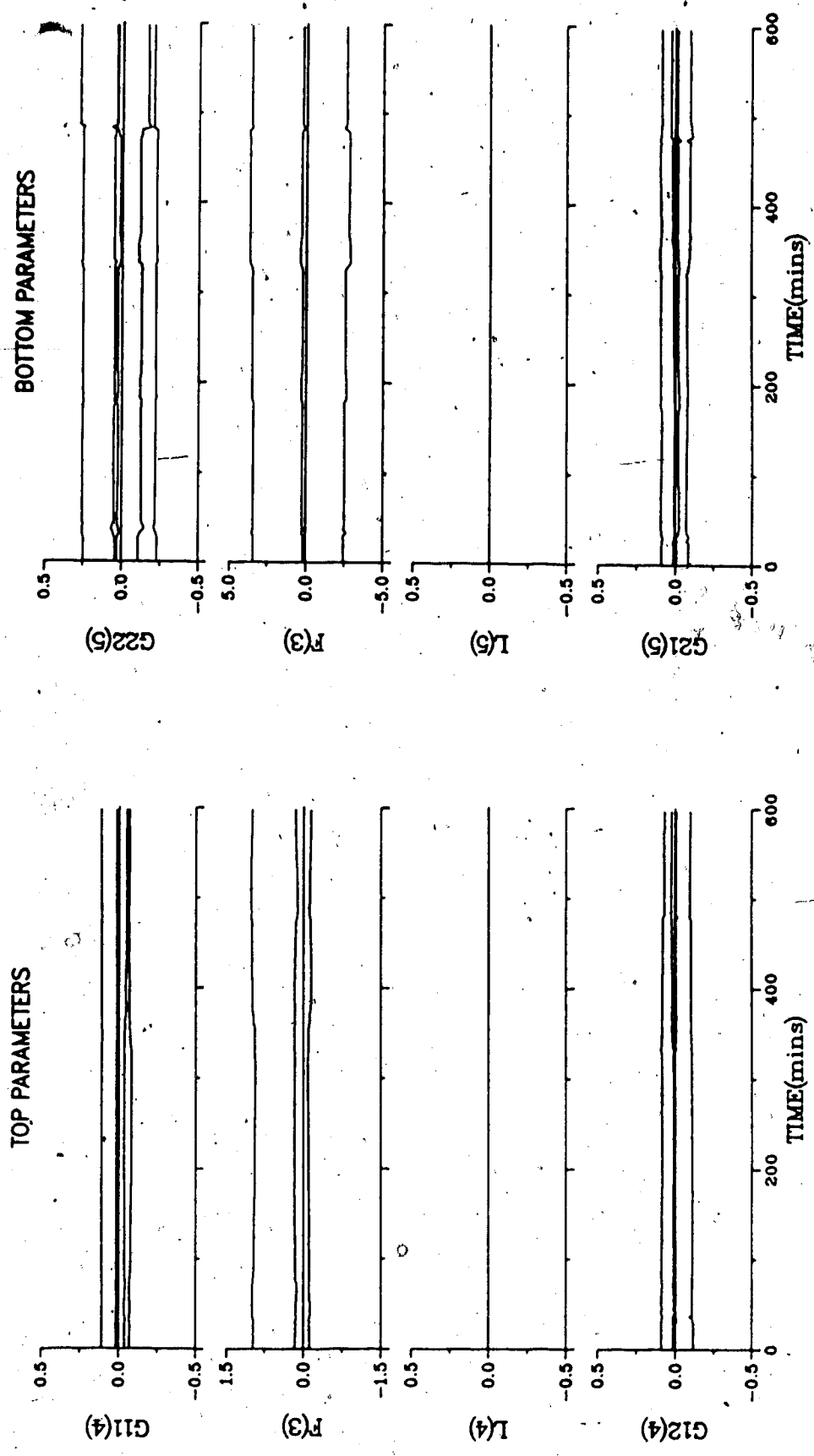


Figure 8.10 - Parameters for GMV Control with Q Weighting based on PI/PID constants (SR,NFF)

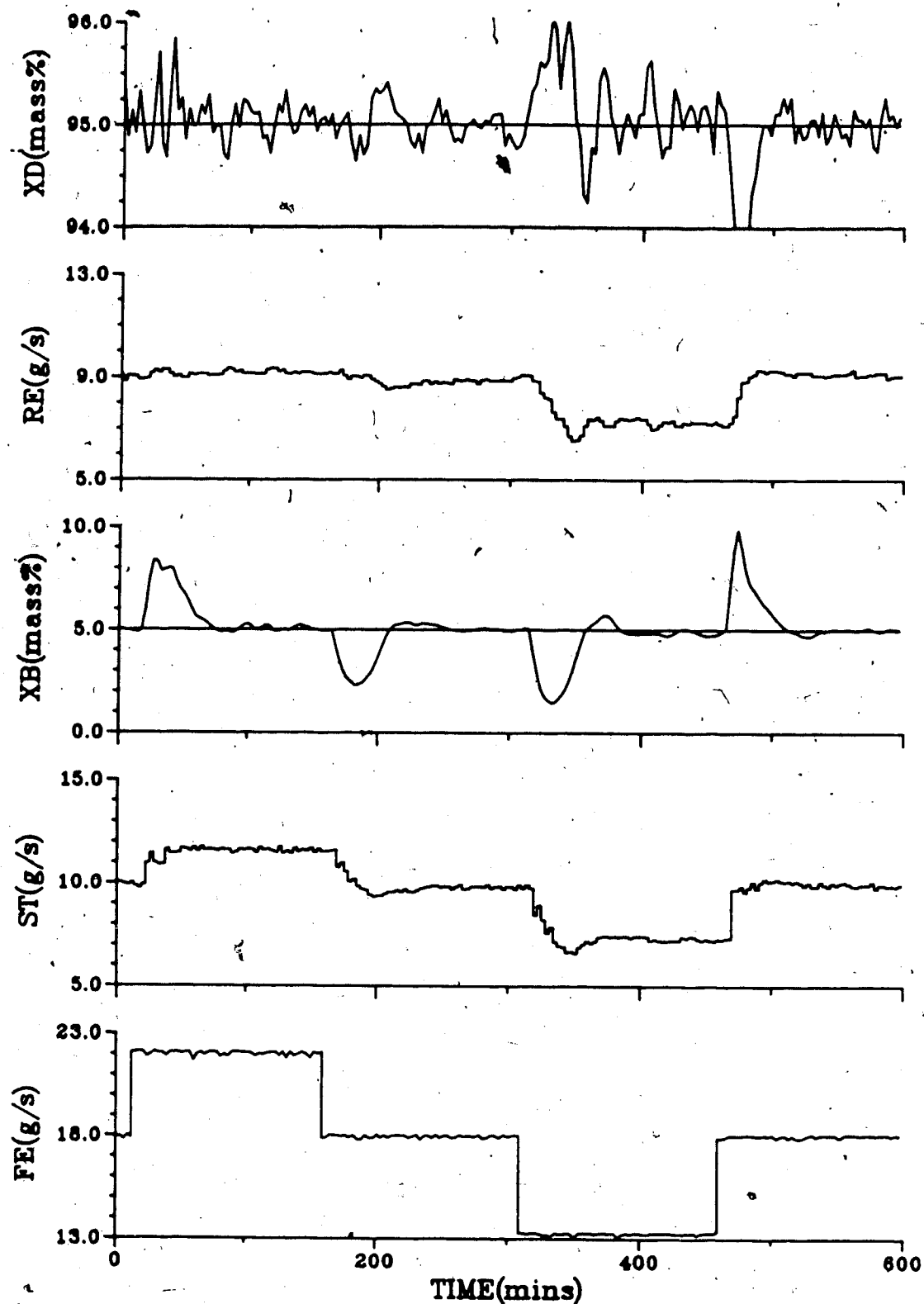


Figure 8.11 - Generalized Minimum Variance Control with Q Weighting based on PI/PID constants (SR,EFF)

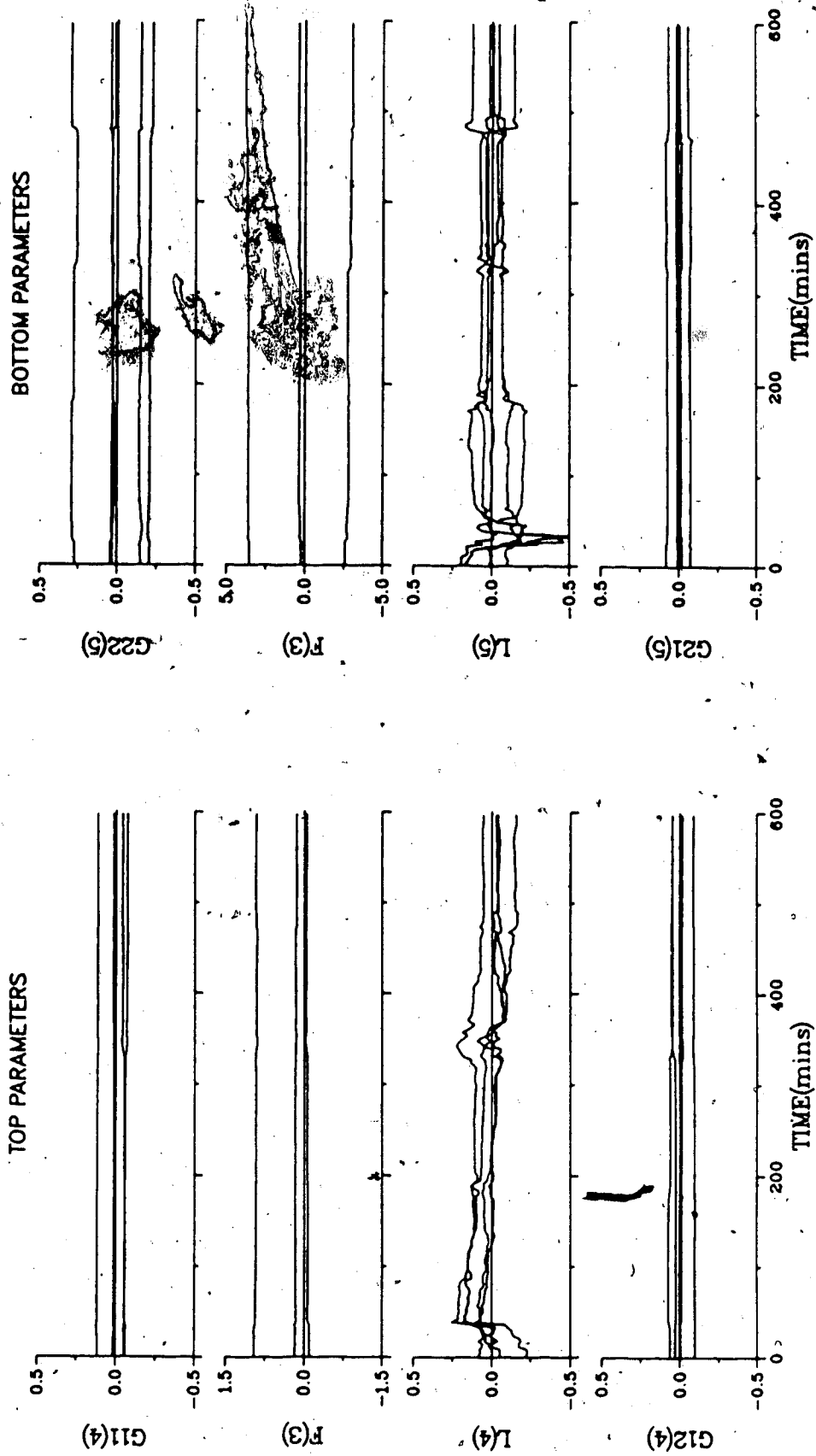


Figure 8.12 - Parameters for GMV Control with Q Weighting based on PI/PID constants (SR,EFF)

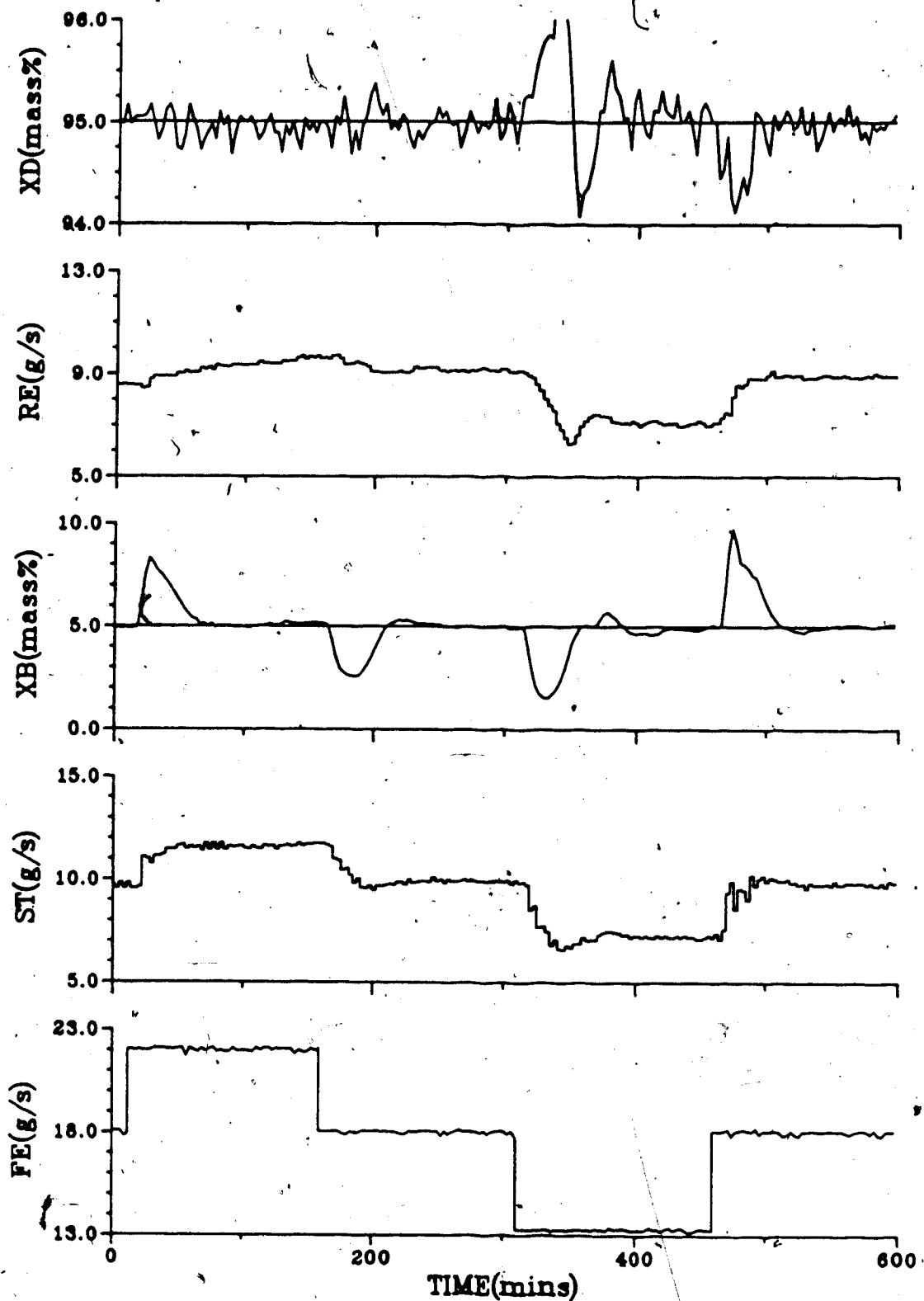


Figure 8.13 - Generalized Minimum Variance Control  
with Q Weighting based on PI/PID  
constants (SR,MFF)

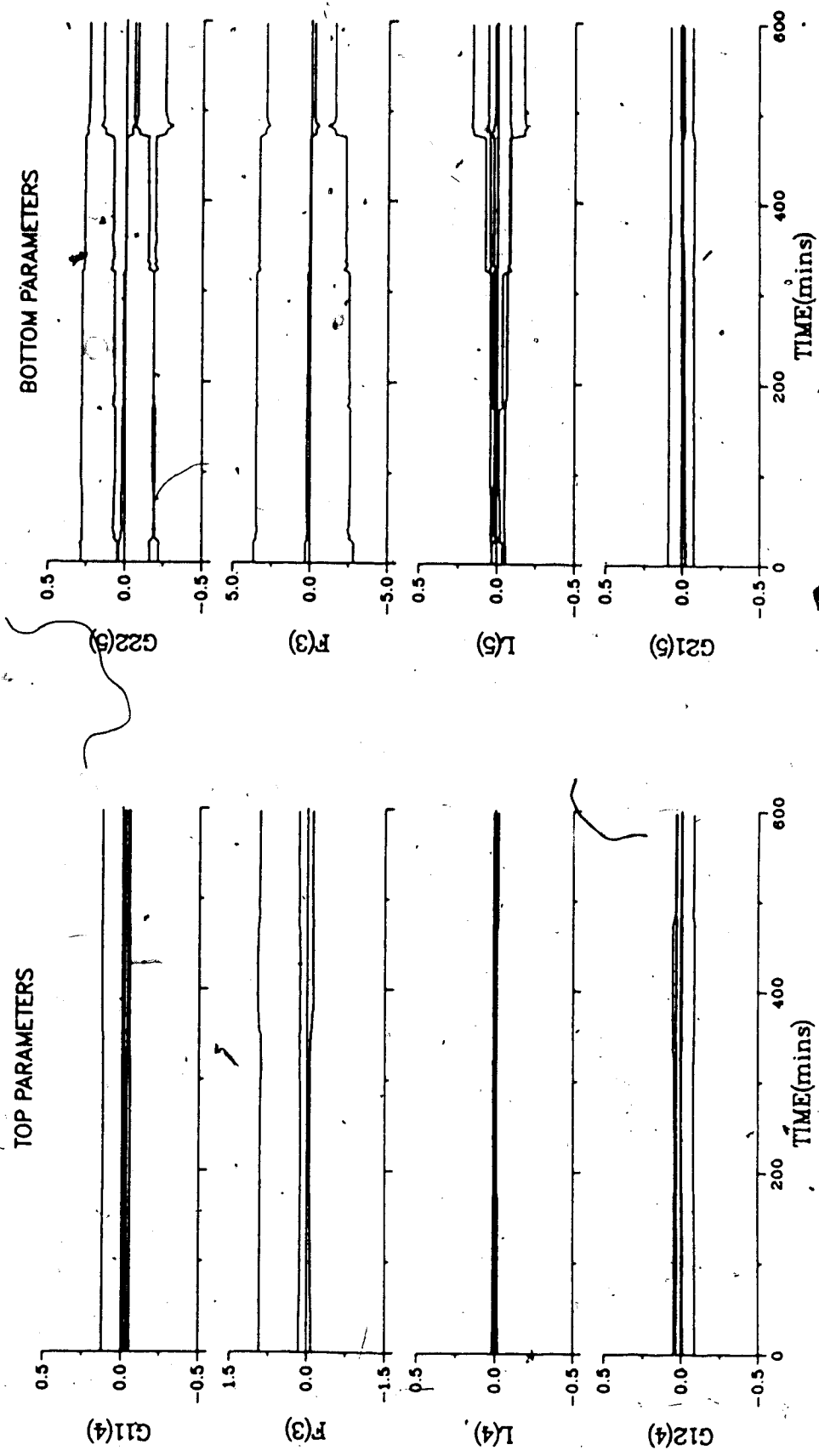


Figure 8.14 - Parameters for GMV Control with Q Weighting based on PI/PID constants (SR,MFF)

For the tests performed using the multirate sampling form of the algorithm, the controller constants used to calculate the Q polynomial coefficients were  $PB = 20.0$  and  $TI = 170.0$  for the top loop and  $PB = 65.0$ ,  $TI = 425.0$  and  $TD = 125.0$  for the bottom loop. This yields Q coefficients for the top loop of:  $q_0 = 5.05$  and  $q_1 = -4.99$ . Q coefficients for the bottom loop are unchanged from the values given previously. Comparison of the responses of the controlled variables from the single sampling rate tests with those of the three multirate tests, presented in Figures 8.15, 8.17 and 8.20, show that the control of the top composition has improved at the expense of the bottom composition control. The parameter adaption patterns displayed in Figures 8.16, 8.18 and 8.20 shows no marked difference from those shown in Figures 8.10, 8.12 and 8.14 for single rate sampling. The SAE values for the single and multirate cases are given in Table 8.2.



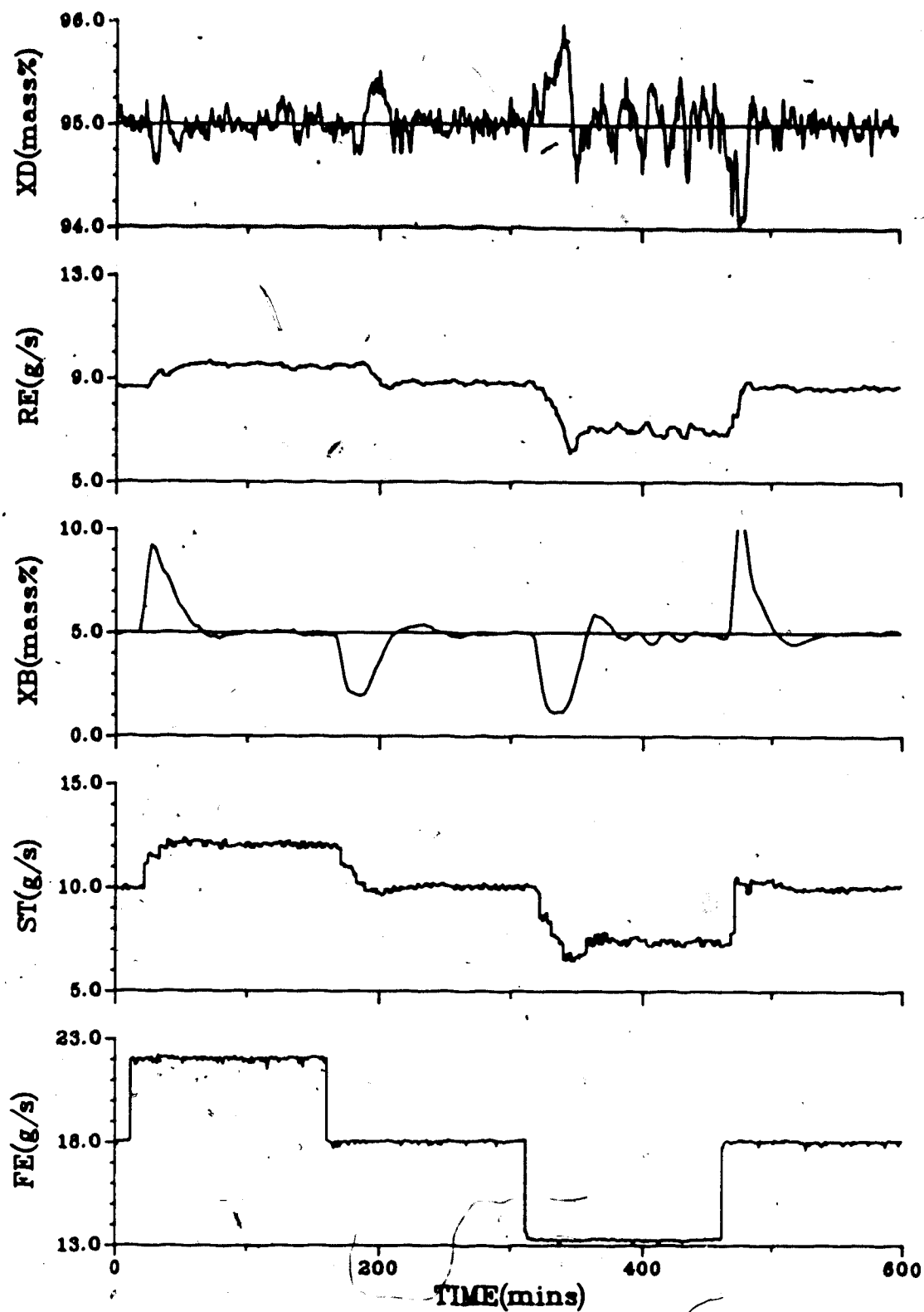


Figure 8.15 - Generalized Minimum Variance Control  
with Q Weighting based on PI/PID  
constants (MR,NFF)

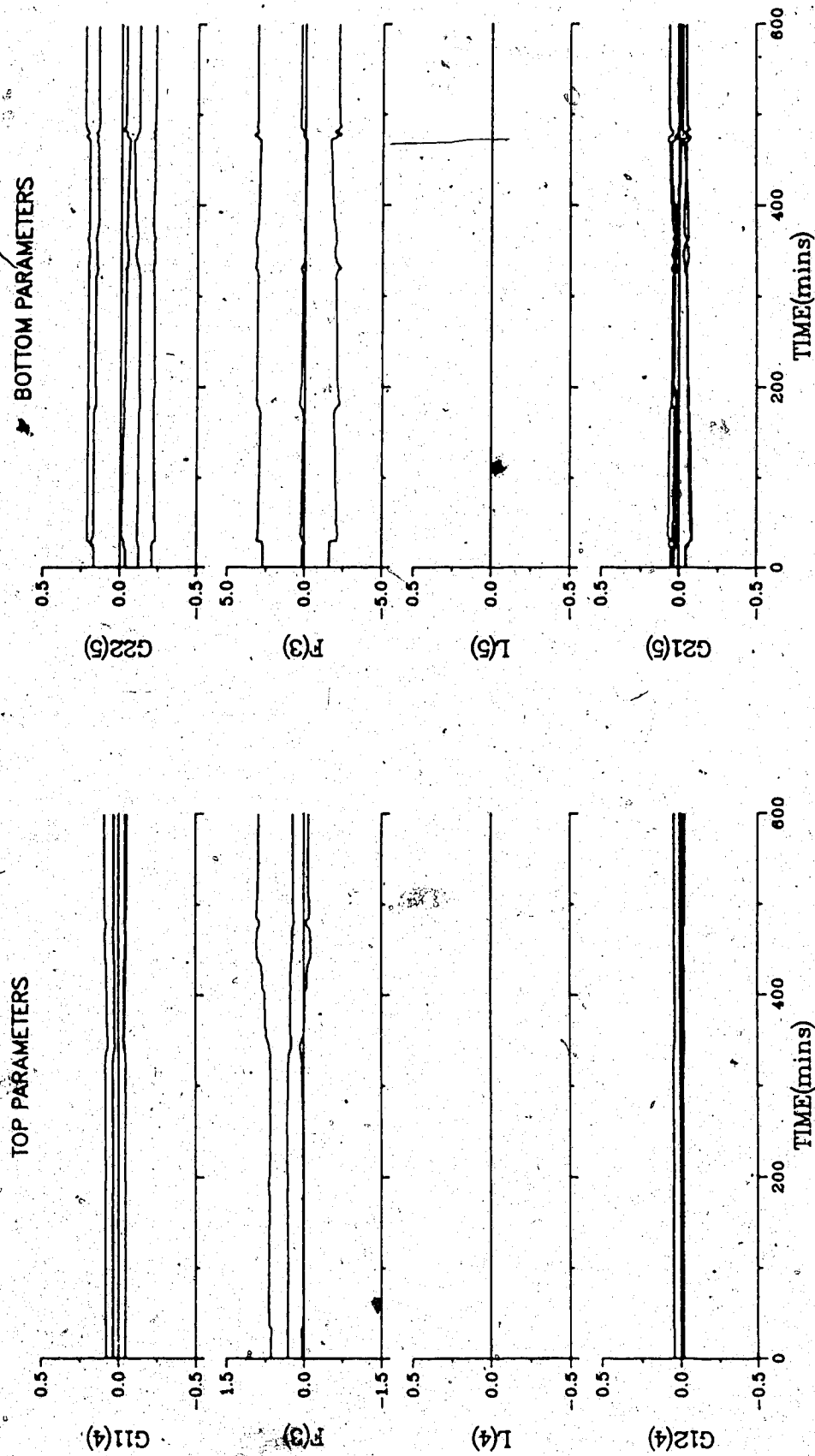


Figure 8.16 - Parameters for GMV Control with Q Weighting based on PI/PID constants (MR,NFF)

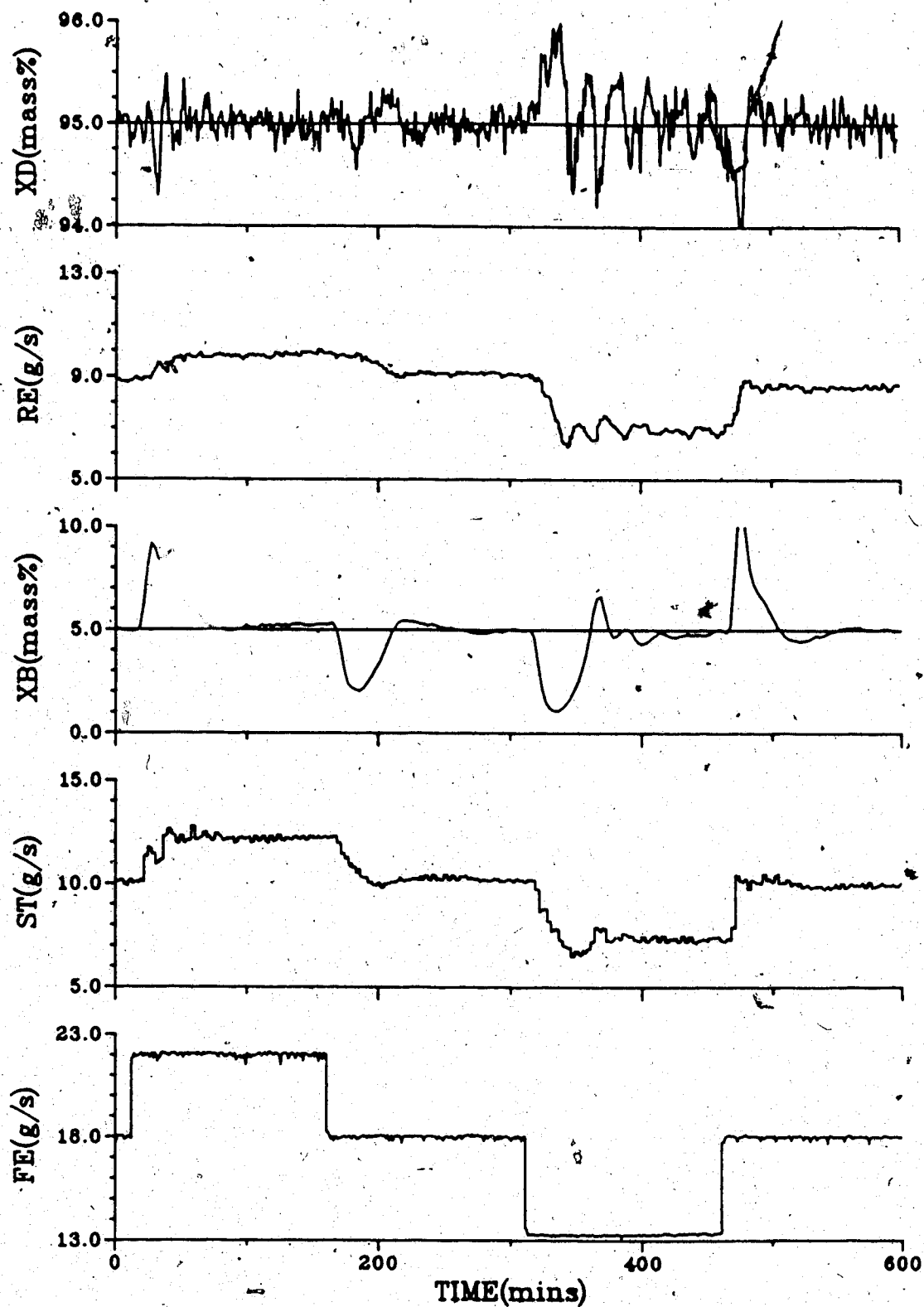


Figure 8.17 - Generalized Minimum Variance Control with Q Weighting based on PI/PID constants (MR, EFF)

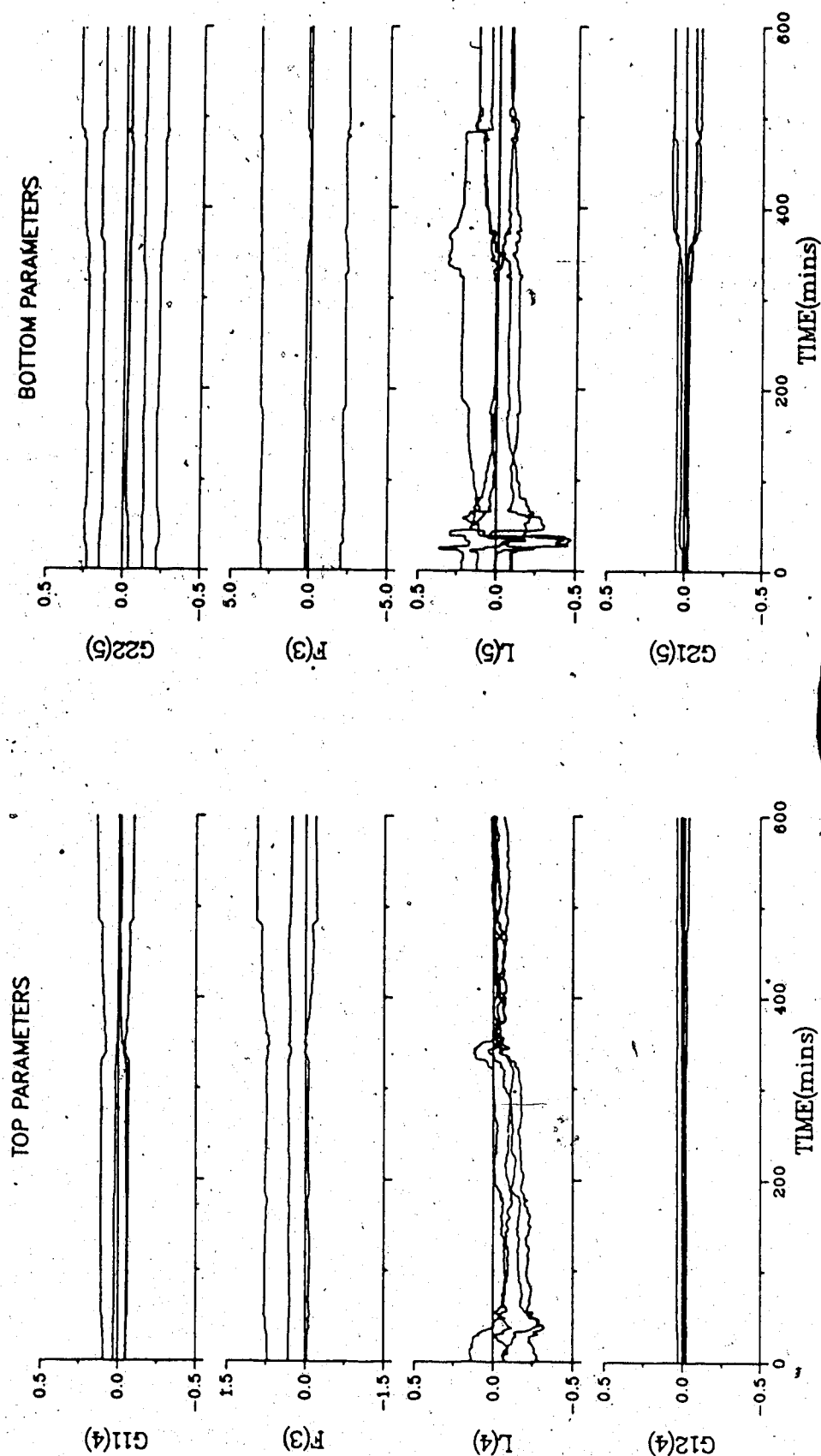


Figure 8.18 - Parameters for GMV Control with Q Weighting based on PI/PID constants (MR, EFF)

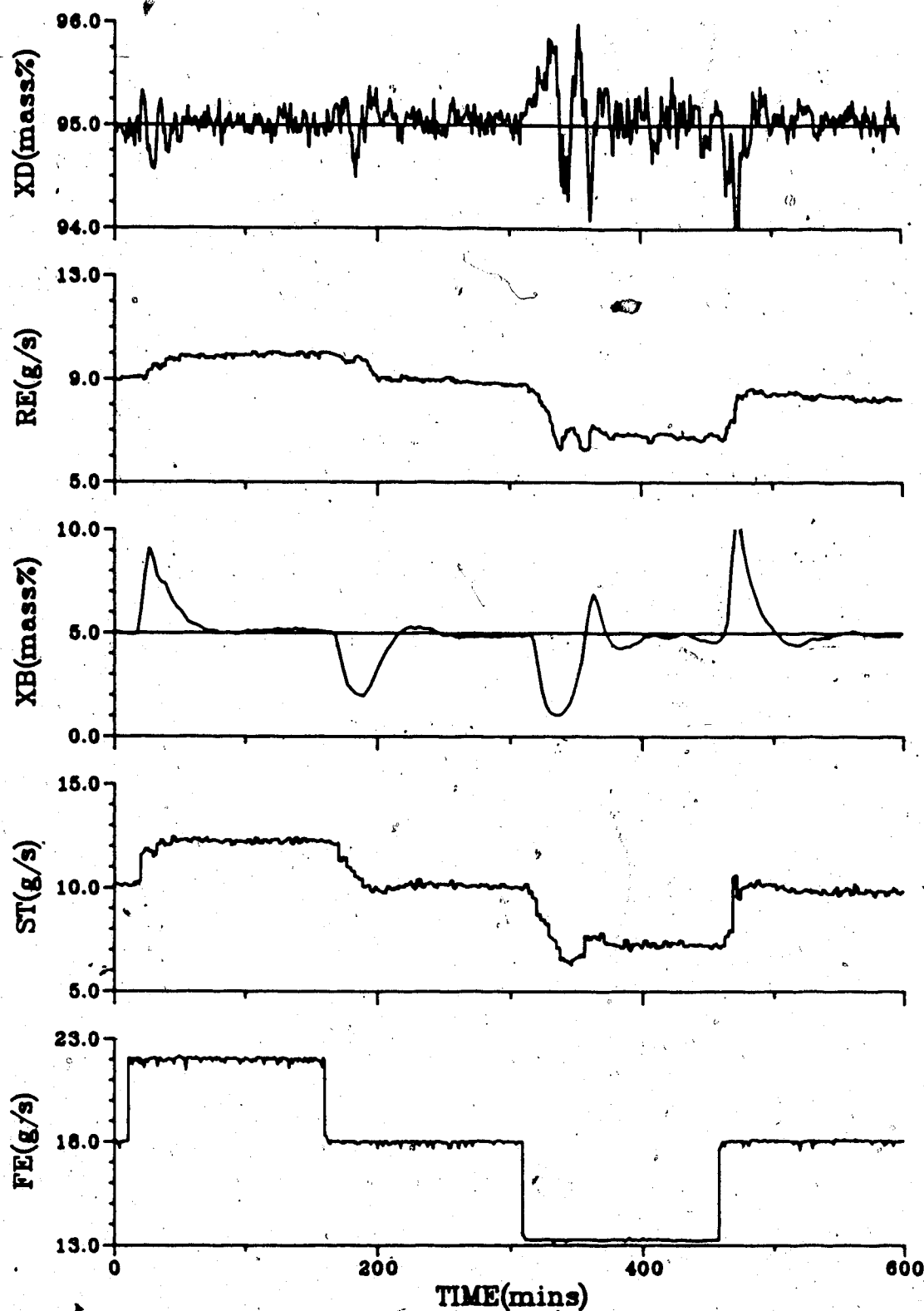


Figure 8.19 - Generalized Minimum Variance Control with Q Weighting based on PI/PID constants (MR,MFF)

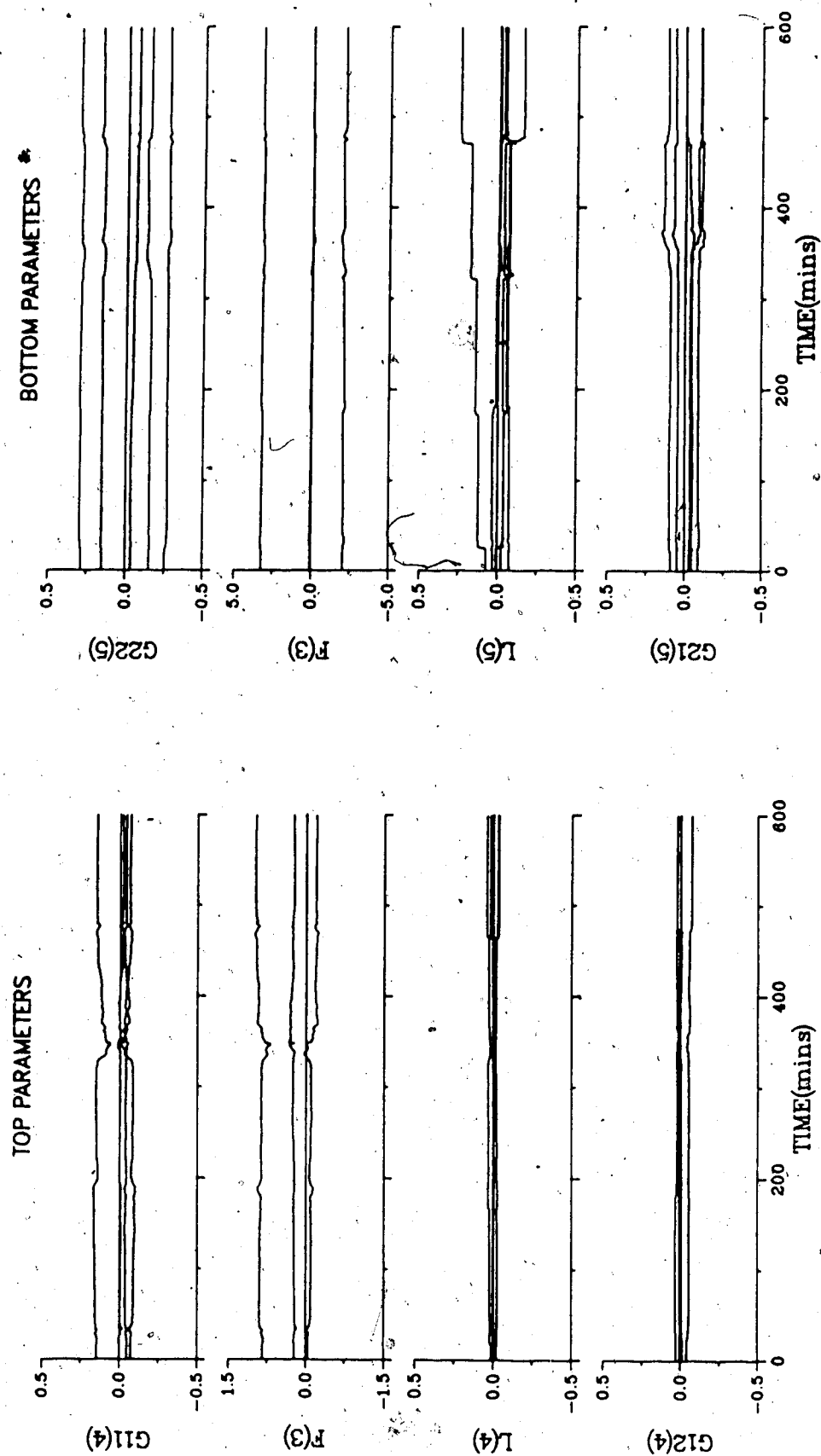


Figure 8.20 - Parameters for GMV Control with Q Weighting based on PI/PID constants (MR,MFF)

Table 8.2  
SAE Values for Q Weighting based on PI/PID constants

Loop	SAE Values:		
	NFF	EFF	MFF
Single Rate Control			
Figure	8.9	8.11	8.13
Top	142.0	129.0	110.0
Bottom	403.0	412.0	392.0
Both	545.0	541.0	502.0
Multirate Control			
Figure	8.15	8.17	8.19
Top	86.7	102.3	91.3
Bottom	434.8	488.3	460.3
Both	521.5	590.6	551.6

### 8.5.3 Q Weighting Established from PI/PI Constants

For the test results presented in this section the derivative action of the PID controller on the bottom composition control loop has been dropped in the calculations of the Q coefficients so that for both loops the Q weighting was assumed to take the inverse PI structure, ignoring the  $q_0$  term. The constants for the single rate case were  $PB = 30.0$  and  $TI = 170.0$  for the top loop and  $PB = 65.0$  and  $TI = 425.0$  for the bottom loop. The only change in the Q coefficients occurs in the bottom loop, where the values are now:  $q_0 = 1.54$  and  $q_1 = -1.53$  ( $q_2$  is no longer used). The responses of the manipulated and controlled variables and of the parameters for no

feedforward action, estimated and measured feedforward action are plotted in Figures 8.21, 8.23 and 8.25, with the corresponding parameter plots given in Figures 8.22, 8.24 and 8.26.

As was the case in Section 8.5.2, the ability to use a measured value of the disturbance when employing feedforward action improved the top composition control at the expense of the control of the bottom composition. For the case of estimated feedforward action it can be seen from Figure 8.23 that changes in the steam flow are somewhat erratic for a short time after the first and third steps in feed flow rate. From the plot of the parameters for this test, displayed in Figure 8.24, it can be seen that a considerable amount of parameter adaptation takes place with the first feed step change. In particular, the  $L$  parameters for the bottom loop change significantly, so until the parameters have adapted, the control performance suffers. In the tests which use multirate sampling, it can be seen from the responses in Figures 8.27, 8.29 and 8.31 that control of the top composition has improved considerably. This is confirmed by the  $\$AE$  values for the single and multirate tests presented in Table 8.3.



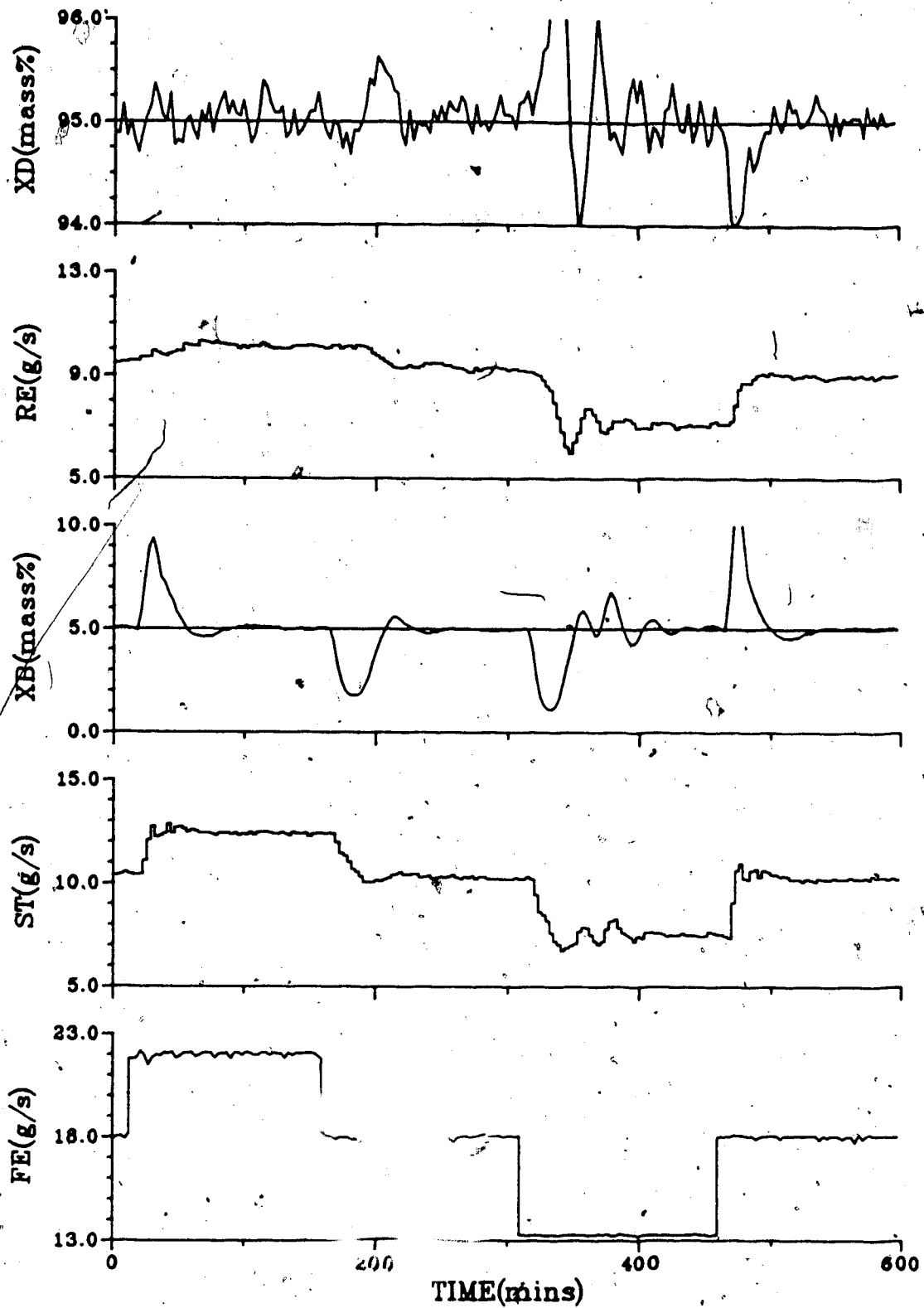


Figure 8.21 - Generalized Minimum Variance Control  
with Q Weighting based on PI/PI  
constants (SR,NFF)

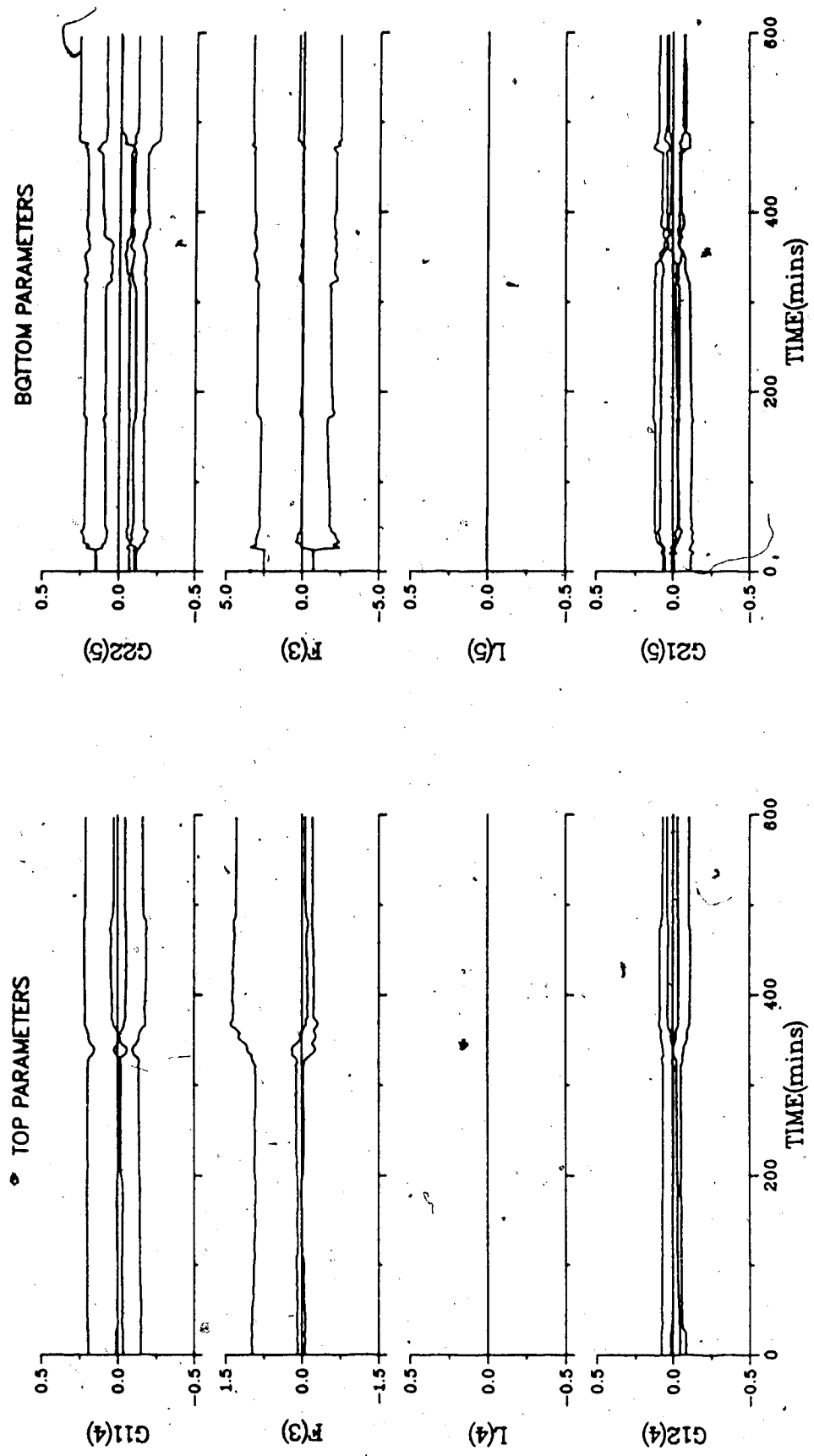


Figure 8.22 - Parameters for  $G_{xy}$  Control using Q Weighting based on PI/PI constants (SR,NFF)

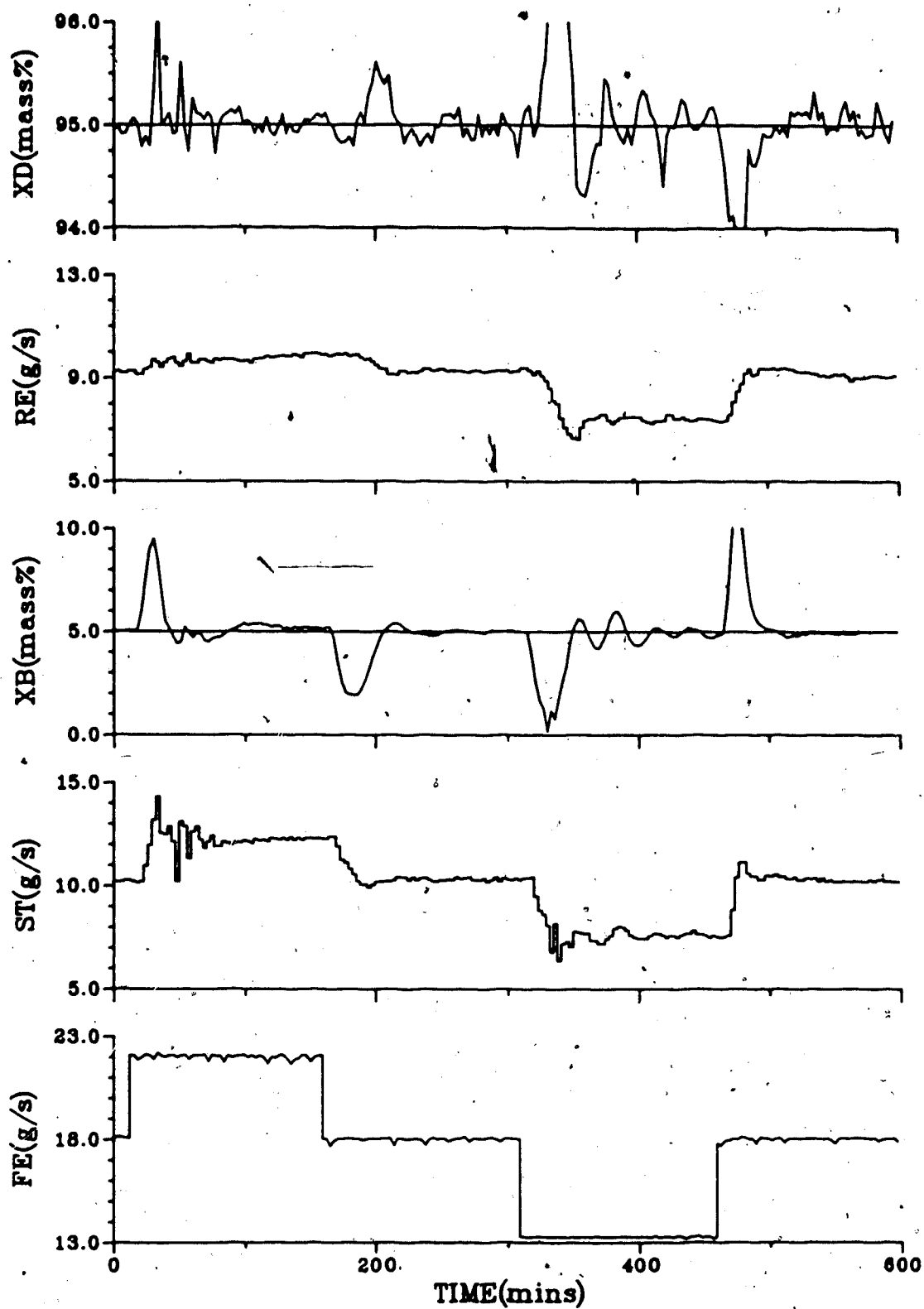


Figure 8.23 - Generalized Minimum Variance Control  
with Q Weighting based on PI/Pi  
constants (SR,EFF)

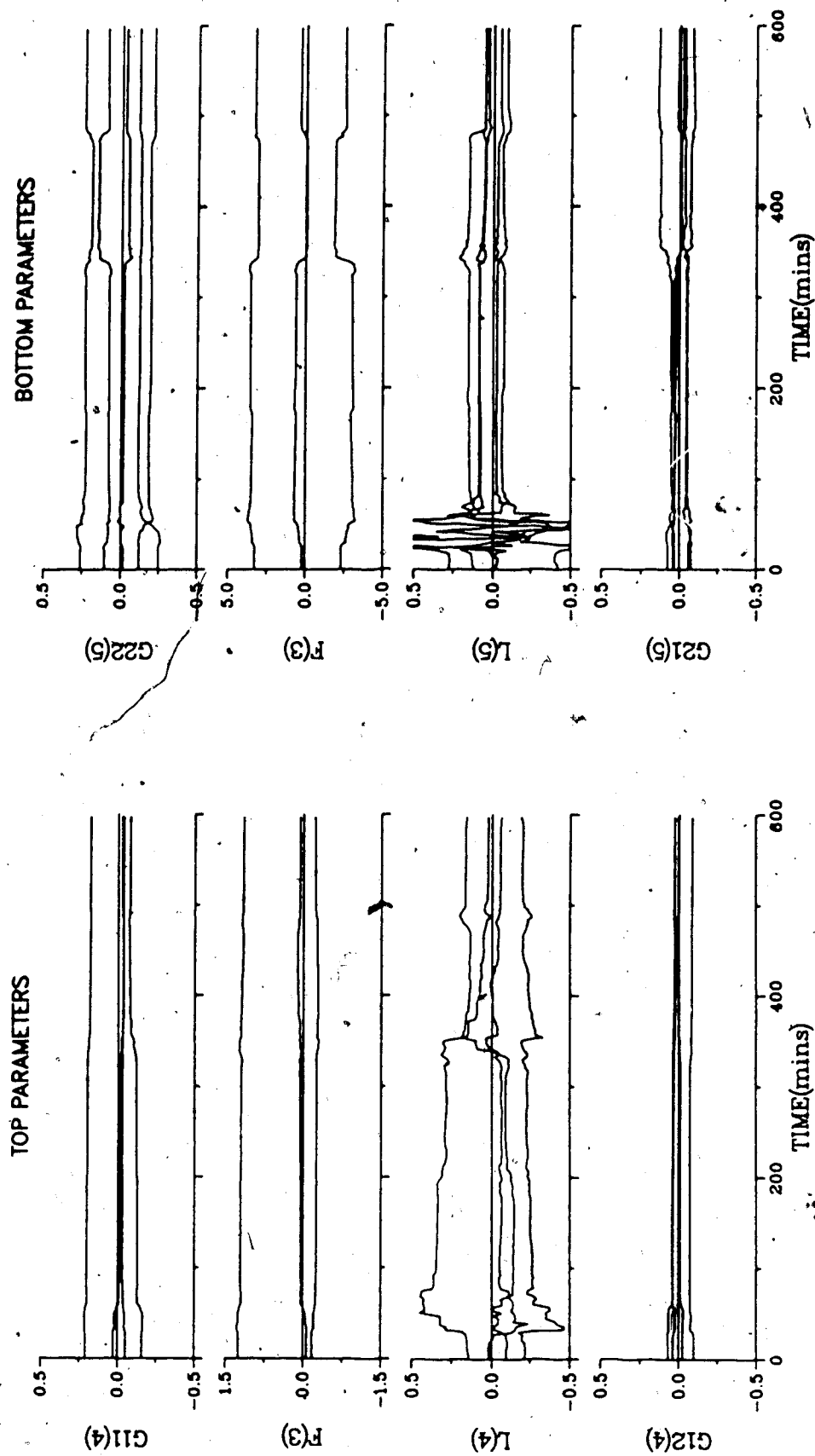


Figure 8.24 - Parameters for GMV Control using Q Weighting based on PI/PI constants (SR, EFF)

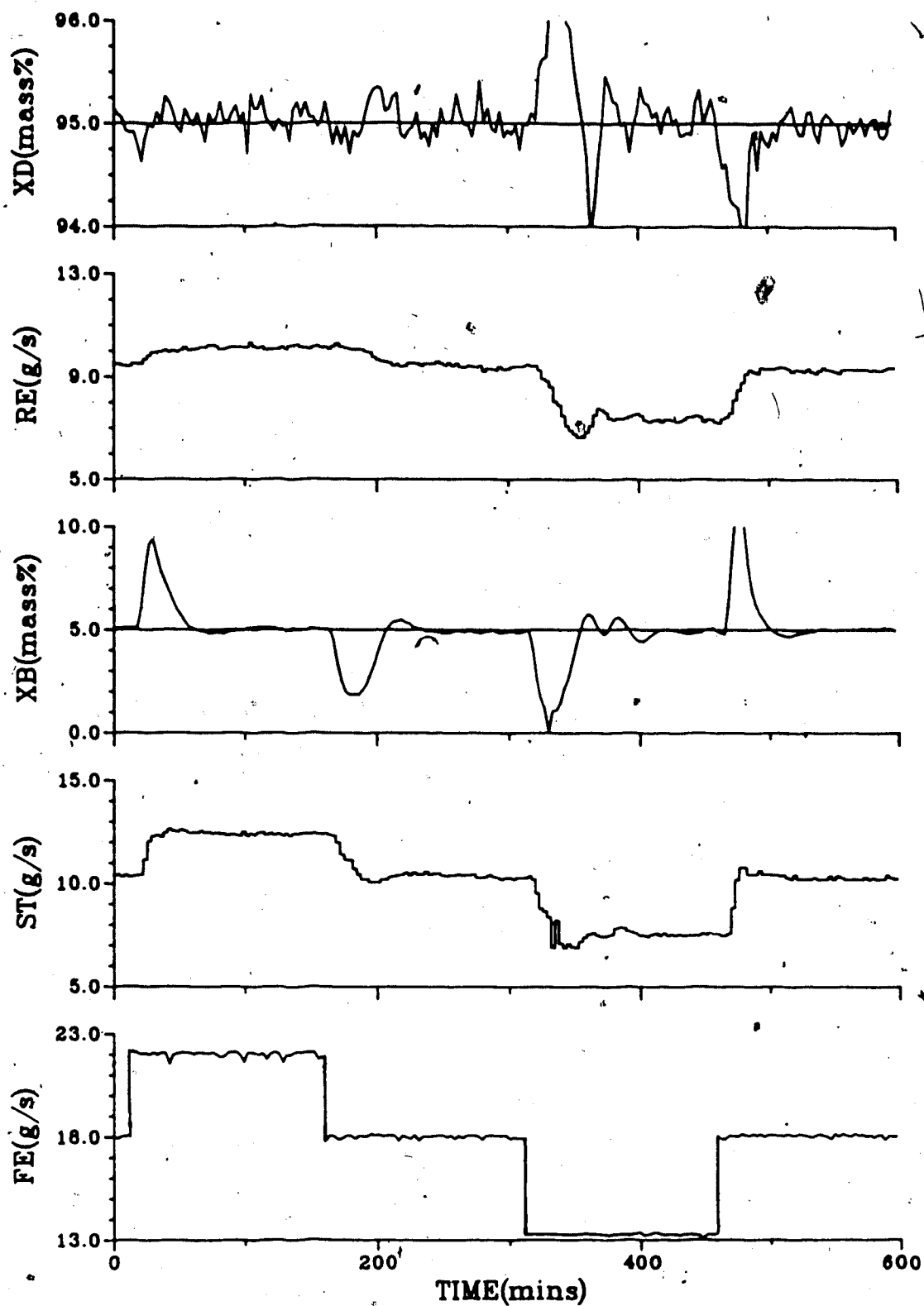


Figure 8.25 - Generalized Minimum Variance Control with Q Weighting based on PI/PI constants, (SR,MFF)

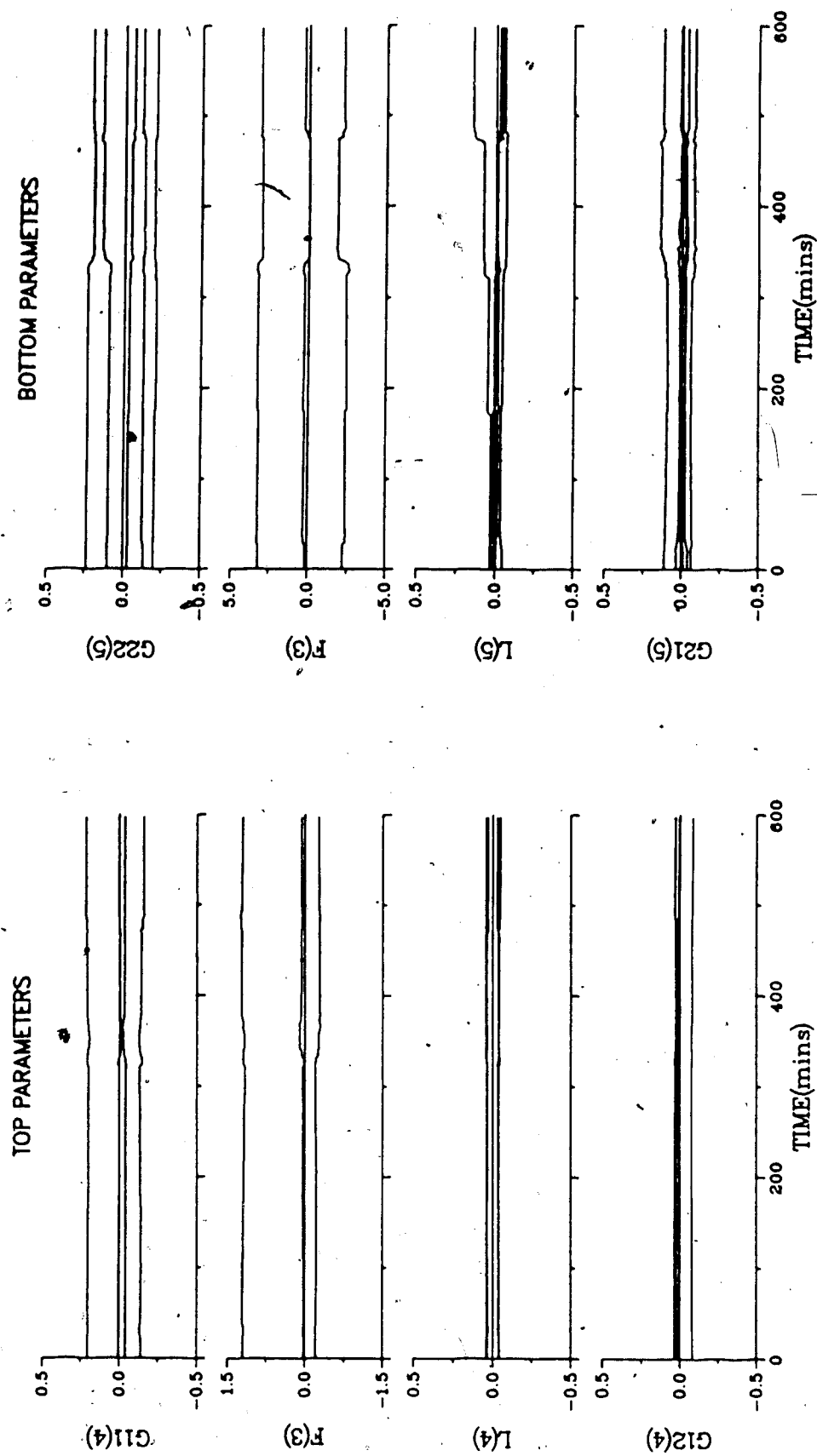


Figure 8.26 - Parameters for GMV Control using Q Weighting based on PI/PI constants (SR,MFF)

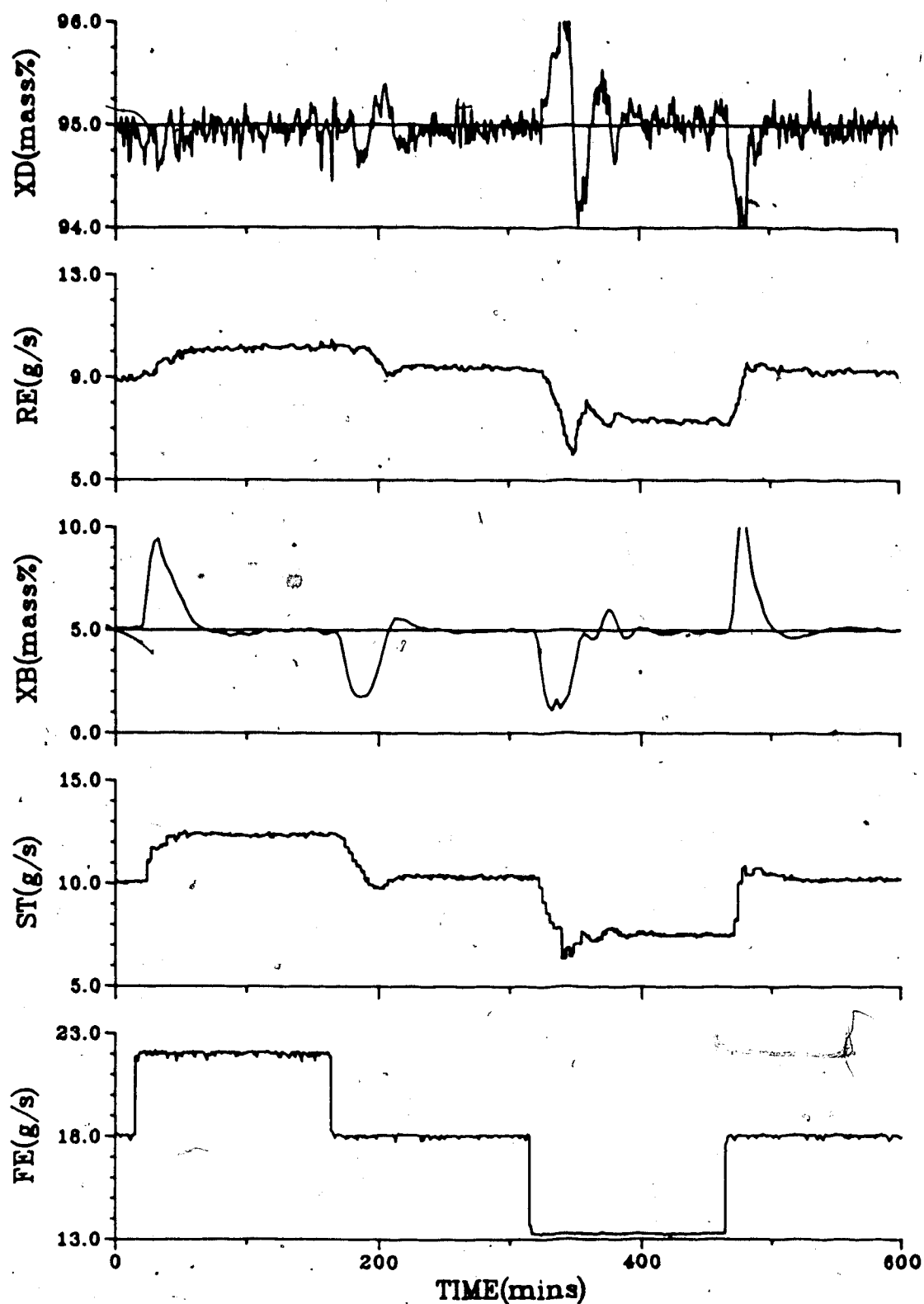


Figure 8.27 - Generalized Minimum Variance Control with Q Weighting based on PI/PI constants (MR,NFF)

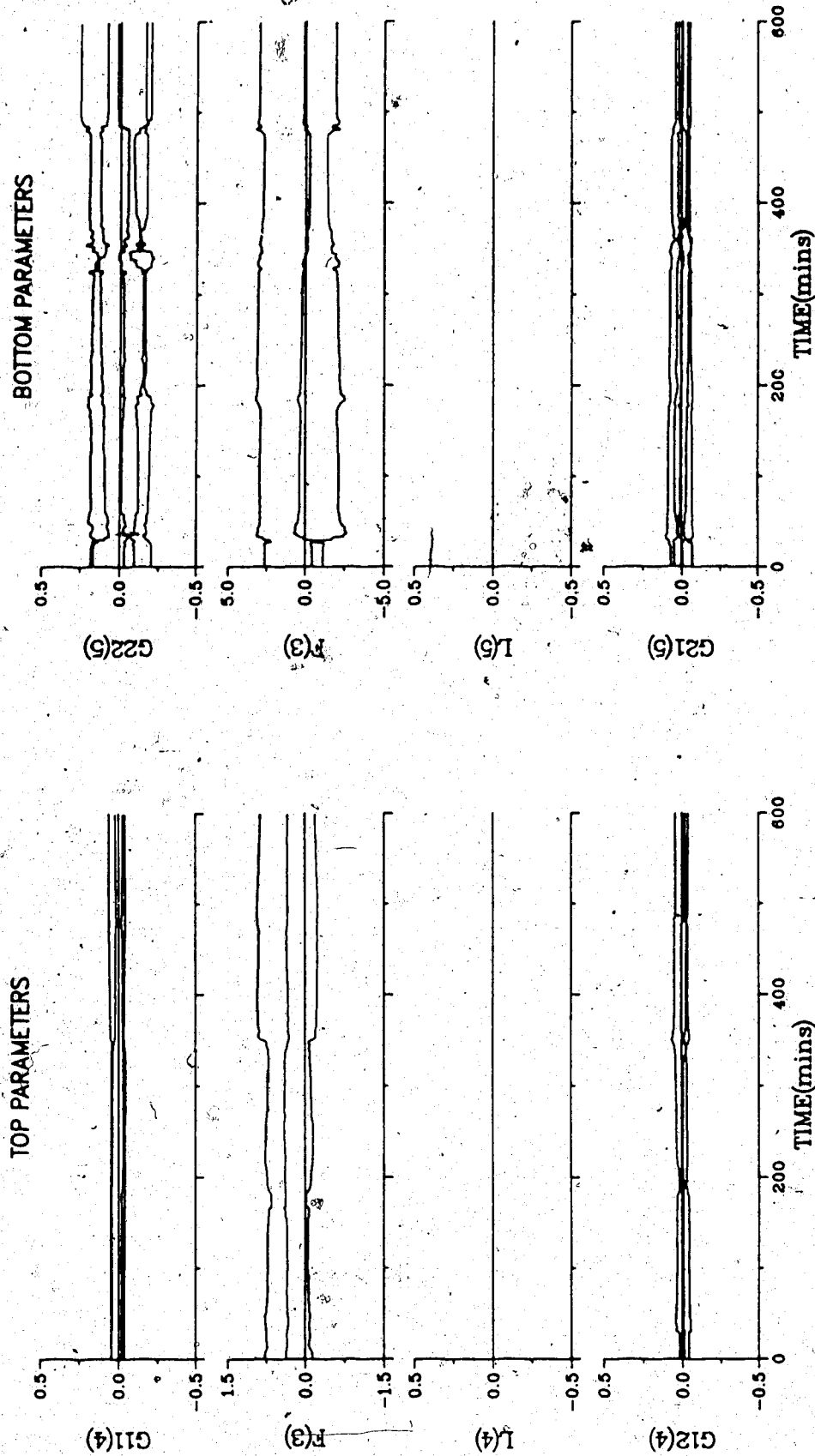


Figure 8,28 - Parameters for GMV Control using Q Weighting based on PI/PI constants (MR,NFF)



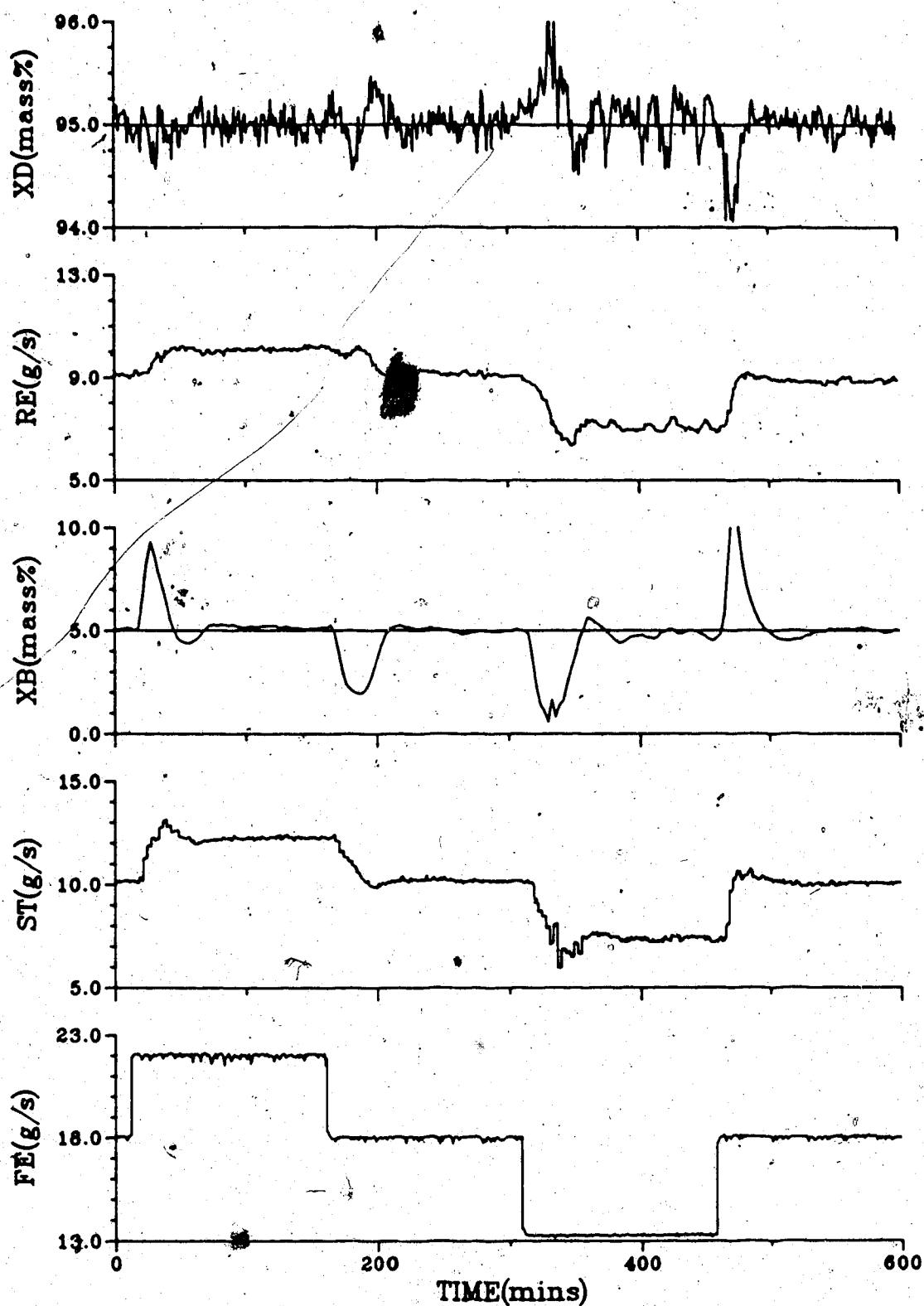


Figure 8.29 - Generalized Minimum Variance Control with Q Weighting based on PI/PI constants (MR,EFF)

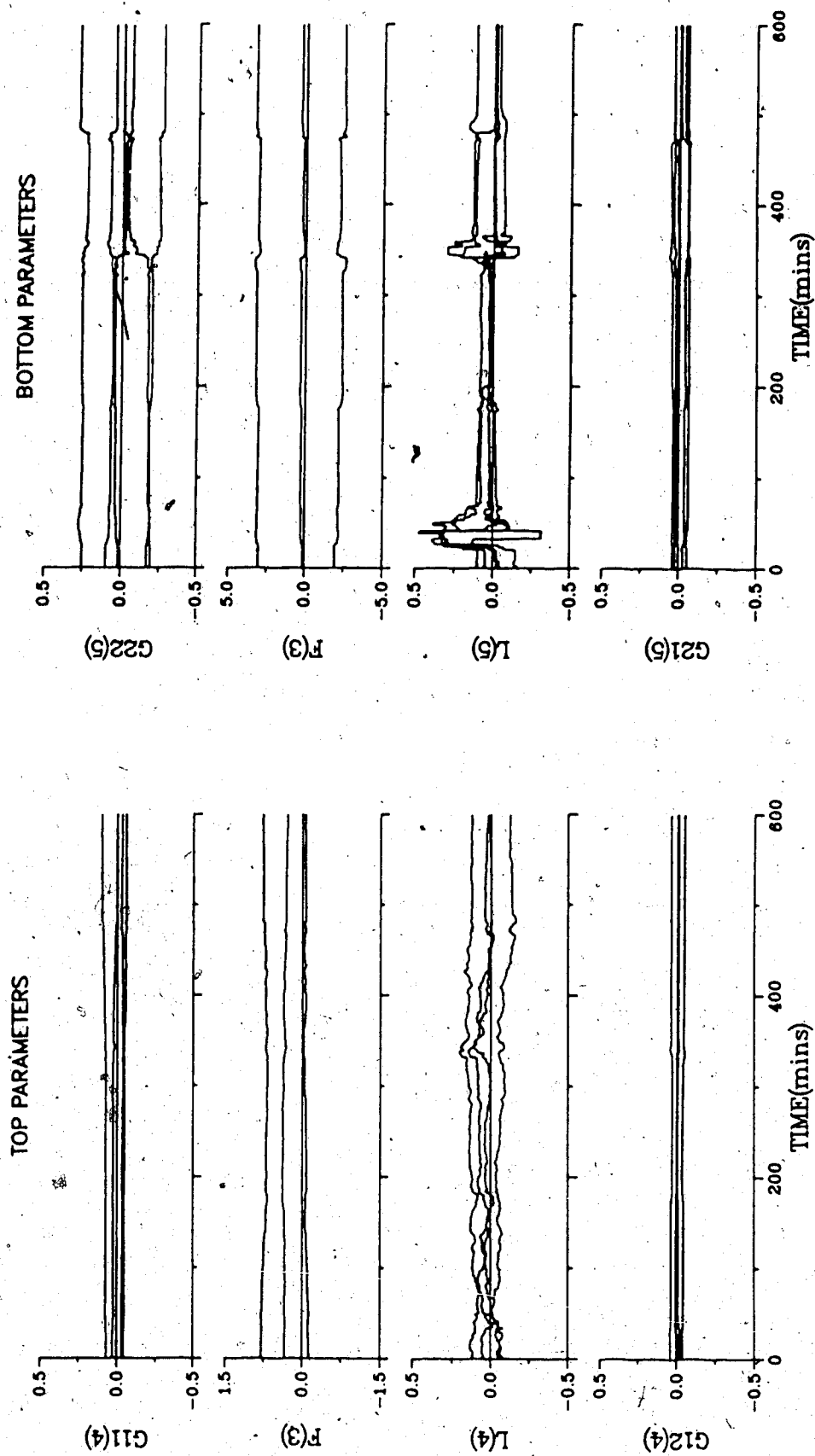


Figure 8.30 - Parameters for GMV Control using Q Weighting based on PI/PI constants (MR, EFF)

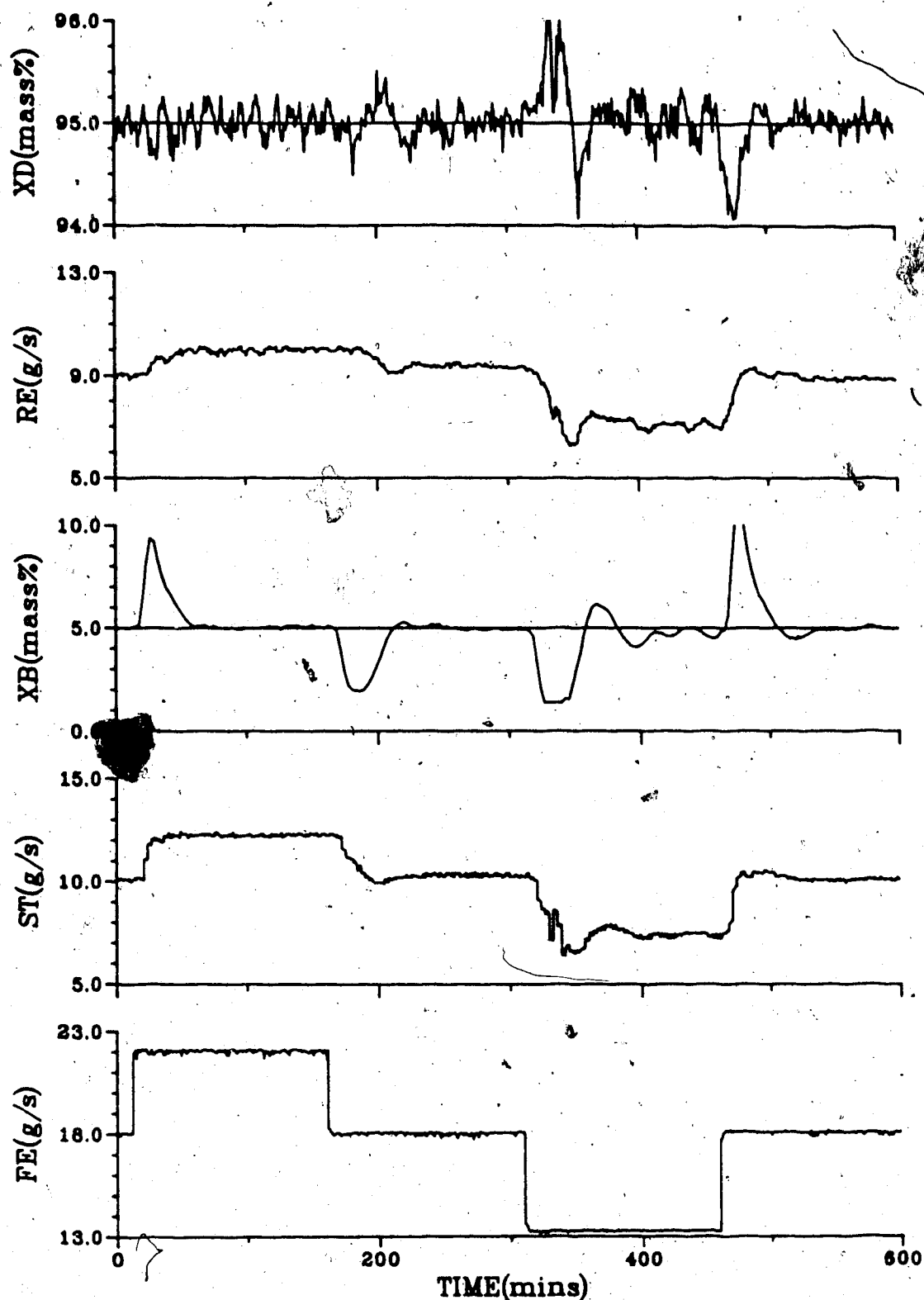


Figure 8.31 - Generalized Minimum Variance Control with Q Weighting based on PI/PI constants (MR,MFF)

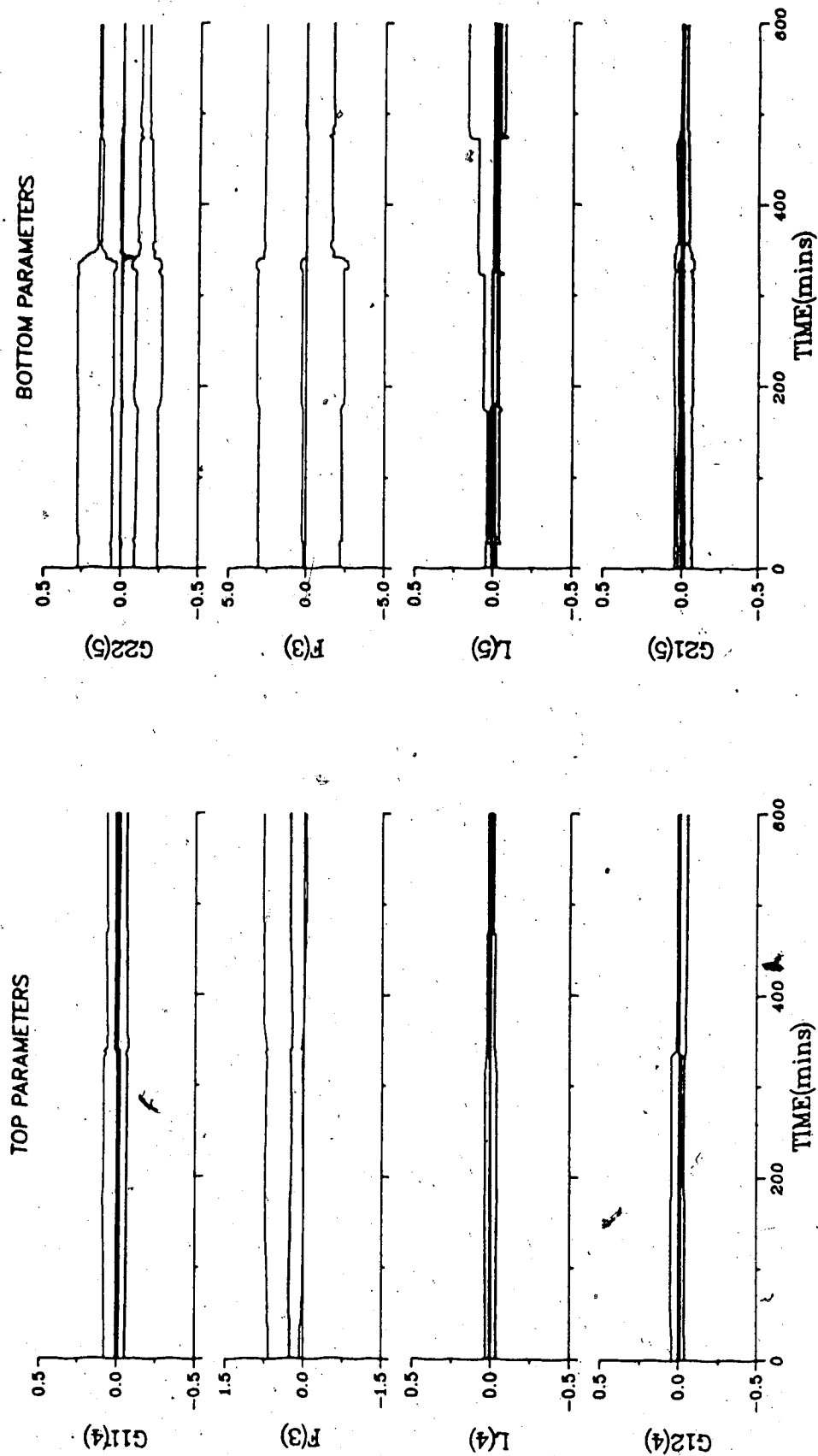


Figure 8.32 - Parameters for GMV Control using Q Weighting based on PI/PI constants (MR, MFF)

Table 8.3  
SAE Values for Q Weighting based on PI/PI-constants

Loop	SAE Values:		
	NFF	EFF	MFF
Single Rate Control			
Figure	8.21	8.23	8.25
Top	132.9	124.6	115.3
Bottom	422.6	397.8	418.7
Both	555.5	522.4	534.0
Multirate Control			
Figure*	8.27	8.29	8.31
Top	97.7	96.9	92.0
Bottom	415.5	412.9	453.8
Both	513.2	499.8	545.8

#### 8.5.4 Modified PI/PI Controller constants for Q Weighting

Vagi, [1987], recommended changing the PI controller constants for use in determining the Q weighting coefficients by assuming there is no time delay on the basis that the self-tuning control algorithm provides prediction and hence accounts for any time delays.

For estimating controller constants for single rate sampling, the Cohen-Coon method, as outlined in Section 6.3, was employed. For the case of no time delay, the modified PI constants were found to be  $PB = 31.93$  and  $TI = 166.6$  for the top loop and  $PB = 45.43$  and  $TI = 238.1$  for the bottom loop. The modified constants and the tuned constants of the top loop are in close agreement. These modified PI controller constants correspond to Q weighting coefficient values of:  $q_0 = 3.16$  and  $q_1 = -3.10$  for the top loop and  $q_0 = 2.22$  and  $q_1 = -2.18$  for the bottom loop. Testing of column control performance using the modified PI constants to calculate the Q weighting lead to the responses given in Figures 8.33, 8.35 and 8.37, with the parameter plots shown in Figures 8.34, 8.36 and 8.38. It can be seen from Figures 8.33, 8.35 and 8.37 that the bottom composition response is much more oscillatory than that observed in the previous tests. This could be due to the gain being too high or too much integral action, that is, the integral time,  $TI$ , being too small. In fact, the oscillatory response may have been expected since the proportional band and integral time are both smaller than the tuned values. Because the values of the tuned and

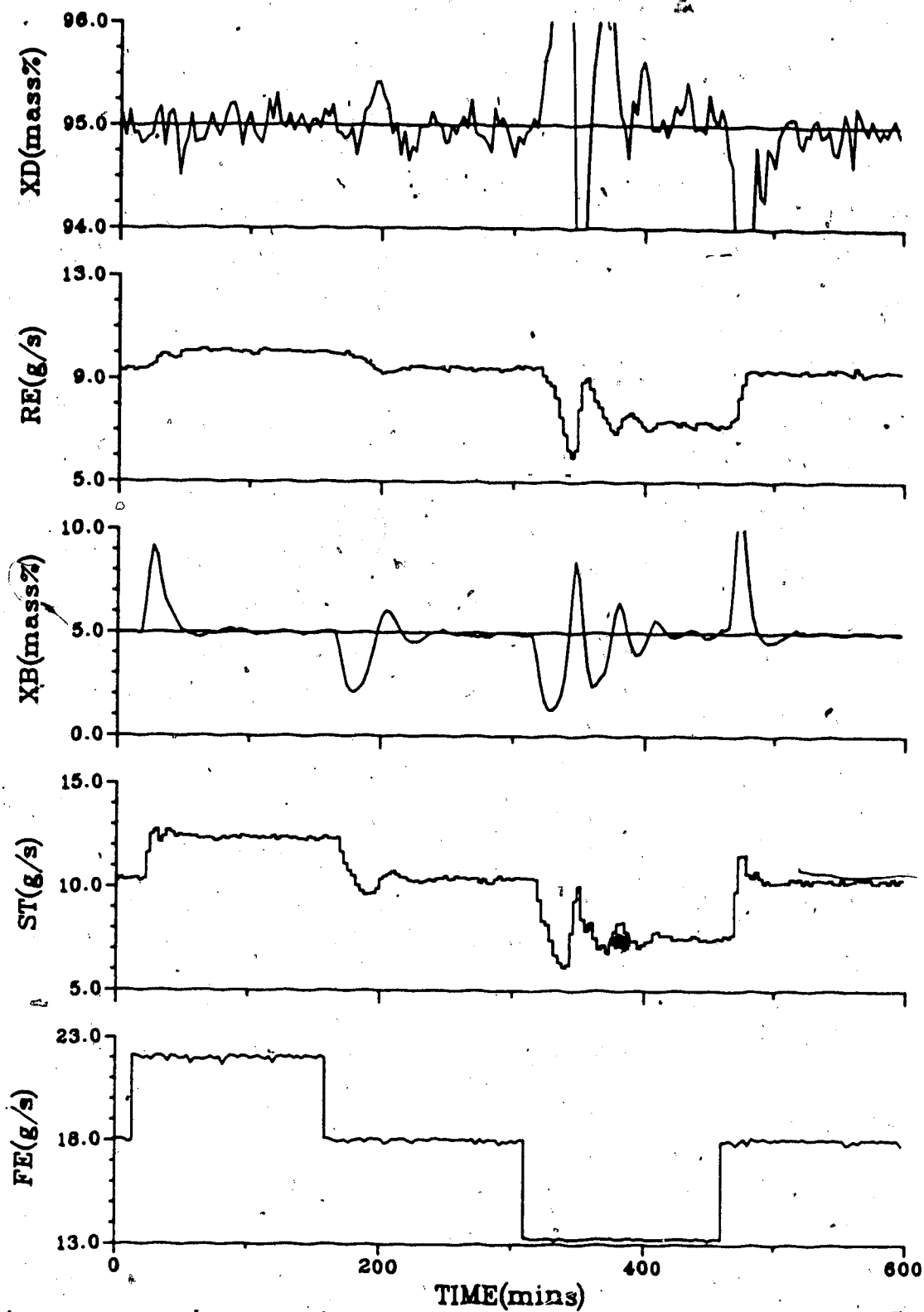


Figure 8.33 - Generalized Minimum Variance Control  
based on Modified PI/PI constants  
(SR,NFF)

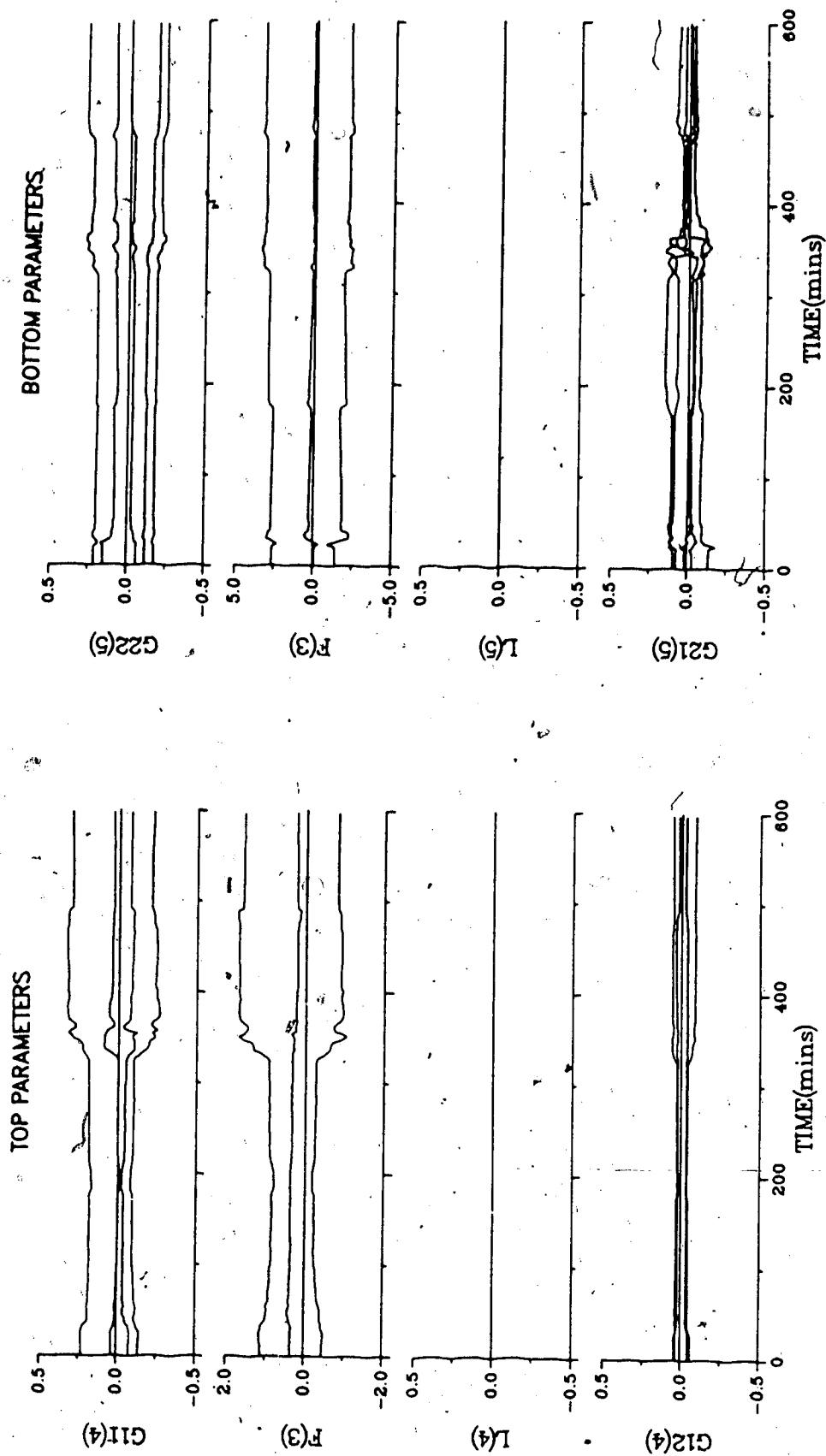


Figure 8.34 - Parameters for GMV Control using Q Weighting based on Modified PI/PI constants (SR,NFF)



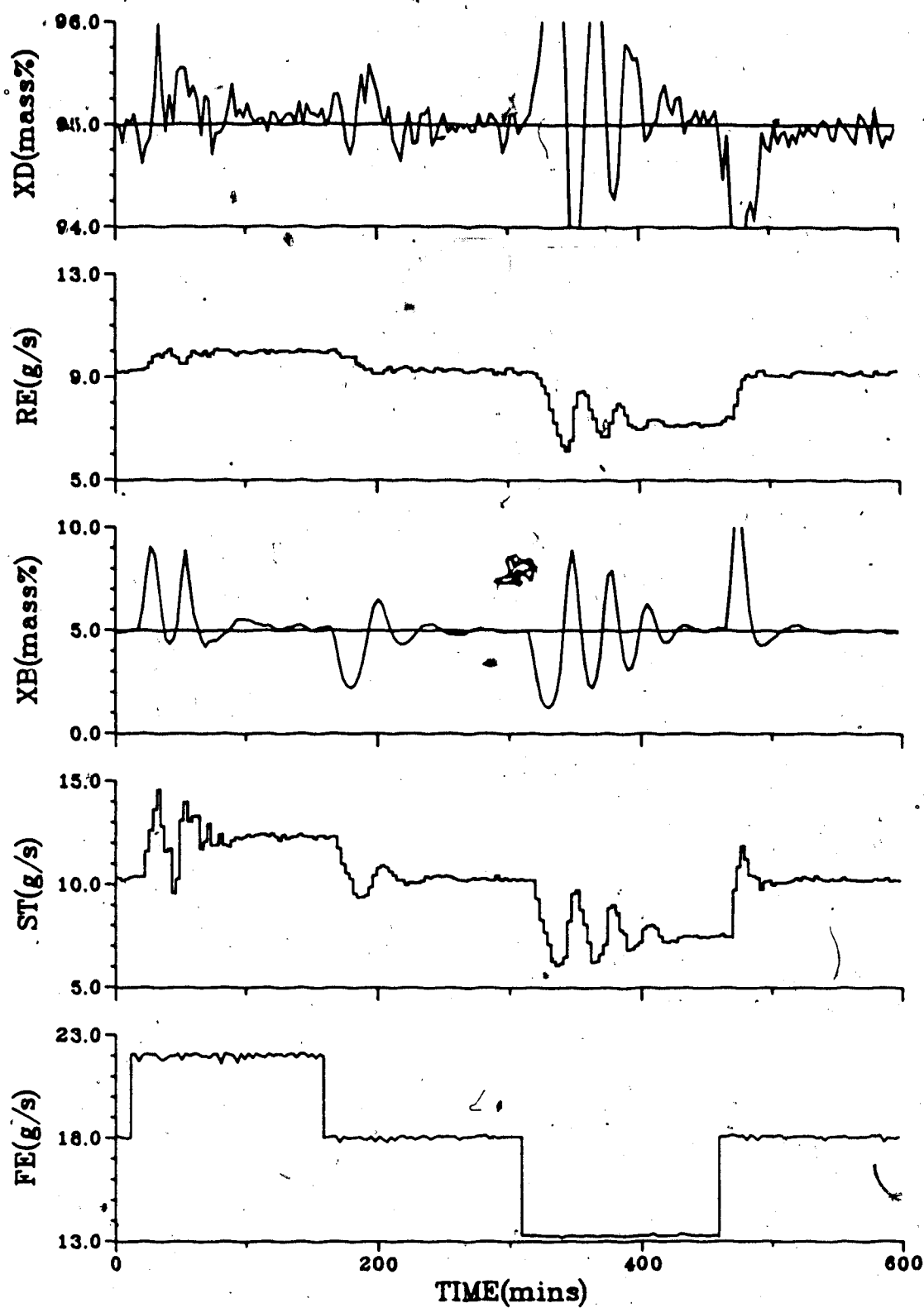


Figure 8.35 - Generalized Minimum Variance Control  
based on Modified PI/PI constants  
(SR, EFF)

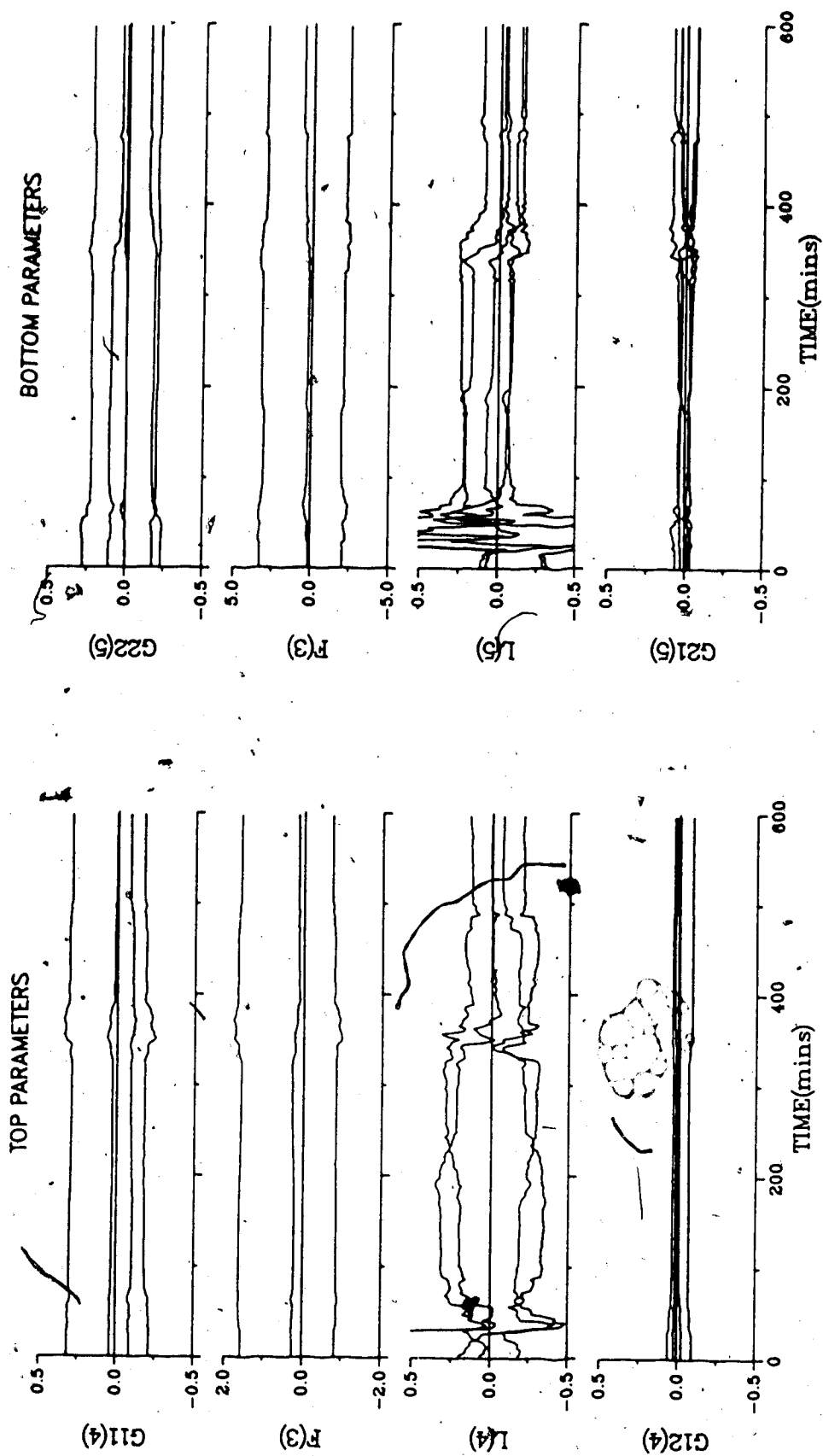


Figure 8.36 - Parameters for GMV Control using Q Weighting based on Modified PI/PI constants (SR, EFF)

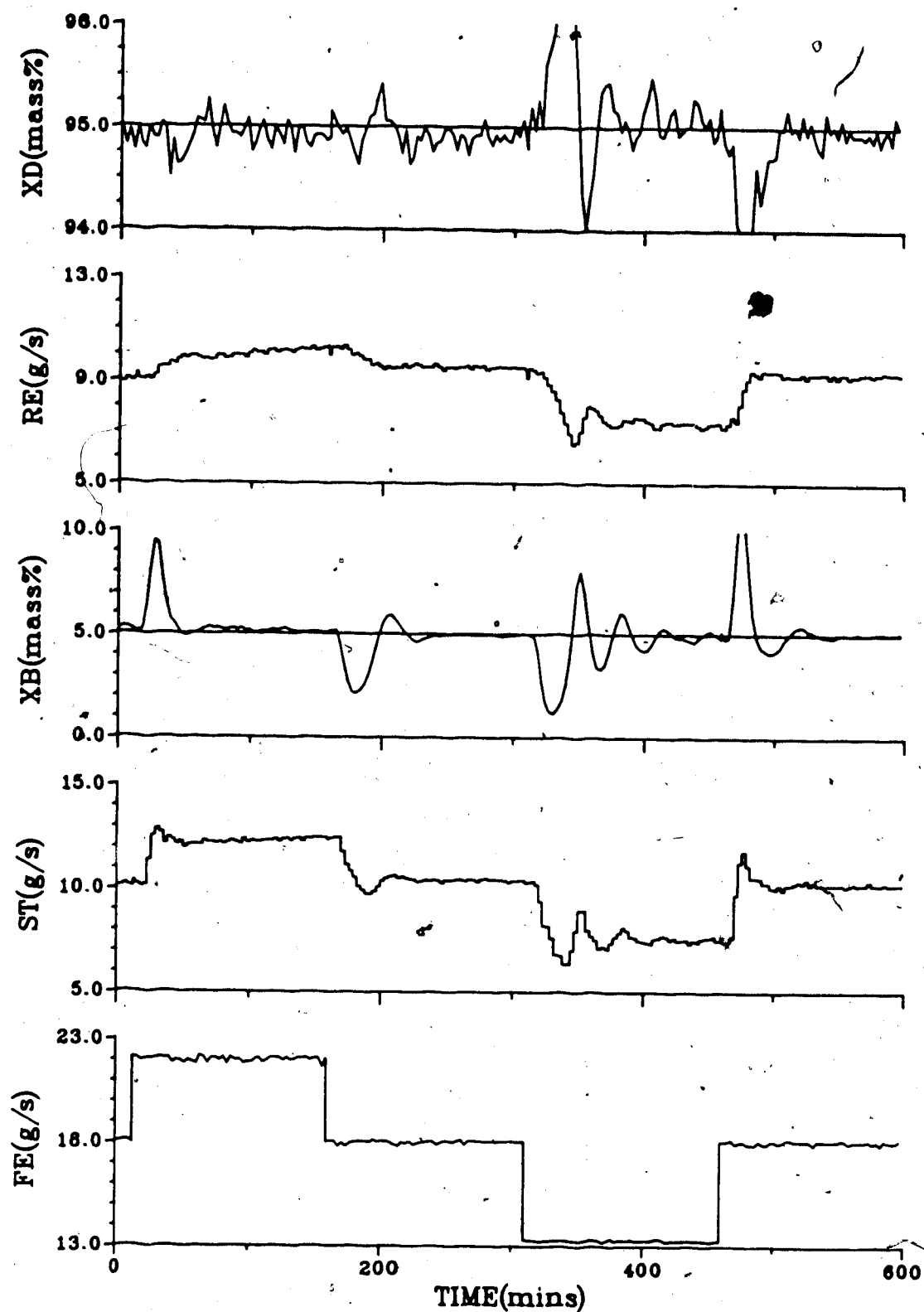


Figure 8.37 - Generalized Minimum Variance Control  
based on Modified PI/PI constants  
( $S^*$ , MFF)

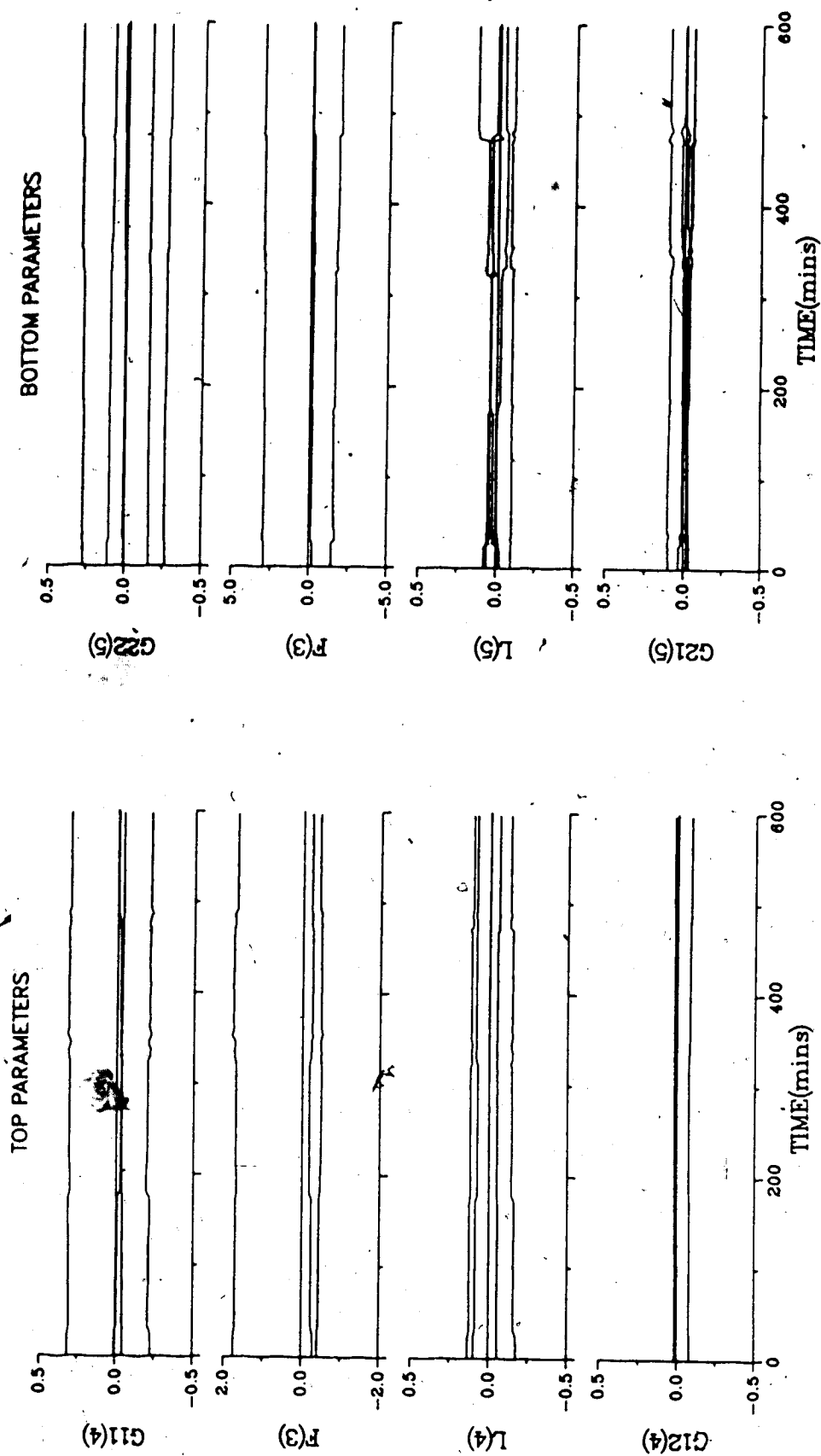


Figure 8.38 - Parameters for GMV Control using Q Weighting based on Modified PI/PI constants (SR, MFF)

modified constants are quite close for the top loop controller, the oscillations that occur in the reflux flow are probably in response to the interactions from the bottom loop. In Figure 8.35 the steam flow responds quite erratically to the first step change. This is probably due to the large amount of adaptation that takes place in the L parameters as shown in Figure 8.36.

In the multirate case, based on the recommendations of Vagi, the PI constants were recalculated using the integral of the absolute error technique. This method is similar to the Cohen-Coon technique, except that the constants given in Table 8.4 are used in equations 6.3 and 6.4 to calculate the controller constants.

Table 8.4  
Integral of Absolute Error Constants  
[Miller et al, 1967]

Mode	A	B	C	D	E	F
PI	.984	.986	1.644	.707		

The controller constants were calculated to be  $PB = 9.54$  and  $TI = 110.0$  for the top loop and  $PB = 38.75$  and  $TI = 308.9$  for the bottom loop. Since the proportional bands and integral times are lower than the corresponding tuned controller constants, oscillatory behavior may again be expected, following the results of the single rate sampling

tests. The  $Q$  coefficients calculate from the PI constants that have been recalculated for the multirate case are found to be:  $q_0 = 10.5$  and  $q_1 = -10.4$  for the top loop, and  $q_0 = 2.58$  and  $q_1 = -2.58$  for the bottom loop. As is evident in the responses from the multirate tests shown in Figures 8.39, 8.41 and 8.43, the oscillatory behavior is most noticeable during the third step of the disturbance. Comparison of the responses in Figure 8.39 with those in Figures 8.41 and 8.43 shows that the best bottom composition control performance and least oscillatory response in the top loop resulted without feedforward action. The response from all three of the multirate sampling tests shows that improved top composition control was obtained compared with that from the single rate tests.

In an effort to improve the control performance using measured feedforward action, and to demonstrate the relationship between the PI constants and the  $Q$  weighting parameters and their effect on the control action, a series of tests were performed with a different choice of  $Q$  weighting parameters. Since the previous multirate, tuned constants in the top loop resulted in very little oscillation in the top composition loop, the constants used to calculate the  $Q$  weighting coefficients for the top loop were  $PB = 20.0$  and  $TI = 170.0$ , which resulted in  $q_0 = 5.05$  and  $q_1 = -4.99$ . For the bottom composition loop the  $PB$  of 38.75 was maintained, but to attempt to reduce the oscillations a  $TI$  of 425.0 was used. The responses of these

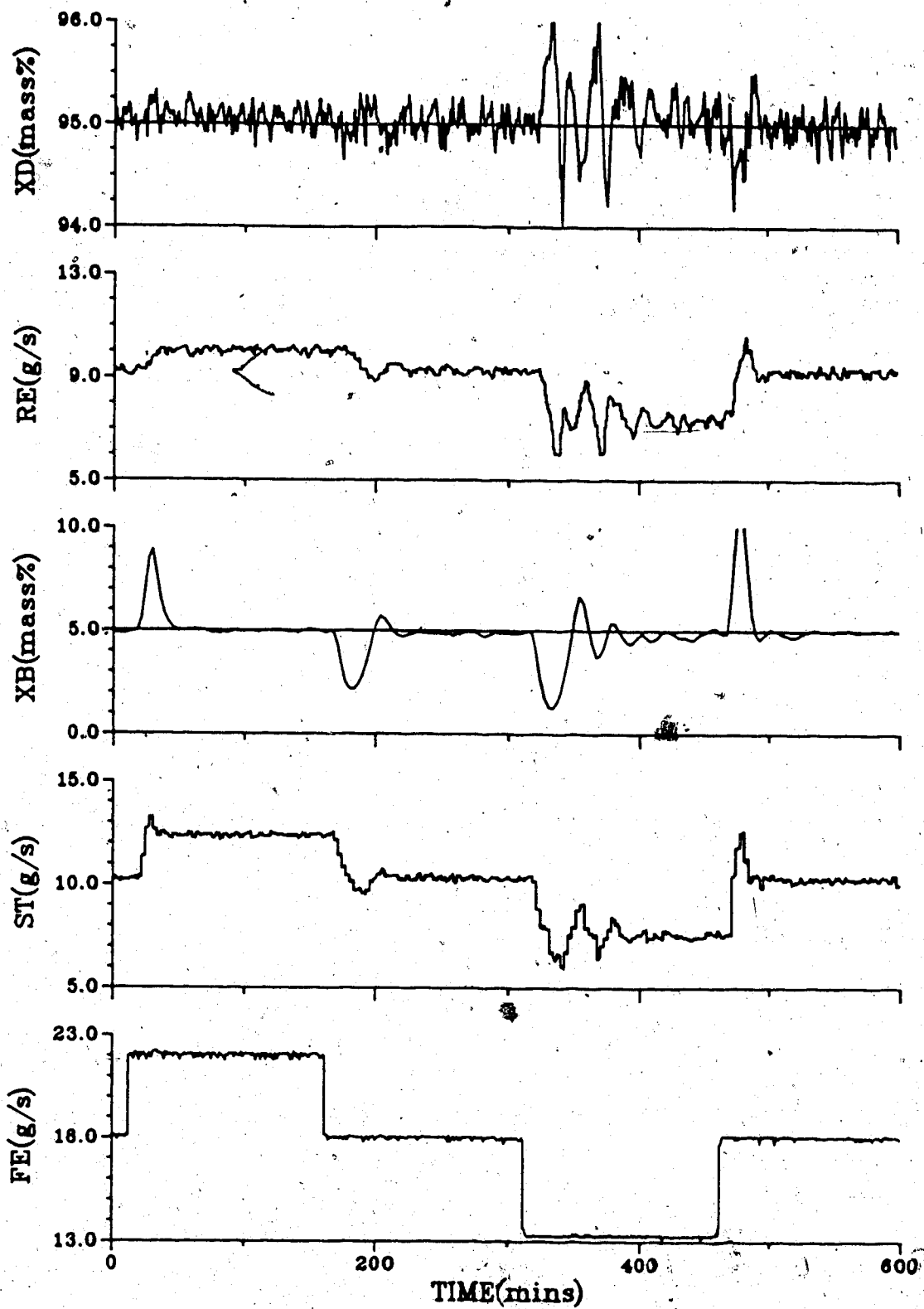


Figure 8.39 - Generalized Minimum Variance Control  
based on Modified PI constants  
(MR, NFF)

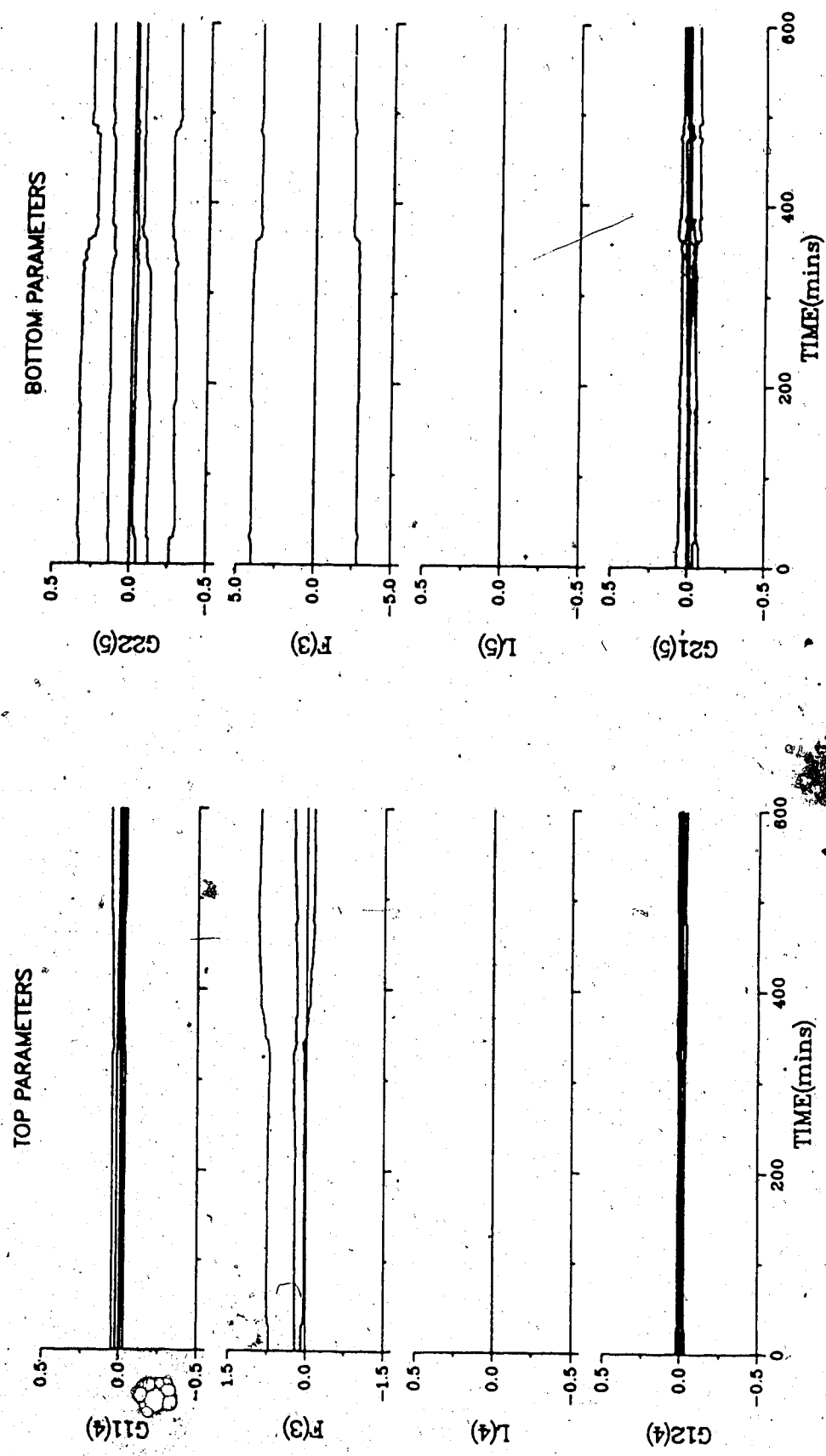


Figure 8.40 - Parameters for GMV 51 using Q Weighting based on Modified PI/PI constant  $K_p(MR, NFE)$



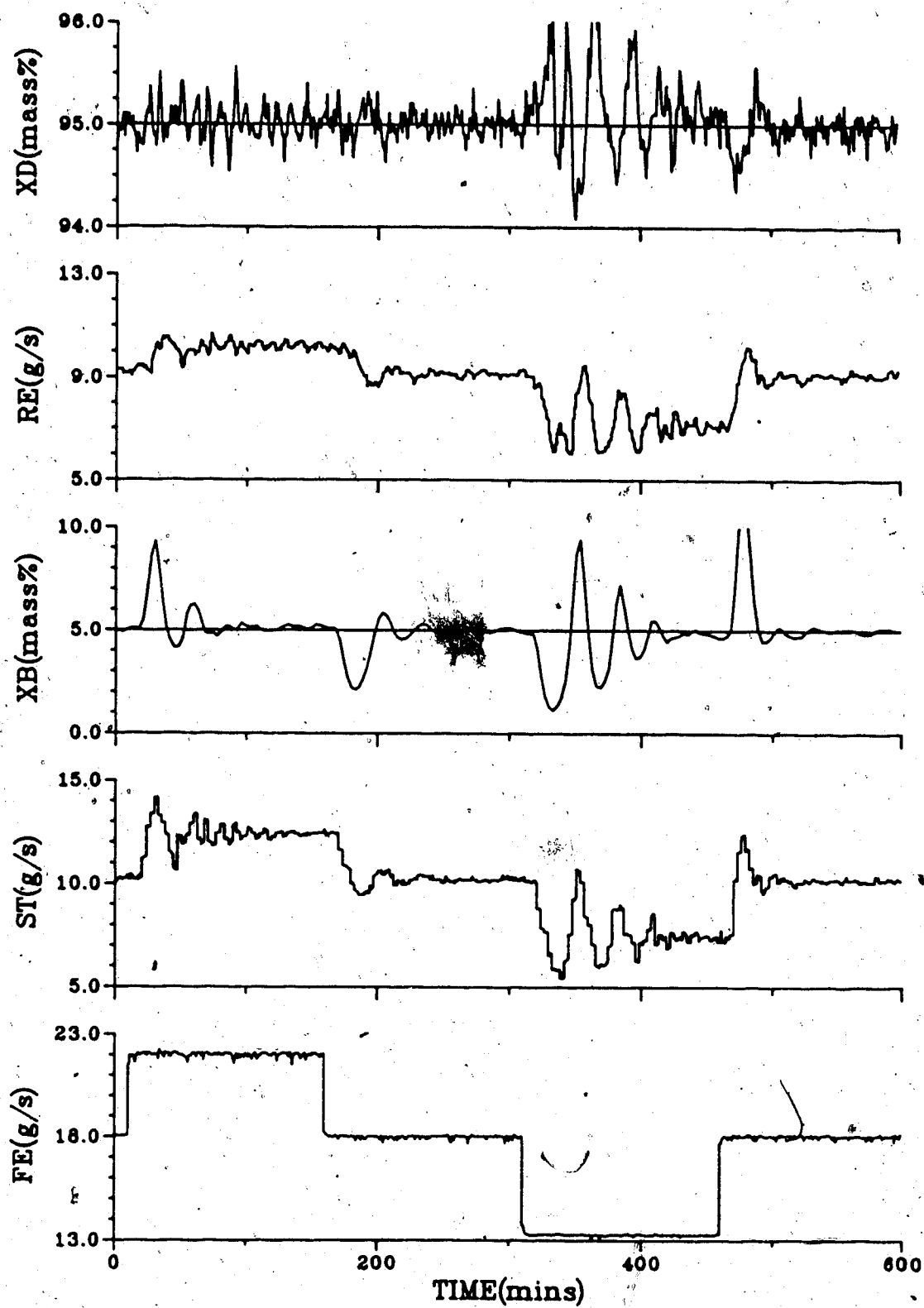


Figure 8.41 - Generalized Minimum Variance Control  
based on Modified PI/PI constants  
(MR, EFF)

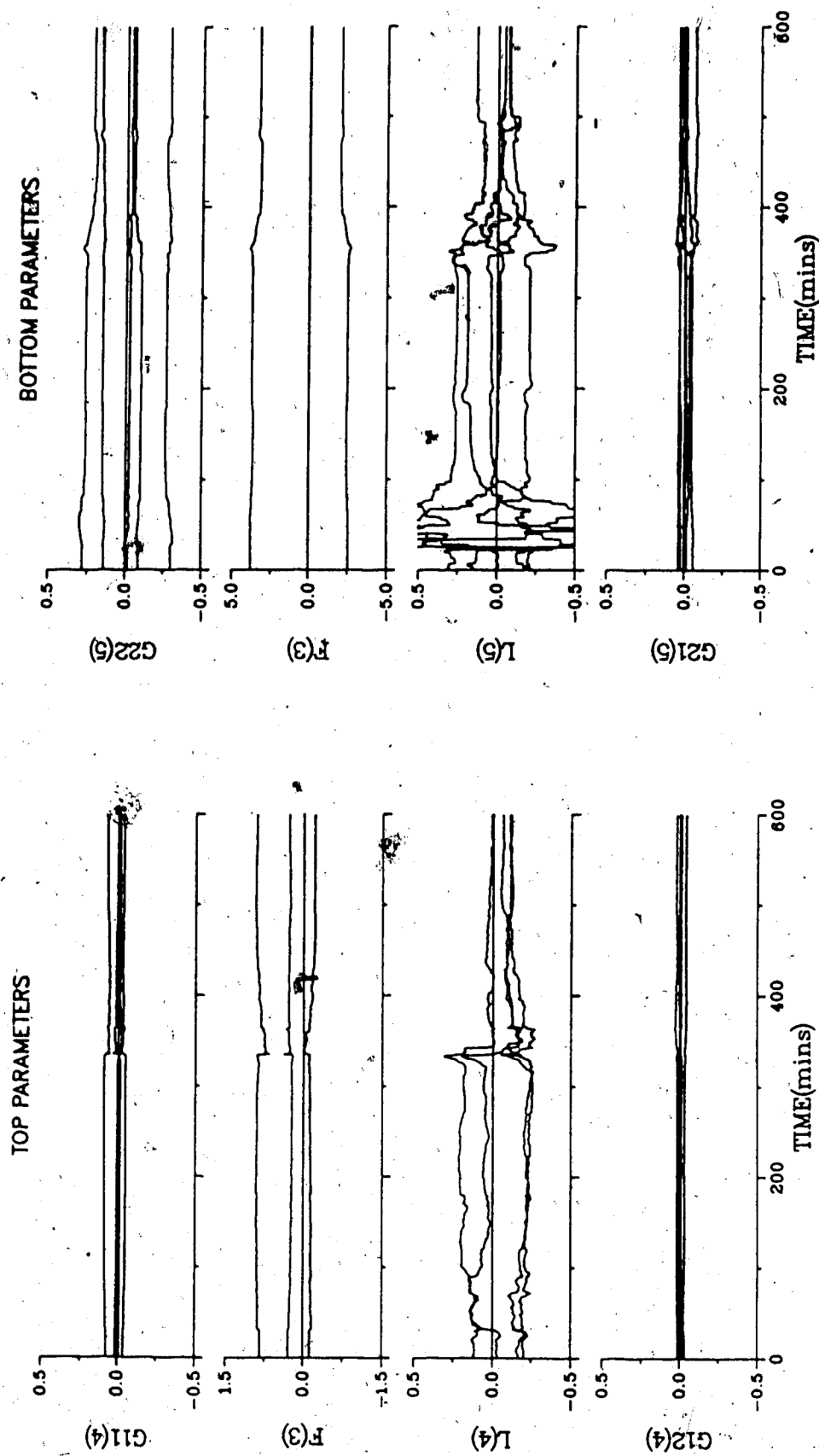


Figure 8.42 - Parameters for GMV Control using Q Weighting based on Modified PI/PI constants (MR, EFF)

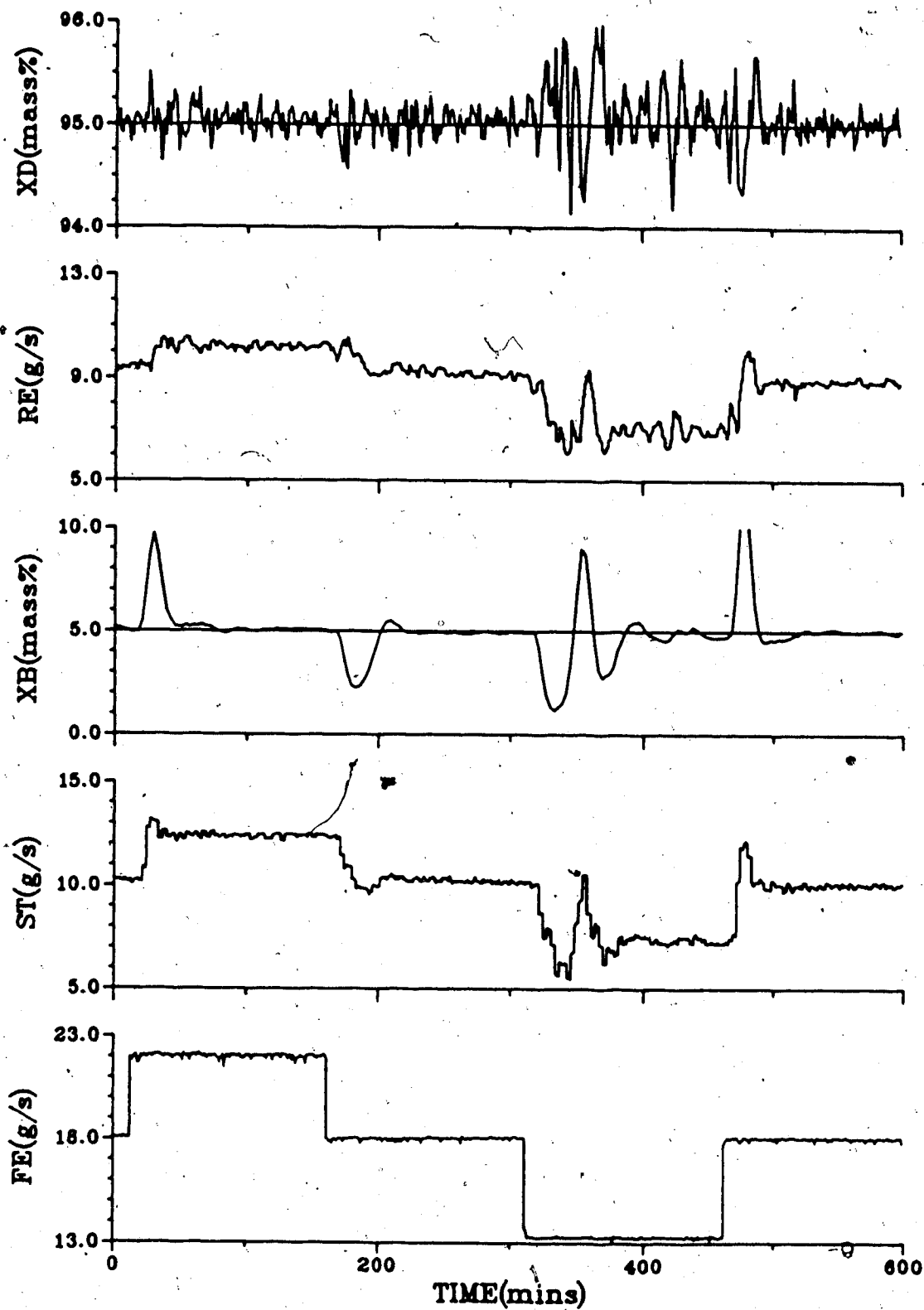


Figure 8.43 - Generalized Minimum Variance Control  
based on Modified PI/PI constants  
(MR,MFF)

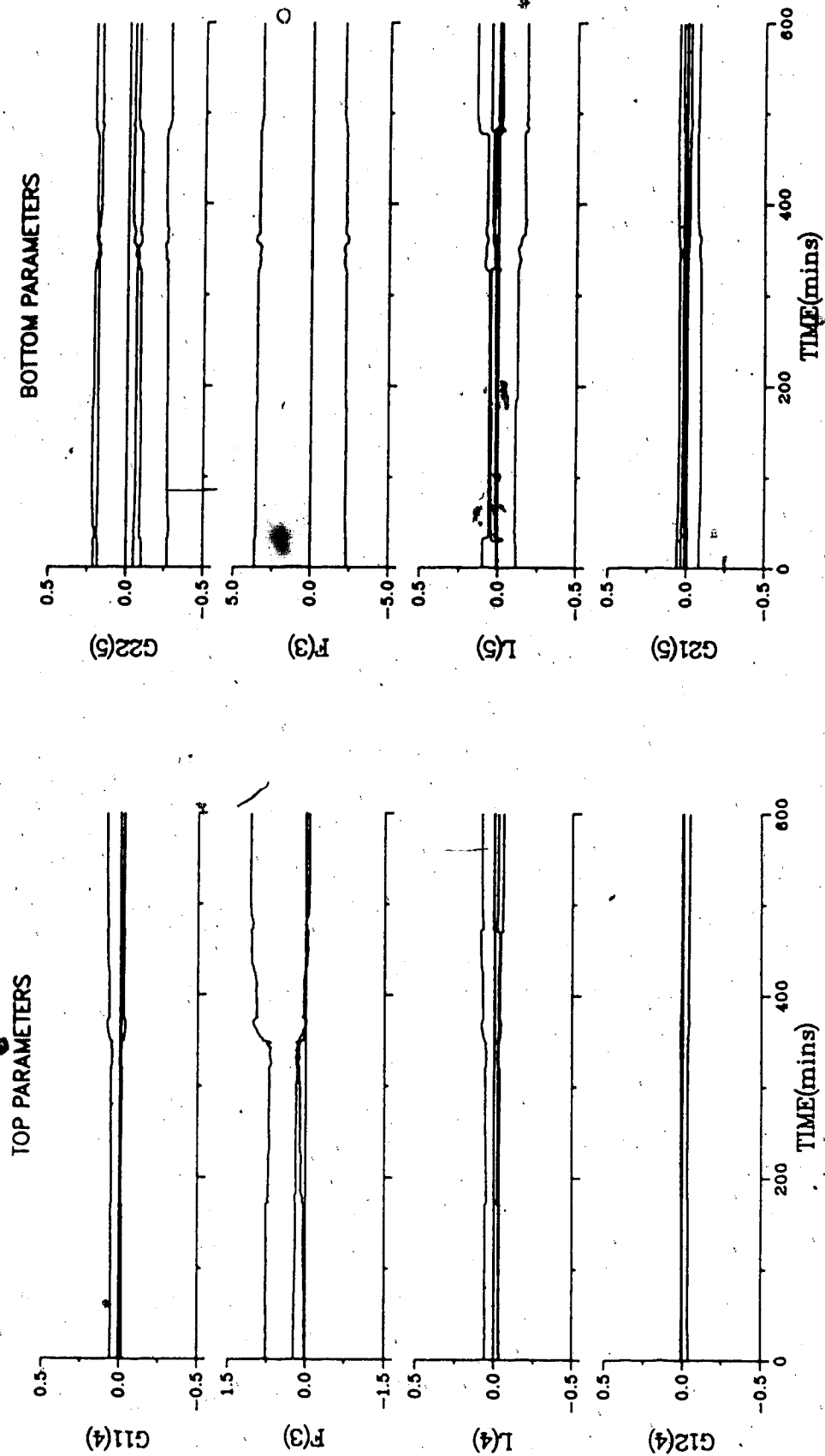


Figure 8.44 - Parameters for GMV Control using Q Weighting based on Modified PI/PI constants (MR, MFF)

tests are plotted in Figures 8.45, 8.47 and 8.49 and from these plots the oscillatory behavior is seen to be damped out. However, as observed by closely comparing Figures 8.39, 8.41 and 8.43 to Figures 8.45, 8.47 and 8.49, the changes in the steam flow in response to the feed flow changes are smaller in magnitude than those shown in Figures 8.45, 8.47 and 8.49, where "tuned" PI constants were used to calculate the  $Q$  weighting coefficients. The control performance that resulted was poorer in the tests where no feedforward action and an estimate for the feedforward action was used. Damping out the oscillations improved the overall control when the disturbance can be measured and used for the feedforward action, but not by much, as can be seen from the SAE values in Table 8.5 for the tests using the tuned constants. It is possible to assume that by following a procedure of tuning the PI constants further, an even better response may be obtained. The tuning should, however, be carried out for the no feedforward, estimated feedforward or measured feedforward schemes individually.

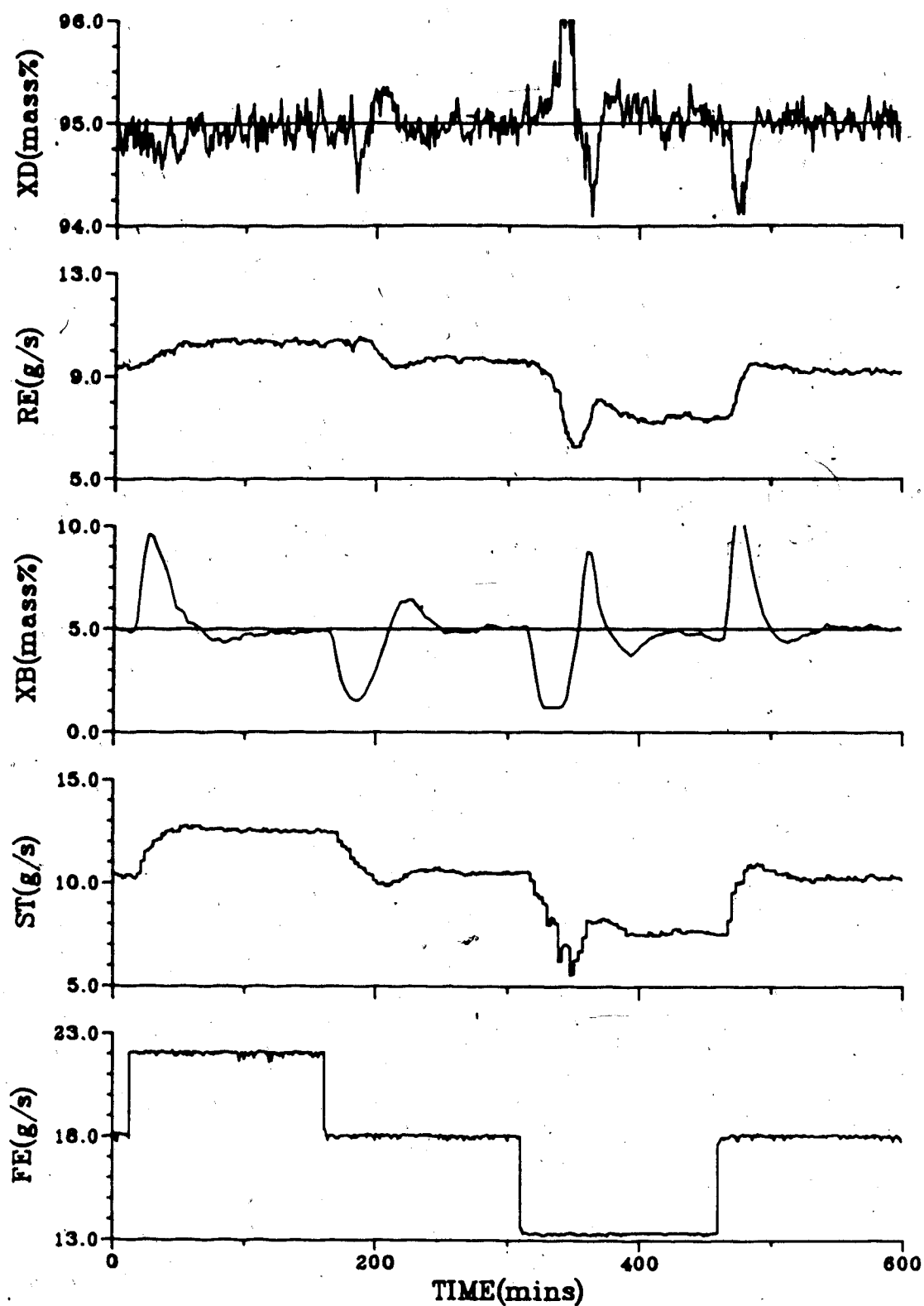


Figure 8.45 - Generalized Minimum Variance Control  
based on Tuned PI/PI constants  
(MR,NFF)

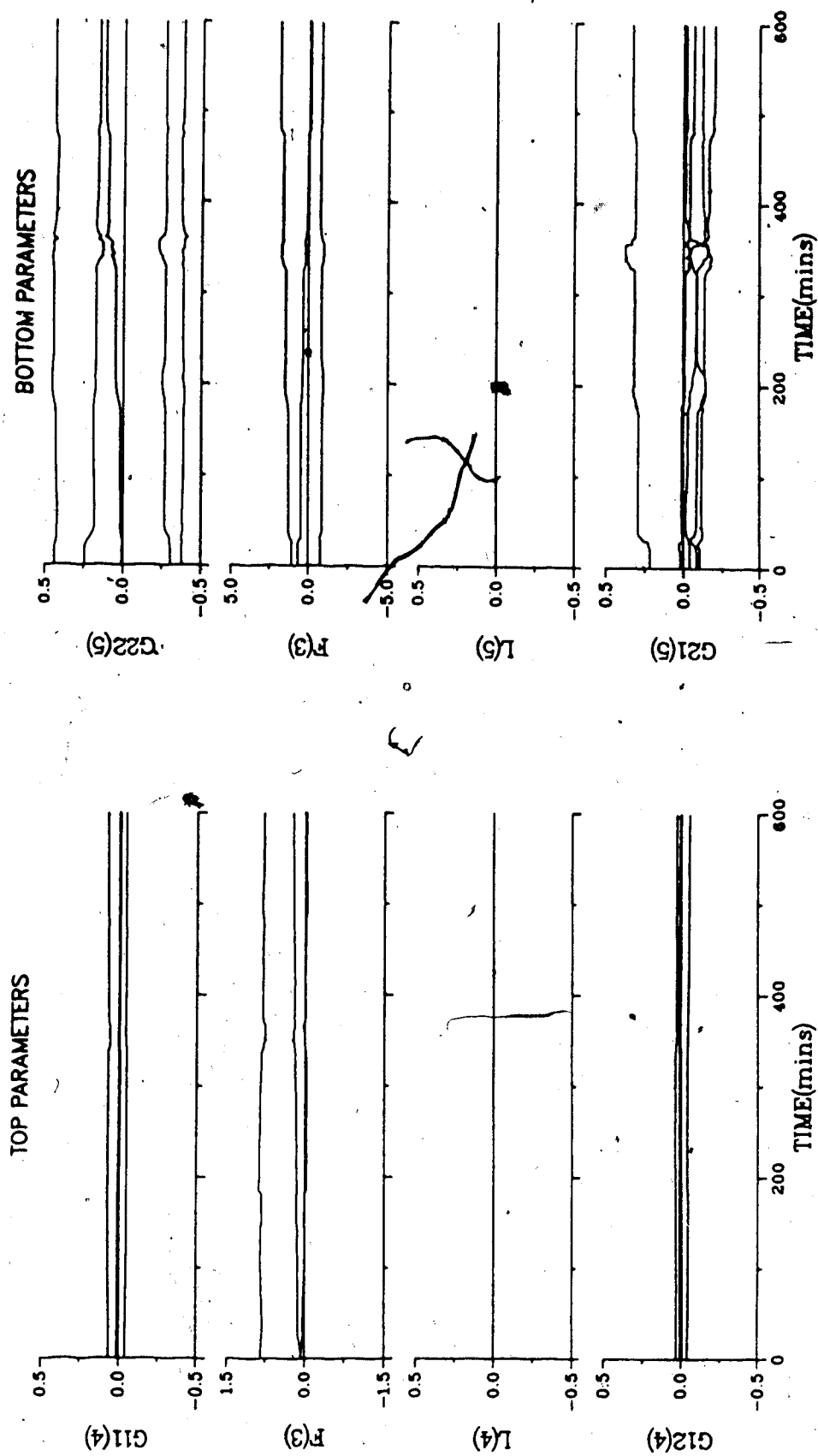


Figure 8.46 - Parameters for GMV Control using Q Weighting based on Tuned PI/PI constants (MR,NFF)

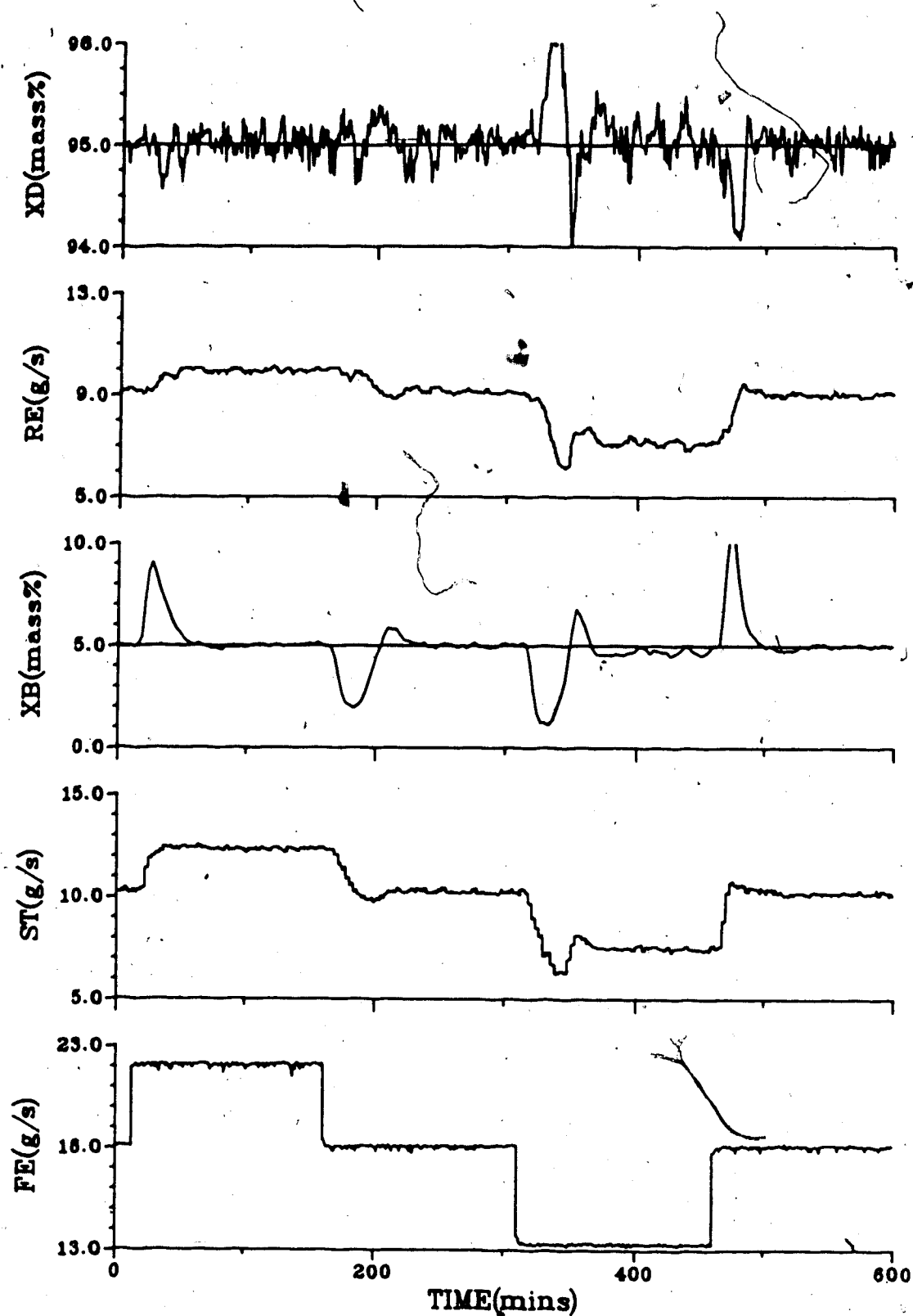


Figure 8.47 - Generalized Minimum Variance Control  
based on Tuned PI/PI constants  
(MR,EFF)



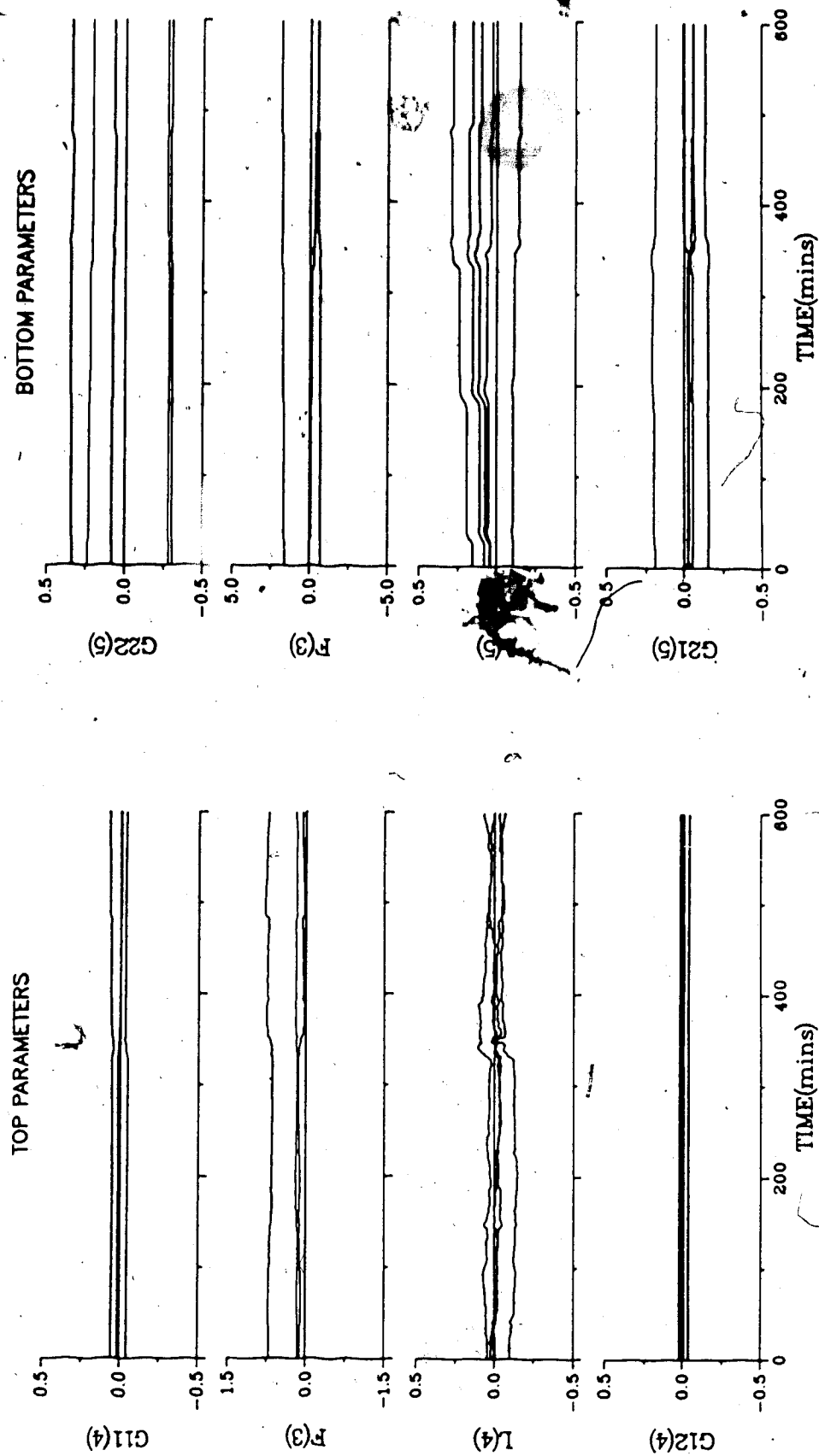


Figure 8.48 - Parameters for GMV Control using Q Weighting based on Tuned PI/PI constants (MR, EFF)

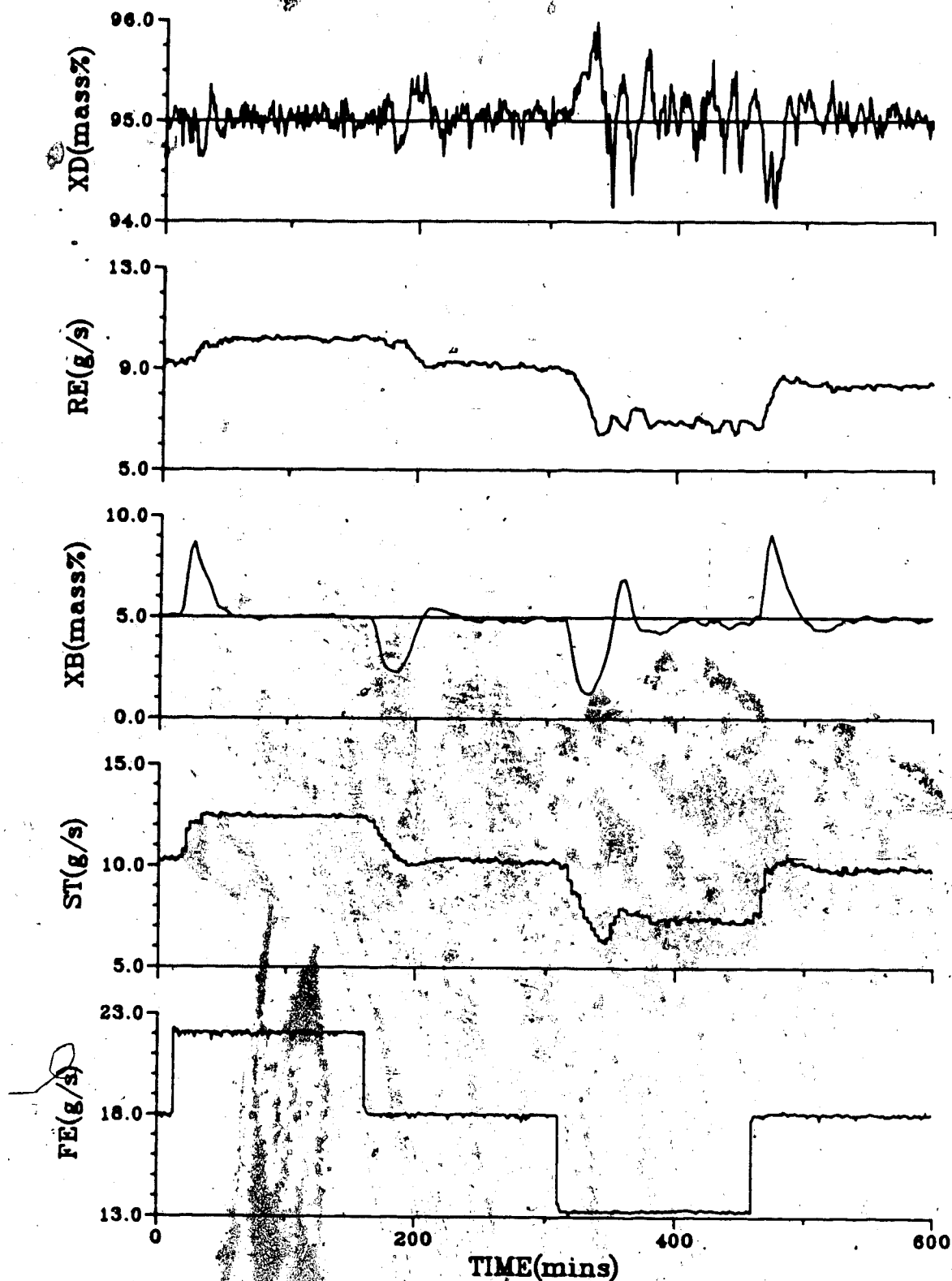


Figure 8.49 - Generalized Minimum Variance Control  
based on Tuned PI/PI constants  
(MR, MFF)

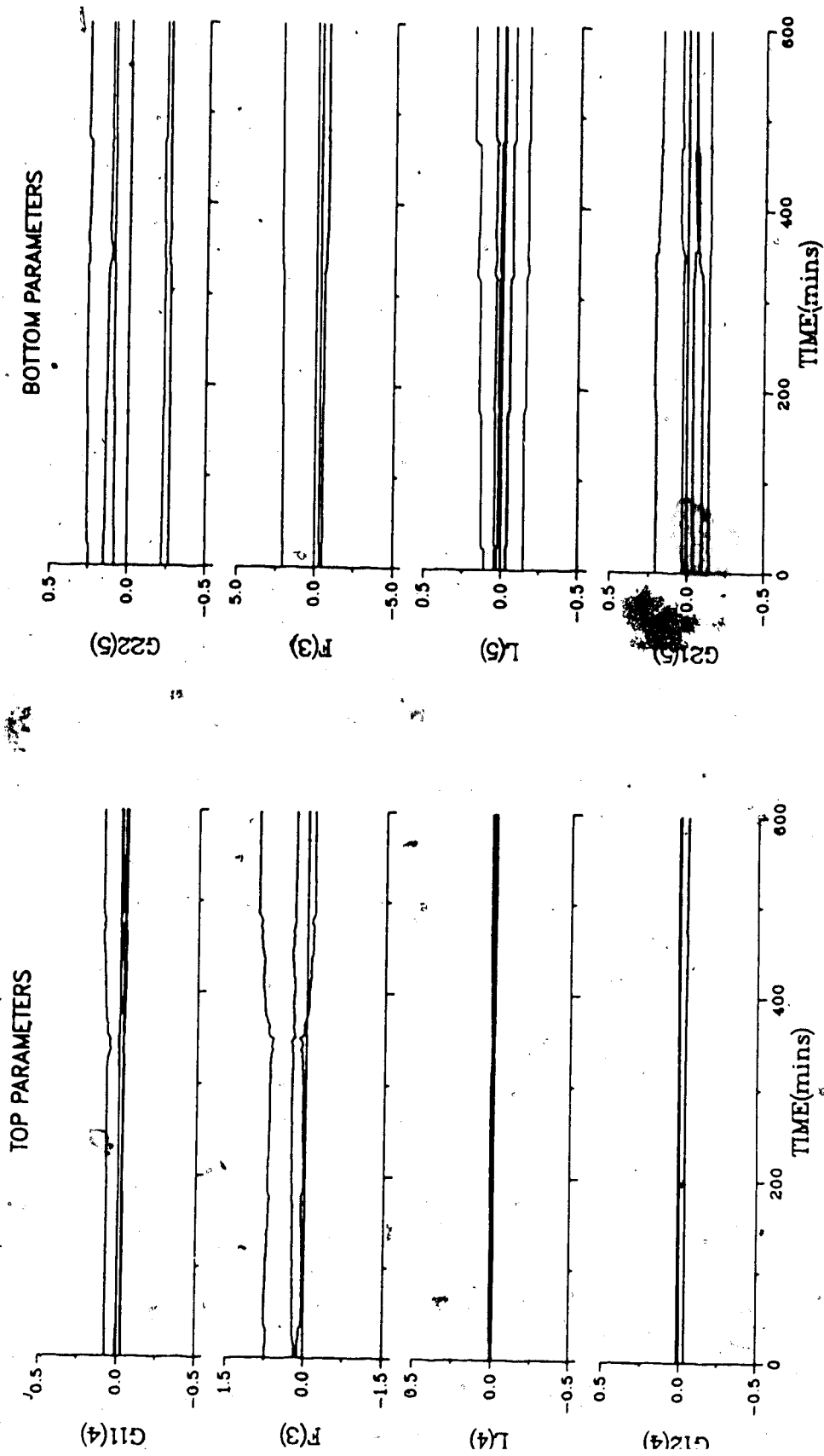


Figure 8.50 - Parameters for GMV Control using Q Weighting based on Tuned PI/PI constants (MR, MFF)

Table 8.5  
SAE Values for GMV Control based on Modified PI/PI constants

Loop	SAE Values:		
	NFF	EFF	MFF
Single Rate Control - Q parameters calculated from Cohen-Coon PI constants			
Figure	8.33	8.35	8.37
Top	162.5	174.9	129.0
Bottom	390.8	467.4	392.8
Both	553.3	642.3	521.8
Multirate Control - Q parameters calculated from Integral of Absolute Error PI constants			
Figure	8.39	8.41	8.43
Top	93.1	106.2	92.3
Bottom	324.0	440.7	390.7
Both	417.1	546.9	483.0
Multirate Control - Q parameters calculated from "Tuned" P constants			
Figure	8.45	8.47	8.49
Top	97.3	100.0	92.7
Bottom	584.7	389.0	380.0
Both	682.0	489.0	472.7

### 8.5.5 Q Weighting based on PI/PID constants with $g_0=0$

In order to completely remove the effect of  $g_0$  and to allow Q weighting coefficients to directly correspond to the compensator, one option available, as discussed in Section 6.4.2, is to set  $g_0 = 0.0$ . For the single rate sampling tests the Q weighting coefficients were calculated earlier from top loop PI constants of  $PB = 30.0$  and  $TI = 170.0$  and PID constants of  $PB = 65.0$ ,  $TI = 425.0$  and  $TD = 125.0$  for the bottom loop. Very similar responses were found for all three on the tests, as can be seen from the results presented in Figures 8.51, 8.53 and 8.55.

Although use of the multirate control algorithm does improve the control of the top composition, as can be seen from the results shown in Figures 8.57, 8.59 and 8.61, it is again difficult to distinguish between the three techniques of employing no feedforwarding, an estimated value and a measured value of the disturbance for the feedforward action. For the multirate tests the constants used in calculating the Q weighting coefficients were  $PB = 20.0$  and  $TI = 170.0$  for the top loop and  $PB = 65.0$ ,  $TI = 425.0$  and  $TD = 125.0$  for the bottom loop. Table 8.6 contains a summary of the SAE values for this series of single and multirate sampling tests.

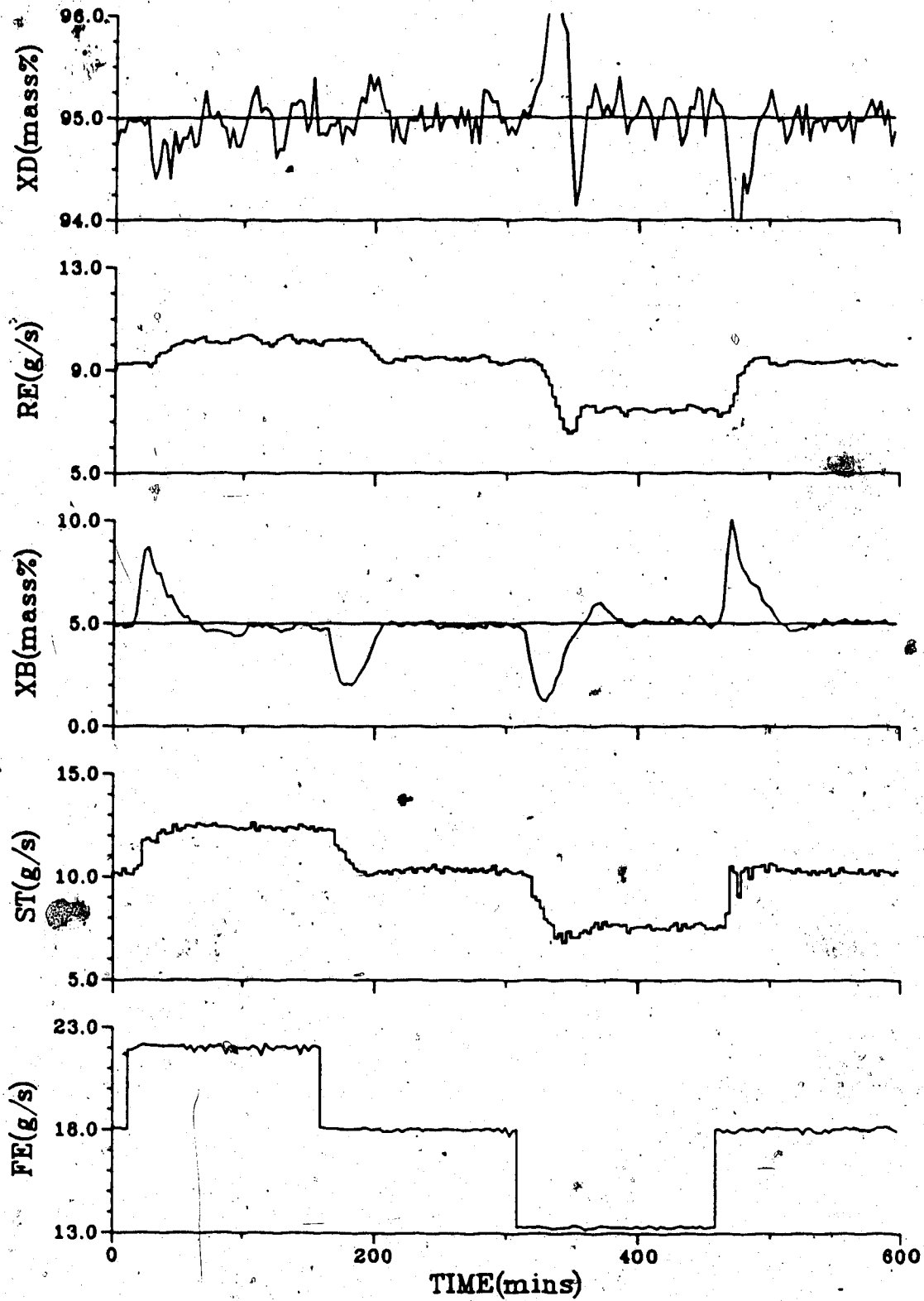


Figure 8.51 - Generalized Minimum Variance Control  
with  $g_0=0.0$  (SR,NFF)

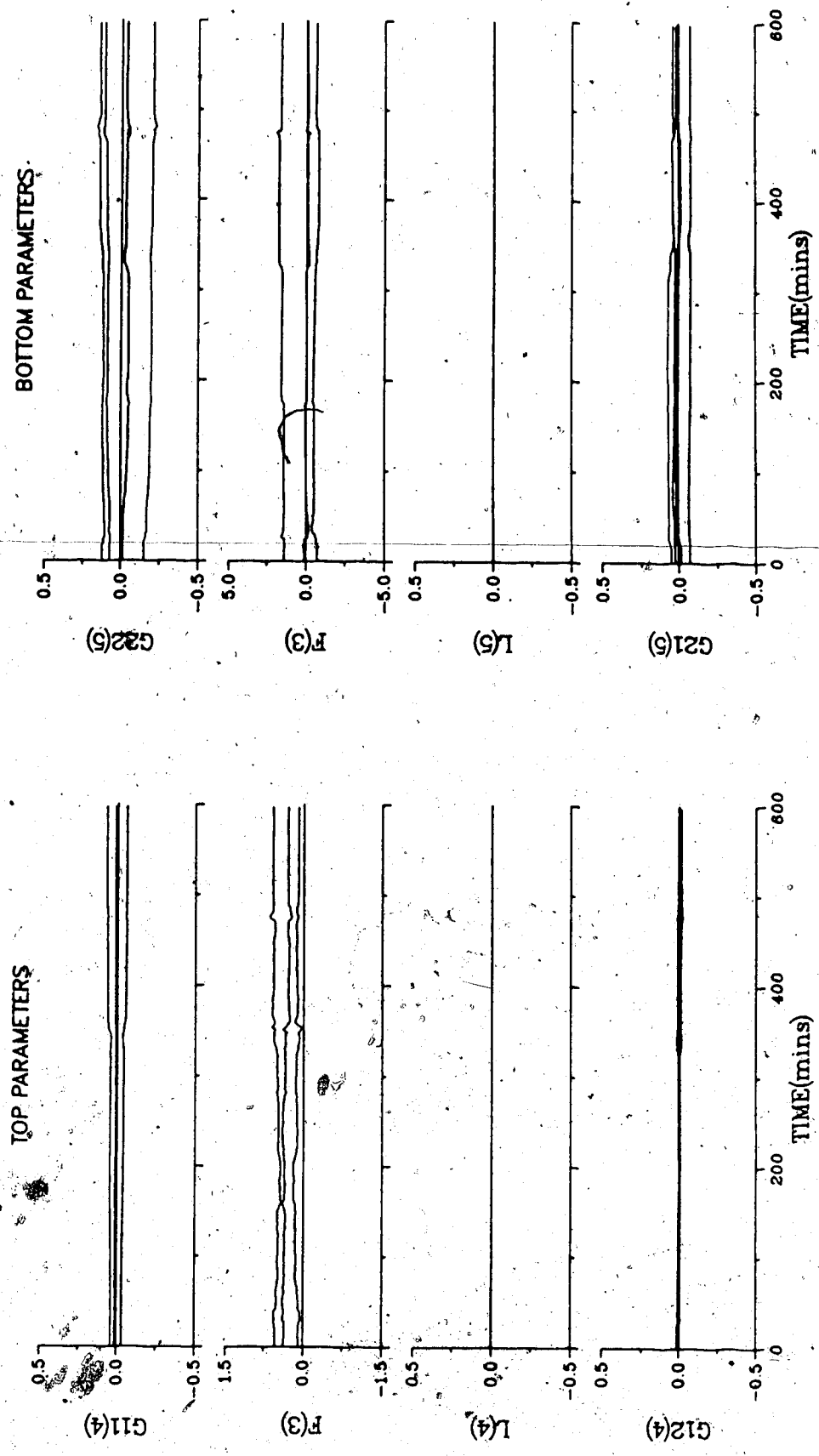


Figure 8.52 - Parameters for GMV Control with  $g_0 = 0.0$  (SR, EFF)

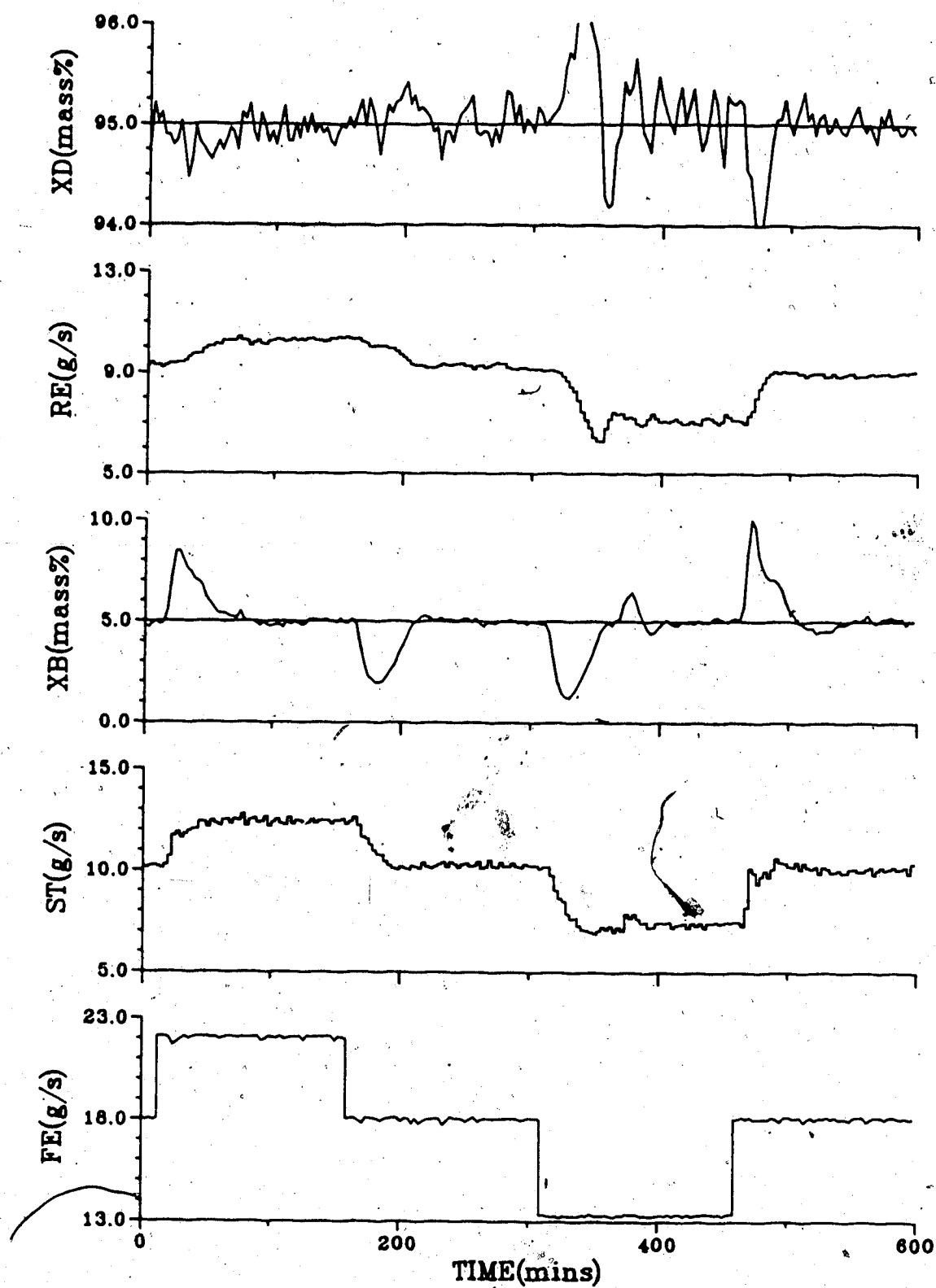


Figure 8.53 - Generalized Minimum Variance Control  
with  $g_0=0.0$  (SR, EFF)



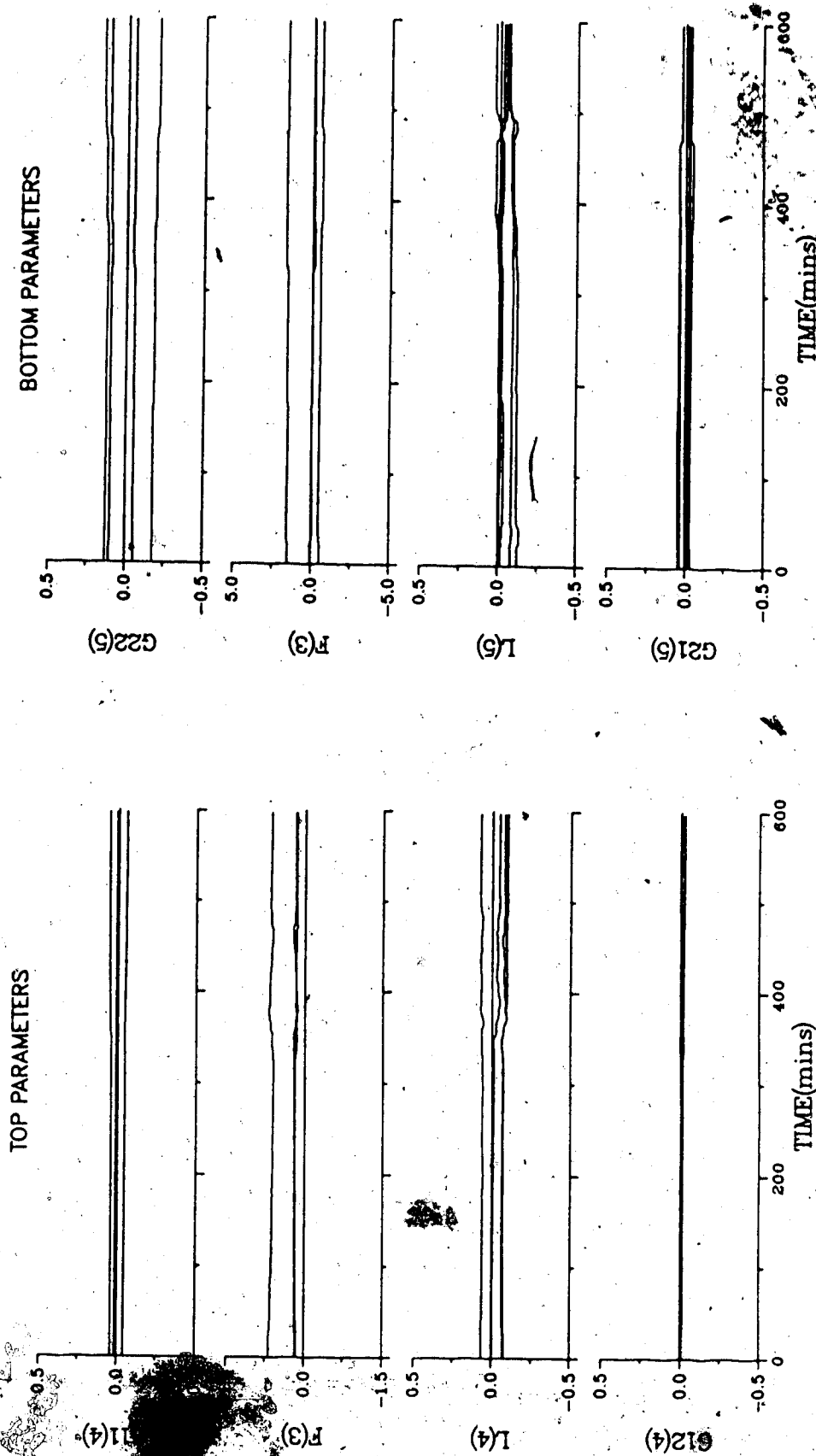


Figure 8.54 - Parameters for GMV Control with  $g_0 = 0.0$  (SR, EFF).

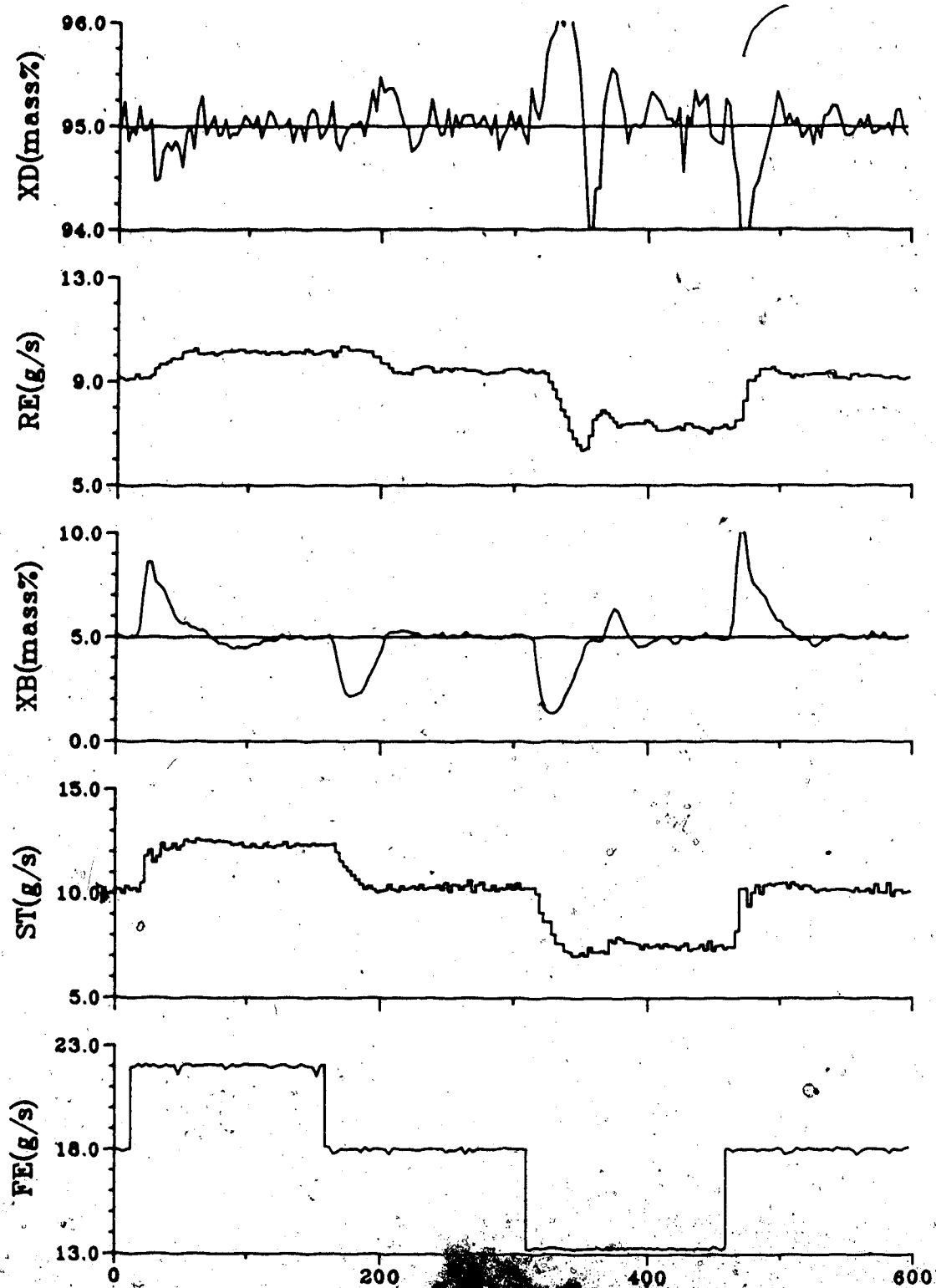


Figure 8.55 Generalized M...ance Control  
with  $g_0=0.0$  (S...)

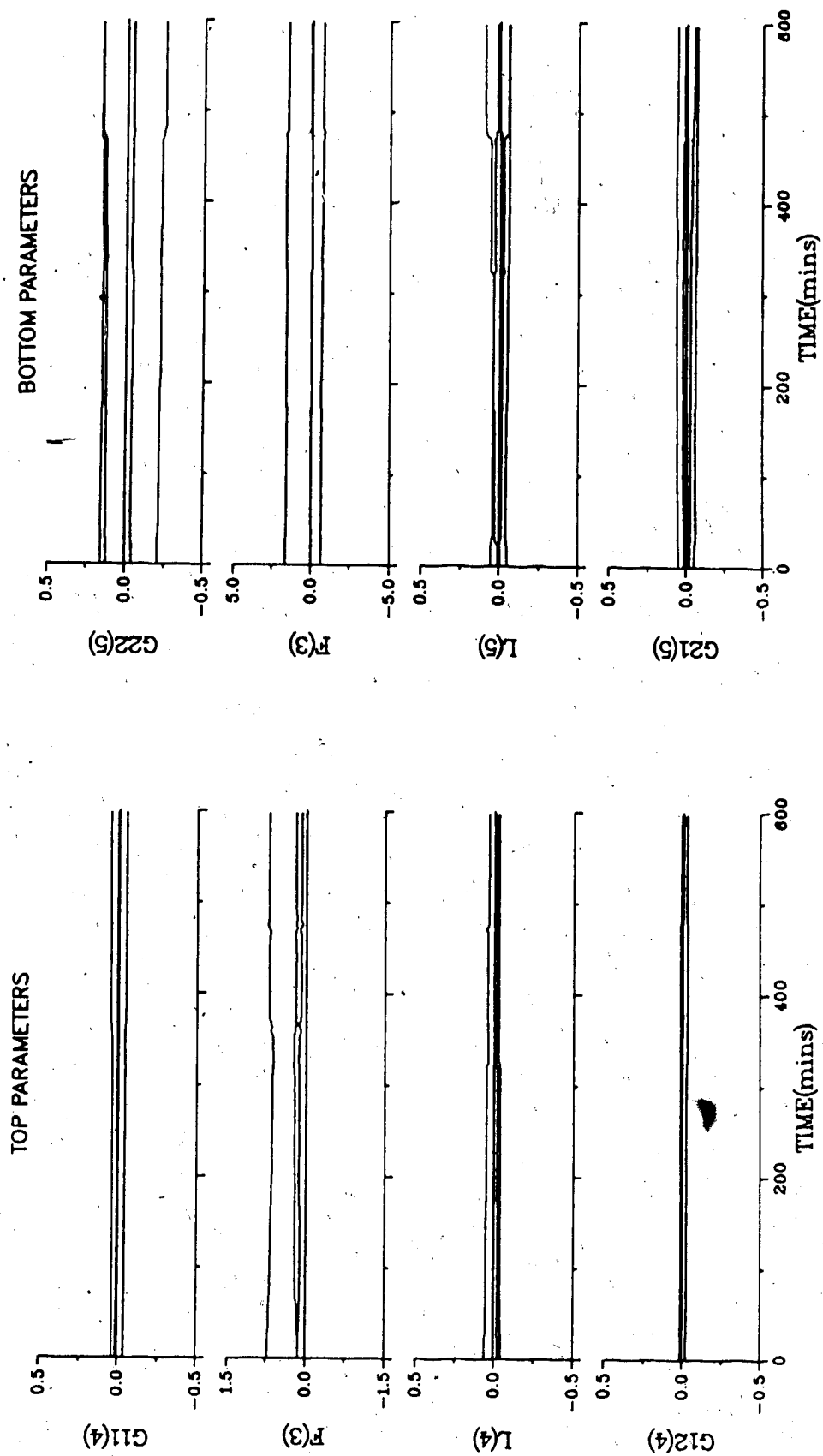


Figure 8.56 - Parameters for GMV Control with  $g_0 = 0.0$  (SR, MFF)

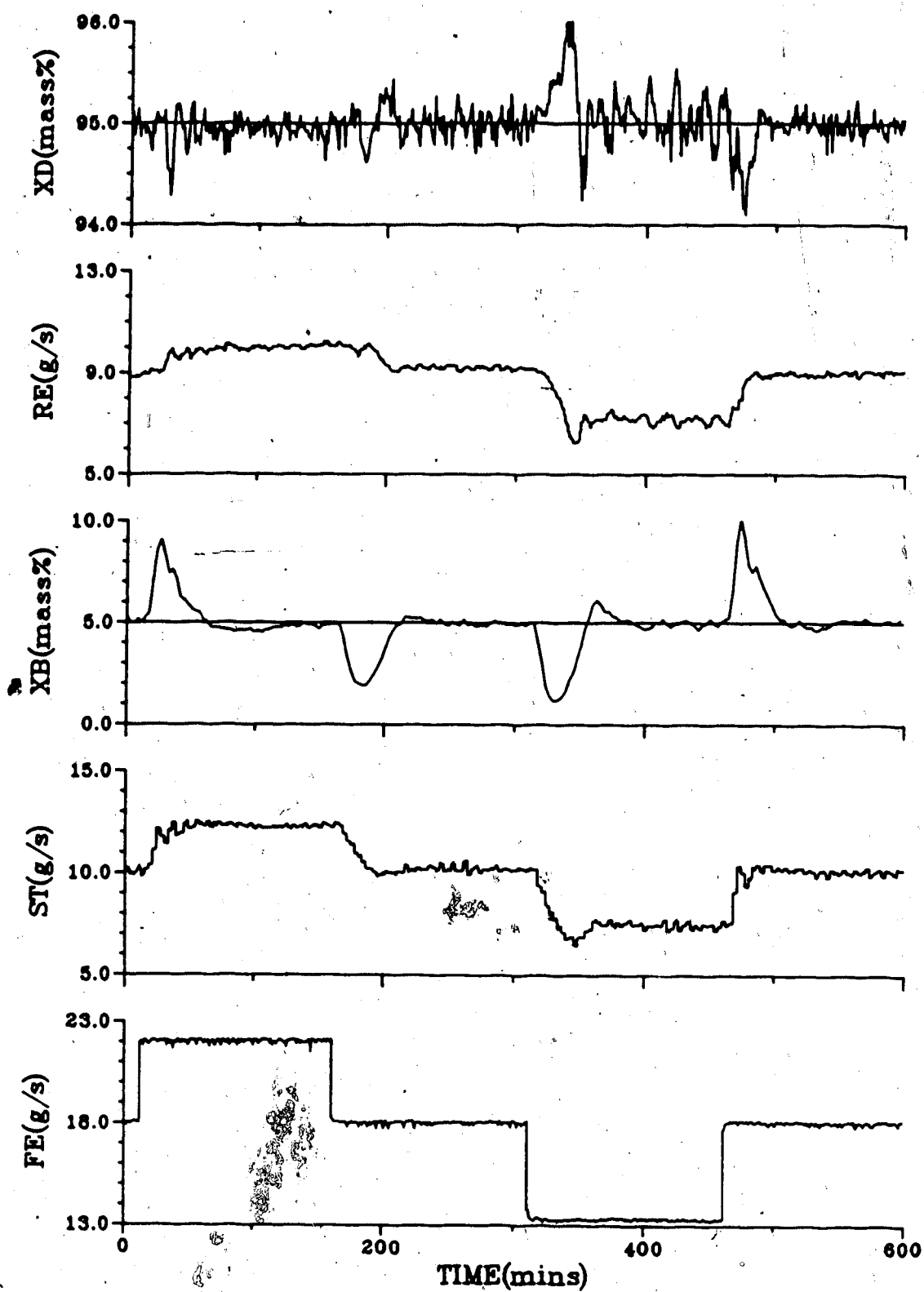


Figure 8.57 - Generalized Minimum Variance Control  
 with  $g_0=0.0$  (MR,NFF)

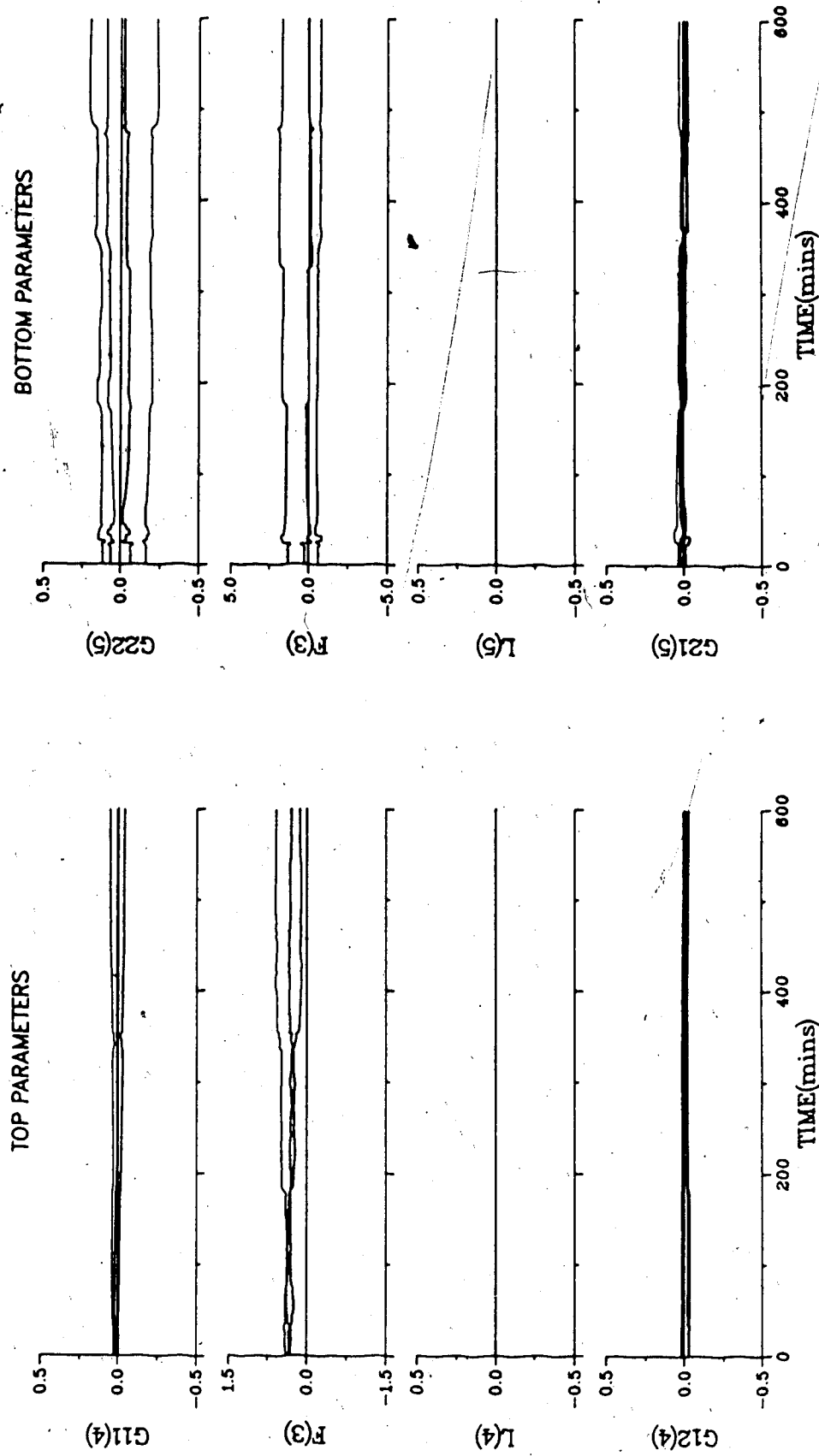


Figure 8.58 - Parameters for GMV Control with  $g_0 = 0.0$  (MR,NFF)

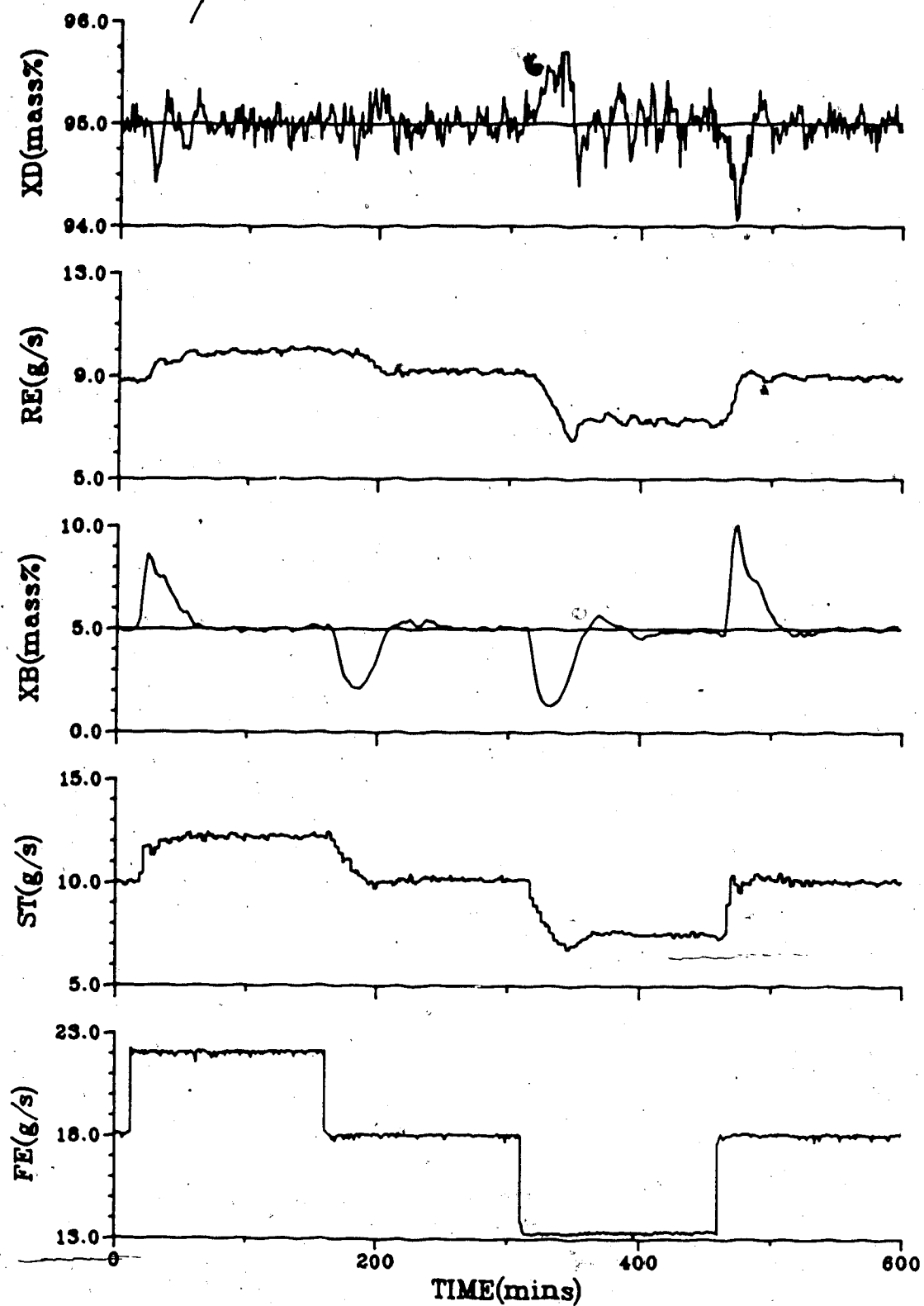


Figure 8.59 - Generalized Minimum Variance Control  
with  $g_0=0.0$  (MR,EFF)

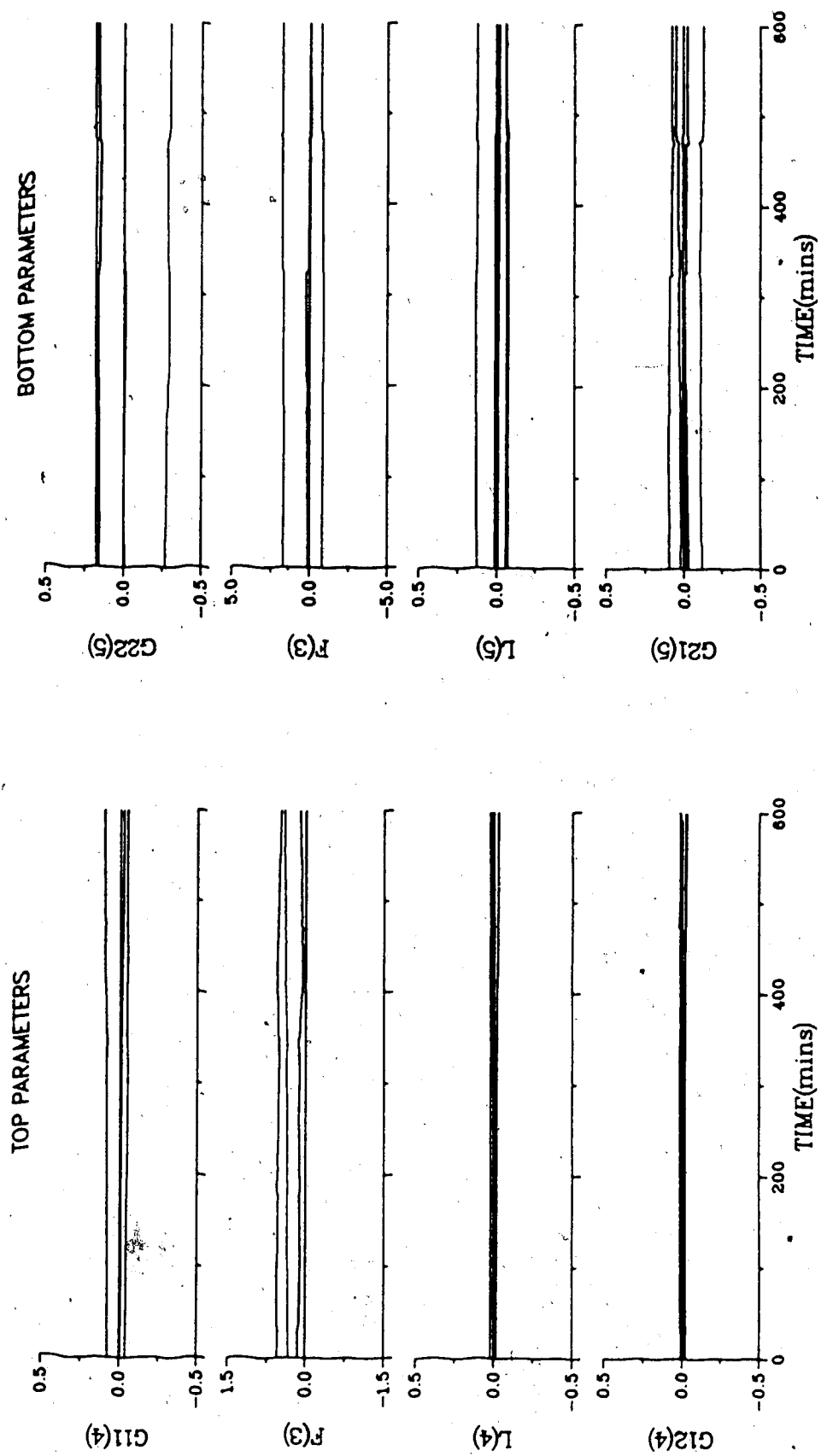


Figure 8.60 - Parameters for GMV Control with  $g_0 = 0.0$  (MR, EFF)

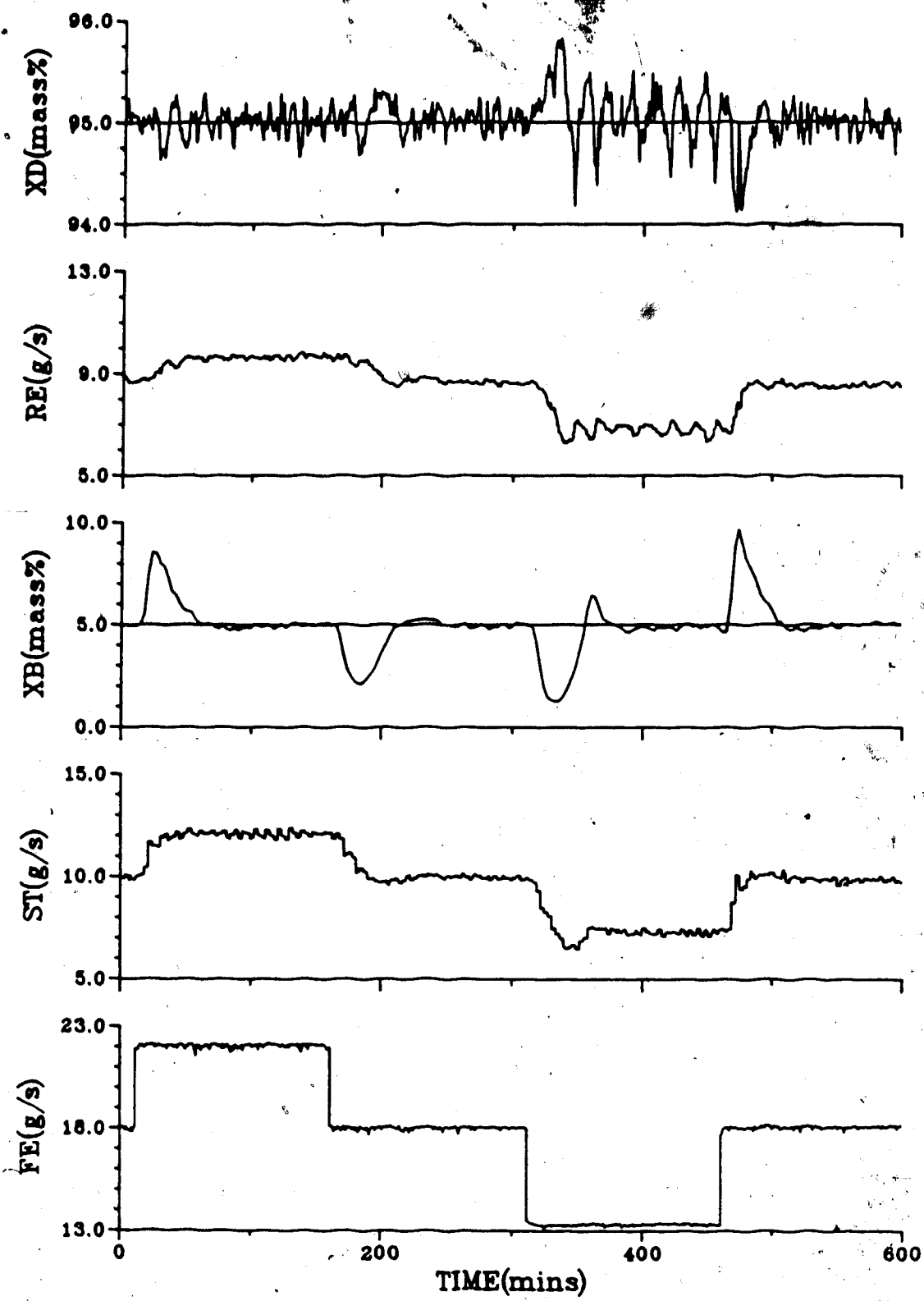


Figure 8.61 - Generalized Minimum Variance Control  
with  $g_0=0.0$  (MR,MFF)



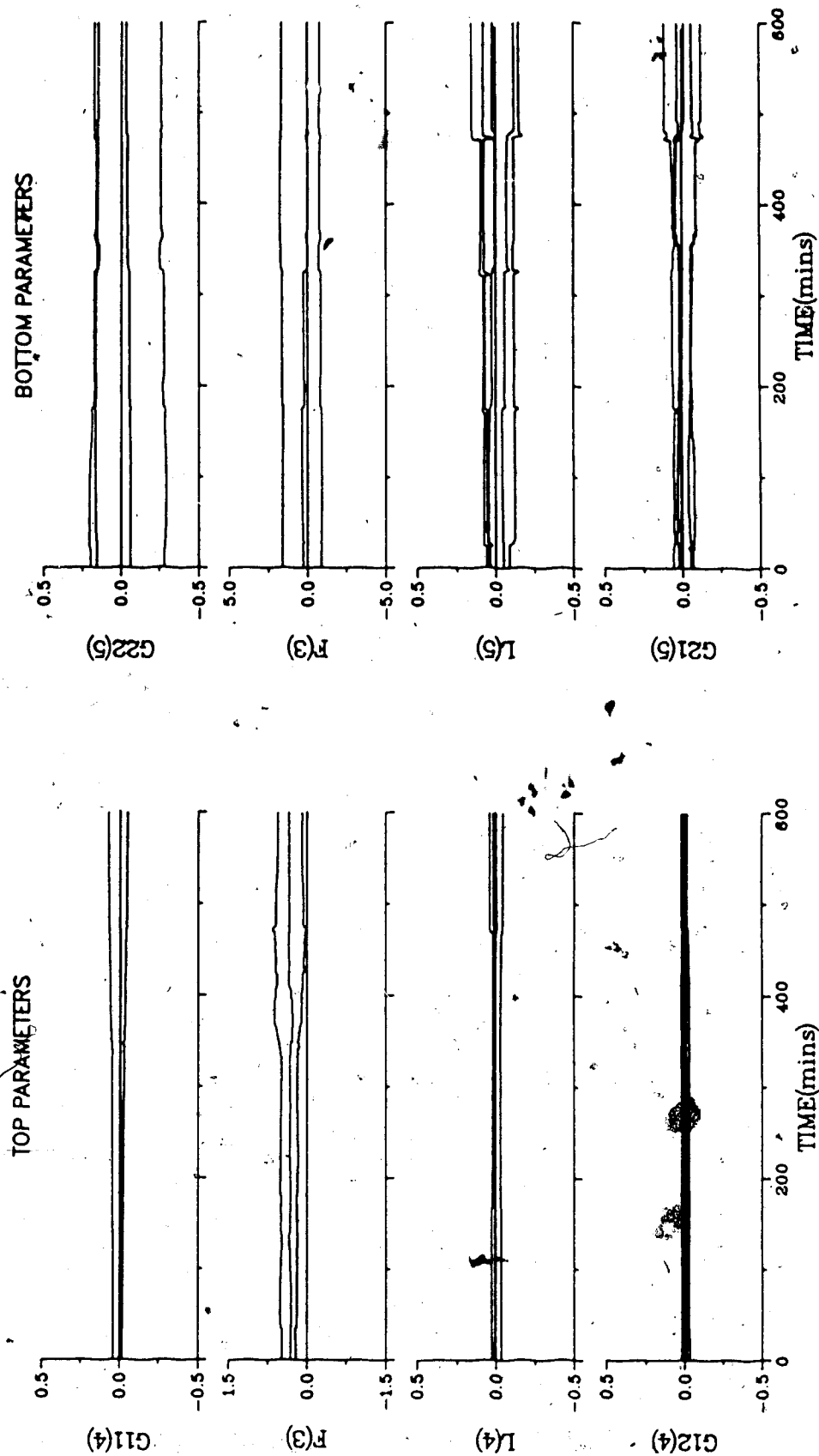


Figure 8.62 - Parameters for GMV Control with  $g_0 = 0.0$  (MR, MFF)

Table 8.6  
SAE Values for GMV Control using  $g_0=0$

Loop	SAE Values:		
	NFF	EFF	MFF
Single Rate Control			
Figure	8.51	8.53	8.55
Top	119.9	125.5	122.3
Bottom	416.4	436.5	411.6
Both	536.3	562.0	533.9
Multirate Control			
Figure	8.57	8.59	8.61
Top	88.8	80.6	91.0
Bottom	423.6	409.6	399.6
Both	512.4	490.2	490.6

#### 8.5.6 Underestimating the Time Delay

Another option to improve the correspondence between the  $Q$  weighting polynomial and the inverse structure of a PI compensator, as discussed in Section 6.4.2, is to set  $g_0 = 0.0$  and underestimate the time delay relating the manipulated variable and the output for the loop. For this set of tests the  $Q$  weighting coefficients were calculated from the tuned PID constants used in Section 8.2, except that the derivative action was not used in calculating the  $q$ 's for the bottom loop.

The responses obtained using the single rate sampling form of the algorithm are plotted in Figures 8.63, 8.65 and 8.67. Examination of the responses shows that it is difficult to detect any noticeable difference in performance between any of the results presented. However, relatively good control performance was obtained compared to the results reported so far in this chapter. In fact, for this particular technique better control behavior resulted with the single rate algorithm than when using the multirate form of the algorithm, as can be seen from the responses in Figures 8.69, 8.71 and 8.73. Use of the multirate form of the algorithm considerably reduced the large deviations in the top composition compared with the single rate performance, but an oscillatory response exists. The bottom composition does not appear to be as well controlled as it was during the single rate sampling tests, and this is confirmed by the SAE values in Table 8.7 where it can

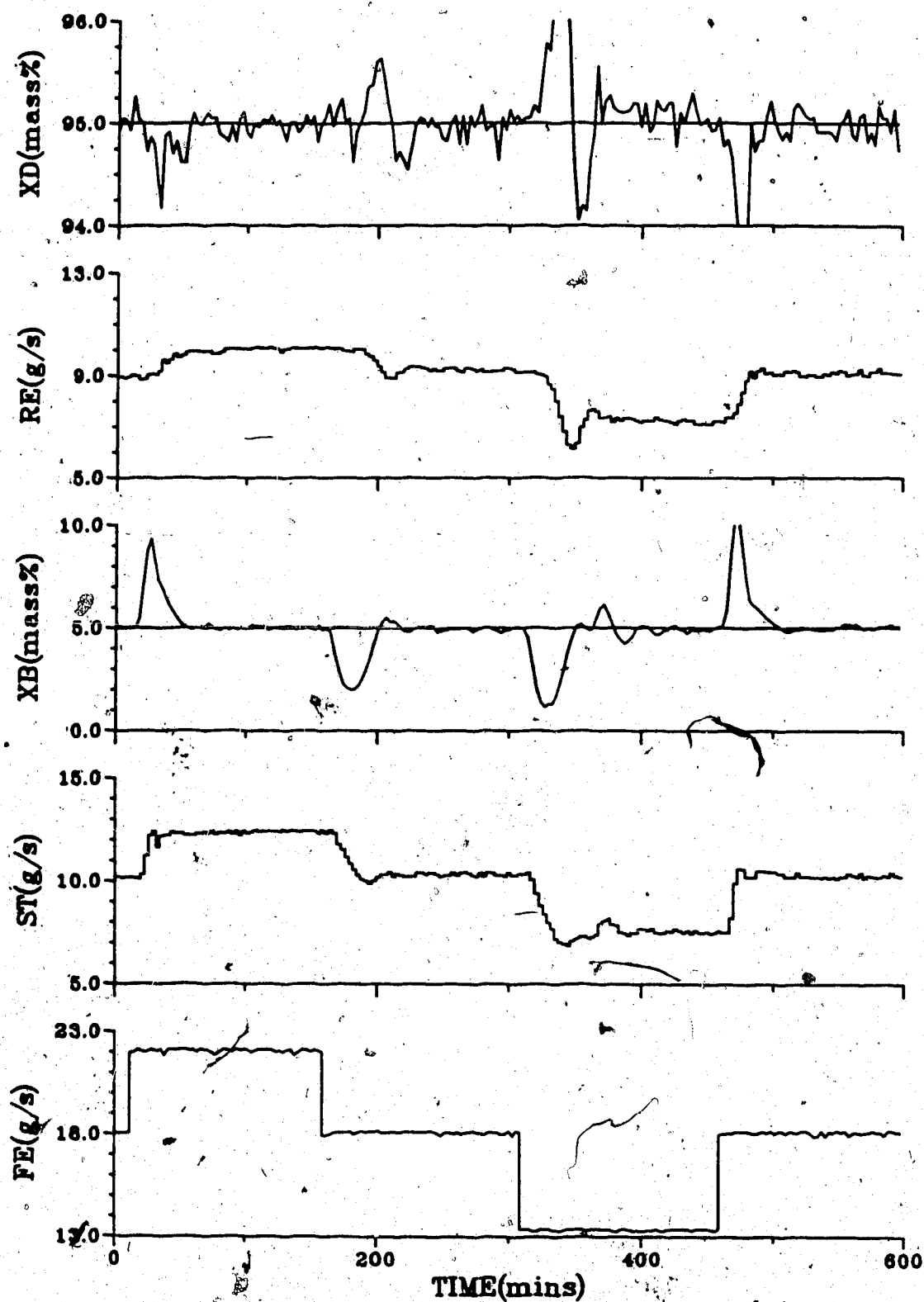


Figure 8.63 - Generalized Minimum Variance Control  
with  $g_0=0.0$  and the Time Delay  
Underestimated (SR, NFE)

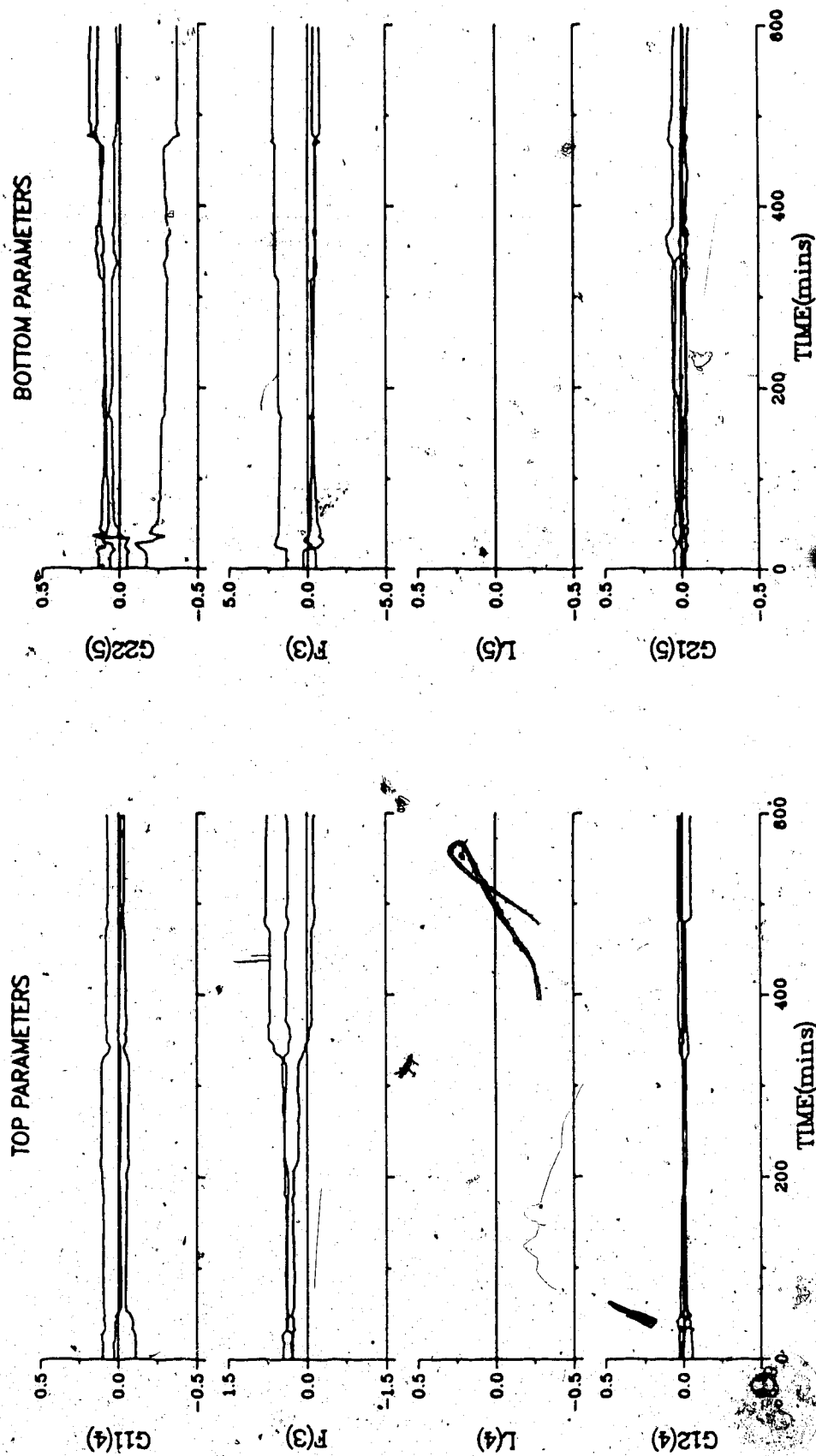


Figure 8.64 - Parameters for GMV Control with  $g_0 = 0.0$  and the Time Delay Underestimated (SR, NFF)

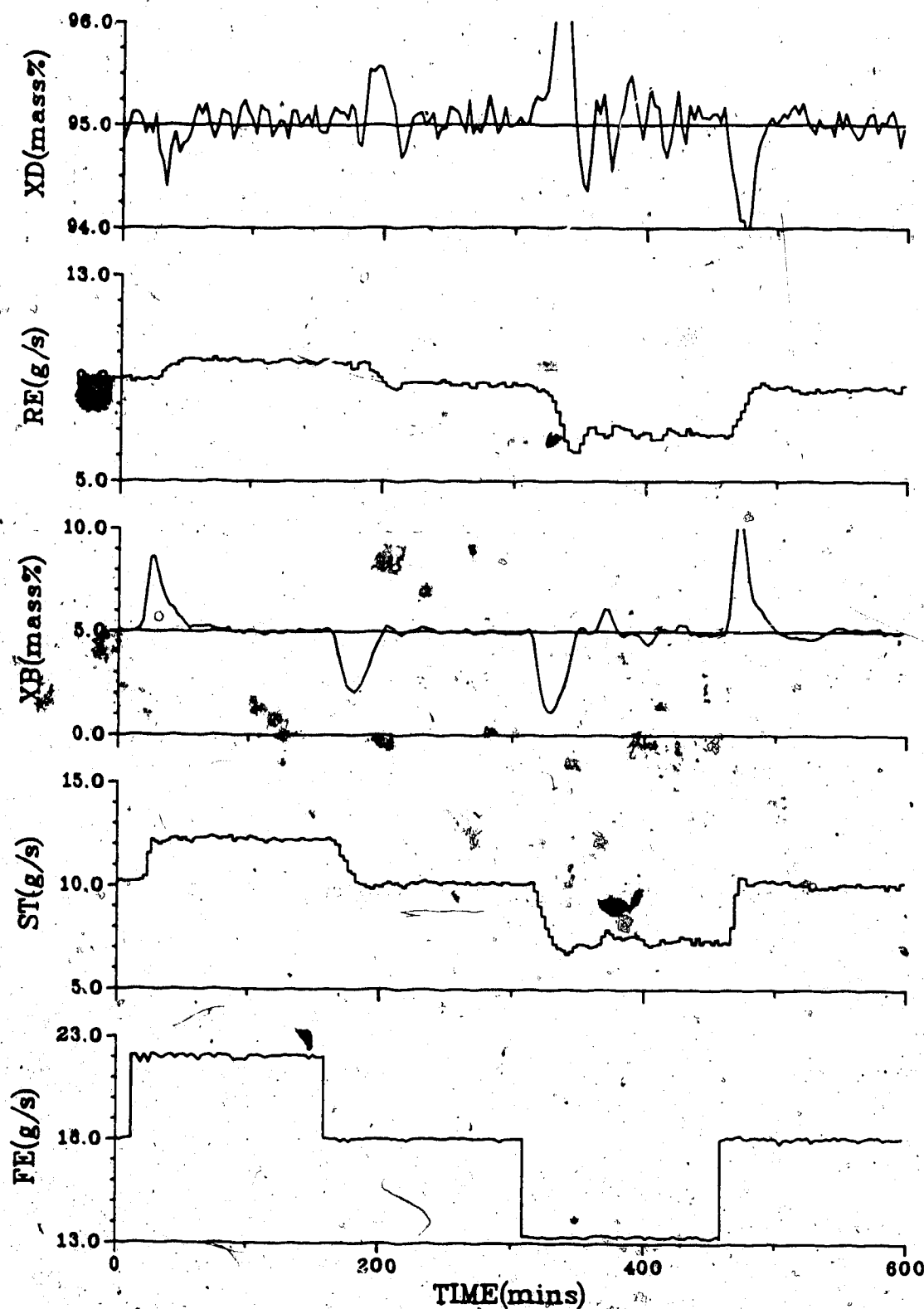


Figure 8.65 - Generalized Minimum Variance Control with  $g_0=0.0$  and the Time Delay, Underestimated (SR,EFF)

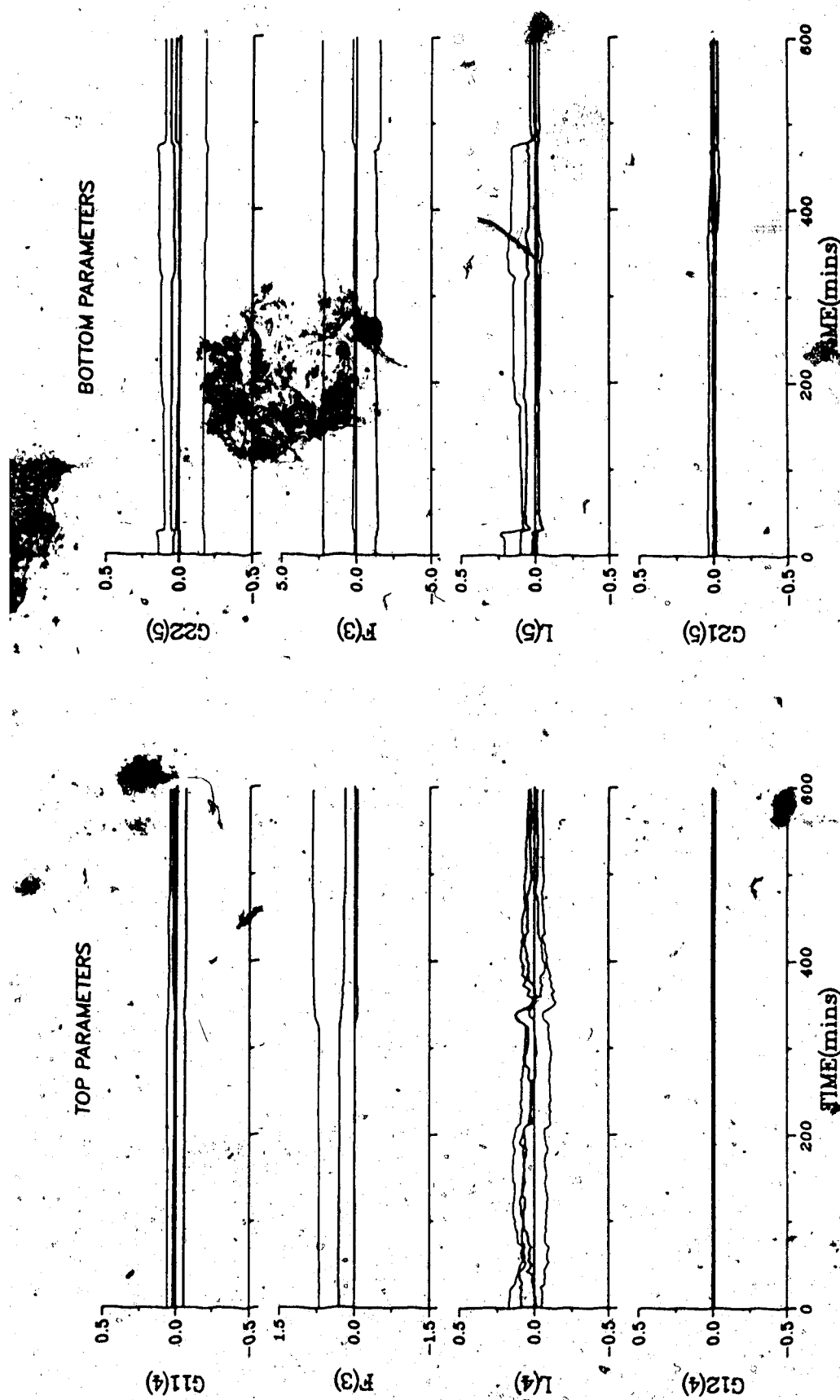


Figure 8.66 - Parameters for GMV Control with  $g_0 = 0.0$  and the Time Delay Underestimated (SR, EFF)

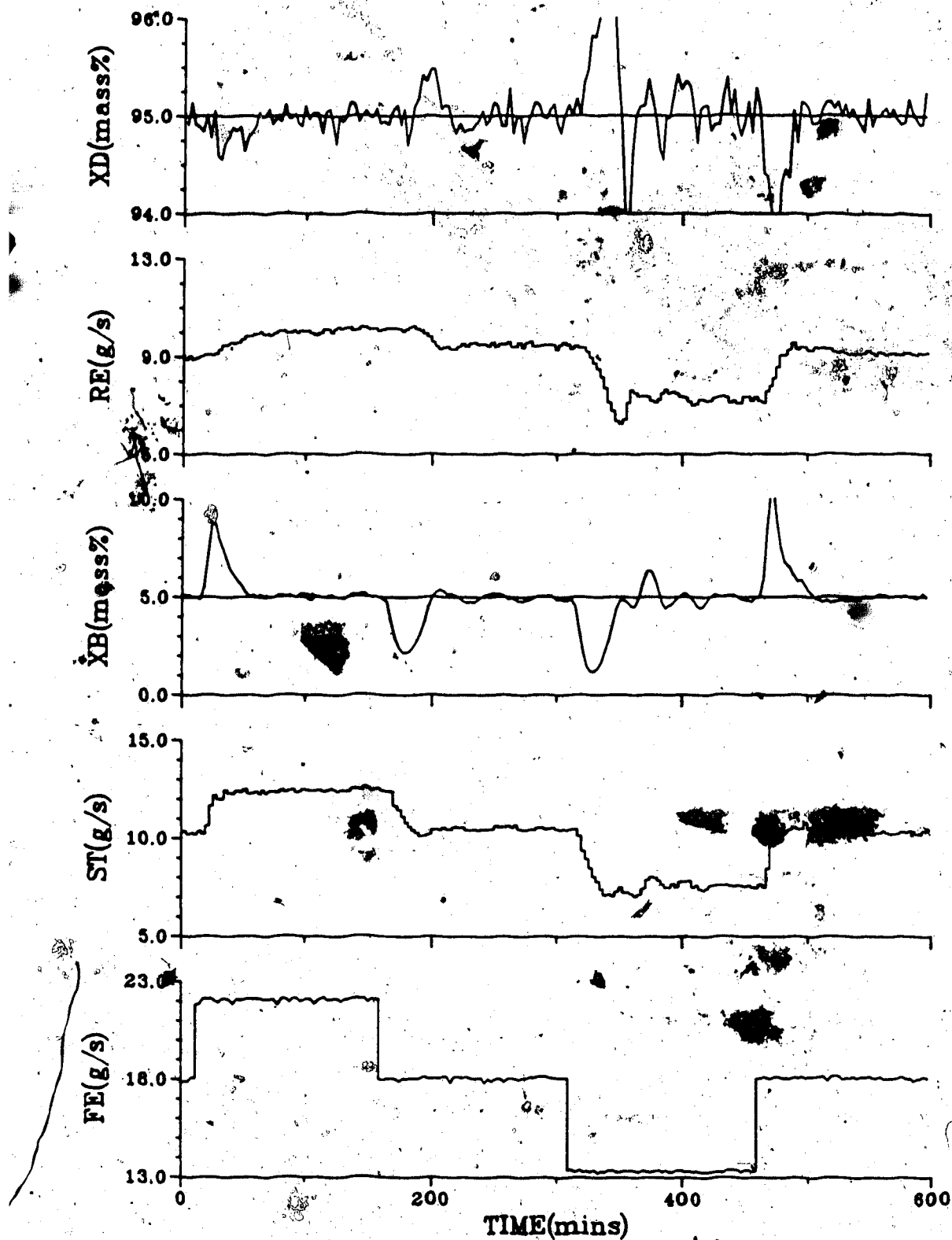


Figure 8.67 - Generalized Minimum Variance Control  
with  $g_0=0.0$  and the Time Delay  
Underestimated (SR,MFF)



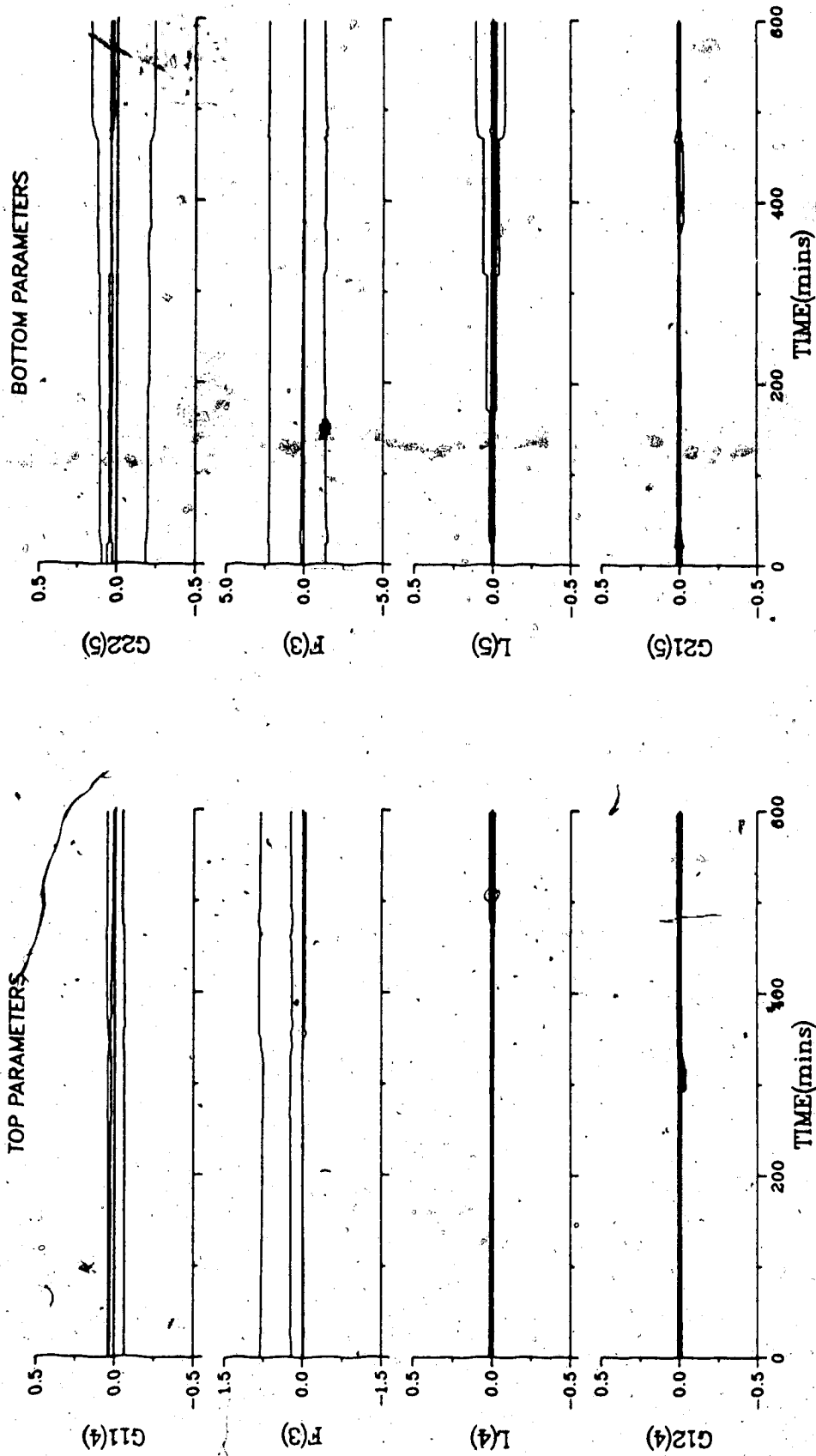


Figure 8.68 - Parameters for GMV Control with  $g_0 = 0.0$  and the Time Delay Underestimated (SR, MFF)

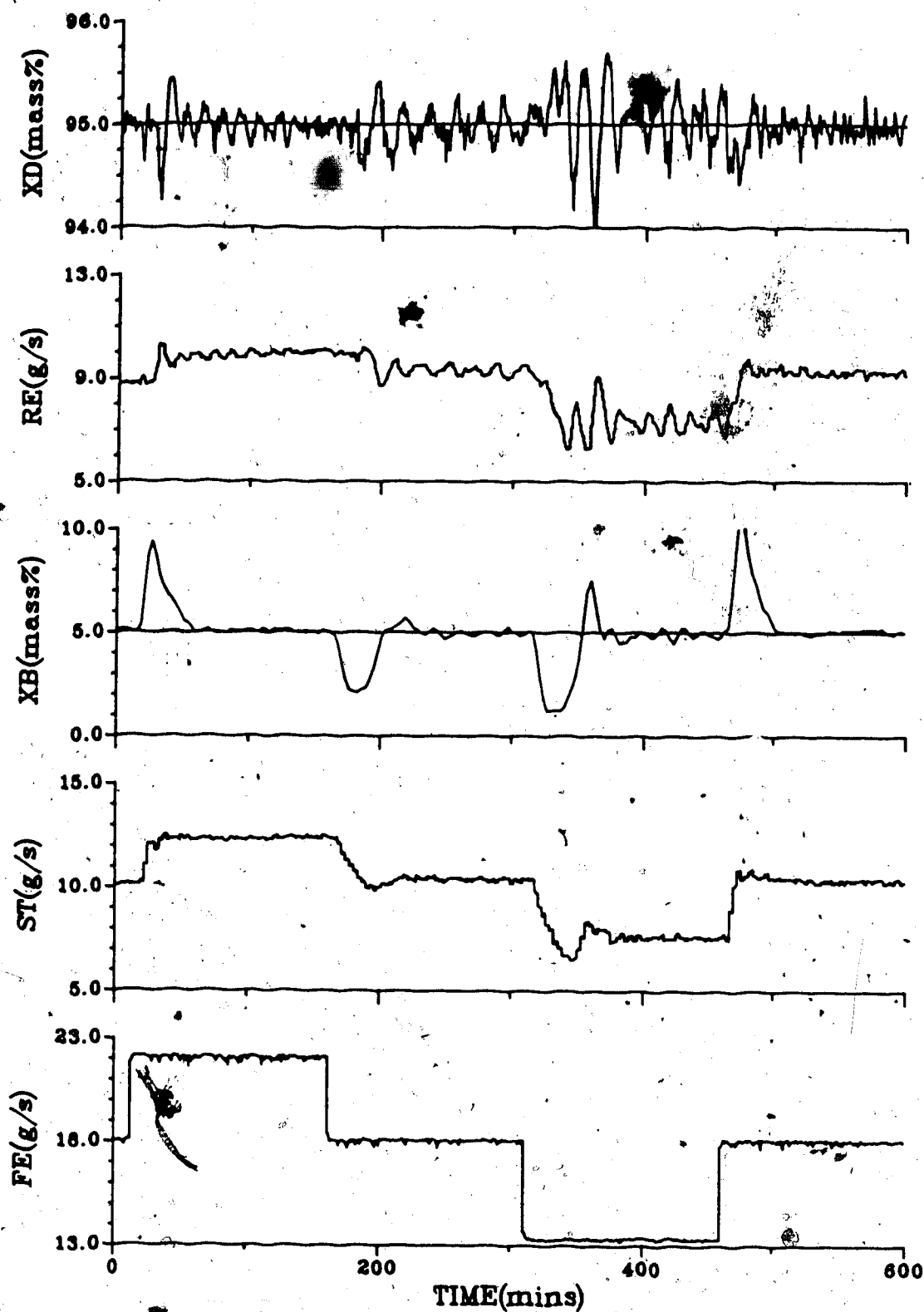


Figure 8.69 - Generalized Minimum Variance Control  
with  $g_0=0.0$  and the Time Delay  
Underestimated (MR,NFF)

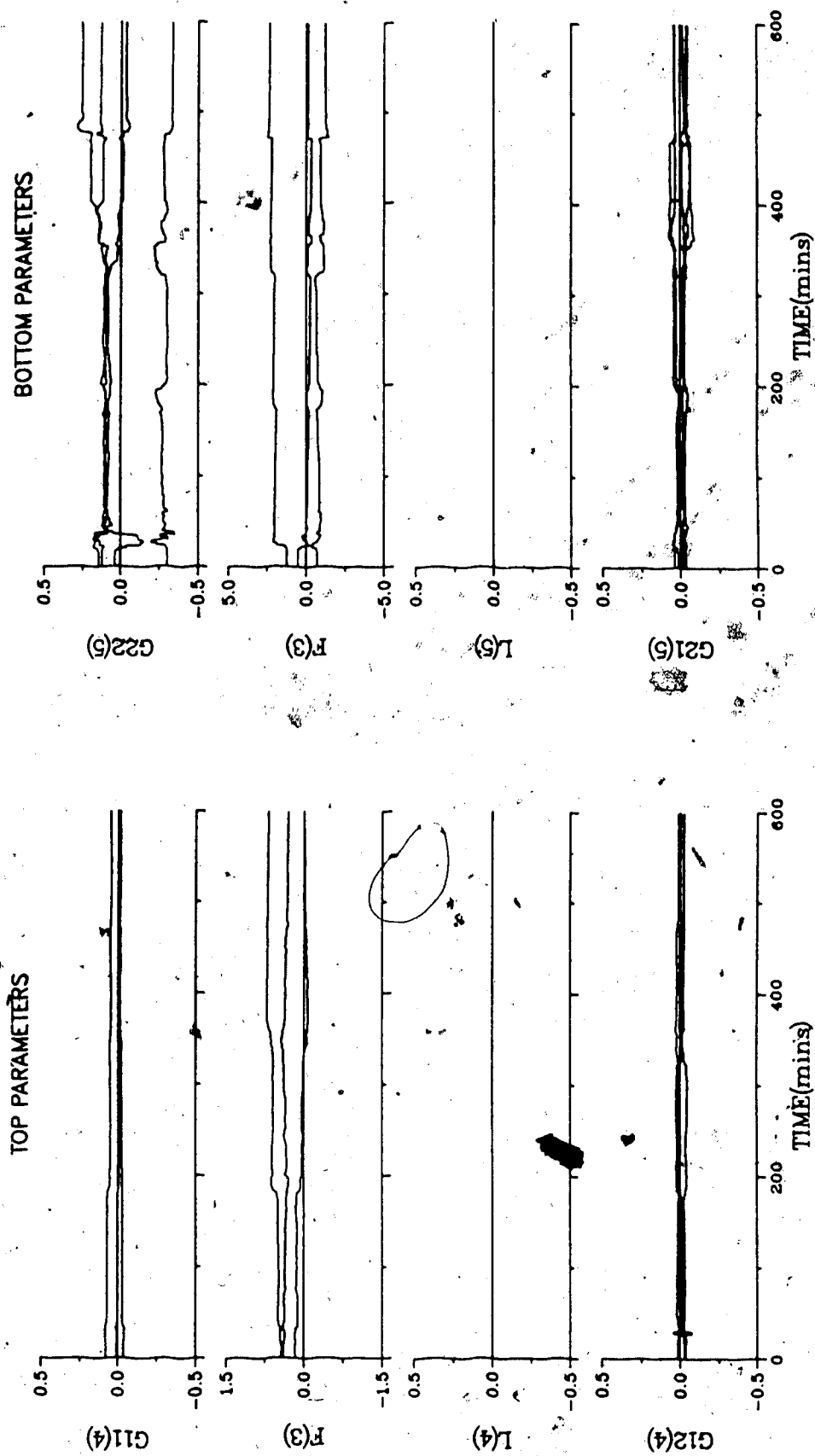


Figure 8.70 - Parameters for GMV Control with  $g_0 = 0.0$  and the Time Delay Underestimated (MR, NFF)

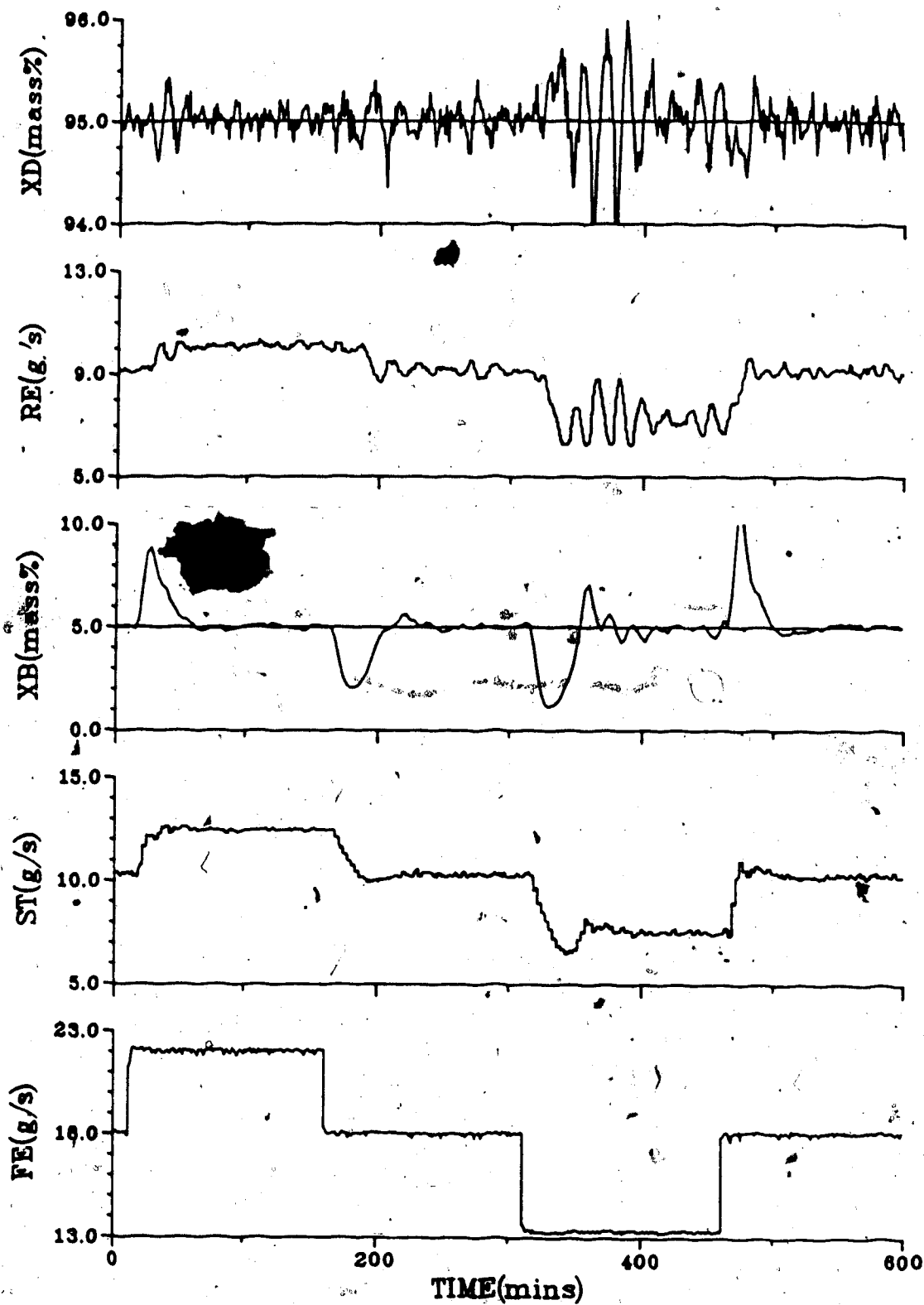


Figure 8.71 - Generalized Minimum Variance Control  
with  $g_0=0.0$  and the Time Delay  
Underestimated (ME,EFF)

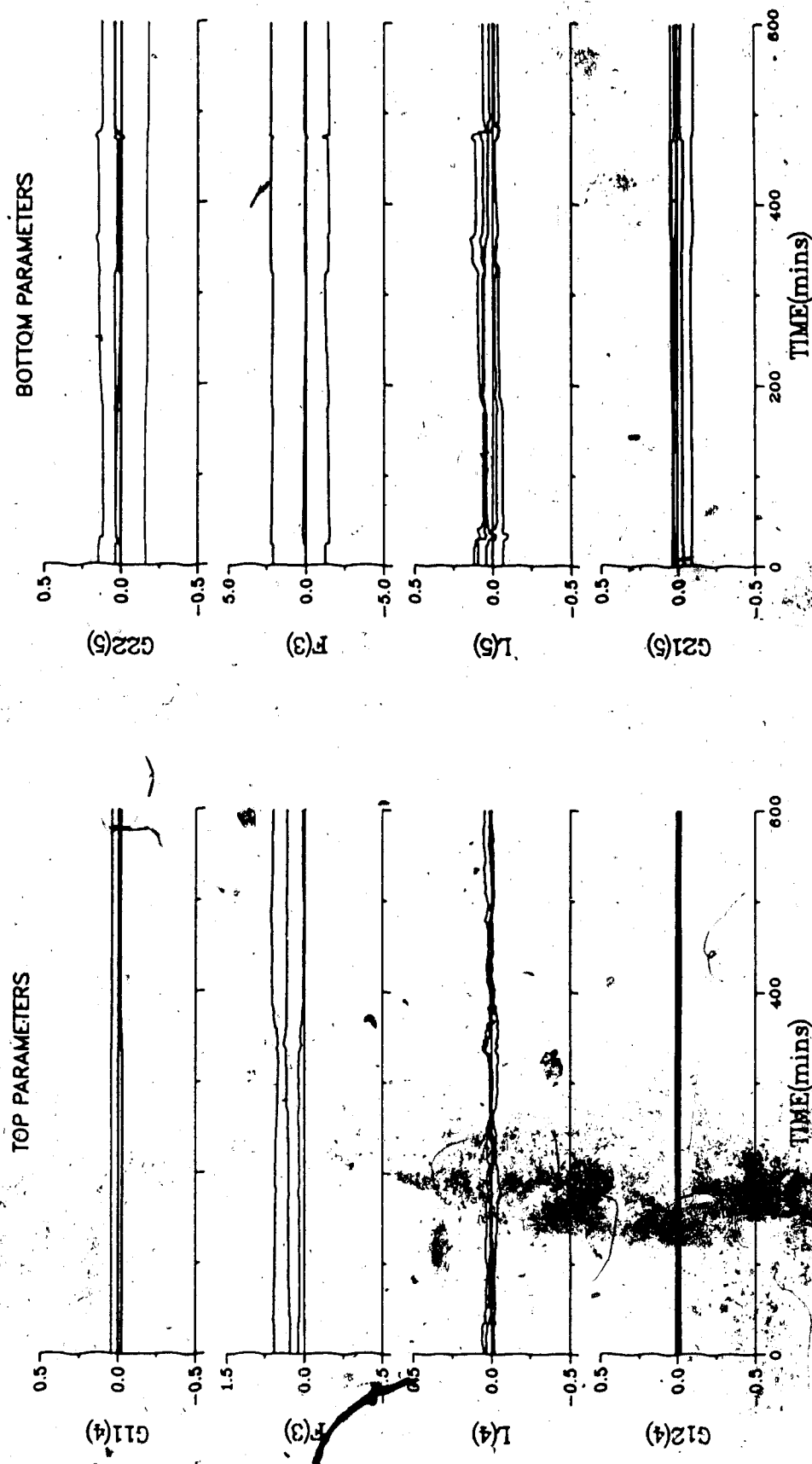


Figure 8.72 - Parameters for GMV Control with  $g_d = 0.0$  and the Time Delay Underestimated (MR, EFF)

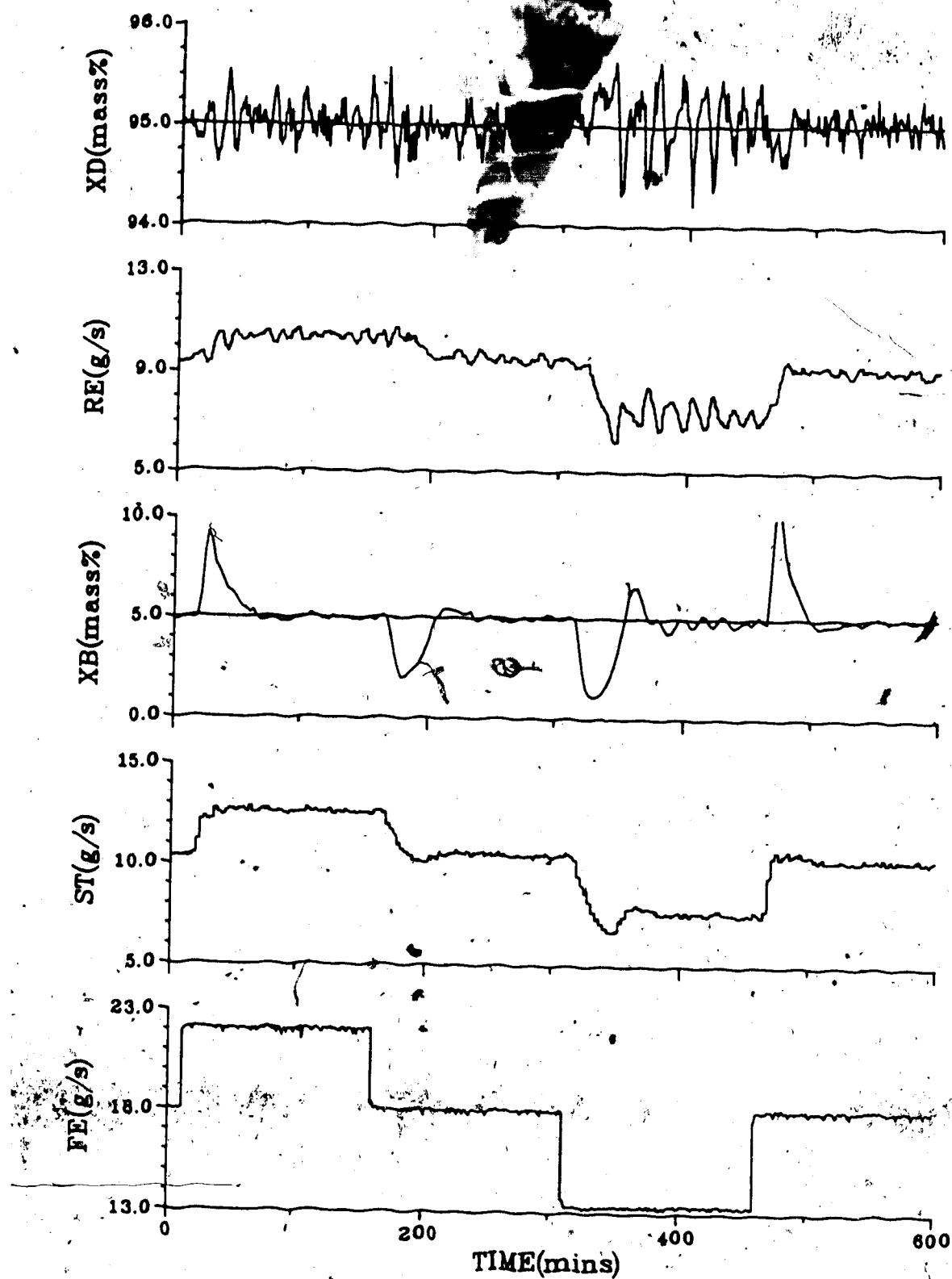


Figure 8.73 - Generalized Minimum Variance Control  
with  $g_0=0.0$  and the Time Delay  
Underestimated (MR,MFF)

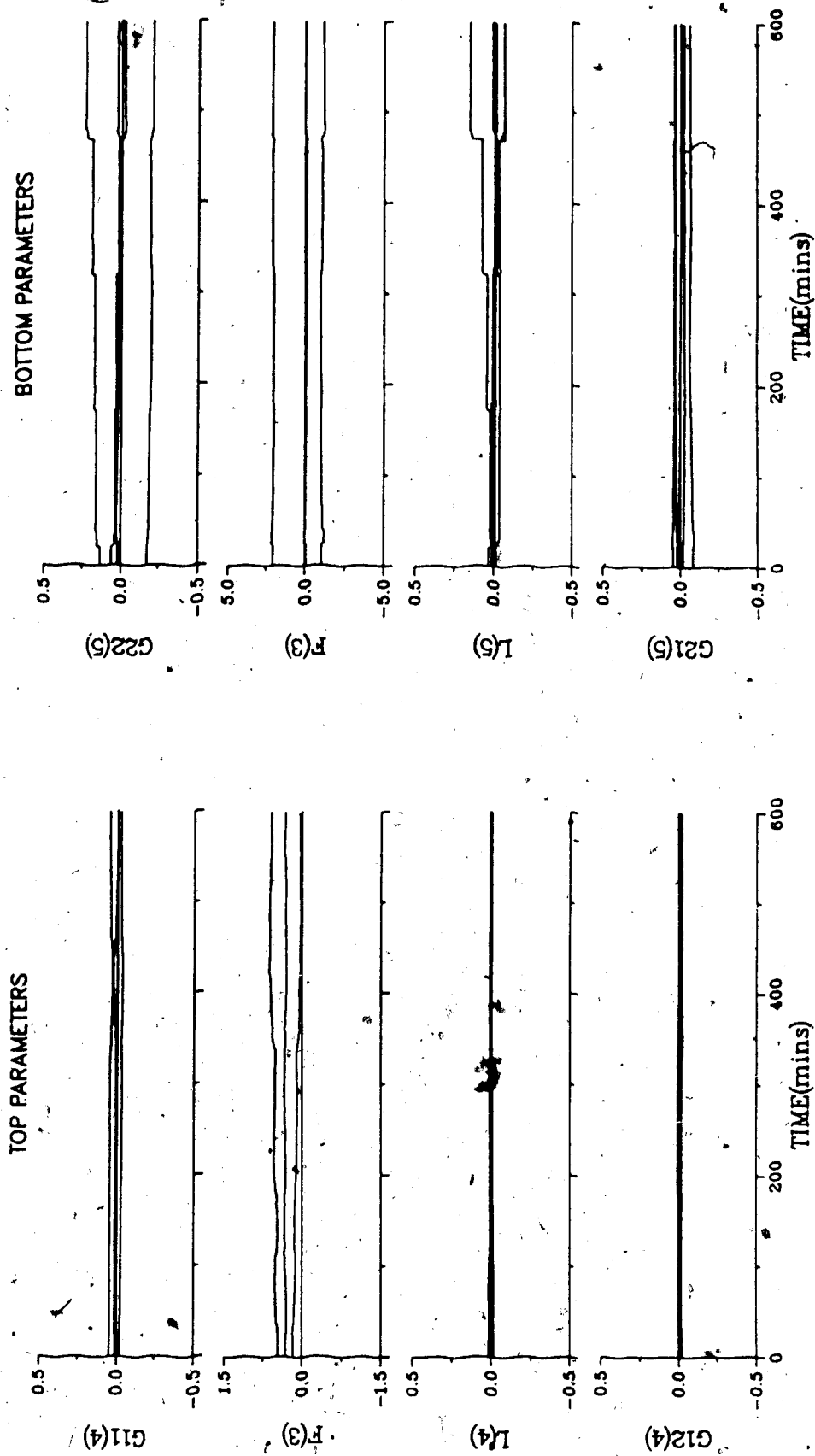


Figure 8.74 - Parameters for GMV Control with  $g_0 = 0.0$  and the Time Delay Underestimated (MR, MFF)

Table 8.7  
SAE Values for GMV Control using  $g_0=0$   
with the Time Delay Underestimated

Loop	NFF	SAE Values: EFF	MFF
Single Rate Control			
Figure	8.63	8.65	8.67
Top	123.0	115.1	120.2
Bottom	365.1	361.7	380.4
Both	488.1	476.8	500.6
Multirate Control			
Figure	8.69	8.71	8.73
Top	92.9	96.6	90.8
Bottom	414.1	403.2	410.5
Both	507.0	499.8	501.3

he observed that the improvement in top composition control performance under multirate sampling is outweighed by the decrease in performance for bottom composition control.

#### 8.5.7 Q Weighting Adapting with $g_0$

The final method considered in determining Q weighting coefficients was to allow the coefficients to adapt along with  $g_0$  as in equation 6.29. This was attempted on the column, but problems starting up the controller prevented any tests from actually being performed. Difficulties arose since any problems with parameter tuning are compounded by



using  $g_0$  to determine the  $Q$  coefficients. As a result, the  $Q$  weighting coefficients varied considerably as  $g_0$  was identified, and the control action that resulted was very erratic during the tuning-in phase of the controller.

### 8.6 Summary of Experimental Work

To facilitate a comparison of the control performance obtained using the different control algorithms for control of the column, the SAE values have been tabulated in Table 8.7. On the basis of the information in this table it is difficult to state specific conclusions, especially considering that the experimental work is only reproducible to within  $\pm 8\%$ . In general, however, multirate control improved control of the top composition, although frequently the bottom composition control suffered as the result.

Any of the methods employed to allow the  $Q$  weighting polynomial to take on the inverse structure of the PID compensator, in conjunction with no feedforward action, resulted in a controller performance as good or better than the performance obtained using the tuned multiloop PI/PID controllers. Tuning of the constants used to calculate the  $Q$  weighting coefficients can improve the performance of the self-tuning controller. However, this tuning was not performed in this study except to show that the tuning may follow a procedure similar to that used in tuning a PID controller. Without tuning the constants used to calculate the  $Q$  weighting coefficient in the situations where an

Table 8.8  
Summary of Experimental Results

Control / Strategy	NFF	SAE Values:	
		EFF	MFF
Single Rate Control			
PID / Constants from Cohen-Coon	770.8		
PID / Well Tuned Constants	539.4		
GMV / Q's from PI/PID	545.0	541.0	502.0
GMV / Q's from PI	555.5	522.4	534.0
GMV / Q's from Modified PI	553.5	642.3	521.8
GMV / Q's from PI/PID with $g_0=0$	536.3	562.0	538.9
GMV / Q's from PI with $g_0=0$ and the delay underestimated	488.1	476.8	500.6
Multirate Control			
PID / Constants from Cohen-Coon	753.8		
PID / Well Tuned Constants	492.4		
GMV / Q's from PI/PID	521.5	590.6	551.6
GMV / Q's from PI	513.1	499.8	545.8
GMV / Q's from Modified PI	417.7	546.9	483.0
GMV / "Tuned" Q's	682.0	489.0	472.7
GMV / Q's from PI/PID with $g_0=0$	512.4	490.2	490.6
GMV / Q's from PI with $g_0=0$ and the delay underestimated	507.0	499.8	501.3

estimated or measured value of the disturbance is used to provide the feedforward action. It is unfair to compare the performance of the self-tuning controller to the performance of a self-tuning controller that utilized no feedforward signal. In Figures 8.23 and 8.35 erratic behavior was noticed in the steam flow. This may have resulted from parameters that had not properly identified. It could possibly have been avoided by the introduction of a small

disturbance after switching from utilizing no feedforward action to using an estimate of the disturbance to provide feedforward action, then letting the controller reach steady state before the feed flow steps. This would give the parameters a chance to identify since the switch to feedforward control may not have caused enough of a deviation in the outputs to allow for proper identification.

## 9. Conclusions

This work has concentrated on the use of PID controller constants to determine coefficients to be used in the  $Q$  weighting polynomial of a self-tuning controller. The underlying incentive has been the desire to implement a self-tuning controller on an existing plant operating under PID control with a minimum amount of effort, making use of the PID controller constants.

In order to evaluate the optimum methods used in calculating the  $Q$  weighting, the column was first run under PID control and the controller constants tuned on the basis of the total SAE value. Under similar conditions of not using any feedforward action, a variety of techniques for calculating the  $Q$  weighting coefficients from the PID constants were employed. Through experiments performed on the pilot plant distillation column, the control performance was evaluated compared with that using conventional multiloop PID control.

With no feedforward action, all tests demonstrated that the self-tuning controller could perform at least as well as the PID controller, within experimental accuracy. Whether or not the derivative term of the PID controller was included in the  $Q$  weighting coefficient calculations had little effect on the control behavior. Under single rate sampling the only test to provide significantly better control performance than any other was that which used  $Q$  coefficients calculated from the PID constants but ignoring

the derivative term, setting  $g_0 = 0.0$  and underestimating the time delay. This technique should provide the best control performance since it allows the  $Q$  weighting polynomial to take the form of the inverse PID compensator as well as allowing the prediction term in the control law to be unaffected by factoring out  $g_0 u(t)$ .

The above-mentioned technique was outperformed under multirate sampling for one test, that being when  $Q$  weighting parameters were determined from the modified PI controller constants. This result implies that tuning of the  $Q$  weighting parameters calculated from tuned PID controller constants would improve the control performance. Although it appears that this tuning procedure could significantly improve the performance, the difficulties associated with manual tuning would then be introduced to the self-tuning controller.

In general, use of the multirate form of the control algorithms provided slightly better overall control of the column. The control of the top composition improved considerably by using multirate sampling, but there was a deterioration in the bottom composition control performance. It was not possible under either single or multirate control to get the self-tuning controller operating at steady state while allowing the  $Q$  weighting coefficients to be calculated from a function of  $g_0$ . The variation of  $g_0$  during the parameter tuning-in phase was echoed in the values of the  $Q$  coefficients to produce unstable control. Minimum variance

control was also found to be unsuccessful in controlling the column.

As a result of the tests using an estimated and measured values of the disturbance to provide the feedforward action, it was seen that the use of feedforward action may be desired when using the single rate sampling form of the controller, and not desired when using the multirate sampling form. However, any comparison with the PID tests that were performed when no feedforward action was used would be unfair. If feedforward action is combined with an existing feedback control loop containing PID control action, then the PID controller constants would need to be retuned, which was not done in this study. Hence there is no reason to expect that the PID controller constants used in calculating the  $Q$  coefficients were the best constants to use when feedforward action was employed. It should be noted how easy it was to incorporate the use of feedforward action in the self-tuning controller.

The results of this study have shown that it is difficult to improve on tuned, conventional PID controllers. The driving force behind the development of the self-tuning controller is the desire to improve the control of time-varying processes, non-linear processes, or processes that are both non-linear and time-varying. The distillation column does exhibit non-linear dynamics and therefore represents a challenge when tuning a PID controller. However, over the course of this study it can be assumed

that the distillation column was a time-invariant process and hence the benefits of a self-tuning controller have not been fully demonstrated.

## 10. Recommendations

Several areas of future studies on the column using the self-tuning controller may be considered.

Initialize the data vectors with typical values for the flows, setpoints and compositions. In starting up the self-tuning controller, the data vectors are initialized to zeros, making it necessary to collect data for some time before using the identification routine.

Initialize all the coefficients to nonzero values of the same order of magnitude as the expected value of the coefficients. It was demonstrated that in the simulation results presented in Figure 7.10, the use of a nonzero initial value for  $g_0$  resulted in a slightly smoother tuning-in phase for the controller.

Refine the technique of allowing the  $Q$  weighting coefficients to be functions of  $g_0$ . This looked very promising in the simulations but it was not possible to conduct an experimental test due to the difficulties in starting the controller. It may be possible to use this technique if the  $Q$  coefficients were taken as constant values for the initial tuning-in period. Then, once the self-tuning controller was operating at steady state, the  $Q$  coefficients could be changed on-line to be functions of  $g_0$ . This is not possible with the current software.

Incorporate one of the many on-line self-tuning PID structured controllers, cf Chapter 2, to tune the  $Q$  weighting coefficients after the self-tuning controller is



operating at steady state. This would combine two self-tuning controllers into one, and would avoid the necessity of manually tuning the  $Q$  weighting coefficients. It was obvious from this study that  $Q$  weighting coefficients calculated from tuned PID constants can be tuned further to obtain a better response to disturbances.

All of the tests performed during this work have used a constant forgetting factor. In view of the fact that frequently very little parameter adaptation took place during the course of a test, the possibility of turning the identification routine off or using a variable forgetting factor to cut down on the computer usage should be investigated.

Study the effect on control performance on reducing (or increasing) the number of coefficients of each polynomial used in the control law. This would help to indicate how adequate the linear representation of the column is as far as determining the required number of parameters, and could affect the computational requirements of the algorithm considerably.

It would be very useful to study the performance of the self-tuning controller under conditions where the process characteristics are time varying. This would be difficult to accomplish with the pilot scale column so another pilot plant unit should be considered for further studies involving the self-tuning controller.

On the distillation column, the use of inferential control, to infer a value for the bottom composition from tray temperature measurements between available G.C. analyses, should be examined. By reducing the effective sampling time in the bottom composition control loop, the overall control may be improved.

An investigation into the possibility of an automatic start-up procedure should be conducted. Some industrial applications require frequent shut-downs and start-ups and a complicated start-up procedure would be detrimental to acceptance of the algorithm.

A comparison of some of the various available self-tuning controllers would be of value. As more and more algorithms become available it becomes increasingly difficult to determine which of the algorithms are best suited for individual applications, or even how to compare the various methods.

From the experience of operating the column during the course of this study, several areas of possible improvements have been noticed.

Adding a check in the main program of the column software to set the system state to "WAIT" if, for instance, the feed flow drops below 10g/s. The current emergency shutdown program in the HP1000 turns off the reflux, feed and bottoms pumps and shuts off the steam flow to the column. However, in the event of an emergency shutdown, the LSI 11/03 continues to operate the GC. Once the column has

drained no liquid sample can be sent to the GC and, if the GC continues to operate without any samples, recalibrating the GC will be inevitable. Similarly, shutting off the GC sample pump should be included in the emergency shutdown procedure.

It may be possible to improve the analysis of both the top and bottom compositions. Comparing any of the plots showing the top composition with those obtained in a previous study, (Vagi, 1987), the current top composition signal appears to exhibit a much noisier response. If it is not possible to decrease the sensitivity of the analyzer, filtering of the top composition should be considered. Since it is possible to sample the top composition very frequently, sampling every six seconds and averaging the last three values to obtain a current value for the identification and control would eliminate much of the undesirable variance.

In the bottom loop a significant difference between this and the previous study is that a portion of the tube leading to the GC sampling valve had plugged and has been replaced with a tube of a smaller inside diameter. As the result, plugging in the line occurs more frequently resulting in more down-time. Replacing the valve would be necessary to overcome the problem although scheduling weekly maintenance for the valve would help to prevent both plugging and interrupted tests.

During the current study the domestic cooling water system was used as the water supplied to the condenser. An attempt should be made to again use the constant head water supply to reduce utility costs.

To improve the portability of the University of Alberta self-tuning package to make it more accessible for possible industrial implementations, a HP3390A Reporting Integrator should be used to replace the HP1000 in providing the LSI with a suitable GC report.

## Bibliography

- Allidina, A.Y. and F.M. Hughes, "Self-tuning Controller with Integral-Action", *Optimal Control Appl. & Methods*, 3, pp 355-362 (1982).
- Allidina, A.Y. and H. Yin, "Explicit Pole-Assignment Self-tuning Algorithms", *Int. J. Control* 42, No 5, pp 1113-1130 (1985).
- Aloisi, P., D. Bertin, S. Bittanti and R. Scattolini, "Self-tuning Control of a Binary Distillation Column - A Simulation Test Case", Presented at Adaptive Control of Chemical Processes, 1st IFAC Workshop, Frankfurt, Oct 21-22 (1985).
- Aström, K.J., Introduction to Stochastic Control Theory, Academic Press, New York (1970).
- Aström, K.J., "Theory and Applications of Adaptive Control - A Survey", *Automatica*, 19, No 5, pp 471-486 (1983a).
- Aström, K.J., "LQG Self-Tuner", *IFAC Adaptive Systems in Control and Signal Processing*, San Francisco, pp 137-146 (1983b).
- Aström, K.J., U. Borrisson, L. Ljung and B. Wittenmark, "Theory and Applications of Adaptive Regulators Based on Recursive Parameter Estimation", Dept. of Automatic Control, Inst. of Technology, Lund, Sweden (1975).
- Aström, K.J., U. Borrisson, L. Ljung and B. Wittenmark, "Theory and Applications of Self-Tuning Regulators", *Automatica*, 13, pp 457-476 (1977).
- Aström, K.J. and B. Wittenmark, "Problems of Identification and Control", *J. of Math. Anal. and Appl.*, 34, pp 90-113 (1971).
- Aström, K.J. and B. Wittenmark, "On Self-Tuning Regulators", *Automatica*, 9, pp 185-199 (1973).
- Barcenas-Urbe, L. and J. Alvarez-Gallegos, "Adaptive Multi-variable Control Applied to a Binary Distillation Column", *IFAC Adaptive Systems in Control and Signal Processing*, San Francisco, pp 109-114 (1983).

- Bar-Kana, I. and H. Kaufman, "Discrete Direct Multivariable Adaptive Control", IFAC Adaptive Systems in Control and Signal Processing, San Francisco, pp 357-362 (1983).
- Bartolini, G., G. Casaliño, F. Davoli, R. Minciardi and R. Zoppoli, "Adaptive Control Systems: A Survey of Algorithms and of Implementation Problems", Control of Industrial Processes, 2, Instrumentation, Oct 6-7, 1981, Milan, Italy, pp 357-385.
- Bayoumi, M.M., K.Y. Wong and M.A. El-Bagoury, "A Self-Tuning Regulator for Multivariable Systems", Automatica, 17, No 6, pp 575-592 (1981).
- Belanger, P.R., "On Type 1 Systems and the Clarke-Gawthrop Regulator", Automatica, 19, No 1, pp 91-94 (1983).
- Bezanson, L.W. and S.L. Harris, "State-space Design of Multivariable Self-tuning Regulators", Int. J. Control, 39, No 2, pp 395-411 (1984).
- Bierman, G.J., "Measurement Updating Using the U-D Factorization", Automatica, 12, pp 375-382 (1976).
- Bilec, R.J., "Modelling and Dual Control of a Binary Distillation Column", MSc Thesis, University of Alberta, Edmonton (1980).
- Bittanti, S. and R. Scattolini, "Multivariable Self-tuning Control: A Model-following Approach", Int. J. Control, 42, No 5, pp 1037-1045 (1985).
- Bristol, E.H., "The Design of Industrially Useful Adaptive Controllers", ISA Transactions, 22, No 3, pp 17-25 (1983).
- Cameron, F. and D.E. Seborg, "A Self-tuning Controller with a PID Structure", IFAC Adaptive Systems in Control and Signal Processing, San Francisco, pp 613-622 (1983).
- Clarke, D.W., "Some Implementation Considerations of Self-Tuning Controllers", Numerical Techniques for Stochastic Systems, Archetti and Cugiani (Eds), North Holland Publishing Company, pp 81-101 (1980).
- Clarke, D.W. and P.J. Gawthrop, "Self-Tuning Controller", Proceedings IEE, 122, No 9, pp 929-934 (1975).
- Clarke, D.W. and P.J. Gawthrop, "Self-Tuning Control", Proceedings IEE, 126, No 6, pp 663-640 (1979).

Clarke, D.W. and P.J. Gawthrop, "Self-Tuning Control and Its Application", Interkama, pp 542-560 (1980).

Clarke, D.W., A.J.F. Hodgson and P.S. Tuffs, "Offset Problems and K-incremental Predictors in Self-tuning Control", IEE Proc., Pt D, 130, No 5, pp217-225 (1983).

Clarke, D.W., P.P. Kanjilal and C. Mohtadi, "A Generalized LQG Approach to Self-tuning Control. Part I Aspects of Design", Int. J. Control, 41, No 6, pp 1509-1523 (1985a).

Clarke, D.W., P.P. Kanjilal and C. Mohtadi, "A Generalized LQG Approach to Self-tuning Control. Part II Implementation and Simulation", Int. J. Control, 41, No 6, pp 1525-1544 (1985b).

Cordero, A.O. and D.Q. Mayne, "Deterministic Convergence of a Self-tuning Regulator with Variable Forgetting Factor", IEE Proc., Part D 128, No 1, pp19-23 (1981).

Costin, M.H. and B.M.R. Buchner, "Minimum Variance Control for Multivariable Systems with Different Deadtimes in Individual Loops", IFAC Adaptive Systems in Control and Signal Processing, San Francisco, pp 115-117 (1983).

Costin, M.H. and B.M.R. Buchner, "Distributed Control Using Self-Tuning Regulators", IFAC Adaptive Systems in Control and Signal Processing, San Francisco, pp 301-307 (1983).

Dahlqvist, S.A., "Control of the Top and Bottom Compositions in a Pilot Distillation Column", I. Chem. E. Symposium Series No 56, pp 2.6/45-50 (1979).

Deshpande, P.B. and R.H. Ash, Elements of Computer Process Control with Advanced Control Applications, Instrument Society of America, North Carolina (1981).

Dickmann, K. and H. Unbehauen, "Recursive Identification of Multi-input, Multi-output Systems", Proc. of the 5th IFAC Symp., Darmstadt, Germany, Sept 1979, 7, pp 423-428.

Dion, J.M. and R. Lozano, "An Indirect Adaptive Control Scheme for MIMO Systems", IFAC Adaptive Systems in Control and Signal Processing, San Francisco, pp 347-350 (1983).

Elliott, H. and W.A. Wolovich, "Parameterization Issues in Multivariable Adaptive Control", Automatica, 20, No 5, pp 533-545 (1984).

Falb, P.L. and W.A. Wolovich, "Decoupling and Synthesis of Multivariable Control Systems", IEEE Transactions on Automatic Control, 12, No 6, pp 651-659 (1969).

Ferreira, A.M.P., T.J. Barker and I.M. MacLeod, "An Application of Self-tuning Control", Presented at the 7th Conf. on Digital Computer Applications to Process Control, Vienna, Sept 17-20 (1985).

Fortescue, T.R., L.S. Kershenbaum and B.E. Ydstie, "Implementation of Self-Tuning Regulators with Variable Forgetting Factors", Automatica, 17, No 6, pp 831-835 (1981).

Foss, B.A., "Composition Control of Binary Distillation Columns using Multivariable Optimal Control", Modeling, Identification and Control, 4, No 4, pp 195-216 (1983).

Goldschmidt, L., S.B. Jorgensen and L. Hallager, "Sparse Process Modelling for Robust Adaptive Surveillance and Control of a Binary Distillation Column", Presented at Adaptive Control of Chemical Processes, 1st IFAC Workshop, Frankfurt, Oct 21-22 (1985).

Goodwin, G.C. and L. Dugard, "Stochastic Adaptive Control with Known and Unknown Interactor Matrices", IFAC Adaptive Systems in Control and Signal Processing, San Francisco, pp 351-355 (1983).

Goodwin, G.C. and E.K. Teoh, "Adaptive Control of a Class of Linear Time Varying Systems", IFAC Adaptive Systems in Control and Signal Processing, San Francisco, pp 1-6 (1983).


Grimble, M.J., "LOG Multivariable Controllers: Minimum Variance Interpretation for Use in Self-tuning Systems", Int. J. Control, 40, No 4, pp 831-842 (1984).

Grimble, M.J. and T.J. Moir, "Multivariable Weighted Minimum Variance Self-Tuning Controllers", IFAC Adaptive Systems in Control and Signal Processing, San Francisco, pp 341-346 (1983).

Habermayer, M. and L. Keviczky, "Investigation of an Adaptive Smith Controller by Simulation", Presented at the 7th Conf. on Digital Computer Applications to Process Control, Vienna, Sept 17-20 (1985).

Hägglund, T., "The Problem of Forgetting Old Data in Recursive Estimation", IFAC Adaptive Systems in Control and Signal Processing, San Francisco, pp 231-214 (1983).



- Hallager, L. and S.B. Jorgensen, "Adaptive Control of Chemical Engineering Processes", IFAC Adaptive Systems in Control and Signal Processing, San Francisco, pp 323-330 (1983).
- Hahn, V., "A Direct Adaptive Controller for Non-minimum Phase Multivariable Systems with Arbitrary Time Delays", Presented at the 7th Conf. on Digital Computer Applications to Process Control, Vienna, Sept 17-20 (1985).
- Hetthessy, J., L. Keviczky and Cs. Banyasz, "On a Class of Adaptive PID Regulators", IFAC Adaptive Systems in Control and Signal Processing, San Francisco, pp 81-82 (1983).
- Huang, H.P., Y.C. Chao and P.H. Lio, "Predictive Adaptive Control System for Unmeasured Disturbances", Ind. Eng. Chem. Proc. Des. Dev., 24, pp 666-673 (1985).
- Kam, W.Y., A.J. Morris, M.T. Tham and R.W. Jones, "A Comparison of Several Single Variable Parameter Adaptive Controllers", Presented at the 7th Conf. on Digital Computer Applications to Process Control, Vienna, Sept 17-20 (1985a).
- Kam, W.Y., A.J. Morris, M.T. Tham and R.W. Jones, "A Comparison of Several Multivariable Parameter Adaptive Controllers", Presented at the 7th Conf. on Digital Computer Applications to Process Control, Vienna, Sept 17-20 (1985b).
- Kan, H.W., "Binary Distillation Column Control: Evaluation of Digital Control Algorithms", MSc Thesis, University of Alberta, Edmonton (1982).
- Kanniah, J. and O.P. Malik, "Self-tuning Regulators with Periodically Constant Control", Int. J. Control, 40, No 3, pp 585-602 (1984).
- Kaya, A. and T.J. Scheib, "A Self-tuning Method for Smith Predictor and PID Controls", ISA Trans., pp 843-855 (1984).
- Kershenbaum, L.S. and T.R. Fortescue, "Implementation of On-line Control in Chemical Process Plants", Automatica, 17, No 6, pp 777-788 (1981).
- Koivo, H.N., "A Multivariable Self-tuning Controller", Automatica, 16, pp 351-366 (1980).
- 

Kraus, T., "Self-tuning Control: An Expert System Approach", ISA Trans., pp 695-704 (1984).

Kurz, H., R. Isermann and R. Schumann, "Experimental Comparison and Application of Various Parameter-Adaptive Control Algorithms", Automatica, 16, pp 117-133 (1980).

Lang, S.J., X.Y. Gu and T.Y. Chai, "A Multivariable Generalized Self-tuning Controller with Decoupling Design", Proc. of the American Control Conf., Boston, June 19-21, (1985).

Latawiec, K. and M. Chyra, "On Low Frequency and Long-Run Effects in Self-Tuning Control", Automatica, 19, No 4, pp 419-424 (1983).

Lieuson, H.Y., "Experimental Evaluation of Self-Tuning Control of a Binary Distillation Column", MSc Thesis, University of Alberta, Edmonton (1980).

Lopez, A.M., J.A. Miller, C.L. Smith and P.W. Murrill, "Tuning Controllers with Error-Integral Criteria", Instrumentation Technology, No 11, pp 57-62 (1967).

MacFarlane, A.G., "The Development of Frequency-Response Methods in Automatic Control", IEEE Transactions on Automatic Control, AC-24, No 2, pp 250-263 (1979).

Marino-Galarraga, M., T.E. Marlin and T.J. McAvoy, "Using the Relative Disturbance Gain to Analyze Process Operability", Proc. of the American Control Conf., Boston, June 19-21 1985, pp 1078-1083.

Martin-Sanchez, J.M. and S.L. Shah, "Multivariable Adaptive Predictive Control of a Binary Distillation Column", Automatica, 20, No 5, pp 607-620 (1984).

Martin-Sanchez, J.M., S.L. Shah and D.G. Fisher, "A Stable Adaptive Predictive Control System", Int. J. Control, 39, No 1, pp 215-224 (1984).

McDermott, P.E. and D.A. Mellichamp, "An Auto-pole-placement Self-tuning Controller", Int. J. Control, 40, No 6, pp 1131-1147 (1984).

Miller, J.A., A.M. Lopez, C.L. Smith and P.W. Murrill, "A Comparison of Controller Tuning Techniques", Control Engineering, 14, No 12, pp 72-75 (1967).

- Mizuno, N. and S. Fuji, "Discrete Time Multivariable Adaptive Control for Non-minimum Phase Plants with Unknown Dead Time", IFAC Adaptive Systems in Control and Signal Processing, San Francisco, pp 363-368 (1983).
- Moir, T.J. and M.J. Grimble, "Optimal Self-tuning Filtering, Prediction and Smoothing for Discrete Multivariable Processes", IEEE Trans on Automatic Control, AC-29, No 2, pp 128-137 (1984).
- Moore, C.F., C.L. Smith and P.W. Murrill, "Simplifying Digital Control Dynamics for Controller Tuning and Hardware Lag Effects", Instrument Practice, January, pp 45-49 (1969).
- Morris, A.J. and Y. Nazer, "Self-Tuning Process Controllers for Single and Multivariable Systems, Part 1, Theoretical Evaluation of the Control Strategy", Presented at the 5th IFAC/IFIP Conference of Digital Computer Applications to Process Control, The Hague, Netherlands (1977).
- Morris, A.J., Y. Nazer, R.K. Wood and H. Lieuson, "Evaluation of Self-Tuning Controllers for Distillation Column Control", IFAC Digital Computer Applications to Process Control, Isermann and Kaltenecker (Eds), pp 345-354 (1981).
- Morris, A.J., Y. Nazer and R.K. Wood, "Multivariate Self-tuning Process Control", Optimal Control Appl. & Methods, 3, pp 363-387 (1982).
- Onderwater, D., J.F. MacGregor and J.D. Wright, "Temperature Control of a Catalytic Tubular Reactor using Self-tuning Regulators", 36th Annual CSChE Conf., Calgary, Oct 6-9, 1985, pp 173-178.
- Ortega, R. and R. Kelly, "PID Self-tuners. Some Theoretical and Practical Aspects", IEEE Trans. on Indust. Elect., IE-31, No 4, pp 332-338 (1984).
- Pacey, W.C., "Control of a Binary Distillation Column: An Experimental Evaluation of Feedforward and Combined Feedforward-Feedback Control Schemes", MSc Thesis, University of Alberta, Edmonton (1973).
- Peterka, V., "On Steady State Minimum Variance Control Strategy", Kybernetika, 8, No 3 (1972).
- Peterka, V., "Predictor-based Self-tuning Control", Automatica, 20, No 1, pp 39-50 (1984).

- Ray, W.H., "Multivariable Process Control - A Survey", Computers & Chemical Engineering, 7, No 4, pp 367-394 (1983).
- Reinholt, H., "Evaluation of Parameter Estimation Methods for the Self-Tuning Controller", MSc Thesis, University of Alberta, Edmonton (1985).
- Sage, A.P., "Optimum Systems Control", Prentice Hall, Appendix A, (1969).
- Sanchez, G., J.M. Dion and L. Dugard, "Multivariable Adaptive Control of a Binary Distillation Column", Presented at Adaptive Control of Chemical Processes, 1st IFAC Workshop, Frankfurt, Oct 21-22 (1985).
- Sastry, V.A., D.E. Seborg and R.K. Wood, "Self-Tuning Regulator Applied to a Binary Distillation Column", Automatica, 13, pp 417-424 (1977).
- Seborg, D.E., S.L. Shah and T.F. Edgar, "Adaptive Control Strategies for Process Control: A Survey", Presented at the AIChE Diamond Jubilee Meeting, Washington, D.C., Oct 30-Nov 4 (1983).
- Shah, M.K. and W.L. Luyben, "Control of a Binary Distillation Column Using Nonlinear Composition Estimators", I. Chem. E. Symposium Series No 56, pp 2.6/1-24 (1979).
- Shinners, S.M., Modern Control System Theory and Applications, 2nd Ed., Addison Wesley (1978).
- Silveria, H.M. and R. Duraiswami, "New Structure for an Adaptive Servomechanism Controller", IEE Proc., Pt D, 131, No 2, pp 64-68 (1984).
- Simonsmeier, U.F., "Nonlinear Binary Distillation Column Models", MSc Thesis, University of Alberta, Edmonton (1978).
- Sinha, N.K. and A. Sen, "Critical Evaluation of Online Identification Methods", Proc. of the IEE, 122, No 10, pp 1153-1158 (1975).
- Smith, C.A. and A.B. Corripio, Principles and Practice of Automatic Process Control, John Wiley & Sons (1985).
- Song, H.K., D.G. Fisher and S.L. Shah, "Experimental Evaluation of a Robust, Self-Tuning PID Controller", Can. J. of Chem. Eng., 62, No 6, pp 755-763 (1984).

- Stephanopoulos, G., Chemical Process Control, An Introduction to Theory and Practice, Prentice-Hall Inc., New Jersey. (1984).
- Tham, M., "Some Aspects of Multivariable Self-tuning Control", PhD Thesis, University of Newcastle Upon Tyne, England, (1985).
- Tham, M.T., A.J. Morris, F. Vagi and R.K. Wood, "An Online Comparison of Two Multivariable Self-tuning Controllers", Presented at the 7th Conf. on Digital Computer Applications to Process Control, Vienna, Sept 17-20 (1985).
- Toivonen, H.T., "Variable Constrained Self-Tuning Control", *Automatica*, 19, No 4, pp 415-418 (1983).
- Tsitsiklis, J.N. and M. Athans, "Guaranteed Robustness Properties of Multivariable Nonlinear Stochastic Optimal Regulators", *IEEE Trans. on Automatic Control*, AC-29, No 8, pp 690-696 (1984).
- Unbehauen, H., "Theory and Application of Adaptive Control", Presented at the 7th Conf. on Digital Computer Applications to Process Control, Vienna, Sept 17-20 (1985).
- Vagi, F.J., "Multivariable Multirate Self-Tuning Control of a Binary Distillation Column", MSc Thesis, University of Alberta, Edmonton (1987).
- Weimer, P., V. Hahn, C. Schmid and H. Unbehauen, "Application of Multivariable Model Reference Adaptive Control to a Binary Distillation Column", *IFAC Adaptive Systems in Control and Signal Processing*, San Francisco, pp 309-314 (1983).
- Wittenmark, B., "Stochastic Adaptive Control Methods: A Survey", *Int. J. Control*, 21, No 5, pp 705-730 (1975).
- Wittenmark, B. and K.J. Åström, "Practical Issues in the Implementation of Self-tuning Control", *Automatica*, 20, No 5, pp595-605 (1984).
- Wong, K.Y., M.M. Bayoumi and S. Nuyan, "Comparative Study of Some Estimation Algorithms for the Self-Tuning Control of Time Varying Systems", *Proceedings Applied Control and Identification*, Copenhagen, Denmark, pp 18/12-18 (1983).

Wood, R.K., "Improved Control By Application of Advanced Control Techniques", ISA Trans., 16, No 4, pp 31-39 (1977).

Yang, D.R. and W.-K. Lee, "Effects of Model Structure, Nonzero D.C. Value and Measurable Disturbance on Adaptive Control", IFAC Adaptive Systems in Control and Signal Processing, San Francisco, pp 253-259 (1983).

Yuwana, M. and D.E. Seborg, "A New Method for On-Line Controller Tuning", AIChE Journal, 28, No 3, pp 434-440 (1982).

# Appendices

## Appendix A

### Example of Matrix Notation

An example is used to illustrate the multivariable system representation in equation 3.32. A simple 2\*2 system may be represented by the following equations:

$$\begin{aligned}
 & a_{110}y_1(t) + a_{111}y_1(t-1) + \dots \\
 & + a_{120}y_2(t) + a_{121}y_2(t-1) + \dots = \\
 & z^{-k_{11}}b_{110}u_1(t) + z^{-k_{11}}b_{111}u_1(t-1) + \dots \\
 & + z^{-k_{12}}b_{120}u_2(t) + z^{-k_{12}}b_{121}u_2(t-1) + \dots \\
 & + z^{-d_{11}}d_{110}u_1(t) + z^{-d_{11}}d_{111}u_1(t-1) + \dots \\
 & + z^{-d_{12}}d_{120}u_2(t) + z^{-d_{12}}d_{121}u_2(t-1) + \dots \\
 & + c_{110}\xi_1(t) + c_{111}\xi_1(t-1) + \dots \\
 & + c_{120}\xi_2(t) + c_{121}\xi_2(t-1) + \dots \quad (A.1a)
 \end{aligned}$$

and

$$\begin{aligned}
 & a_{210}y_1(t) + a_{211}y_1(t-1) + \dots \\
 & + a_{220}y_2(t) + a_{221}y_2(t-1) + \dots = \\
 & z^{-k_{21}}b_{210}u_1(t) + z^{-k_{21}}b_{211}u_1(t-1) + \dots \\
 & + z^{-k_{22}}b_{220}u_2(t) + z^{-k_{22}}b_{221}u_2(t-1) + \dots \\
 & + z^{-d_{21}}d_{210}u_1(t) + z^{-d_{21}}d_{211}u_1(t-1) + \dots \\
 & + z^{-d_{22}}d_{220}u_2(t) + z^{-d_{22}}d_{221}u_2(t-1) + \dots \\
 & + c_{210}\xi_1(t) + c_{211}\xi_1(t-1) + \dots \\
 & + c_{220}\xi_2(t) + c_{221}\xi_2(t-1) + \dots \quad (A.1b)
 \end{aligned}$$



With the following substitutions to replace the polynomials in the backshift operator:

$$A_{11} = a_{110} + a_{111}z^{-1} + \dots$$

$$A_{12} = a_{120} + a_{121}z^{-1} + \dots$$

$$A_{21} = a_{210} + a_{211}z^{-1} + \dots$$

$$A_{22} = a_{220} + a_{221}z^{-1} + \dots$$

$$B_{11} = b_{110} + b_{111}z^{-1} + \dots$$

$$B_{12} = b_{120} + b_{121}z^{-1} + \dots$$

$$B_{21} = b_{210} + b_{211}z^{-1} + \dots$$

$$B_{22} = b_{220} + b_{221}z^{-1} + \dots$$

$$D_{11} = d_{110} + d_{111}z^{-1} + \dots$$

$$D_{12} = d_{120} + d_{121}z^{-1} + \dots$$

$$D_{21} = d_{210} + d_{211}z^{-1} + \dots$$

$$D_{22} = d_{220} + d_{221}z^{-1} + \dots$$

$$C_{11} = c_{110} + c_{111}z^{-1} + \dots$$

$$C_{12} = c_{120} + c_{121}z^{-1} + \dots$$

$$C_{21} = c_{210} + c_{211}z^{-1} + \dots$$

$$C_{22} = c_{220} + c_{221}z^{-1} + \dots$$

equations A.1a and A.1b may then be represented as:

$$\begin{aligned} A_{11}y_1(t) + A_{12}y_2(t) = & z^{-k_{11}}B_{11}u_1(t) + z^{-k_{12}}B_{12}u_2(t) + \\ & z^{-d_{11}}D_{11}v_1(t) + z^{-d_{12}}D_{12}v_2(t) + \\ & C_{11}\xi_1(t) + C_{12}\xi_2(t) \end{aligned} \quad (A.2a)$$

and

$$\begin{aligned}
 A_{21}y_1(t) + A_{22}y_2(t) = & z^{-k+1}B_{21}u_1(t) + z^{-k+1}B_{22}u_2(t) + \\
 & z^{-d+1}D_{21}v_1(t) + z^{-d+1}D_{22}v_2(t) + \\
 & C_{21}\xi_1(t) + C_{22}\xi_2(t) \quad (A.2b)
 \end{aligned}$$

In matrix notation equations A.2a and A.2b can be expressed as:

$$\begin{aligned}
 \begin{bmatrix} A_{11} & A_{12} \\ A_{21} & A_{22} \end{bmatrix} \begin{bmatrix} y_1 \\ y_2 \end{bmatrix} = & z^{-k+1} \begin{bmatrix} B_{11} & B_{12} \\ B_{21} & B_{22} \end{bmatrix} \begin{bmatrix} u_1 \\ u_2 \end{bmatrix} + \\
 & z^{-d+1} \begin{bmatrix} D_{11} & D_{12} \\ D_{21} & D_{22} \end{bmatrix} \begin{bmatrix} v_1 \\ v_2 \end{bmatrix} + \\
 & \begin{bmatrix} C_{11} & C_{12} \\ C_{21} & C_{22} \end{bmatrix} \begin{bmatrix} \xi_1 \\ \xi_2 \end{bmatrix} \quad (A.3)
 \end{aligned}$$

Using the following vector and matrix definitions:

$$Y = \begin{bmatrix} y_1 \\ y_2 \end{bmatrix}; \quad U = \begin{bmatrix} u_1 \\ u_2 \end{bmatrix}; \quad \Xi = \begin{bmatrix} \xi_1 \\ \xi_2 \end{bmatrix}; \quad V = \begin{bmatrix} v_1 \\ v_2 \end{bmatrix}$$

$$A = \begin{bmatrix} A_{11} & A_{12} \\ A_{21} & A_{22} \end{bmatrix}; \quad B = \begin{bmatrix} B_{11} & B_{12} \\ B_{21} & B_{22} \end{bmatrix}$$

$$C = \begin{bmatrix} C_{11} & C_{12} \\ C_{21} & C_{22} \end{bmatrix}; \quad D = \begin{bmatrix} D_{11} & D_{12} \\ D_{21} & D_{22} \end{bmatrix}$$

allows equation A.3 to be written as:

$$AY(t) = z^{-k} BU(t) + CZ(t) + z^{-d} DV(t) \quad (A.4)$$

which is equivalent to equation 3.32 except the  $z^{-1}$  arguments are not shown explicitly.

## Appendix B

### Differentiation of Cost Function

The details of the differentiation of the cost function in equation 3.46 are presented here. The cost function to be minimized in the derivation of the control law is:

$$J = [PY^*(t+k_{ii}|t) - RW(t)]'[PY^*(t+k_{ii}|t) - RW(t)] + [Q'U(t)][Q'U(t)] + \sigma_{i,k_{ii}}^2 \quad (B.1)$$

The above cost function is minimized by selecting  $U(t)$  such that the partial derivative of the cost function with respect to  $U(t)$  is zero. Since  $\sigma_{i,k_{ii}}^2$  is assumed to not be a function of  $U(t)$ , then:

$$\begin{aligned} \frac{\partial J}{\partial U(t)} &= \frac{\partial}{\partial U(t)} \{ [PY^*(t+k_{ii}|t) - RW(t)]'[PY^*(t+k_{ii}|t) - RW(t)] \} \\ &+ \frac{\partial}{\partial U(t)} \{ [Q'U(t)][Q'U(t)] \} \end{aligned} \quad (B.2)$$

The differentiation is accomplished in several stages. Making use of a relationship developed by Sage, [1968], and corrected to:

$$s = M'NO \quad (B.3)$$

where  $M$  and  $O$  are  $m \times 1$  vectors,  $N$  is a  $m \times m$  matrix, then:

$$\frac{ds}{dt} = \left[ \frac{dM'}{dt} \right] NO + \left[ \frac{dO'}{dt} \right] N'M + M' \left[ \frac{dN}{dt} \right] O \quad (B.4)$$

For the first term of equation B.2 M, N and O become:

$$M = [PY^*(t+k_{11}|t) - RW(t)]$$

$$N = I$$

$$O = [PY^*(t+k_{11}|t) - RW(t)]$$

Then, utilizing the relation of equation B.4, the differentiation of the first portion of equation B.2 becomes:

$$\begin{aligned} & \frac{\partial}{\partial U(t)} \{ [PY^*(t+k_{11}|t) - RW(t)]' I [PY^*(t+k_{11}|t) - RW(t)] + \\ & \frac{\partial}{\partial U(t)} \{ [PY^*(t+k_{11}|t) - RW(t)]' I' [PY^*(t+k_{11}|t) - RW(t)] + \\ & [PY^*(t+k_{11}|t) - RW(t)]' \left[ \frac{\partial I}{\partial U(t)} \right] [PY^*(t+k_{11}|t) - RW(t)] \quad (B.5) \end{aligned}$$

Since  $I$  is not a function of  $U(t)$ ,  $\partial I / \partial U(t) = 0$  and the third term of B.5 may be dropped. It is still necessary to determine an expression for:

$$\frac{\partial}{\partial U(t)} [PY^*(t+k_{11}|t) - RW(t)]' \quad (B.6)$$

In Chapter 3, it was shown that:

$$PY^*(t+k_{ii}|t) = P_d FC^{-1}Y(t) + z^{k_{ii}-k_{ii}} EC^{-1}BU(t) + z^{k_{ii}-d_{ii}} EC^{-1}DV(t) \quad (3.47)$$

And, because  $U(t)$  is the only element on the right hand side which is a function of  $U(t)$ , then:

$$\begin{aligned} \frac{\partial}{\partial U(t)} [PY^*(t+k_{ii}|t)] &= \frac{\partial}{\partial U(t)} [EC^{-1}BU(t)] \\ &= E(0)C(0)^{-1}B(0) \end{aligned} \quad (B.7)$$

Again, it is only the first terms of the  $E$ ,  $B$  and  $C$  polynomials that are of interest.  $RW(t)$  is not a function of  $U(t)$ , hence its derivative with respect to  $U(t)$  is zero. This results in the first term of equation B.5 of the form:

$$E(0)C(0)^{-1}B(0)'[PY^*(t+k_{ii}|t) - RW(t)] \quad (B.8)$$

Following the same procedure for the second term of equation B.5, letting:

$$M = [Q'U(t)]$$

$$N = I$$

$$O = [Q'U(t)]$$

It follows that the derivative of the second term of equation B.5, using equation B.4, becomes:

$$\frac{\partial}{\partial U(t)} \{ [Q'U(t)]' \} I [Q'U(t)] + \frac{\partial}{\partial U(t)} \{ [Q'U(t)]' \} I' [Q'U(t)] \\ + [Q'U(t)]' \frac{\partial \{ I \}}{\partial U(t)} [Q'U(t)] \quad (B.9)$$

The second term of B.9 is zero, and:

$$\frac{\partial}{\partial U(t)} [Q'U(t)]' = Q'(0)' \quad (B.10)$$

Combining equations B.5, B.8, B.9 and B.10 to replace the respective values in equation B.2 results in the differentiation being expressed as:

$$\frac{\partial J}{\partial U(t)} = 2E(0)C(0)'(0)'[PY^*(t+k_1|t) - RW(t)]' \\ + 2Q'(0)'Q'U(t) \quad (B.11)$$

Given as equation 3.47.

## Appendix C

### Calibration Data for the Distillation Column

Table C.1  
Top Product Analyzer Calibration

Chart (%)	mvolts	Composition (mass %)
48.5	2912.4	95.362
30.0	2710.9	95.942
10.5	1404.6	97.084
86.0	4326.5	93.626
70.0	3740.5	94.039

$$\text{Top Composition} = (-0.00119) * (\text{mvolts}) + (98.6867)$$

$$\text{Chart \%} = (0.02575) * (\text{mvolts}) - (25.9586)$$



Table C.2  
Top Product Flow Calibration

Chart (%)	mvolts	Mass (lbs)	Time (min:sec)	g/s	SQRT(mV)
7.0	1184.2	75.0	102:17	5.543	34.412
15.5	1618.2	30.0	30:25	7.456	40.227
94.5	5405.0	35.0	15:41	16.871	73.519
57.0	3737.1	26.0	14:27	13.603	61.132
28.5	2284.2	30.0	24:06	9.411	47.793

$$\text{Top Product Flow (g/s)} = (0.29024) * \text{SQRT(mV)} - (4.3465)$$

Table C.3  
Reflux Flow Calibration

Chart (%)	mvolts	Mass (lbs)	Time (min:sec)	g/s	SQRT(mV)
10.0	1467.0	20.0	32:20	4.676	38.301
20.0	1840.0	29.0	33:57	6.458	42.895
30.0	2216.2	26.0	24:17	8.094	47.077
40.0	2645.6	35.0	29:01	9.119	51.435
50.0	3040.1	32.0	23:12	10.427	55.137
60.0	3425.1	32.0	21:55	11.038	58.524
70.0	3806.8	33.0	20:50	11.975	61.699

$$\begin{aligned}
 \text{Reflux Flow (g/s)} &= (0.30649) * \text{SQRT(mV)} - 6.7198 \\
 &\quad (- \text{ shift of 2.8 g/s in the recorder zero}) \\
 &= (0.30649) * \text{SQRT(mV)} - 3.9198
 \end{aligned}$$

Table C.4  
Feed Flow Calibration

Chart (%)	mvolts	Mass (lbs)	Time (min:sec)	g/s	SQRT(mV)
25.0	1991.0	42.0	24:30	12.960	44.622
35.0	2367.5	45.0	22:58	14.812	48.657
45.0	2734.4	48.0	21:40	16.748	52.292
55.0	3137.7	40.0	16:11	18.686	56.015
65.0	3503.5	41.0	15:24	20.127	59.190
75.0	3913.3	47.0	16:16	21.843	62.556

$$\text{Feed Flow (g/s)} = (0.50797) * \text{SQRT(mV)} - 9.6778$$

Table C.5  
Steam Flow Calibration

Chart (%)	mvolts	Mass (lbs)	Time (min:sec)	g/s	SQRT(mV)
30.0	2173.3	10.5	10:39	7.453	46.619
38.0	2487.3	12.9	11:52	8.218	49.873
46.0	2799.6	12.7	9:19	10.305	52.911
54.0	3118.8	10.6	6:52	11.670	55.846

$$\text{Steam Flow (g/s)} = (0.47818) * \text{SQRT(mV)} - 15.1248$$

Table C.6  
Bottom Product Flow Calibration

Chart (%)	mvolts	Mass (lbs)	Time (min:sec)	g/s	SQRT(mV)
81.0	4979.1	64.0	30:13	16.012	70.563
66.0	4180.1	48.0	24:45	14.662	64.654
55.0	3590.9	45.0	25:51	13.160	59.924
41.0	2884.3	45.0	30:37	11.111	53.706
22.0	1940.3	30.0	28:23	7.990	44.049
6.0	1265.3	17.0	31:32	4.076	35.570

$$\text{Bottom Product Flow (g/s)} = (0.33971) * \text{SQRT(mV)} - 7.4287$$

## Appendix D

### Pseudocode for Distillation Column Routines

Run the main program (MAIN1)

- 1 - Initialize (Call START1 - which reads the main data file, RTMIST.DAT, to obtain the:
    - sampling times and
    - calibration data from the model section,
    - number of each type of parameter,
    - parameter initial values,
    - assumed time delays,
    - type of identification,
    - forgetting factors,
    - initial value of the covariance matrix  
(and initialize the matrix);
    - initial set points and
    - the initial control settings
    - from the system section, and the
    - upper control limit,
    - lower control limit,
    - maximum percentage change in control,
    - control action (direct or indirect),
    - PB, TI and TD to be used in calculating
    - the Q weighting polynomial coefficients,
    - number of Q polynomial coefficients,
    - number of P polynomial coefficients,
    - numerator and denominator polynomial
    - coefficients for Q,
    - numerator and denominator polynomial
    - coefficients for P,
    - PB, TI, TD parameters for PID control and
    - feed initial conditions and disturbance
    - pattern (if any) from the control section.
- START1 also calls:
- COFSET - to calculate the trapezoidal approximation to get coefficients for a PID controller polynomial,
  - ANIN - to get initial feed, reflux and steam flows,
  - DOUT - to start the GC routine and
  - CLOCK - to initialize the timer.

- 2 - Look for an incoming GC report (Call CHARIN).
- 3 - Check the keyboard for any input (Call KEYSC)
- 4 - If there is input, deal with it (Call POCSR - POCSR allows the operator to introduce disturbances, stop control, change parameters, etc.)
- 5 - If there hasn't been a GC report yet - return to (2)
- 6 - If there has been a GC report:
- 7 - Retrieve the report (Call GETGC)
- 8 - Restart the GC routine (Call DOUT)
- 9 - Obtain the latest top composition, feed, reflux and steam flows (Call ANIN)
- 10 - Perform control (Call CONTR1 - CONTR1 will determine if it is time to introduce a disturbance, it will perform the calculations for the STC or PID control algorithms, limit the control action and send the desired set points out to the local flow controllers (Call ANOUT))
- 11 - Generate output and write it out, either to the screen or to a disk for storage
- 12 - Reset the GC routine
- 13 - Return to (2)